ҚАЗАҚСТАН РЕСПУБЛИКАСЫ
ҒЫЛЫМ ЖӘНЕ ЖОҒАРЫ БІЛІМ МИНИСТРЛІГІ
SATBAYEV UNIVERSITY
МЕТАЛЛУРГИЯ ЖӘНЕ КЕН БАЙЫТУ ИНСТИТУТЫ

ISSN 2616-6445 (Online)
ISSN 2224-5243 (Print)
DOI 10.31643/2018/166445

Минералдық шикізаттарды кешенді пайдалану

4(339)

Комплексное Использование Минерального Сырья

Complex Use of Mineral Resources

ҚАЗАН-ЖЕЛТОҚСАН 2026
OCTOBER-DECEMBER 2026
ОКТЯБРЬ-ДЕКАБРЬ 2026

ЖЫЛЫНА 4 РЕТ ШЫҒАДЫ
QUARTERLY JOURNAL
ВЫХОДИТ 4 РАЗА В ГОД

ЖУРНАЛ 1978 ЖЫЛДАН БАСТАП ШЫҒАДЫ
JOURNAL HAS BEEN PUBLISHING SINCE 1978
ЖУРНАЛ ИЗДАЕТСЯ С 1978 ГОДА

АЛМАТЫ - 2026

Редакция мекен жайы:
«Металлургия және кен байыту институты» АҚ
050010, Қазақстан Республикасы, Алматы қ., Шевченко к-сі, Уәлиханов к-нің қиылысы, 29/133,
Fax. +7 (727) 298-45-03, Tel. +7-(727) 298-45-02, +7 (727) 298-45-19
E mail: journal@kims-imio.kz, product-service@kims-imio.kz
http://kims-imio.com/index.php/main

«Минералдық шикізаттарды кешенді пайдалану» журналы ғылыми жұмыстардың негізгі нәтижелерін жариялау үшін Қазақстан Республикасы Білім және ғылым министірлігінің Білім және ғылым сапасын қамтамасыз ету комитеті ұсынған ғылыми басылымдар тізіміне енгізілген.
Меншік иесі: «Металлургия және кен байыту институты» АҚ

Журнал Қазақстан Республикасының Ақпарат және коммуникация министрлігінің Байланыс, ақпараттандыру және бұқаралық ақпарат құралдары саласындағы мемлекеттік бақылау комитетінде қайта тіркелген

2016 ж. 18 қазандағы № 16180-Ж Куәлігі

Address:
"Institute of Metallurgy and Ore Beneficiation" JSC
29/133 Shevchenko Street, corner of Ch. Valikhanov Street, Almaty, 050010, Kazakhstan
Fax. +7 (727) 298-45-03, Tel. +7-(727) 298-45-02, +7 (727) 298-45-19
E mail: journal@kims-imio.kz, product-service@kims-imio.kz
http://kims-imio.com/index.php/main

The Journal "Complex Use of Mineral Resources" is included in the List of publications recommended by the Committee for Control in the Sphere of Education and Science of the Ministry of Education and Science of the Republic of Kazakhstan for the publication of the main results of scientific activities.
Owner: "Institute of Metallurgy and Ore Beneficiation" JSC

The Journal was re-registered by the Committee for State Control in the Sphere of Communication, Information and Mass Media of the Ministry of Information and Communication of the Republic of Kazakhstan.

Certificate № 16180-Ж since October 18, 2016

Адрес редакции:
АО «Институт металлургии и обогащения»
050010, Республика Казахстан, г. Алматы, ул. Шевченко, уг. ул. Валиханова, 29/133,
Fax. +7 (727) 298-45-03, Tel. +7 (727) 298-45-02, +7 (727) 298-45-19
E mail: journal@kims-imio.kz, product-service@kims-imio.kz
http://kims-imio.com/index.php/main

Журнал «Комплексное использование минерального сырья» включен в Перечень изданий, рекомендуемых Комитетом по контролю в сфере образования и науки Министерства образования и науки Республики Казахстан для публикации основных результатов научной деятельности.
Собственник: АО «Институт металлургии и обогащения»

Журнал перерегистрирован в Комитете государственного контроля в области связи, информатизации и средств массовой информации
Министерства информации и коммуникации Республики Казахстан
Свидетельство № 16180-Ж от 18 октября 2016 г.

Crossref

DOI: 10.31643/2026/6445.35
Metallurgy

Investigation of zinc leaching from clinker with pretreatment of raw materials by ultrahigh frequency radiation (microwave)

Berkinbaeva A.N., Surkova T.Yu., *Dosymbayeva Z.D., Umirbekova N.S., Kebekbaeva A.A., Kyussubayeva N.A.

Institute of Metallurgy and Ore Beneficiation JSC, Satbayev University, Almaty, Kazakhstan

**Corresponding author email: z.dosymbaeva@satbayev.university*

Received: *March 5, 2025*
Peer-reviewed: *March 18, 2025*
Accepted: *May 27, 2025*

Abstract

The processing of zinc-containing man-made raw materials is an important task from the point of view of rational use of natural resources and reducing the environmental burden. In recent years, there has been a growing interest in efficient methods of processing such materials, since zinc is an important metal for industry. The leaching of zinc from raw materials with a solution of sulfuric acid is a key step in the hydrometallurgical production of zinc. Optimizing this process is crucial to increase the efficiency of its extraction, reduce costs, and minimize negative environmental impacts. We have investigated the process of leaching zinc from man-made raw materials with a solution of sulfuric acid, with pretreatment of raw materials with microwave radiation. Optimal leaching parameters have been determined. Clinker, a residual product of zinc ore calcination, was used as the starting material. The zinc content in clinker is 1.25%. It is shown that high zinc recovery is achieved after preliminary exposure to microwave radiation at a temperature of 600 °C. The effect of solvent concentration, the ratio of solid and liquid phases, and temperature on the degree of zinc extraction has been studied.

Keywords: leaching, zinc, clinker, ultrahigh frequency radiation.

Information about authors:

Berkinbayeva A.N. *Candidate of technical sciences, a head of chemical analytical laboratory, Institute of Metallurgy and Ore Beneficiation JSC, Satbayev University, Shevchenko str., 29/133, 050010, Almaty, Kazakhstan. E-mail: a.berkinbayeva@satbayev.university; ORCID ID: https://orcid.org/0000-0002-2569-9087*

Surkova T.Yu. *Candidate of technical sciences, a leading researcher of the B.B. Beisembayeva laboratory of special methods of hydrometallurgy, Institute of Metallurgy and Ore Beneficiation JSC, Satbayev University, Shevchenko str., 29/133, 050010, Almaty, Kazakhstan. Email: t.surkova@satbayev.university; ORCID ID: https://orcid.org/0000-0001-8271-125X*

Dosymbayeva Z.D. *Researcher, Institute of Metallurgy and Ore Beneficiation JSC, Satbayev University, Shevchenko str., 29/133, 050010, Almaty, Kazakhstan. Email: z.dosymbaeva@satbayev.university; ORCID ID: https://orcid.org/0000-0001-9144-208X*

Umirbekova N.S. *Researcher, Institute of Metallurgy and Ore Beneficiation JSC, Satbayev University, Shevchenko str., 29/133, 050010, Almaty, Kazakhstan. Email: n.umirbekova@satbayev.university; ORCID ID: https://orcid.org/0000-0001-5860-3179*

Kebekbayeva A.A. *Junior Researcher, Institute of Metallurgy and Ore Beneficiation JSC, Satbayev University, Shevchenko str., 29/133, 050010, Almaty, Kazakhstan. Email: a.kebekbaeva@satbayev.university*

Kyussubayeva N.A. *Leading engineer, Institute of Metallurgy and Ore Beneficiation JSC, Satbayev University, Shevchenko str., 29/133, 050010, Almaty, Kazakhstan. Email: n.kyussubayeva@satbayev.university*

Introduction

Zinc, being one of the most common metal elements in the world, is widely used in industries such as automotive, construction, shipbuilding, and aerospace. It is used in the form of electroplating, zinc alloys, zinc oxide, and other forms to protect steel surfaces from corrosion [1]. Key mining and processing facilities for zinc-containing resources are located in China, Peru, Australia, India, the United States, Mexico, and Bolivia. These seven countries together produce more than 76% of zinc in concentrates [2]. The main components of zinc ores are zinc sulfide, zinc oxide, or a combination of the two. Currently, 70% of the world's zinc production comes from primary zinc ores, while the remaining 30% comes from secondary zinc sources [[3], [4]].

Pyro- and hydrometallurgical methods are used for processing zinc-containing technogenic materials [5]. Pyrometallurgical processes are based on the reduction of zinc with carbon-containing materials at high temperatures. The most common

pyrometallurgical method is rolling (reduction and ignition firing). As a result of rolling, zinc lotions and clinker are obtained. Zinc sublimations are directed to sulfuric acid leaching [6]. To date, 4.5 – 5.7 million tons of zinc industry waste have accumulated in Kazakhstan [7].

Traditionally, acids such as [[8], [9]], sulfuric acid and hydrochloric acid are used for zinc leaching, which can be environmentally hazardous. Modern research focuses on the use of less toxic and more stable reagents and methods, which contributes to improving the environmental safety of the process [[10], [11], [12]]. In recent years, the use of bacteria such as *Thiobacillus ferrooxidans* to leach zinc from man-made waste, such as ash or slag, has been actively investigated. It is an environmentally friendly alternative to chemical methods, which shows high results at low temperatures and pressures. Despite its advantages over traditional enrichment methods, bio-leaching technology has a significant disadvantage, which is the high duration of the technological process due to the weak kinetics of redox reactions [13]. Modern methods, such as the use of ultrasound and microwave radiation, are becoming increasingly popular to improve material recycling processes [14]. These methods affect the structure of the material, which can help improve leaching performance. In [15], ultrasonic technology using the ammonia-ammonium-chloride-water system was used to leach zinc from industrial waste. Some studies combine microwave treatment and ultrasound leaching with a microbiological process, where microwave and ultrasound treatment activates bacteria that promote additional dissolution of metals, including zinc [16]. This can become an important area for processing ores and waste.

One of the promising methods for increasing extraction efficiency is the pretreatment of raw materials by microwave firing, which makes it possible to intensify subsequent leaching processes. This review examines the mechanisms of the influence of microwave processing on the structure of raw materials, changes in its phase composition, and an increase in the degree of extraction of germanium from zinc oxide (ZnO) dust [17]. For the processing of lead oxides, their preliminary purification from chlorides and fluorides is necessary. For this purpose, technologies for washing welz oxides with aqueous and aqueous-alkaline solutions were used. Pyrometallurgical calcination is an alternative method of halogen removal. Microwave heating is a promising method of heat treatment of welz oxides, having a number of advantages, such as the transfer of electromagnetic energy instead of heat, high heating rate, selective heating of materials and the volumetric nature of heating [[18], [19]].

Clinker, as an intermediate product of ore processing, can contain various metals, including zinc, which is an important element for various industries. For efficient processing and extraction of zinc, it is necessary to increase the efficiency of leaching, which is usually carried out using acids. However, the use of traditional leaching methods may be limited by low productivity, as well as high energy consumption of the process. Hydrometallurgical processes remain the main ones for processing zinc-containing raw materials, as they allow obtaining high-purity metals with minimal energy costs. The leaching of zinc from raw materials with a solution of sulfuric acid is a key step in the hydrometallurgical production of zinc. Optimizing this process is crucial to increase the efficiency of its extraction, reduce costs, and minimize negative environmental impacts. In recent years, more and more attention has been paid to the use of non-traditional methods of intensifying leaching processes, such as microwave heating and ultrasonic treatment.

Optimizing this process is crucial to increase the efficiency of its extraction, reduce costs, and minimize negative environmental impacts. In recent years, more and more attention has been paid to the use of non-traditional methods of intensifying leaching processes, such as microwave heating and ultrasonic treatment.

In recent years, more and more attention has been paid to the use of non-traditional methods to intensify leaching processes, such as microwave heating. Therefore, the purpose of this study is to optimize the process of zinc leaching from man-made raw materials (clinker) with pretreatment by microwave radiation, by determining the effect of parameters on the efficiency of zinc extraction, which will increase efficiency and reduce the environmental burden during the processing of zinc-containing materials.

Methodology and Materials

Technogenic zinc-containing raw materials, clinker, were used as the starting material. The chemical composition of the sample is represented by the main elements: Fe (25.39%), Zn (1.25%) and Cu (0.81%), as well as gold (1.53 g/t) and silver (71.81 g/t), calcium (3.81%), silicon (4.58%), copper

(1.04%), zinc (more than 1.2%) and other substances.

The effect of microwave radiation on clinker occurred in a high-temperature microwave reactor "Energy K-50" (915 MHz, 25 kW). Figure 1 shows a single installation of the Energiya K family. The complex is designed to process the initial product by dielectric heating it in ultrahigh frequency electromagnetic fields in the mode of continuous movement of the material in a rotating dielectric retort (tube) installed in the waveguides of the drying chamber of the Complex.

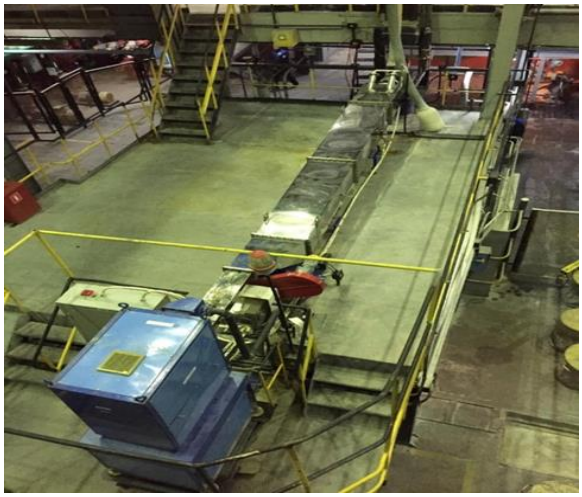

Figure 1 - A single installation of the «Energy K» family

Test experiments were conducted on leaching of the initial technogenic zinc-containing raw materials in order to determine the optimal conditions. An installation was used for leaching, including a reactor with a PE 8399 mechanical stirrer from Ekros.

The kinetics of the leaching process was studied by placing a solution of 0.1 dm3 sulfuric acid or alkali in conical flasks with a volume of 0.25 dm3 (acid concentration ranged from 60-140 g/dm3, sodium hydroxide from 25-150 g/dm3) and ore in the ratio S:L=1:5. The leaching was carried out with intensive stirring; the duration of the process was 6 hours, the mixing speed was 300 rpm, and the temperature ranged from 22-80 °C.

The leaching conditions are chosen to ensure an optimal balance between extraction efficiency, reaction rate, mass transfer, and process economy.

Methods of analysis

Modern analytical methods were used in the work. The phase composition of the samples was determined using a D8 Advance X–ray diffractometer (BRUKER), Cu-Ka radiation. The elemental analysis was performed using an X-ray fluorescence spectrometer with an Axios wavelength of 1 kW (PANalytical). The microstructure of the surface was monitored using a JXA-8230 electron probe microanalyzer from JEOL (Jeol, Tokyo, Japan). The quantitative zinc content in the solutions after leaching was determined using an Optima 8000DV inductively coupled plasma atomic emission spectrometer.

Results and discussion

In the course of the research, the following experimental scheme was used: crushing clinker to 90 % of the class size -0.071+0 mm, microwave processing and leaching (Fig.2) [20].

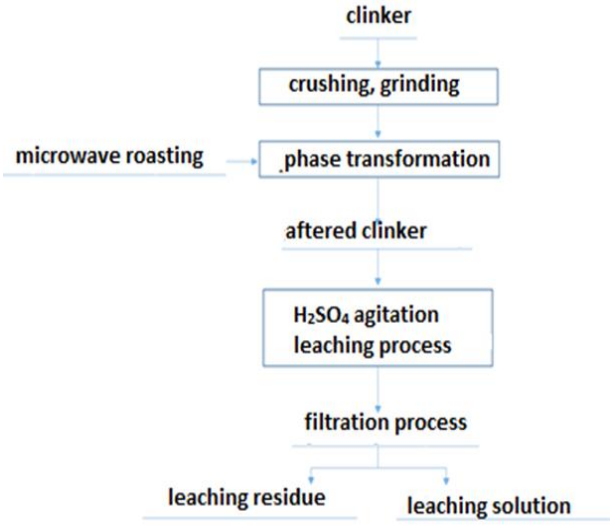

Figure 2 – Block diagram of the experiment

According to the above scheme, the crushed and crushed clinker has passed the stage of microwave firing. The parameters of the effect of microwave radiation on clinker are shown in Table 1.

Table 1 – Parameters of experiments on a microwave installation

Naming of indicators	Experience No. 1	Experience No. 2	Experience No. 3	Experience No. 4
Microwave power, kW	25	25	25	25
Frequency of waves, MHz	915	915	915	915
Duration of experience, min	5-7	5-7	5-7	5-7
Temperature, °C	250	460	600	700

When studying the microwave effect on clinker, the following parameters were taken: radiation power — 25 kW, frequency — 915 MHz, treatment duration — 5-7 minutes. These parameters remained unchanged in all experiments, while the heating temperature varied (from 250 to 700 °C), which made it possible to evaluate the influence of the temperature factor, all other things being equal. The frequency of 915 MHz is the industry standard for microwave processing, providing deep penetration of microwave energy into the processed material. The duration of 5-7 minutes was chosen experimentally as sufficient to achieve a stable thermal effect at a given power. Increasing the time does not give a significant increase in temperature or effect, but increases energy consumption.

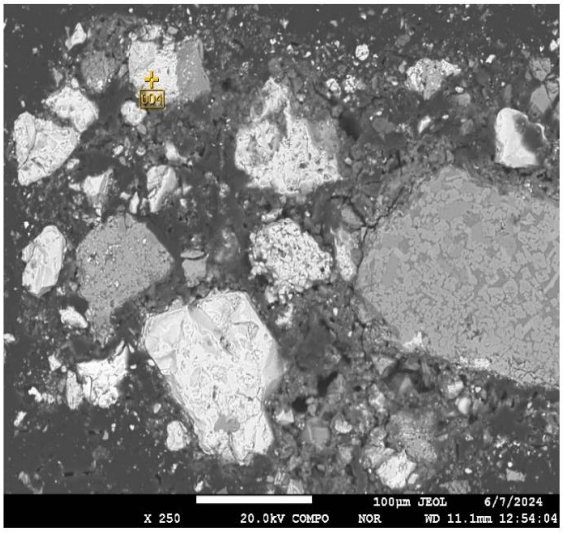

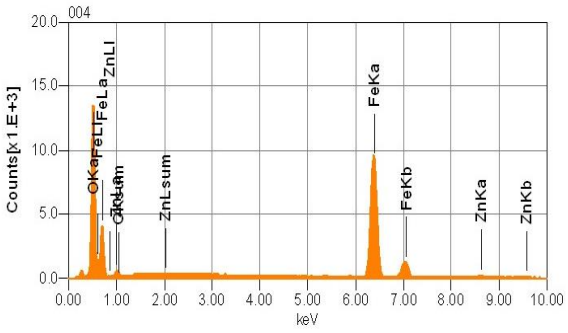

Chemical formula	ms%	mol%	Sigma	Net	K ratio	Line
O	36.51	66.87	0.13	2926850	0.3257862	K
Fe	61.12	32.07	0.42	5578589	0.6352698	K
Zn	2.37	1.06	1.16	98005	0.0225208	K
Total	100.00	100.00				

Figure 3 - Microstructure and energy dispersion analysis of clinker after exposure to microwave radiation at 700 °C

The temperature range covers both the initial stages of dehydration and structural transformations (250-460 °C) and high-temperature effects, including phase transformations and activation of chemically inert compounds (600-700 °C).

As can be seen from the table, the microwave heating temperature range ranges from 250 – 700 °C. According to the results of energy dispersion analysis of clinker after exposure to microwave radiation, it was found that when the microwave heating temperature reaches 460 °C, cracks form in the sphalerite grain as a result of thermally induced mechanical stresses. When the temperature rises to 600 °C, the zinc-containing phase is mainly ZnO [20]. At the same time, zinc oxide is well soluble in dilute acids by the reaction:

$$ZnO + H_2SO_4 = ZnSO_4 + H_2O \quad (1)$$

$$ZnO + 2NaOH + H_2O = Na_2[Zn(OH)_4] \quad (2)$$

With a further increase in temperature (up to 700 °C), a complex ferritic compound (ZnO · Fe2O3) is synthesized, demonstrating a high degree of chemical resistance in weakly concentrated acidic media (Fig. 3). Thus, the temperature of the clinker phase transformation by microwave heating was chosen to be 600 °C.

In the course of the research, the process of leaching clinker pretreated with microwave radiation in different temperature conditions with a solution of sulfuric acid concentration of 100 g/dm^3 at a temperature of 22 ±2 ° C was studied (Fig. 4).

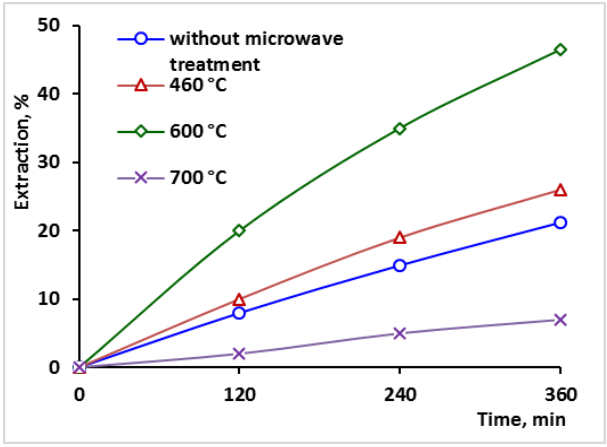

Figure 4 - Comparison of zinc extraction efficiency during clinker leaching with sulfuric acid before and after exposure to microwave radiation

The figure 4 shows that the degree of zinc recovery from clinker was: - from the feedstock – 21.12%; after preliminary exposure to microwave radiation at 460 ° C – 23.45%, at 600 ° C – 46.47%, at

700 ° C – 5.12%. Thus, the highest zinc recovery was achieved after preliminary exposure Microwave radiation at a temperature of 600 °C. Increasing the temperature to 700 ° C reduces the leaching process. This fact is probably related to the formation of a complex ferritic compound ($ZnO*Fe_2O_3$), which demonstrates a high degree of chemical resistance in weakly concentrated acids. In subsequent experiments, clinker was pretreated with microwave radiation at a temperature of 600 ° C.

Then, training using sulfuric acid of various concentrations from 25 to 125 was studied (Fig. 5). The kinetic curves shown in the figure show that with an increase in the concentration of sulfuric acid, zinc extraction increases from 15.0 to 46.47 %. At a higher concentration of H_2SO_4, the formation of insoluble iron sulfate ($Fe_2(SO_4)_3$ is possible, which can reduce the extraction of impurity elements.

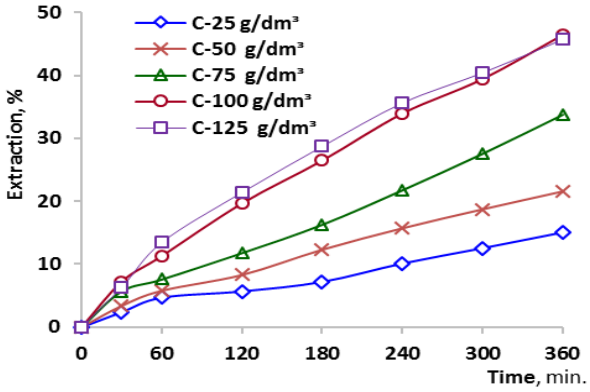

Figure 5 - Effect of sulfuric acid (H_2SO_4) concentration on zinc extraction from clinker after exposure to microwave radiation

When studying the effect of the concentration of the leaching reagent on the zinc dissolution process, sodium hydroxide (NaOH) was also used, the concentration of which varied between 25-150 g/dm^3 (Fig. 6).

Figure 5 shows the kinetic curves of the interaction of clinker pretreated with alkali depending on its concentration, which shows that with an increase in the concentration of sodium hydroxide from 25 to 50 g/dm^3, the degree of zinc leaching increases from 4.8 to 6.9 %. An increase in the alkali concentration leads to a sharp decrease in zinc extraction to 5.9 %. The reason for the decrease in zinc extraction at high NaOH concentrations may be the formation of insoluble compounds or the passivation of the clinker surface.

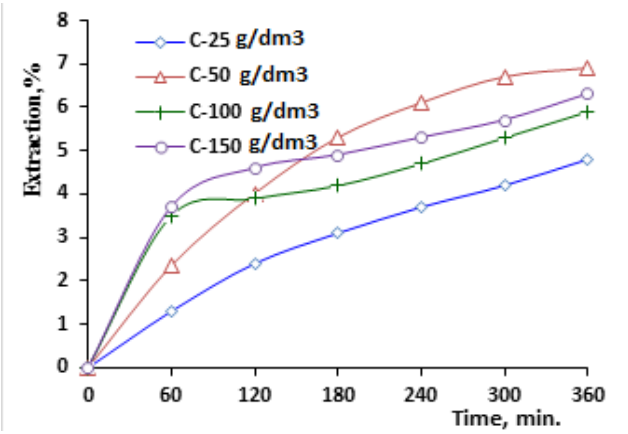

Figure 6 - Effect of sodium hydroxide (NaOH) concentration on zinc extraction from clinker after exposure to microwave radiation

The results shown in Figures 7 and 8 demonstrate the effect of the liquid–solid ratio, as well as the temperature of the leaching of clinker with sulfuric acid.

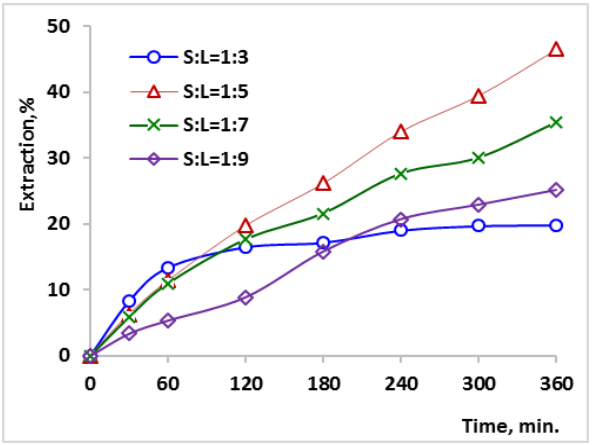

Figure 7 - The effect of the S:L ratio on zinc extraction from clinker after exposure to microwave radiation

It is shown that with an increase in the S:L ratio from 1:3 to 1:5, an increase in the degree of zinc extraction is observed from 32.0 to 46.0 %, and a further increase contributes to a decrease in extraction from 46.0 to 25.07 % (Fig. 7). The optimal solid-liquid ratio is 1:5.

As for the effect of temperature, the relationship is simpler: An increase in the clinker leaching temperature from 22 to 80 °C contributes to an increase in the degree of zinc extraction from 46.47 to 68.18 % (Fig. 8).

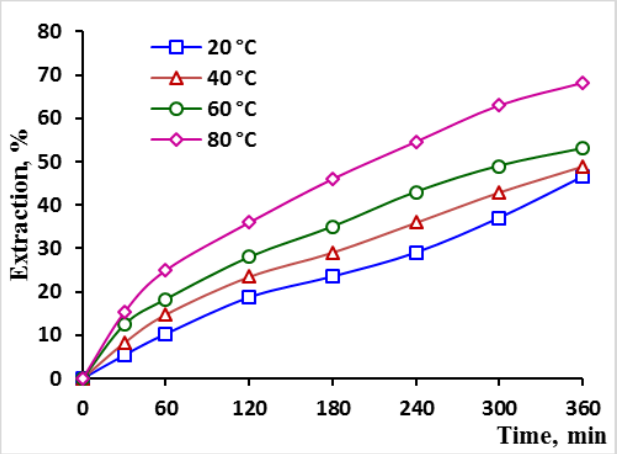

Figure 8 - Effect of temperature on zinc leaching from clinker after exposure to microwave radiation

Thus, the studies carried out and the results obtained have shown that the optimal conditions for exposure to microwave radiation are: a temperature of 600 ° C, and a leaching concentration of sulfuric acid of 100 g/l, a liquid–solid ratio of 5:1, and a leaching temperature of 80 °C.

Conclusion

Pretreatment of clinker using microwave and ultrasonic exposure is a promising method for increasing the efficiency of zinc leaching. The use of these methods can reduce energy consumption and increase the productivity of processing processes, which is important for the modern metallurgical and chemical industries.

Studies have shown that the highest zinc recovery is achieved after preliminary exposure to microwave radiation at a temperature of 600 °C. Increasing the temperature to 700 ° C reduces the leaching process. This fact is probably related to the formation of a complex ferritic compound ($ZnO*Fe_2O_3$), which demonstrates a high degree of chemical resistance in weakly concentrated acids.

A study of the effect of acid and alkali concentrations on the degree of zinc leaching from clinker pretreated with microwave radiation showed that the optimal concentration of sulfuric acid is 100 g/dm^3, and alkali is 50 g/dm^3.

Studies have shown that the optimal parameters for the leaching process are the temperature of 80 °C and the ratio of solid and liquid phases (S:L) 1:5. Under these conditions, a balanced ratio is achieved between the efficiency of chemical interaction and the processability, which allows for sufficient contact between the reagent (sulfuric acid) and the processed material. Under these conditions, the degree of extraction by sulfuric acid was 46.47%. Sulfuric acid leaching is the most common method, providing a high degree of recovery. In this study, sulfuric acid leaching showed a higher level of zinc recovery than alkaline leaching, which makes it the preferred method under the conditions studied.

Conflict of interest. There are no competing interests for all authors.

CRediT author statement: **A. Berkinbayeva:** Conceptualization, Methodology, and Software; **T. Surkova:** Data curation and Writing - Original draft preparation; **Z. Dossymbayeva**: Visualization and Investigation; **N. Umirbekova**: Visualization and Investigation; **A. Kebekbayeva**: Software and Validation; **N. Kyusubaeva**: Software and Validation.

Funding statement. This research is funded by the Science Committee of the Ministry of Science and Higher Education of the Republic of Kazakhstan (Grant No AP19675985).

Acknowledgements. The authors would like to thank the research team at the Institute of Metallurgy and Ore Beneficiation, Satbayev University, Kazakhstan for their support in this study.

Cite this article as: Berkinbaeva AN, Surkova TYu, Dosymbayeva ZD, Umirbekova NS, Kebekbaeva AA, Kyussubayeva NA. Investigation of zinc leaching from clinker with pretreatment of raw materials by ultrahigh frequency radiation (microwave). Kompleksnoe Ispolzovanie Mineralnogo Syra = Complex Use of Mineral Resources. 2026; 339(4):5-13. https://doi.org/10.31643/2026/6445.35

Ультра жоғары жиілікте сәулелендіру арқылы (микротолқынды пеш) алдын ала өңделген клинкерден мырыштың шаймалануын зерттеу

Беркинбаева А.Н., Суркова Т.Ю, Досымбаева З.Д., Умирбекова Н.С., Кебекбаева А.А., Кюсубаева Н.А.

Металлургия және кен байыту институты АҚ, Сәтбаев университеті, Алматы, Қазақстан

Мақала келді: *5 наурыз 2025*
Сараптамадан өтті: *18 наурыз 2025*
Қабылданды: *27 мамыр 2025*

ТҮЙІНДЕМЕ

Құрамында мырыш бар техногендік шикізатты қайта өңдеу табиғи ресурстарды ұтымды пайдалану және экологиялық жүктемені азайту тұрғысынан маңызды міндет болып табылады. Соңғы жылдары мұндай материалдарды өңдеудің тиімді әдістеріне қызығушылық артып келеді, өйткені мырыш өнеркәсіп үшін маңызды металл болып табылады. Шикізаттан мырышты күкірт қышқылының ерітіндісімен шаймалау мырыштың гидрометаллургиялық өндірісіндегі негізгі қадам болып табылады. Бұл процесті оңтайландыру өндіру тиімділігін арттыру, шығындарды азайту және қоршаған ортаға теріс әсерді азайту үшін өте маңызды. Біз мырышты техногендік шикізаттан күкірт қышқылының ерітіндісімен микротолқынды сәулелендірумен алдын ала өңдеу арқылы шаймалау процесін зерттедік. Оңтайлы шаймалау параметрлері анықталды. Бастапқы шикізат ретінде мырыш кенінің вельцтеу өндірісінің қалдық өнімі клинкер пайдаланылды. Клинкердегі мырыш мөлшері - 1,25 %. Мырыштың жоғары экстракциясына 600 °С температурада микротолқынды сәулелендірудің алдын ала әсерінен кейін қол жеткізілгені көрсетілді. Шаймалаудың оңтайлы параметрлері анықталды.

Түйін сөздер: шаймалау, мырыш, клинкер, ультра жоғары жиілікті сәулелендіру.

Авторлар туралы ақпарат:

Беркинбаева А.Н. *Химия-аналитикалық зертханасының меңгерушісі, техника ғылымдарының кандидаты, Металлургия және кен байыту институты АҚ, Сәтбаев университеті, Шевченко көш., 29/133, 050010, Алматы, Қазақстан. E-mail: a.berkinbayeva@satbayev.university; ORCID ID: https://orcid.org/0000-0002-2569-9087*

Суркова Т.Ю. *Техника ғылымдарының кандидаты, Б.Б.Бейсембаев атындағы гидрометаллургияның арнайы әдістері зертханасының жетекші ғылыми қызметкері, Металлургия және кен байыту институты АҚ, Сәтбаев университеті, Шевченко көш., 29/133, 050010, Алматы, Қазақстан. Email: t.surkova@satbayev.university; ORCID ID: https://orcid.org/0000-0001-8271-125X*

Досымбаева З.Д. *Ғылыми қызметкер, Металлургия және кен байыту институты АҚ, Сәтбаев университеті, Шевченко көш., 29/133, 050010, Алматы, Қазақстан. Email: z.dosymbaeva@satbayev.university; ORCID ID: https://orcid.org/0000-0001-9144-208X*

Умирбекова Н.С. *Ғылыми қызметкер, Металлургия және кен байыту институты АҚ, Сәтбаев университеті, Шевченко көш.,29/133, 050010, Алматы, Қазақстан. Email: n.umirbekova@satbayev.university; ORCID ID: https://orcid.org/0000-0001-5860-3179*

Кебекбаева А.А. *Кіші ғылыми қызметкер, Металлургия және кен байыту институты АҚ, Сәтбаев университеті, Шевченко көш., 29/133, 050010, Алматы, Қазақстан. Email: a.kebekbaeva@satbayev.university*

Кюсубаева Н.А. *Жетекші инженер, Металлургия және кен байыту институты АҚ, Сәтбаев университеті, Шевченко көш., 29/133, 050010, Алматы, Қазақстан. Email: n.kyussubayeva@satbayev.university*

Исследование выщелачивания цинка из клинкера с предварительной обработкой сырья сверхвысокочастотным излучением

Беркинбаева А.Н., Суркова Т.Ю, Досымбаева З.Д., Умирбекова Н.С., Кебекбаева А.А., Кюсубаева Н.А.

АО Институт металлургии и обогащения, Satbayev University, Алматы, Казахстан

Поступила: *5 марта 2025*
Рецензирование: *18 марта 2025*
Принята в печать: *27 мая 2025*

АННОТАЦИЯ

Переработка цинкосодержащего техногенного сырья представляет собой важную задачу с точки зрения рационального использования природных ресурсов и снижения экологической нагрузки. В последние годы наблюдается рост интереса к эффективным методам переработки таких материалов, поскольку цинк является важным металлом для промышленности. Выщелачивание цинка из сырья раствором серной кислоты является ключевым этапом в гидрометаллургическом производстве цинка. Оптимизация этого процесса имеет решающее значение для повышения эффективности его извлечения, снижения затрат и минимизации негативного воздействия на окружающую среду. Нами исследован процесс выщелачивания цинка из техногенного сырья раствором серной кислоты с предварительной обработкой сырья СВЧ-излучением. Определены оптимальные параметры выщелачивания. В качестве исходного сырья использовали клинкер – остаточный продукт вельцевания цинковых руд. Содержание цинка в клинкере - 1,25 %. Показано, что высокое извлечение цинка достигнуто после предварительного воздействия СВЧ излучения при температуре 600 °С. Изучено влияние концентрации растворителей, соотношения твердой и жидкой фаз, температуры на степень извлечения цинка.

Ключевые слова: выщелачивание, цинк, клинкер, сверхвысокочастотное излучение.

Беркинбаева А.Н.	***Информация об авторах:*** *Кандидат технческих наук, заведующая химико-аналитической лабораторией АО Институт металлургии и обогащения, Satbayev University, ул.Шевченко 29/133, 050010, Алматы, Казахстан. E-mail: a.berkinbayeva@satbayev.university; ORCID ID: https://orcid.org/0000-0002-2569-9087*
Суркова Т. Ю.	*Кандидат технческих наук, ведущий научный сотрудник лаборатории спецметодов гидрометаллургии им.Б.Б.Бейсембаева, АО Институт металлургии и обогащения, Satbayev University, ул.Шевченко 29/133, 050010, Алматы, Казахстан. Email: t.surkova@satbayev.university; ORCID ID: https://orcid.org/0000-0001-8271-125X*
Досымбаева З.Д.	*Научный сотрудник, АО Институт металлургии и обогащения, Satbayev University, ул. Шевченко 29/133, 050010, Алматы, Казахстан. Email: z.dosymbaeva@satbayev.university; ORCID ID: https://orcid.org/0000-0001-9144-208X*
Умирбекова Н.С.	*Научный сотрудник, АО Институт металлургии и обогащения, Satbayev University, ул. Шевченко 29/133, 050010, Алматы, Казахстан. Email: n.umirbekova@satbayev.university; ORCID ID: https://orcid.org/0000-0001-5860-3179*
Кебекбаева А.А.	*Младший научный сотрудник, АО Институт металлургии и обогащения, Satbayev University, ул. Шевченко 29/133, 050010, Алматы, Казахстан. Email: a.kebekbaeva@satbayev.university*
Кюсубаева Н.А.	*Ведущий инженер, АО Институт металлургии и обогащения, Satbayev University, ул. Шевченко 29/133, 050010, Алматы, Казахстан. Email: n.kyussubayeva@satbayev.university*

References

[1] Nayak A, Jena MS, Mandre NR. Beneficiation of lead-zinc ores—A review. Miner. Process. Extr. Metall. Rev. 2021; 43:1-20. https://doi.org/10.1080/08827508.2021.1903459

[2] TSINK. Mirovoy reyting stran [ZINC. World ranking of countries]. 2022. (in Russ). https://nedradv.ru/nedradv/ru/msr?obj=ca79a46078f5785d6a24f2c3830d0b9

[3] Esezobor DE, Balogun SA. Zinc accumulation during recycling of iron oxide wastes in the blast furnace. Ironmaking & Steelmaking. 2006; 33(5):419-425. https://doi.org/10.1179/174328106X114020

[4] Muammer Kaya, Shokrullah Hussaini, Sait Kursunoglu, Critical review on secondary zinc resources and their recycling technologies, Hydrometallurgy. 2020; 195:105362. https://doi.org/10.1016/j.hydromet.2020.105362

[5] Yevtushevich II, Dzgoev ChT, Epifanov AV, Gudkov SS, Yemelyanov YuE, Belikov SV. Avtoklavno-pirometallurgicheskiy sposob pererabotki zolotosoderzhashchikh i svintsovo-tsinkovykh kontsentratov [Autoclave-pyrometallurgical method of processing gold-containing and lead-zinc concentrates] Journal of Siberian Federal University. Chemistry. 2017; 1. (in Russ). https://cyberleninka.ru/article/n/avtoklavno-pirometallurgicheskiy-sposob-pererabotki-zolotosoderzhaschih-i-svintsovo-tsinkovyh-kontsentratov

[6] Kozlov PA. Extraction of a range of non-ferrous and rare metals from industrial waste: Physico-chemical basis and technical solutions. Tsvetnye Metally. 2020; 5:28-36. https://doi.org/10.17580/tsm.2020.05.05

[7] Kolesnikov A, Fediuk R, Kolesnikova O, Akhmetova E, Shal A. Processing of Waste from Enrichment with the Production of Cement Clinker and the Extraction of Zinc. Materials. 2022; 15(1):324. https://doi.org/10.3390/ma15010324

[8] Abdel-Aal EA. Kinetics of sulfuric acid leaching of low-grade zinc silicate ore, Hydrometallurgy. 2000; 55(3):247-254. ISSN 0304-386X. https://doi.org/10.1016/S0304-386X(00)00059-1

[9] Ruşen A, Sunkar AS, Topkaya YA. Zinc and lead extraction from Çinkur leach residues by using hydrometallurgical method, Hydrometallurgy. 2008; 93(1–2):45-50. https://doi.org/10.1016/j.hydromet.2008.02.018

[10] Kenzhaliyev B, Surkova T, Yessimova D, Baltabekova Z, Abikak Y, Abdikerim B, Dosymbayeva Z. Extraction of noble metals from pyrite cinders. ChemEngineering. 2023; 7(1):14. https://doi.org/10.3390/chemengineering7010014

[11] Kenzhaliyev B, Surkova T, Yessimova D, Abikak Y, Mukhanova A, Fischer D. On the question of the complex processing of pyrite cinders. Inorganics. 2023; 11(4):171. https://doi.org/10.3390/inorganics11040171

[12] Abdulvaliev RA, Surkova TYu, Baltabekova ZhA, Yessimova DM, Stachowicz M, Smailov KM, Dossymbayeva ZD, Berkinbayeva AN. Effect of amino acids on the extraction of copper from sub-conditional raw materials. Kompleksnoe Ispolzovanie Mineralnogo Syra = Complex Use of Mineral Resources. 2025; 335(4):50-58. https://doi.org/10.31643/2025/6445.39

[13] Kiorescu AV. Biovyshchelachivaniye nikelya, medi i kobal'ta iz predvaritel'no obrabotannoy svch-izlucheniyem rudy [Bioleaching of Nickel, Copper and Cobalt from Microwave Pre-Treated Ore] Successes of modern Natural Science. 2019; 12(1):51-56. (in Russ). https://doi.org/10.17513/use.37268

[14] Fuzailov OU, Sayfullaev FI, and Mezhidova I, Zhabborova SG. Issledovaniye sposobov intensifikatsii protsessa obzhiga sul'fidnykh zolotosoderzhashchikh kontsentratov s primeneniyem mikrovolnovogo izlucheniya [Study of methods for intensifying the roasting process of sulphide gold-bearing concentrates using microwave radiation]. Journal of achievements in the field of engineering technologies. 2022; 2(6). (in Russ). https://doi.org/10.24412/2181-1431-2022-2-43-46

[15] Ma A, Li J, Chang J, Zheng X. Mechanism Analysis and Experimental Research on Leaching Zn from Zinc Oxide Dust with an Ultrasound-Enhanced NH3-NH4Cl-H2O System. Sustainability. 2024; 16(7): 2901. https://doi.org/10.3390/su16072901

[16] Li S, Wang H, Wang S, et al. Study on the kinetics and mechanism of ultrasonic-microwave synergistic enhancement for leaching indium from zinc oxide dust. Chem. Pap. 2024; 78: 3667-3685. https://doi.org/10.1007/s11696-024-03338-0

[17] Wankun Wang, Fuchun Wang. Enhancing the extraction of germanium from zinc oxide dust through microwave roasting and the underlying mechanism, Chemical Engineering and Processing - Process Intensification. 2024; 206: 110050. https://doi.org/10.1016/j.cep.2024.110050

[18] Molodtsova MA, Sevastyanova YuV. Vozmozhnosti i perspektivy ispol'zovaniya mikrovolnovogo izlucheniya v promyshlennosti (obzor) [Possibilities and Prospects of Using Microwave Radiation in Industry (Review)]. Lesn. zhurn. 2017; 2:173-187. (Higher Ed. studies. establishments). (in Russ). https://doi.org/10.17238/issn0536-1036.2017.2.173

[19] Ryazanov AG, Kazbekova KK, Baryshev IS, Senin AV, Mikhailov GG. Issledovaniye protsessa vozdeystviya elektromagnitnogo polya svch na nagrev tsinksoderzhashchikh produktov [Study of the process of influence of microwave electromagnetic field on heating of zinc-containing products] Bulletin of SUSU. The Metallurgy series. 2021; 21(2):5-17. (in Russ). https://cyberleninka.ru/article/n/issledovanie-protsessa-vozdeystviya-elektromagnitnogo-polya-svch-na-nagrev-tsinksoderzhaschih-produktov

[20] Kenzhaliyev B, Surkova T, Berkinbayeva A, Baltabekova Zh, Smailov K. Harnessing Microwave Technology for Enhanced Recovery of Zinc from Industrial Clinker. MDPI, Q-2. Metals. 2024; 14:699. https://doi.org/10.3390/met14060699

Crossref

DOI: 10.31643/2026/6445.36
Metallurgy

Physicochemical parameters of lithium sorption from hydromineral raw materials using synthesized inorganic sorbents

[1]Kenzhaliyev B.K., [1]Karshyga Z.B., [1*]Yersaiynova A.A., [2]Muhammad N.A.A., [1]Yessengaziyev A.M.

[1] Institute of Metallurgy and Ore Beneficiation JSC, Satbayev University, Almaty, Kazakhstan
[2] Universiti Pendidikan Sultan Idris, Tanjung Malim, Perak, Malaysia

** Corresponding author email: a.yersaiynova@satbayev.university*

Received: *March 26, 2025*
Peer-reviewed: *April 12, 2025*
Accepted: *May 27, 2025*

ABSTRACT

This paper presents the results of a study on the physicochemical parameters of the lithium sorption process from hydromineral raw materials using synthesized sorbents. The physicochemical parameters of lithium sorption from brine, including the enthalpy change (ΔH, kJ/mol), entropy change (ΔS, kJ/mol·K), and Gibbs free energy (ΔG, kJ/mol), were investigated. The enthalpy value ΔH = -0.698 kJ/mol indicates that the process is exothermic, as it is accompanied by heat release. The positive value of entropy ΔS = 0.0122 kJ/(mol·K) indicates a low degree of order and increased randomness at the interface between the manganese dioxide-based sorbent and the brine during lithium absorption. The negative Gibbs free energy (ΔG) values, ranging from -4.401 to -4.769 kJ/mol at temperatures of 303–333 K, confirm that the lithium sorption process on the manganese oxide sorbent is spontaneous and can proceed without external influence. Additionally, the activation energy value Ea = -0.592 kJ/mol suggests a decrease in the sorption rate as the temperature increases. Using a modified Arrhenius-type equation, the adhesion probability S* was determined to be 0.188. This value indicates the predominance of the chemisorption mechanism in the lithium sorption process.

Keywords: lithium, physicochemical parameters, chemisorption, lithium-ion sieves, hydromineral raw material.

Information about authors:

Kenzhaliyev Bagdaulet Kenzhaliyevich — *Doctor of Technical Sciences, Professor, General Director-Chairman of the Management Board of the Institute of Metallurgy and Ore Beneficiation JSC, Satbayev University, Shevchenko str., 29/133, 050010, Almaty, Kazakhstan. Email: bagdaulet_k@satbayev.university; ORCID ID: https://orcid.org/0000-0003-1474-8354*

Karshyga Zaure Baitaskyzy — *PhD, Associate Professor, Leading Researcher, laboratory of titanium and rare refractory metals, Institute of Metallurgy and Ore Beneficiation JSC, Satbayev University, Shevchenko str., 29/133, 050010, Almaty, Kazakhstan. Email: z.karshyga@satbayev.university; ORCID ID: https://orcid.org/0000-0002-3025-7363*

Yersaiynova Albina Abatkyzy — *Doctoral student, laboratory of titanium and rare refractory metals, Institute of Metallurgy and Ore Beneficiation JSC, Satbayev University, Shevchenko str., 29/133, 050010, Almaty, Kazakhstan. Email: a.yersaiynova@satbayev.university; ORCID ID: https://orcid.org/0000-0003-0638-380X*

Muhammad Noorazlan Abd Azis — *PhD, Faculty of Science and Mathematics, Universiti Pendidikan Sultan Idris, Tanjung Malim, Perak, 35900, Malaysia. Email: azlanmn@fsmt.upsi.edu.my; ORCID ID: https://orcid.org/0000-0002-2792-4145*

Yessengaziyev Azamat Muratovich — *PhD, Head of the titanium and rare refractory metals, Institute of Metallurgy and Ore Beneficiation JSC, Satbayev University, Shevchenko str., 29/133, 050010, Almaty, Kazakhstan. Email: a.yessengaziyev@satbayev.university; ORCID ID: https://orcid.org/0000-0002-4989-4119*

Introduction

Lithium is one of the key elements of modern energy, widely used in the manufacture of batteries, glass, ceramics, and pharmaceutical products [[1], [2], [3], [4], [5]]. However, the extraction of lithium from natural sources such as salt lakes, oil brines, and seawater presents significant technological challenges [6]. In recent years, lithium-ion sieves (LIS) have emerged as an innovative solution for the efficient extraction of lithium from liquid media [[7], [8]]. Li-ion sieves are characterized by high selectivity toward lithium ions as well as environmental safety, making them a promising tool for the sustainable development of the lithium industry [[9], [10]].

Lithium-ion sieves (LIS) are specialized adsorbents capable of selectively capturing lithium ions (Li^+) from aqueous solutions [[11], [12]]. Their structure is based on porous materials containing lithium, which is replaced by hydrogen ions (H^+) when interacting with the solution. The principle of

operation of LIS is illustrated in Figure 1. The synthesis of LIS involves several steps: preparation of the precursor, its calcination, and acid treatment of the precursor to obtain the sorbent. The vacant sites in the crystal lattice formed during this process are able to retain ions whose radius does not exceed that of the target lithium ions.

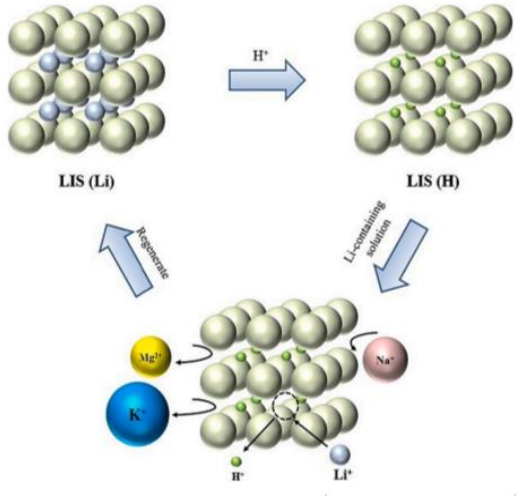

Figure 1 - Schematic representation of LISs process [13]

Among the many materials used in LIS, manganese-based oxides are the most widespread. From the precursors $LiMn_2O_4$, $Li_{1.33}Mn_{1.67}O_4$, and $Li_{1.6}Mn_{1.6}O_4$, scientists have developed manganese oxide-based sorbents such as λ-MnO_2, $MnO_2 \cdot 0.3H_2O$, and $MnO_2 \cdot 0.5H_2O$ [[14], [15]]. These sorbents exhibit excellent adsorption capacity. For example, precursor sorbents have sorption capacities of 39.9 mg/g for $LiMn_2O_4$, 59 mg/g for $Li_4Mn_5O_{12}$, and a high capacity of 72.3 mg/g for the $Li_{1.6}Mn_{1.6}O_4$ precursor sorbent [[16], [17]].

In previous papers, the results of studies on the synthesis of inorganic sorbents based on manganese oxide compounds were presented, along with the results of lithium sorption from formation brines of oil fields. Additionally, the kinetic model of lithium sorption from hydro-mineral raw materials on the synthesized sorbent was determined, and the synthesized manganese dioxide sorbent was studied after its saturation with lithium from brine [[18], [19]].

To gain a more detailed understanding of lithium sorption from brine and to increase the completeness of sorption extraction, it is particularly important to study the physicochemical parameters characterizing the process.

Research methods

Experimental methodology. Experiments on lithium sorption from brines were conducted in a thermostated reactor with a capacity of 0.5 dm^3, equipped with a mechanical stirrer (VELP Scientifica LS F201A0151, Italy) operating at a fixed number of revolutions. The temperature was maintained constant using a LOIP LT-100 circulation thermostat. A specific amount of brine was poured into the reactor and heated to the desired temperature. Once the target temperature was reached, the required amount of sorbent was added to the brine in the reactor, and stirring was initiated. The start of the process was then recorded. At the end of the experiment, the brine was separated from the sorbent, and the lithium content in the brine was analyzed.

Analysis methods. The quantitative content of lithium in the initial brine and filtrates after sorption was determined on an Optima 8300DV inductively coupled plasma atomic emission spectrometer and on a SHIMADZU AA-7000 atomic absorption spectrophotometer (Japan).

Results and Discussion

The study of the physicochemical characteristics of the sorption process provides important information regarding the Gibbs free energy of the system and other thermodynamic parameters during the sorption of lithium from brine. This information can be used to determine the type and mechanism of the process.

The physicochemical parameters of lithium sorption from brine such as enthalpy change (ΔH, kJ/mol), entropy change (ΔS, kJ/mol·K) and Gibbs free energy (ΔG, kJ/mol) are calculated using the following equations:

$$\Delta G = -2{,}303\ RT \log K_d \quad (1)$$

$$\log K_d = \frac{\Delta S}{2{,}303R} - \frac{\Delta H}{2{,}303RT} \quad (2)$$

$$\Delta G = \Delta H - T\Delta S \quad (3)$$

where, K_d is the sorption equilibrium constant, dm^3/g; R is the universal gas constant, 8.314 J/(mol·K); T is the absolute temperature, K.

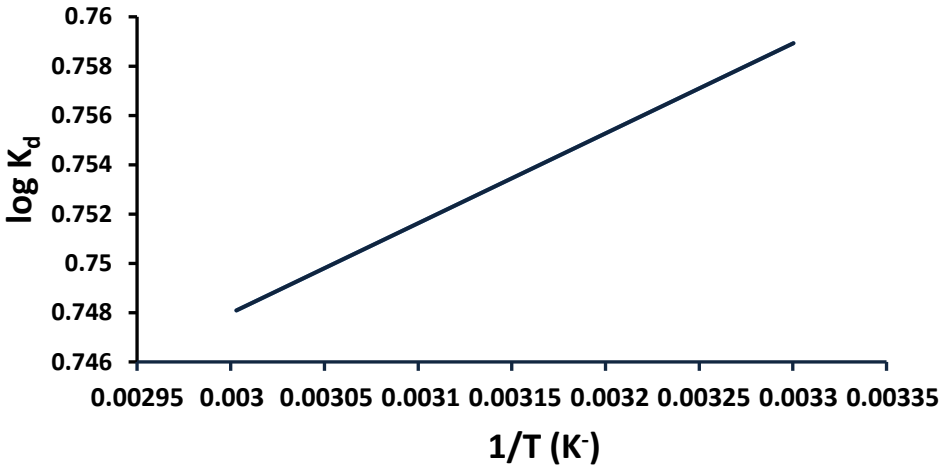

Figure 2 - Graph of dependence of the logarithm of the equilibrium constant of lithium sorption on manganese-oxide sorbent log K_d on the inverse temperature 1/T

By constructing a line graph in the coordinates log K_d versus 1/T, in accordance with equation (2), we can determine the values of the enthalpy change (ΔH) and the entropy change (ΔS) from the slope of the line and its intersection with the ordinate axis, respectively.

The process of lithium sorption from brines with initial lithium concentration of 5.477 mg/dm^3 under the following conditions was studied: temperature from 30 to 60 °C (step 10 °C); duration 24 h; ratio of sorbent mass to brine volume = 1: 1000. According to the obtained results, K_d values were calculated and a graph in log K_d - 1/T coordinates was plotted (Figure 2). The parameters calculated from the graph of Figure 2 are shown in Table 1. The negative value of Gibbs energy (ΔG) indicates that lithium sorption on manganese oxide sorbent under these conditions can proceed spontaneously, i.e. spontaneously. The negative value of the enthalpy change (ΔH) indicates that the sorption process proceeds with heat release. The positive value of entropy change (ΔS) indicates a low degree of order and indicates that randomness increases at the manganese dioxide sorbent/salt interface during lithium adsorption.

Table 1 - Physicochemical parameters for lithium sorption process on manganese oxide sorbent

Parameters	Temperature, K	Value
ΔG, kJ/mol	303	–4.401
	313	–4.528
	323	–4.645
	333	–4.769
ΔH, kJ/mol		–0.698
ΔS, kJ /(mol·K)		0.0122
E_a, kJ/mol		–0.592
S^*		0.188

The modified Arrhenius-type equation related to surface coverage (θ) is the sticking probability (S*), which is a function of the adsorbate/adsorbent system under consideration and depends on the temperature of the system. The value of S* is a measure of the ability of the adsorbate to remain on the adsorbent indefinitely [20]. The effect of temperature on the sticking probability is estimated by calculating the surface coverage at different temperatures and can be expressed as [21]:

$$S^* = (1-\theta)\exp-\left(\frac{E_a}{RT}\right) \quad (4)$$

$$\ln(1-\theta) = \ln S^* + \frac{E_a}{RT} \quad (5)$$

$$\theta = 1 - \frac{C_e}{C_0} \quad (6)$$

where, θ is the fraction of the sorbent surface occupied by adsorbed lithium; E_a is the apparent activation energy, kJ/mol; C_0 and C_e are initial and equilibrium concentrations of lithium in brine, respectively, mg/dm^3.

The probability of adhesion under optimal conditions of the sorption process was evaluated as a function of the degree of coverage of the sorbent surface and temperature in the range of 303–333 K. Based on the linear dependence plotted in the coordinates of ln(1-θ) versus 1/T, it is possible to determine ln S* and E_a/R (Figure 3).

The calculated values of apparent activation energy (E_a) and sticking probability (S*) are presented in Table 1. The sorption process in the studied temperature range of 303-333K is exothermic and proceeds with heat release. The

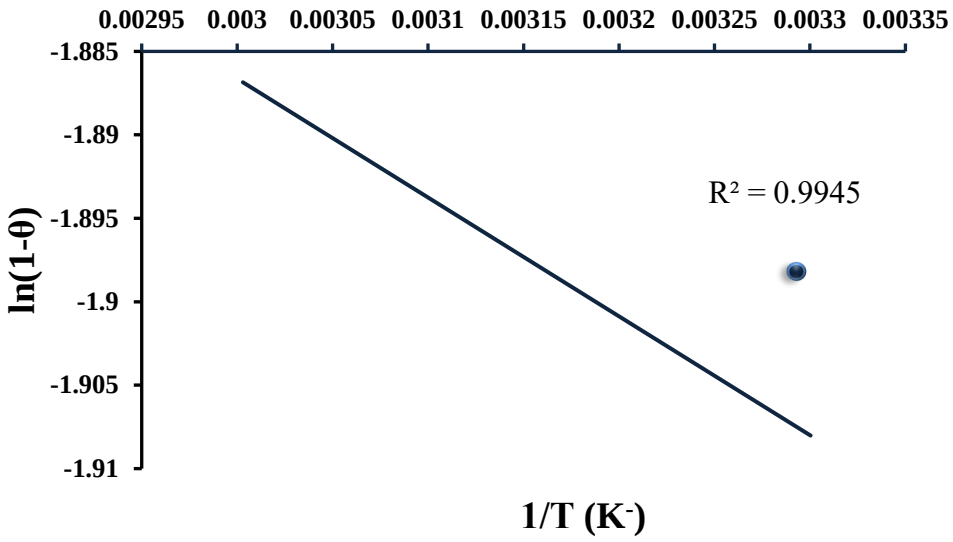

Figure 3 - Graph of ln(1-θ) versus 1/T for lithium sorption on manganese oxide sorbent

negative value of activation energy shows that sorption slows down with increasing temperature. The sticking probability should lie in the range $0 < S^{*}<1$ [21].

The sticking probability $S^{*} > 1$ indicates the adhesion of adsorbate from adsorbent (no sorption), $S^{*} = 1$ implies a linear dependence of adhesion between adsorbate and adsorbent and a mixture of physical and chemisorption mechanisms is possible, S* = 0 means unlimited adhesion of adsorbate to adsorbent in which the chemisorption mechanism prevails.

Finally, in the region of values $0 < S^{*}< 1$ means favourable adhesion of adsorbate to adsorbent with predominance of physical sorption mechanism. The calculated value of S*, which is 0.188, is closer to 0 in the range of 0 to 1, indicating the predominance of the chemisorption mechanism [22].

Therefore, the physicochemical parameters derived from both calculations and experiments can be utilized for scientific research.

Conclusions

The study of the physicochemical parameters of the lithium sorption process from hydromineral raw materials was conducted. The physicochemical parameters of lithium sorption from brine, such as enthalpy change (ΔH, kJ/mol), entropy change (ΔS, kJ/mol·K), and Gibbs free energy (ΔG, kJ/mol), were calculated. The enthalpy change ΔH = -0.698 kJ/mol indicates that the lithium sorption process is exothermic, accompanied by heat release. The entropy changes ΔS = 0.0122 kJ/(mol·K) suggest a low degree of ordering and an increase in chaos at the manganese dioxide sorbent/salt interface during lithium adsorption. The negative values of Gibbs free energy (ΔG), ranging from -4.401 to -4.769 kJ/mol within the temperature range of 303–333 K, demonstrate that the sorption of lithium on the manganese oxide sorbent can proceed spontaneously. A negative activation energy E_a = -0.592 kJ/mol, was obtained, indicating that the sorption process slows down as the temperature increases. The sticking probability S* = 0.188 was calculated, which suggests the predominance of a chemisorption mechanism.

Conflicts of interest. On behalf of all authors, the corresponding author states that there is no conflict of interest.

CRediT author statement: **B. Kenzhaliyev**: Conceptualization, Validation, Visualization; **Z. Karshyga**: Supervision, Validation, Original draft preparation, Reviewing and Editing; **A. Yersaiynova**: Investigation, Methodology, Data curation, Writing draft preparation; **N. Muhammed**: Validation; **A. Yessengaziyev**: Investigation, Software.

Acknowledgements. This research is funded by the Science Committee of the Ministry of Science and Higher Education of the Republic of Kazakhstan (Grant No. AP23488932).

Cite this article as: Kenzhaliyev BK, Karshyga ZB, Yersaiynova AA, Muhammad NAA, Yessengaziyev AM. Physicochemical parameters of lithium sorption from hydromineral raw materials using synthesized inorganic sorbents. Kompleksnoe Ispolzovanie Mineralnogo Syra = Complex Use of Mineral Resources. 2026; 339(4):14-20. https://doi.org/10.31643/2026/6445.36

Синтезделген сорбенттер көмегімен гидроминералды шикізаттан литийді сорбциялау процесінің физика-химиялық көрсеткіштерін зерттеу

[1]Кенжалиев Б.К., [1]Қаршыға З.Б., [1]Ерсайынова А.А., [2]Muhammad N.A.A., [1]Есенгазиев А.М.

[1] Металлургия және кен байыту институты АҚ, Сәтбаев университеті, Алматы, Қазақстан
[2] Пендидикан Сұлтан Идрис университеті, Танжунг Малим, Перак, Малайзия

Мақала келді: *26 наурыз 2025*
Сараптамадан өтті: *12 сәуір 2025*
Қабылданды: *27 мамыр 2025*

ТҮЙІНДЕМЕ

Бұл жұмыста синтезделген сорбенттерді қолдана отырып, гидроминералды шикізаттан литийді сорбциялау процесінің физика-химиялық параметрлерін зерттеу нәтижелері келтірілген. Тұзды ерітіндіден литийді сорбциялаудың физика-химиялық параметрлері, мысалы, энтальпияның өзгеруі (ΔH кДж/моль), энтропияның өзгеруі (ΔS, кДж/моль) және Гиббстің бос энергиясы (ΔG, кДж/моль) есептелді. Энтальпия мәні ΔH = -0,698 кДж / моль процестің жылу шығарумен бірге жүретінін растайды, бұл оның экзотермиялық сипатын көрсетеді. Энтропияның оң мәні ΔS = 0,0122 кДж / (моль·К) марганец диоксиді негізіндегі сорбент пен литийді сіңіру кезінде тұзды ерітінді арасындағы фазалық интерфейсте реттіліктің төмен дәрежесін және ретсіздіктің жоғарылауын көрсетеді. 303-333 К температурада -4,401-ден -4,769 кДж/моль диапазонында алынған Гиббс бос энергиясының теріс мәндері (ΔG) марганец-оксид сорбентіндегі литий сорбциясы процесі өздігінен жүретінін және сыртқы әсерсіз жүруі мүмкін екенін растайды. E_a = -0,592 кДж/моль активтендіру энергиясының мәні температура жоғарылағанда сорбция жылдамдығының төмендейтінін көрсетеді. Модификацияланған Аррениус типті теңдеуді қолдана отырып, 0,188-ге тең S* жабысу ықтималдығы анықталды, бұл литийді сорбциялау процесінде хемосорбциялық механизмінің басым екендігін көрсетеді.

Түйін сөздер: литий, физика-химиялық параметрлер, хемосорбция, литий-ионды елек, гидроминералды шикізат.

Авторлар туралы ақпарат:

Кенжәлиев Бағдәулет Кенжәліұлы — *Техника ғылымдарының докторы, профессор, Металлургия және кен байыту институты АҚ Бас директоры - Басқарма төрағасы, Сәтбаев университеті, Шевченко көш., 29/133, 050010, Алматы, Қазақстан. Email: bagdaulet_k@satbayev.university; ORCID ID: https://orcid.org/0000-0003-1474-8354*

Қаршыға Зәуре Байтасқызы — *PhD, жетекші ғылыми қызметкер, қауымдастырылған профессор, титан және сирек қиын балқитын металдар зертханасы, Металлургия және кен байыту институты АҚ, Сәтбаев университеті, Шевченко көш., 29/133, 050010, Алматы, Қазақстан. Email: z.karshyga@satbayev.university; ORCID ID: https://orcid.org/0000-0002-3025-7363*

Ерсайынова Альбина Абатқызы — *Докторант, титан және сирек қиын балқитын металдар зертханасы, Металлургия және кен байыту институты АҚ, Сәтбаев университеті, Шевченко көш., 29/133, 050010, Алматы, Қазақстан. Email: a.yersaiynova@satbayev.university; ORCID ID: https://orcid.org/0000-0003-0638-380X*

Muhammad Noorazlan Abd Azis — *PhD, ғылым және математика факультеті, Пендикан Сұлтан Идрис университеті, 35900 Танджонг Малим, Перак, Малайзия. Email: azlanmn@fsmt.upsi.edu.my; ORCID ID: https://orcid.org/0000-0002-2792-4145*

Есенгазиев Азамат Муратович — *PhD, титан және сирек қиын балқитын металдар зертханасының меңгерушісі, Металлургия және кен байыту институты АҚ, Сәтбаев университеті, Шевченко көш., 29/133, 050010, Алматы, Қазақстан. Email: a.yessengaziyev@satbayev.university; ORCiD ID: https://orcid.org/0000-0002-4989-4119*

Физико-химические параметры процесса сорбции лития из гидроминерального сырья с использованием синтезированных сорбентов

[1] Кенжалиев Б.К., [1]Қаршыға З.Б., [1]Ерсайынова А.А., [2]Muhammad N.A.A., [1]Есенгазиев А.М.

[1] АО Институт металлургии и обогащения, Satbayev University, Алматы, Казахстан
[2] Университет Пендидикан Султан Идрис, Танджунг Малим, Перак, Малайзия

Поступила: *26 марта 2025*
Рецензирование: *12 апреля 2025*
Принята в печать: *27 мая 2025*

АННОТАЦИЯ

В данной работе представлена результаты изучения физико-химических параметров процесса сорбции лития из гидроминерального сырья с использованием синтезированных сорбентов. Рассчитаны термодинамические параметры сорбции лития из рассола, такие как изменение энтальпии (ΔH кДж/моль), изменение энтропии (ΔS, кДж/моль·К) и свободная энергия Гиббса (ΔG, кДж/моль). Значение энтальпии ΔH = –0,698 кДж/моль подтверждает, что процесс сопровождается выделением тепла, что указывает на его экзотермический характер. Положительное значение энтропии ΔS = 0,0122 кДж/(моль·К) свидетельствует о низкой степени упорядоченности и увеличении хаотичности на границе раздела фаз между сорбентом на основе диоксида марганца и рассолом при поглощении лития. Полученные отрицательные значения свободной энергии Гиббса (ΔG) в диапазоне от –4,401 до –4,769 кДж/моль при температурах 303–333 К подтверждают, что процесс сорбции лития на марганцево-оксидном сорбенте является спонтанным и может протекать без внешнего воздействия. Значение энергии активации E_a = –0,592 кДж/моль свидетельствует о снижении скорости сорбции с ростом температуры. С использованием модифицированного уравнения типа Аррениуса определена величина вероятности прилипания S^*, равная 0,188, которая указывает на преобладание хемосорбционного механизма процесса сорбции лития.

Ключевые слова: литий, физико-химические параметры, хемосорбция, литий-ионное сито, гидроминеральное сырье.

Информация об авторах:

Кенжәлиев Багдаулет Кенжалиевич *Доктор технических наук, профессор, Генеральный директор - Председатель правления АО Институт металлургии и обогащения, Satbayev University, ул.Шевченко 29/133, 050010, Алматы, Казахстан. Email: bagdaulet_k@satbayev.university; ORCID ID: https://orcid.org/0000-0003-1474-8354*

Қаршыға Зәуре Байтасқызы *PhD, ведущий научный сотрудник, ассоциированный профессор, лаборатория титана и редких тугоплавких металлов, АО Институт металлургии и обогащения, Satbayev University, ул.Шевченко 29/133, 050010, Алматы, Казахстан. Email: z.karshyga@satbayev.university; ORCID ID: https://orcid.org/0000-0002-3025-7363*

Ерсайынова Альбина Абатқызы *Докторант, лаборатория титана и редких тугоплавких металлов, АО Институт металлургии и обогащения, Satbayev University, ул. Шевченко 29/133, 050010, Алматы, Казахстан. Email: a.yersaiynova@satbayev.university; ORCID ID: https://orcid.org/0000-0003-0638-380X*

Muhammad Noorazlan Abd Azis *PhD, факультет естественных наук и математики, Университет Пендидикан Султан Идрис, 35900 Танджонг Малим, Перак, Малайзия. Email: azlanmn@fsmt.upsi.edu.my; ORCID ID: https://orcid.org/0000-0002-2792-4145*

Есенгазиев Азамат Муратович *PhD, заведующий лабораторией титана и редких тугоплавких металлов, АО Институт металлургии и обогащения, Satbayev University, ул.Шевченко, 29/133, 050010, Алматы, Казахстан. Email: a.yessengaziyev@satbayev.university; ORCiD ID: https://orcid.org/0000-0002-4989-4119*

References

[1] Garret ED: Handbook of Lithium and Natural Calcium Chloride. Elsevier. 2004.

[2] Gunther M, Lars R, Michael H, Martin B. Lithium market research – global supply, future demand and price development. Energy Storage Materials. 2017; 6:171-179. https://doi.org/10.1016/j.ensm.2016.11.004

[3] Jamie S, Marcello C, Yassine H, Robert G. The future of lithium availability for electric vehicle batteries. Renewable and Sustainable Energy Reviews. 2014; 35:83-193. https://doi.org/10.1016/j.rser.2014.04.018

[4] Azlina Y, Azlan MN, Hajer SS, Halimah MK, Suriani AB, Umar SA, Hisam R, Zaid MHM., Iskandar SM, Kenzhaliyev BK, Nitsenko AV, Yusof NN., Boukhris I. Graphene oxide deposition on neodymium doped zinc borotellurite glass surface: Optical and polarizability study for future fiber optics. Optical Materials. 2021; 117. https://doi.org/10.1016/j.optmat.2021.111138

[5] Kenzhaliyev B, Yesimova DM, Surkova TY, Soemowidagdo A, Amanzholova LU, Egorov NB. Transformation of the rare earth elements and impurity elements combinations in the course of pH pregnant solution modification. News of the National Academy of Sciences of the Republic of Kazakhstan, Series of Geology and Technical Sciences. 2020; 2(440):87-95, https://doi.org/10.32014/2020.2518-170X.35

[6] Zi HF, John HL. Emerging membrane technologies for sustainable lithium extraction from brines and leachates: Innovations, challenges, and industrial scalability. Desalination. 2025; 598:118411. https://doi.org/10.1016/j.desal.2024.118411

[7] Chitrakar R, Kanoh H, Miyai Y, Ooi K. A New Type of Manganese Oxide ($MnO_2 \cdot 0.5H_2O$) Derived from $Li_{1.6}Mn_{1.6}O_4$ and Its Lithium Ion-Sieve Properties. Chem. Mater. 2000; 12:3151-3157.

[8] Sun Y, Wang Q, Wang Y, Yun R, Xiang X. Recent Advances in Magnesium. Lithium Separation and Lithium Extraction Technologies from Salt Lake Brine. Separation and Purification Technology. 2020. https://doi.org/10.1016/j.seppur.2020.117807

[9] Ding W, Haoyue D, Yacong H, Jing H, Lei Ch, Fang Zh, Jiadao W. Introduction of manganese based lithium-ion Sieve-A review. Progress in Natural Science: Materials International. 2020; 30(2);139-152. https://doi.org/10.1016/j.pnsc.2020.01.017

[10] Orooji Y, Nezafat Z, Nasrollahzadeh M, Shafiei N, Afsari M, Pakzad Kh, Razmjou A. Recent advances in nanomaterial development for lithium ion-sieving technologies. Desalination. 2022; 529:115624. https://doi.org/10.1016/j.desal.2022.115624

[11] Hanwei Y, Gayathri N, Chunyao Zh, Chen W, Amir R, Dong SH, Tao H, Hokyong Sh. Metal-based adsorbents for lithium recovery from aqueous resources. Desalination. 2022; 539:115951. https://doi.org/10.1016/j.desal.2022.115951

[12] Ooi K, Miyai Y, Katoh S. Recovery of Lithium from Seawater by Manganese Oxide Adsorbent. Separation Science and Technology. 1986; 21(8):755-766. https://doi.org/10.1080/01496398608056148

[13] Xu X, Chen Y, Wan P, Gasem Kh, Wang K, He T, Adidharma H, Fan M. Extraction of lithium with functionalized lithium ion-sieves. Progress in Materials Science. 2016; 84:276-313.

[14] Murodjon S, Yu X, Li M, Duo J, Deng T. Lithium Recovery from Brines Including Seawater, Salt Lake Brine, Underground Water and Geothermal Water. 2020.

[15] Demir MM, Toprak S, Oncel C, Yilmaz S, BABA A, Aksoy KG. Lithium Extraction from Geothermal Brine Using Γ-MnO_2: A Case Study for Tuzla Geothermal Power Plant. http://dx.doi.org/10.2139/ssrn.4239318

[16] Chitrakar R, Sakane K, Umeno A, Kasaishi Sh, Takagi N, Ooi K. Synthesis of orthorhombic $LiMnO_2$ by solid-phase reaction under steam atmosphere and a study of its heat and acid-treated phases. Journal of Solid State Chemistry. 2002; 169:66-74.

[17] Guotai Zh, Jingze Zh, Jinbo Z, Yanxia S, Yue Sh, Xiang Li, Xiufeng R, Chunxi H, Yuan Zh, Weiping T. Improved structural stability and adsorption capacity of adsorbent material $Li_{1.6}Mn_{1.6}O_4$ via facile surface fluorination, Colloids and Surfaces A: Physicochemical and Engineering Aspects. 2020; 629:127465. https://doi.org/10.1016/j.colsurfa.2021.127465

[18] Karshyga Z, Yersaiynova A, Yessengaziyev A, Orynbayev B, Kvyatkovskaya M, Silachyov I. Synthesis of Manganese Oxide Sorbent for the Extraction of Lithium from Hydromineral Raw Materials. Materials. 2023; 16:7548. https://doi.org/10.3390/ma16247548

[19] Abdulvaliyev R, Karshyga Z, Yersaiynova A, Yessengaziyev A, Orynbayev B, Kvyatkovskaya M. Physical and chemical study of manganese dioxide sorbent after sorption of lithium from brines. Kompleksnoe Ispolzovanie Mineralnogo Syra = Complex Use of Mineral Resources. 2024; 334(3):59-69. https://doi.org/10.31643/2025/6445.28

[20] Sundaram CS, Viswanathan N, Meenakshib S. Defluoridation chemistry of synthetic hydroxyapatite at nano scale: Equilibrium and kinetic studies. Journal of Hazardous Materials. 2008; 155:206-215.

[21] Horsfall M Jr, Spiff AI. Effects of temperature on the sorption of Pb^{2+} and Cd^{2+} from aqueous solution by caladium bicolor (Wild Cocoyam) biomass. Electronic Journal of Biotechnology. 2005; 8:162-169.

[22] Kou TY, Wang YZ, Zhang C, Sun JZ, Zhang ZH. Adsorption behavior of methyl orange onto nanoporous core-shell Cu@Cu2O nanocomposite. Chemical Engineering Journal. 2013; 223:76-83.

Crossref
DOI: 10.31643/2026/6445.37
Metallurgy

Study of the kinetics of sorption of praseodymium and neodymium ions using interpolymer systems based on KU-2-8 and AB-17-8 in salt forms

[1]Jumadilov T.K., [1]Kabzhalelov K.R., [1*]Khimersen Kh., [1]Totkhuskyzy B., [2]Mukatayeva Zh.S.

[1]A.B. Bekturov Institute of Chemical Sciences JSC, Almaty, Kazakhstan
[2]Abai Kazakh National Pedagogical University, Almaty, Kazakhstan

** Corresponding author email: khuana88@gmail.com*

Received: *April 10, 2025*
Peer-reviewed: *May 22, 2025*
Accepted: *June 5, 2025*

ABSTRACT
This paper presents a study of the kinetics of neodymium and praseodymium ions sorption using interpolymer systems based on KU-2-8 and AB-17-8 in salt forms. Sorption of target ions was carried out in a dynamic mode (with constant stirring) in interpolymer systems in molar ratios of 4:2 and 3:3 (cation exchanger to anion exchanger). Aliquots were collected during certain time intervals, then widely known kinetic models of sorption were used to construct linear graphs. According to the obtained results, the best model for describing sorption was pseudo-first order (the highest value for the 4:2 system = 0.97885 and 0.98112; for the 3:3 system = 0.9647 and 0.98779). Such results are important for understanding the mechanisms of the sorption process and establishing the limiting factor that can slow down this process. The kinetic model of pseudo-first order may indicate the need to improve the washing out of counterions from the polyelectrolyte matrix for their high ionization and accessibility of functional groups for metal ions. This assumption can be used in the future to optimize industrial schemes of ion-exchange sorption of REE.

Keywords: interpolymer systems, kinetic models, sorption, neodymium and praseodymium ions, cation exchanger KU-2-8, anion exchanger AB-17-8.

Information about authors:

Jumadilov Talkybek Kozhatayevich — *Doctor of Chemical Sciences, Professor, Head of the laboratory Synthesis and physics and chemistry of polymers, A.B. Bekturov Institute of Chemical Sciences JSC, Almaty, Kazakhstan. E-mail: jumadilov@mail.ru; ORCID ID: https://orcid.org/0000-0001-9505-3719*

Kabzhalelov Kamil — *Engineer, A.B. Bekturov Institute of Chemical Sciences JSC, Almaty, Kazakhstan. Email: kamil_kabhzalelov@outlook.com; ORCID ID: https://orcid.org/0009-0008-6030-052X*

Khimersen Khuangul — *PhD, Researcher, A.B. Bekturov Institute of Chemical Sciences JSC, Almaty, Kazakhstan. E-mail: khuana88@gmail.com; ORCID ID: https://orcid.org/0000-0002-5138-5997*

Totkhuskyzy Bakytgul — *PhD, Researcher, A.B. Bekturov Institute of Chemical Sciences JSC, Almaty, Kazakhstan. E-mail: bakytgul.sakenova@mail.ru; ORCID ID: https://orcid.org/0000-0001-8119-668X*

Mukatayeva Zhazira Sagatbekovna — *Candidate of Chemical Sciences, Associate Professor, Abai Kazakh National Pedagogical University, Almaty, Kazakhstan. E-mail: jazira-1974@mail.ru; ORCID ID: https://orcid.org/0000-0002-1584-5810*

Introduction

Rare earth metals are a strategic resource and are increasingly used in various fields. Rare earth elements are a group of 17 metallic elements that share similar chemical properties [1]. REEs consist of the 15 lanthanides, as well as scandium and yttrium lanthanides [[2], [3]]. REEs are typically categorized into light rare earth elements and heavy rare earth elements. The latter have grown crucial for numerous emerging technologies, especially in the green energy sector, including wind turbines, large-scale energy storage systems, and new energy vehicles [4]. They also provide a bridge from fossil fuels to low-carbon energy [5]. As for the metals themselves, which are studied in this article, they also have a huge variety of applications, and therefore, the demand for them will only grow in the future. For example, Nd is applied in supermagnets for disk drives [6], Nd-Fe-B magnets [7], in AL-Mgalloys, and steel, also for magnetic resonance imaging (MRI) contrasting agents [8]. Praseodymium is widely used in magnets [9], optical Fibres, carbon-arc lamps [7], in alloys for aircraft engines, capacitors, sensors, and semiconductors, in flat display electronics [8]. Therefore, considering the great need for these rare earth metals, this study aims to study the sorption kinetics to better understand the absorption mechanism, which will improve the technologies of concentration and extraction of target ions. This goal was achieved through several steps: 1) selection of interpolymer

systems for sorption from a model solution; 2) sampling aliquots at certain time intervals; 3) selection of the most suitable kinetic model among the most common in the literature; 4) based on the selection of the most suitable kinetic model, suggest a possible sorption mechanism, a limiting factor, and how this factor can be compensated. The selection of sorption and the composition of interpolymer systems are also supported by the fact that "adsorption provides advantages such as simplicity, low capital investment, low energy usage, and good environmental sustainability, making it the ideal choice for separating and removing rare earth elements"[10]. The development of simple but effective sorbents that can be used repeatedly is an urgent need in modern realities [11].

By now, a huge number of works have accumulated on various methods of extracting REE from primary and secondary sources. Some of them also pay attention to kinetic factors, especially in articles where sorption is the main process. The authors [12] introduced a technique for extracting neodymium from permanent magnet waste (WPM) through a hydrometallurgical process that includes separation using a hollow fiber liquid membrane (HFSLM). Neodymium in WPM was recovered via solvent extraction with D2EHPA. The separation of Nd from Fe was achieved successfully using 0.6 M D2EHPA at an O/A phase ratio of 3, with a pH range of 1.26–2.0, resulting in a neodymium recovery rate of 97.48%.

The extraction of neodymium and other REE from recycled magnets was also studied in the work [13]. They were extracted as oxalates using various amounts of oxalic acid relative to its stoichiometric quantity. When oxalic acid was used in stoichiometric amounts, about 93% of the rare earth elements present in the solution precipitated [13].

Miguel Nogueira et al. [14] used activated carbon obtained from tire rubber after CO_2 activation for sorption, and the most effective adsorbent achieved a maximum absorption capacity of 24.7 mg g^{-1} for Nd^{3+} and 34.4 mg g^{-1} for Dy^{3+}. The authors also noted that the synthesized adsorbents made from waste materials demonstrated better performance than commercially available activated carbon. This study also has environmental implications, as it demonstrated the potential use of waste to create effective adsorbents.

Organic acids, such as acetic and oxalic acids, have been used for Nd leaching, showing promising efficiencies. Under standard conditions (27°C, 3 M acid concentration, 20 g/L pulp density, 200 rpm stirring, 500 µm particle size, 300 min leaching), Nd extraction reached 50% with acetic acid and 44% with oxalic acid [15]. However, optimized parameters (80°C, 0.4 M acetic acid, 10 g/L pulp density, 106–150 µm particle size) significantly increased Nd extraction to 99.99% [16].

Recent research introduces electrokinetic mining (EKM) as an innovative technique for extracting REEs from ion-adsorption deposits (IADs) while addressing environmental concerns associated with conventional ammonium-salt-based leaching methods. Traditional methods exhibit low recovery efficiencies (40–60%) and contribute to significant water contamination and soil degradation. EKM applies an electric field to facilitate the selective migration of ions, significantly reducing the need for chemical leaching agents (by up to 80%). Experimental results demonstrate that EKM achieves 90–96% recovery efficiency, outperforming conventional techniques. Furthermore, the method results in higher purity REEs, with up to 70% fewer metallic impurities [4].

Deep eutectic solvents (DESs) have gained attention as a viable substitute for aqueous solutions in the recovery of valuable metals from NdFeB magnets. A study [17] investigated a DES composed of choline chloride and lactic acid in a 1:2 molar ratio for the leaching of REEs and other metals. A separation process was devised using Aliquat 336 SCN diluted in toluene to effectively extract Fe, B, and Co from Nd and Dy. Purified Dy was recovered by water stripping, while Nd was precipitated using oxalic acid, yielding Nd_2O_3 (99.87% purity) and Dy_2O_3 (99.94% purity).

The use of chelate sorbents has also become a popular direction for research and development for the selective extraction of REE ions. For example, ion-exchange resins IRC-747 and TP-260 have shown high affinity for REEs from highly concentrated 4 M H_3PO_4 produced by OCP. These resins achieve REE extraction yields ranging from 20% to 60% [18].

The ion exchange process is highly selective and environmentally friendly, making it effective for treating low metal concentrations. However, at the same time, there are also some difficulties: high cost of selective chelating separation materials and limited capacity, slow desorption kinetics and the need for selection of desorbing reagents [[19], [20], [21]].

It is worth noting that many works have been devoted to the problem of extracting REE from model solutions, as well as from primary and secondary sources using various cross-linked polyelectrolytes. The general direction of all these works is the search for high extraction efficiency,

selectivity, and optimal conditions. For example, industrial sorbents Purolite S940 and Lewatit TP 260 were used in the work [[22], [23]] to extract neodymium and scandium from sulfate solutions. According to the results, neodymium strongly bound with functional groups to form coordination bonds, and scandium sorption was strongly dependent on the sulfate concentration. In two other experiments 22] were used cation exchangers with the same functional group as in our work (sulfo group) to extract neodymium and separate it from calcium, iron and strontium. An important discovery was that calcium and neodymium ions compete with each other during sorption on the polymer matrix.

Our research is aimed at using interpolymer systems, which are composed of cationite and anionite. When in one solution, they mutually activate each other, changing the most important characteristics (pH, electrical conductivity, and swelling degree increase) [[24], [25], [26]]. In our previous studies, we considered interpolymer systems based on various industrial sorbents for the extraction of REE from solutions [[27], [28]]. In these works, the sorption characteristics of a mixture of praseodymium and neodymium, as well as lute-tium individually, were demonstrated using mutually activated cross-linked polyelectrolytes. It was possible to find that the interpolymer system has increased sorption characteristics compared to its application. It was also possible to find that in the static mode, greater selectivity to one of the REEs is possible. However, at the moment, no experiments have been conducted to study the kinetics of sorption in such systems, so this work will pay more attention to this aspect.

Experimental part

Equipment. The required mass of the ion exchanger was measured using a Shimadzu TX-423 electronic analytical balance. The residual concentration was determined using an atomic emission analysis (Thermo Scientific™ iCAP™ PRO XP ICP-OES, USA).

Materials. In the experiment, aqueous solutions of neodymium and praseodymium hexahydrate nitrate with a concentration of 30 mg/l were used (Sigma-Aldrich, Darmstadt, Germany). Ion-exchange resins in salt forms: KU-2-8 (Na^+) strongly acidic (Azot, Cherkassy, Ukraine) cation exchanger and strongly basic AB-17-8 (Cl^-) (Azot, Cherkassy, Ukraine) gel-type anion, were used.

Experiment. An interpolymer system was created using KU-2-8 and AB-17-8 in a molar ratio of 4:2 and 3:3. These ratios were chosen for study based on previous work. In it, these interpolymer systems showed satisfactory sorption indices (extraction degree and sorption capacity). The masses of ionites in these systems were: 4:2 (0.079 g.: 0.041g.); 3:3 (0.059 g.: 0.062g.). Then, sorption was carried out in solutions containing neodymium and praseodymium nitrates. Aliquots were collected during the following time intervals: 5 min, 10 min, 15 min, 30 min, 1 h, 2 h, 3 h, 4.5 h, 6 h. The solutions were stirred using a magnetic stirrer, since in static mode, the sorption processes occur slowly. The main task of the algorithm of this experiment is to find which of the kinetic models best describes the process of sorption of these rare earth metals by interpolymer systems.

Results and Discussion

Kinetics in sorption processes characterizes the rates of sorbate adsorption and desorption from an aqueous solution onto a solid phase. The kinetic analysis can be linear or nonlinear, depending on the system's complexity and the underlying mechanisms. In our work, we used several popular models of sorption kinetics to establish the mechanism and limiting factors of REE extraction using activated interpolymer systems. These models are: pseudo-first order, pseudo-second order, Elovich model, and intraparticle diffusion.

Pseudo first-order kinetic model fit

Widely used models to describe adsorption kinetics are the pseudo-second order (PS2) and pseudo-first order models (PS1) [[29], [30]]. These models are adaptations for heterogeneous systems, in which it is assumed that the concentration of the sorbent does not change over time. Also, in these models, the value of adsorption capacity is important. The equation for the pseudo-first order model and its linear form are usually presented as follows [[29], [31]]:

$$q(t) = q_e(1 - e^{-k_1 t}) \quad (1)$$

$$ln[q_e - q(t)] = -k_1 t + lnq_e \quad (2)$$

The Pseudo-First-Order (PFO) kinetic model posits that the adsorption rate is directly proportional to the difference between the maximum adsorption capacity and the current amount of adsorbate already adsorbed at any given time. This means the adsorption process is primarily controlled by the concentration of the sorbate in the solution. It is typically used when the adsorption

process is diffusion-controlled, meaning mass transfer plays a significant role.

In this work, we used the linear form of the equation to plot the graph. Figures 1 and 2 show a linear approximation for the sorption kinetics of neodymium and praseodymium in different systems.

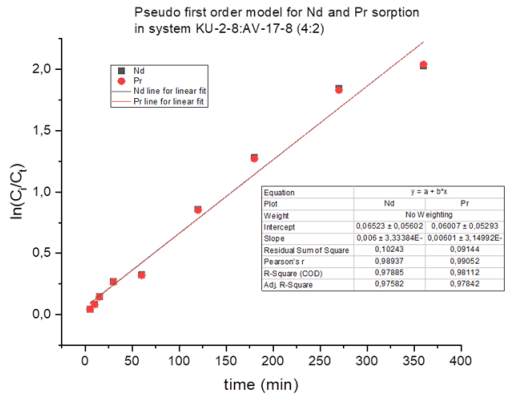

Figure 1 - Pseudo first order kinetics for neodymium and praseodymium sorption in a 4:2 system

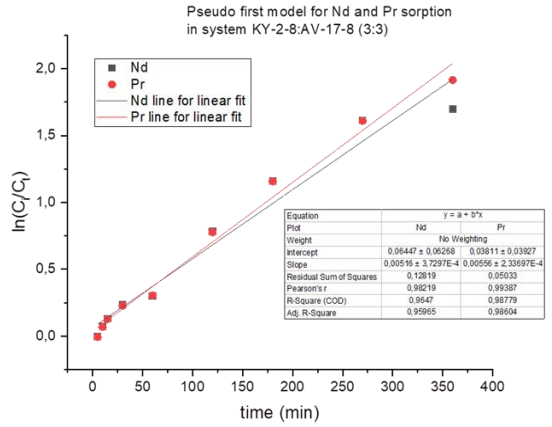

Figure 2 - Pseudo first order kinetics for neodymium and praseodymium sorption in a 3:3 system

According to the values of the quantity, the pseudo-first-order model describes well the sorption of both ions on the cation exchanger in interpolymer systems. However, this partly contradicts expectations because this model assumes physical adsorption and dependence on the concentration gradient. In turn, it is known that cross-linked polyelectrolytes contain functional groups with which metal ions directly interact (formation of ionic or coordination bonds). The model suggests that adsorption is driven by mass transfer, which occurs due to a concentration gradient between the solution and the adsorbent surface [32]. Therefore, the unexpected good pseudo-first-order correspondence can be explained by the following assumptions. A field of counterions is formed around the charged polyelectrolyte, which is replaced by metal ions. At a certain moment, counterions begin to prevent the solution and other REE ions from penetrating the polymer matrix, so despite the chemical interaction between the functional groups and REE ions in the solution, the limiting factor becomes mass transfer.

Pseudo-second order kinetic model fit

The linear form of the equation for pseudo second order is represented by the following formula [31]:

$$\frac{t}{q_t} = \left(\frac{1}{q_e}\right) t + \frac{1}{k_2 q_e^2} \qquad (3)$$

The Pseudo-Second-Order (PSO) model, also referred to as the Ho and McKay equation [33], is commonly employed to describe the adsorption of solutes from solution. The model is most applicable when adsorption is controlled by chemical interactions (chemisorption) rather than diffusion. The adsorption process depends on the availability of active sites rather than just mass transfer, meaning it is not solely controlled by diffusion [34].

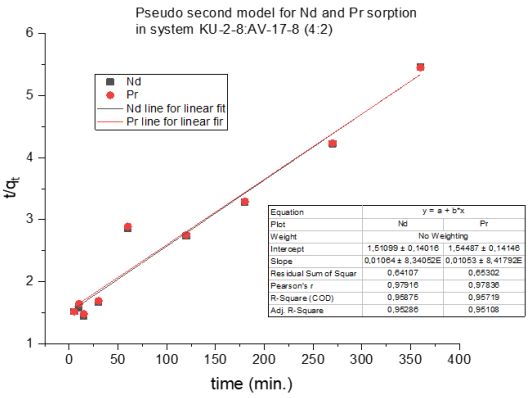

Figure 3 - Pseudo second order kinetics for neodymium and praseodymium sorption in a 4:2 system

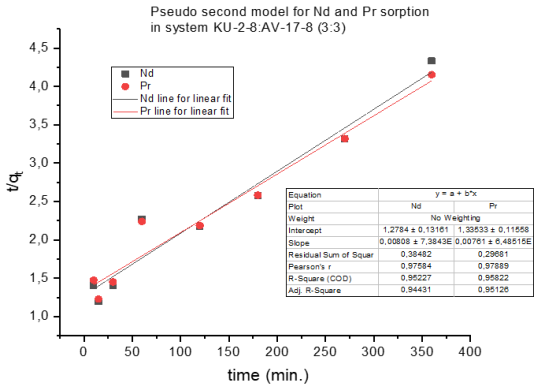

Figure 4 - Pseudo second order kinetics for neodymium and praseodymium sorption in a 3:3 system

According to the coefficient of determination in both systems (figures 3 and 4), both praseodymium and neodymium also correspond well to the pseudo-second order, but slightly less than the pseudo-first order. This is also contrary to expectations, since sorption on polyelectrolytes is usually a chemical process. But based on previous discussions of mass transfer, we conclude that although both models yielded high coefficients of determination, the actual mechanism and limiting factors are complex processes.

Elovich model

The Elovich model is commonly employed to characterize adsorption kinetics, particularly in systems where the sorbent surface is energetically heterogeneous and chemisorption is the rate-controlling step [[35], [36]]. This model posits that the adsorption rate diminishes over time as the surface coverage increases, resulting in a progressive reduction of available active sites. The linear equation for this model can be expressed by the following formula [36]:

$$q_t = \frac{1}{\beta} ln(\alpha\beta) + \frac{1}{\beta} ln(t) \qquad (4)$$

where α is the initial rate of adsorption (mg.g-1.min^{-1}) and β is the desorption constant (g.mg^{-1}) Figures 5 and 6 show graphs for the Elovich model.

According to the determination coefficient, this model describes the kinetics of neodymium and praseodymium sorption worse than the pseudo-first and pseudo-second order. This indirectly confirms that chemisorption is not a determining factor.

Intra-particle diffusion

The intraparticle diffusion model explains how adsorbate molecules, like dyes, move from the bulk solution into the solid adsorbent phase. This transport process often acts as the rate-limiting step in adsorption, especially in rapidly stirred batch reactors [37]. The formula that describes this model can be represented as follows:

$$q_t = K_{dif} t^{0.5} + C \qquad (5)$$

where C (mg*g^{-1}) is the intercept and Kdif is the intraparticle diffusion rate constant (in mg*g^{-1} min$^{-1/2}$).

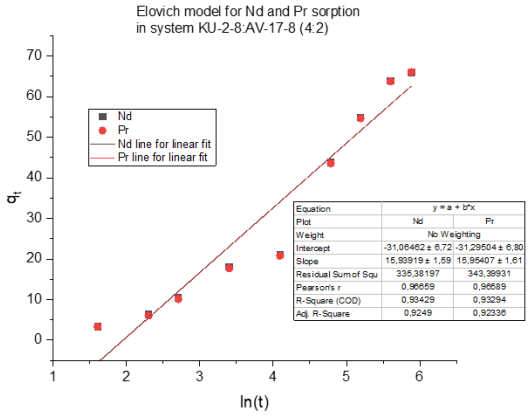

Figure 5 - Elovich model for neodymium and praseodymium sorption in a 4:2 system

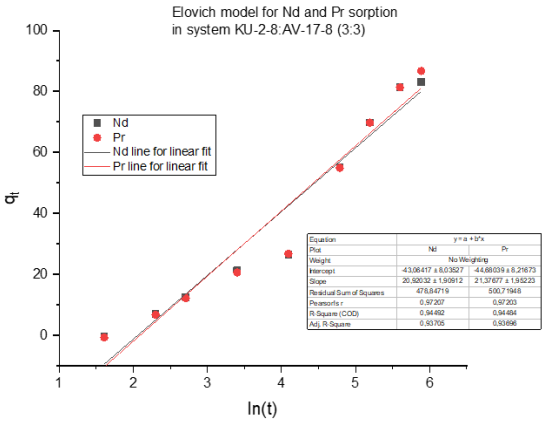

Figure 6 - Elovich model for neodymium and praseodymium sorption in a 3:3 system

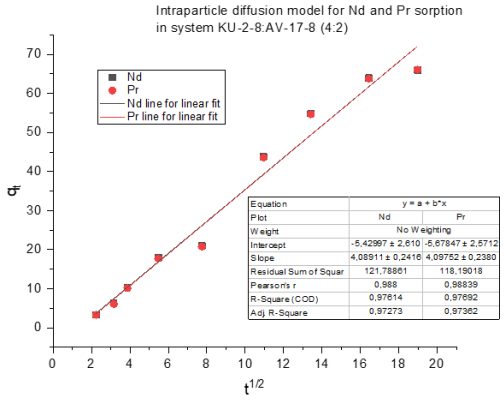

Figure 7 - Intraparticle diffusion model for neodymium and praseodymium sorption in a 4:2 system

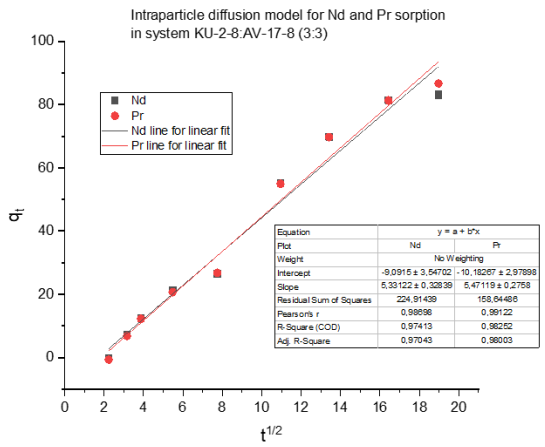

Figure 8 - Intraparticle diffusion model for neodymium and praseodymium sorption in a 3:3 system

Based on the determination coefficient, it can be concluded that this model also satisfactorily describes the sorption kinetics for neodymium and praseodymium in two systems (Figures 7 and 8). Thus, the pseudo-first-order and Elovich models turned out to be the most suitable for describing the processes occurring in interpolymer systems. The good fit of the intraparticle diffusion model suggests that mass transfer resistance within the resin plays a significant role.

Tables 1, 2 summarise the results of the linear correlation of all four sorption models (in the 4:2 system and 3:3 system) relative to the determination coefficient presented in the work.

Table 1 - Determination coefficient for Nd and Pr in 4:2 system

Kinetic model	Nd (R^2)	Pr (R^2)
Pseudo first	0.97885	0.98112
Pseudo second	0.95875	0.95719
Elovich	0.93429	0.93294
Intraparticle diffusion	0.97614	0.97692

Table 2 - Determination coefficient for the Nd and Pr 3:3 system

Kinetic model	Nd (R^2)	Pr (R^2)
Pseudo first	0.9647	0.98779
Pseudo second	0.95227	0.95822
Elovich	0.94492	0.94484
Intraparticle diffusion	0.97043	0.98003

Conclusions

This study investigated the sorption kinetics of neodymium (Nd^{3+}) and praseodymium (Pr^{3+}) ions using interpolymer systems KU-2-8:AB-17-8. Experimental data were fitted to pseudo-first-order, pseudo-second-order, Elovich, and intraparticle diffusion models to determine the best kinetic description.

The pseudo-first-order model (PFO) provided the best fit, with R2 values of 0.97885–0.98779, suggesting that mass transfer limitations and external diffusion play a key role in sorption kinetics. The pseudo-second-order model (PSO) also showed good agreement but performed slightly worse, indicating that chemisorption is not the sole controlling mechanism. The Elovich model, which typically describes heterogeneous chemisorption, exhibited the poorest fit, confirming that physical interactions and counterion exchange dominate the process. The intraparticle diffusion model demonstrated that internal diffusion resistance contributes to the sorption rate but is not the only limiting step.

The findings indicate that sorption kinetics in interpolymer systems are influenced by the counterion exchange effect, external mass transfer, and intraparticle diffusion. These insights can be applied to improve industrial ion-exchange sorption technologies for rare earth element recovery. Future studies should focus on the thermodynamics of the process, the effect of pH control, and the long-term regeneration efficiency of the interpolymer system. Another important conclusion is that under active stirring both metals are sorbed almost equally, which confirms our previous results regarding static and dynamic regimes.

Conflicts of interest. The authors declare no conflict of interest.

CRediT author statement: **T. Jumadilov:** Conceptualization, Methodology, Validation and Data curation; **K. Kabzhalelov:** Formal analysis, Investigation, Data curation and Writing - Original draft preparation; **Kh. Khimersen:** Writing - review and editing, Data curation, Visualization; **B. Totkhuskyzy:** Validation and Supervision; **Zh. Mukatayeva:** Software and Validation. All authors have read and agreed to the published version of the manuscript.

Funding. This work was supported by the Ministry of Science and Higher Education of the Republic of Kazakhstan [Grant No. BR27101179].

Cite this article as: Jumadilov TK, Kabzhalelov KR, Khimersen Kh, Totkhuskyzy B, Mukatayeva Zh. Study of the kinetics of sorption of praseodymium and neodymium ions using interpolymer systems based on KU-2-8 and AB-17-8 in salt forms. Kompleksnoe Ispolzovanie Mineralnogo Syra = Complex Use of Mineral Resources. 2026; 339(4):21-29. https://doi.org/10.31643/2026/6445.37

Тұз түріндегі КУ-2-8 және АВ-17-8 негізіндегі интерполимерлі жүйелерді қолдану арқылы празеодим және неодим иондарының сорбциялану кинетикасын зерттеу

[1]Джумадилов Т.К., [1]Кабжалелов К.Р, [1*]Химэрсэн Х., [1]Тотхусқызы Б., [2]Мукатаева Ж.С.

[1]Ә.Б. Бектұров атындағы химия ғылымдары институты АҚ, Алматы, Қазақстан
[2]Абай атындағы Қазақ ұлттық педагогикалық университеті, Алматы, Қазақстан

Мақала келді: *10 сәуір 2025*
Сараптамадан өтті: *22 мамыр 2025*
Қабылданды: *5 маусым 2025*

ТҮЙІНДЕМЕ

Бұл жұмыста тұз түріндегі КУ-2-8 және АВ-17-8 негізіндегі интерполимерлі жүйелерді қолдану арқылы неодим және празеодим иондарының сорбциялану кинетикасын зерттеу ұсынылған. Мақсатты иондарды сорбциялау динамикалық режимде (тұрақты араластырумен) 4:2 және 3:3 молярлық қатынастағы интерполимерлі жүйелерде (катион алмастырғыштан анион алмастырғышқа) жүргізілді. Белгіленген уақыт аралықтарында аликвоттар алынып, сызықтық графиктерді құру үшін сорбцияның белгілі кинетикалық үлгілері пайдаланылды. Алынған нәтижелер бойынша сорбцияны сипаттаудың ең жақсы үлгісі псевдо-бірінші ретті модель болды (4:2 жүйесі үшін ең жоғары мән = 0,97885 және 0,98112; 3:3 жүйесі үшін = 0,9647 және 0,98779). Мұндай нәтижелер сорбция процесінің механизмдерін түсіну және осы процесті баяулататын шектеуші факторды анықтау үшін маңызды. Псевдо-бірінші ретті кинетикалық моделі полимерлердің жоғары иондануы және металл иондары үшін функционалдық топтардың қолжетімділігі үшін полиэлектролиттік матрицадан қарсы иондарды жууды жақсарту қажеттілігін көрсетуі мүмкін. Бұл болжамды болашақта СЖЭ ионалмасу сорбциясының өнеркәсіптік схемаларын оңтайландыру үшін пайдалануға болады.

Түйін сөздер: интерполимерлі жүйелер, кинетикалық модельдер, сорбция, неодим және празеодим иондары, катионалмастырғыш КУ-2-8, анионалмастырғыш АВ-17-8.

Авторлар туралы ақпарат:

Джумадилов Т.Қ — *Химия ғылымдарының докторы, профессор, полимерлер синтезі және физика химиясы зертханасының меңгерушісі, Ә.Б. Бектұров атындағы химия ғылымдары институты АҚ, Алматы, Қазақстан. E-mail: jumadilov@mail.ru; ORCID ID: https://orcid.org/0000-0001-9505-3719*

Кабжалелов К.Р. — *Бакалавр, инженер, Ә.Б. Бектұров атындағы химия ғылымдары институты АҚ, Алматы, Қазақстан. Email: kamil_kabhzalelov@outlook.com; ORCID ID: https://orcid.org/0009-0008-6030-052X*

Химэрсэн Х. — *PhD, ғылыми қызметкер, Ә.Б. Бектұров атындағы химия ғылымдары институты АҚ, Алматы, Қазақстан. E-mail: khuana88@gmail.com; ORCID ID: https://orcid.org/0000-0002-5138-5997*

Тотхусқызы Б. — *PhD, ғылыми қызметкер, Ә.Б. Бектұров атындағы химия ғылымдары институты АҚ, Алматы, Қазақстан. E-mail: bakytgul.sakenova@mail.ru; ORCID ID: https://orcid.org/0000-0001-8119-668X*

Мукатаева Ж. С. — *Химия ғылымдарының кандидаты, қауымдастырылған профессор, Абай атындағы Қазақ ұлттық педагогикалық университеті, Алматы, Қазақстан. E-mail: jazira-1974@mail.ru; ORCID ID: https://orcid.org/0000-0002-1584-5810*

Изучение кинетики сорбции ионов празеодима и неодима интерполимерными системами на основе КУ-2-8 и АВ-17-8 в солевых формах

[1]Джумадилов Т.К., [1]Кабжалелов К.Р, [1*]Химэрсэн Х., [1]Тотхусқызы Б., [2]Мукатаева Ж.С.

[1]АО Институт химических наук им. А.Б.Бектурова, Алматы, Казахстан
[2]Казахский национальный педагогический университет имени Абая, Алматы, Казахстан

Поступила: *10 апреля 2025*
Рецензирование: *22 мая 2025*
Принята в печать: *5 июня 2025*

АННОТАЦИЯ

В данной работе представлено исследование кинетики сорбции ионов неодима и празеодима интерполимерными системами на основе КУ-2-8 и АВ-17-8 в солевых формах. Сорбцию целевых ионов проводили в динамическом режиме (при постоянном перемешивании) в интерполимерных системах в мольных соотношениях 4:2 и 3:3 (катионит к аниониту). Аликвоты отбирались через определенные промежутки времени, затем для построения линейных графиков использовались широко известные кинетические модели сорбции. Согласно полученным результатам, наилучшей моделью для описания сорбции оказалась модель псевдопервого порядка (наибольшее значение для системы 4:2 = 0,97885 и 0,98112; для системы 3:3 = 0,9647 и 0,98779). Подобные результаты важны для понимания механизмов процесса сорбции и установления лимитирующего фактора, способного замедлить этот процесс. Кинетическая модель псевдопервого порядка может указывать на необходимость улучшения вымывания противоионов из полиэлектролитной матрицы для их высокой ионизации и доступности функциональных групп для ионов металлов. Данное предположение может быть использовано в дальнейшем для оптимизации промышленных схем ионообменной сорбции РЗЭ.

Ключевые слова: интерполимерные системы, кинетические модели, сорбция, ионы неодима и празеодима, катионит КУ-2-8, анионит АВ-17-8.

Информация об авторах:

Джумадилов Т.К. *Доктор химических наук, профессор, заведующий лабораторией синтеза и физикохимии полимеров, АО Институт химических наук им. А.Б.Бектурова, Алматы, Казахстан. E-mail: jumadilov@mail.ru; ORCID ID: https://orcid.org/0000-0001-9505-3719*

Кабжалелов К.Р. *Бакалавр, инженер, АО Институт химических наук им. А.Б.Бектурова, Алматы, Казахстан. Email: kamil_kabhzalelov@outlook.com; ORCID ID: https://orcid.org/0009-0008-6030-052X*

Химэрсэн Х. *PhD, научный сотрудник, АО Институт химических наук им. А.Б.Бектурова, Алматы, Казахстан. E-mail: khuana88@gmail.com; ORCID ID: https://orcid.org/0000-0002-5138-5997*

Тотхусқызы Б. *PhD, научный сотрудник, АО Институт химических наук им. А.Б.Бектурова, Алматы, Казахстан. E-mail: bakytgul.sakenova@mail.ru; ORCID ID: https://orcid.org/0000-0001-8119-668X*

Мукатаева Ж. С. *Кандидат химических наук, ассоциированный профессор, Казахский национальный педагогический университет имени Абая, Алматы, Казахстан. E-mail: jazira-1974@mail.ru; ORCID ID: https://orcid.org/0000-0002-1584-5810*

References

[1] Papagianni S, Moschovi AM, Sakkas KM, Chalaris M, Yakoumis I. Preprocessing and Leaching Methods for Extraction of REE from Permanent Magnets: A Scoping Review. AppliedChem. 2022; 2(14):199-212. https://doi.org/10.3390/appliedchem2040014

[2] Binnemans K, Jones PT, Blanpain B, Van Gerven T, Yang Y, Walton A, Buchert M. Recycling of Rare Earths: A Critical Review. Journal of Cleaner Production. 2013; 51:1–22. http://dx.doi.org/10.1016/j.jclepro.2012.12.037

[3] Gkika DA, Chalaris M, Kyzas GZ. Review of Methods for Obtaining Rare Earth Elements from Recycling and Their Impact on the Environment and Human Health. Processes. 2024; 12:1235. https://doi.org/10.3390/pr12061235

[4] Wang G, Xu J, Ran L, Zhu R et al. A green and efficient technology to recover rare earth elements from weathering crusts. Nature Sustainability. 2022; 6(1):81-92. https://doi.org/10.1038/s41893-022-00989-3

[5] Depraiter L, Goutte S. The role and challenges of rare earths in the energy transition. Resources Policy. 2023; 86(6):104-137. https://doi.org/10.1016/j.resourpol.2023.104137

[6] Balaram V. Rare earth elements: A review of applications, occurrence, exploration, analysis, recycling, and environmental impact. Geoscience Frontiers. 2019; 10(4):1285-1303. https://doi.org/10.1016/j.gsf.2018.12.005

[7] Hurst C. China's Rare Earth Elements Industry: What Can the West Learn? Institute for the Analysis of Global Security; Fort Leavenworth. 2010. KS, USA.

[8] Filho WL. et al. Understanding rare earth elements as critical raw materials. Sustainability. 2023; 15(3):1919.

[9] Humphries M. Rare Earth Elements: The Global Supply Chain: Congressional Research Service. The Library of Congress. 2010. Washington, DC, USA.

[10] Zhang W, Li Ch, Xu Q, Hu K, Chen H, Liu Y, Wan Y, Zhang J, Li X. Effective adsorption and recovery of rare earth elements from wastewater by activated talc. Applied Clay Science. 2024; 251. https://doi.org/107312. 10.1016/j.clay.2024.107312

[11] Asadollahzadeh M, Torkaman R, Torab-Mostaedi M. Extraction and separation of rare earth elements by adsorption approaches: current status and future trends. Separation & Purification Reviews. 2021; 50(4):1-28. https://doi.org/10.1080/15422119.2020.1792930

[12] NI'AM A C. et al. Recovery of neodymium from waste permanent magnets by hydrometallurgy using hollow fibre supported liquid membranes. Solvent Extraction Research and Development. 2020; 27(2):69-80. https://doi.org/10.15261/serdj.27.69

[13] Klemettinen A. et al. Recovery of rare earth elements from the leaching solutions of spent NdFeB permanent magnets by selective precipitation of rare earth oxalates. Minerals. 2023; 13(7):846. https://doi.org/10.3390/min13070846

[14] Nogueira M. et al. Recovery of Nd^{3+} and Dy^{3+} from E-Waste Using Adsorbents from Spent Tyre Rubbers: Batch and Column Dynamic Assays. Molecules. 2024; 30(1):92. https://doi.org/10.3390/molecules30010092

[15] Erust C, Akcil A, Tuncuk A, Deveci H, Yazici EY. A Multi-stage Process for Recovery of Neodymium (Nd) and Dysprosium (Dy) from Spent Hard Disc Drives (HDDs). Miner. Process. Extr. Metall. Rev. 2019; 42:90-101. https://doi.org/10.1080/08827508.2019.1692010

[16] Behera SS, Parhi PK. Leaching kinetics study of neodymium from the scrap magnet using acetic acid. Separation and Purification Technology. 2016; 160:59-66. https://doi.org/10.1016/j.seppur.2016.01.014

[17] Riaño S, Petranikova M, Onghena B. Separation of rare earths and other valuable metals from deep-eutectic solvents: A new alternative for the recycling of used NdFeB magnets. Rsc Advances. 2017; 7(51):32100-32113. https://doi.org/10.1039/c7ra06540j

[18] Hérès X, Blet V, Di Natale P, Ouaattou A, Mazouz H, Dhiba D, Cuer F. Selective extraction of rare earth elements from phosphoric acid by ion exchange resins. Metals. 2018; 8(9):682. https://doi.org/10.3390/met8090682

[19] Chen Z, Zhan L, Chen J, Kallem P. Recent advances in selective separation technologies of rare earth elements: a review. Journal of Environmental Chemical Engineering. 2022; 10(1):107104. https://doi.org/10.1016/j.jece.2021.107104

[20] Pereao O, Bode-Aluko Ch, Fatoba O, Petric L. Rare earth elements removal techniques from water/wastewater: A review. Desalination and water treatment. 2018; 130:71-86. https://doi.org/10.5004/dwt.2018.22844

[21] El Ouardi Y, Sami V, Markku L, Eveliina R, Katri L. The recent progress of ion exchange for the separation of rare earths from secondary resources–A review Hydrometallurgy. 2023; 218:106047. https://doi.org/10.1016/j.hydromet.2023.106047

[22] Virolainen S, Repo E, Sainio T. Recovering rare earth elements from phosphogypsum using a resin-in-leach process: Selection of resin, leaching agent, and eluent. Hydrometallurgy. 2019; 189:105125. https://doi.org/10.1016/j.hydromet.2019.105125

[23] Bao S, Hawker W, Vaughan J. Scandium loading on chelating and solvent impregnated resin from sulfate solution. Solvent extraction and ion exchange. 2018; 36(1):1-14. https://doi.org/10.1080/07366299.2017.1412917

[24] Ismailova ShA, Jumadilov TK, Bekturov EA. Features of complex formation of rare-crosslinked polyacrylic acid with polyacrylamide hydrogel. Izvestiya MES RK NAS RK, ser. chem. 2004; 4:80-85.

[25] Ismailova ShA. Features of interaction of three-dimensional structures based on polycarboxylic acids and nitrogen-containing polymers: dissertation for the degree of candidate of chemical sciences. 02.00.06, Almaty, ICN MES RK. 2006, 109.

[26] Jumadilov T, Totkhuskyzy B, Malimbayeva Z, Kondaurov R, Imangazy A, Khimersen K, Grazulevicius J. Impact of Neodymium and Scandium Ionic Radii on Sorption Dynamics of Amberlite IR120 and AB-17-8 Remote Interaction. Materials. 2021; 14:5402. https://doi.org/10.3390/ma14185402

[27] Talkybek J, Kabzhalelov K, Malimbayeva Z, Korganbayeva Zh. Features of Selective Sorption of Neodymium and Praseodymium Ions by Interpolymer Systems Based on Industrial Sorbents KU-2-8 and AB-17-8. Polymers. 2025; 17(4):440. https://doi.org/10.3390/polym17040440

[28] Jumadilov T, Khimersen Kh, Haponiuk J, Totkhuskyzy B. Enhanced Lutetium Ion Sorption from Aqueous Solutions Using Activated Ion Exchangers. Polymers 2024; 16(2):220. https://doi.org/10.3390/polym16020220

[29] Revellame ED, Fortela D, Sharp W, Hernandez R. Adsorption kinetic modeling using pseudo-first order and pseudo-second order rate laws: A review. Cleaner Engineering and Technology. 2020; 1:100032. https://doi.org/10.1016/j.clet.2020.100032

[30] Vareda JP, Valente AJM, Durães L. Heavy metals in Iberian soils: Removal by current adsorbents/amendments and prospective for aerogels. Advances in Colloid and Interface Science. 2016; 237:28-42. https://doi.org/10.1016/j.cis.2016.08.009

[31] Ho YS, McKay G. Pseudo-second order model for sorption processes. Process biochemistry. 1999; 34(5):451-465.

[32] Fawzy MA, Gomaa M. Use of algal biorefinery waste and waste office paper in the development of xerogels: A low cost and eco-friendly biosorbent for the effective removal of congo red and Fe (II) from aqueous solutions. Journal of Environmental Management. 2020; 262:110380. https://doi.org/10.1016/j.jenvman.2020.110380

[33] Vareda JP. On validity, physical meaning, mechanism insights and regression of adsorption kinetic models. Journal of Molecular Liquids. 2023; 376:121416. https://doi.org/10.1016/j.molliq.2023.121416

[34] Zhang J. Physical insights into kinetic models of adsorption. Separation and Purification Technology. 2019; 229:115832. https://doi.org/10.1016/j.seppur.2019.115832

[35] Musah M, Azeh Y, Mathew JT, Tanko MU. Adsorption kinetics and isotherm models: a review. CaJoST. 2022; 4(1):20-26. https://doi.org/10.4314/cajost.v4i1.3

[36] Farouq R, Yousef NS. Equilibrium and kinetics studies of adsorption of copper (II) ions on natural biosorbent. International Journal of Chemical Engineering and Applications. 2015; 6(5):319. https://doi.org/10.7763/IJCEA.2015.V6.503

[37] Santhi T, Manonmani S, Smitha T. Kinetics and isotherm studies on cationic dyes adsorption onto annona squmosa seed activated carbon. International Journal of Engineering Science and Technology. 2010; 2(3):287-295.

Crossref
DOI: 10.31643/2026/6445.38
Engineering and technology

Morphological and Crystallographic Investigation of CVD-Grown MoS_2

[1] Otunchi Ye., [1] Umirzakov A., [1,2] Dmitriyeva E., [1] Shongalova A., [1,2*] Kemelbekova A.

[1] Institute of Physics and Technology, Satbayev University, Almaty, Kazakhstan
[2] Manul Technologies, Astana, Kazakhstan

** Corresponding author email: a.kemelbekova@satbayev.university*

Received: *February 14, 2025*
Peer-reviewed: *April 8, 2025*
Accepted: *June 9, 2025*

ABSTRACT

This paper presents a study of the structural characteristics of a promising MoS_2-based material obtained by chemical vapor deposition (CVD). Optimization of the synthesis process to obtain the desired structure is also presented. The optimal parameter for the synthesis of CVD MoS_2 crystals was found to be the maximum sulfurization temperature of 780 °C with an exposure time of about 15 minutes, the heating temperature of the sulfur source zone of 250 °C, the distance between the sulfur and molybdenum sources of 25 cm, and the distance between the molybdenum source and the substrate was 1.5 cm. The morphology and elemental composition of the obtained samples were studied using scanning electron microscopy (SEM) with energy dispersive X-ray spectroscopy (EDS). Using SEM, it was revealed that MoS_2 crystals are formed in a triangular shape and are evenly distributed over the surface of the substrate. The maximum sizes of crystallites reach 6 microns. EMF mapping of crystallites confirmed the homogeneous distribution of molybdenum and sulfur in the structure, revealing only minor variations in composition at the grain boundaries. The quality and quantity of the sample layer were studied using Raman spectroscopy. The results showed two characteristic peaks (vibrational modes E_{2g}^1 and A_{1g}) of nanoscale MoS_2. The peaks have a sharp shape and are located at a distance of ≈20.9 cm^{-1}, which may indicate the high quality of the crystal structure of the obtained crystallites. The results obtained emphasize the effectiveness of the chosen approach and the importance of the work for the development of 2D materials technologies.

Keywords: Molybdenum disulfide, CVD synthesis, 2D materials, Raman spectroscopy, morphology.

Information about authors:

Otunchi Yedil — *Master's student, Institute of Physics and Technology, Satbayev University, 050032, Almaty, Kazakhstan. Email: ye.otunchi@sci.kz; ORCID ID: https://orcid.org/0009-0006-4361-8099*

Umirzakov Arman — *PhD candidate, Researcher. Institute of Physics and Technology, Satbayev University, Ibragimov str. 11, 050032, Almaty, Kazakhstan. Email: a.umirzakov@sci.kz ; ORCID ID: https://orcid.org/0000-0002-0941-0271*

Dmitriyeva Elena — *Candidate of Physico-Mathematical Sciences, Professor, Institute of Physics and Technology, Satbayev University, Ibragimov str. 11, 050032, Almaty, Kazakhstan. Email: e.dmitriyeva@sci.kz ORCID ID: https://orcid.org/0000-0002-1280-2559*

Shongalova Aigul — *PhD, Institute of Physics and Technology, Satbayev University, Ibragimov str. 11, 050032, Almaty, Kazakhstan. Email: a.shongalova@sci.kz ; ORCID ID: https://orcid.org/0000-0002-7352-9007*

Kemelbekova Ainagul — *PhD, Institute of Physics and Technology, Satbayev University, Ibragimov str. 11, 050032, Almaty, Kazakhstan; Manul Technologies, Astana, Kazakhstan. Email: a.kemelbekova@sci.kz ; ORCID ID: https://orcid.org/0000-0003-4813-8490*

Introduction

Molybdenum disulfide (MoS_2) is a layered material possessing a set of unique properties—including semiconducting, optical, mechanical, and catalytic characteristics—that make it a subject of intensive research. Its electronic properties are closely related to its structural phase. In its monolayer form, the semiconducting 2H-MoS_2 phase exhibits a direct bandgap of approximately 1.8–1.9 eV, making it a promising candidate for applications in field-effect transistors and photodetectors [1]. In contrast, the metallic 1T-MoS_2 phase broadens its functionality in catalytic and energy systems [2].

MoS_2 is noted for its high mechanical strength, low friction coefficient, and pronounced catalytic activity, particularly in the hydrogen evolution reaction (HER) [[3], [4]]. These attributes have stimulated their application in tribology and renewable energy technologies [[5], [6]]. In the field of nanoelectronics and optoelectronics, MoS_2 has been integrated into field-effect transistors, light-emitting diodes, photodetectors, and solar cells [7].

Its high absorption and emission efficiency facilitate the development of fast and sensitive photonic devices [[8], [9]]. Furthermore, its catalytic properties can be tailored through surface modification to enhance device performance [3]. MoS_2's tribological advantages—such as high wear resistance—make it an effective solid lubricant or protective coating [5], while in sensing applications, MoS_2 demonstrates selective adsorption of target molecules, which is advantageous for gas and biosensors [[10], [11]].

In recent years, efforts have been made to expand MoS_2's application potential via functionalization. Various surface modification techniques have been shown to tune MoS_2's physicochemical properties, improving its environmental stability and performance in devices [[12], [13], [14]]. The creation of hybrid structures by combining MoS_2 with other two-dimensional (2D) materials, such as graphene or metal oxide nanostructures, has been shown to enhance their electrical conductivity and catalytic activity [[15], [16], [17], [18]]. In addition, chemical treatments that increase the density of catalytically active sites are essential for optimizing electrochemical performance [[19], [20]].

Different morphologies and structural qualities of MoS_2 have been obtained using different synthesis routes. Among these, chemical vapor deposition (CVD) is frequently selected because this method is scalable as well as offers layer thickness and uniform control [21]. Mechanical exfoliation [22], hydrothermal synthesis [14], laser ablation, and other methods, such as ultrasound-assisted or biological synthesis [[23], [24], [25]], still have a role in meeting other needs. However, some issues prevent practical deployment. Phase instability is one of the bigger ones. However, the 1T- MoS_2 phase is more active but undergoes irreversible conversion to the stable 2H- MoS_2 phase under normal and ambient conditions [21]. The Stabilising it chemically or structurally is an ongoing challenge. One issue is reproducibility, as growth through CVD is highly dependent on the experimental parameters such as temperature, position of precursor and gas flow dynamics [[26], [27]].

Devices suffer performance limitations as well. In general most basal planes of MoS_2 are less catalytically active and its conductivity is not always high enough for demanding electronic applications. But that progress has been made by forming nanostructures or integration of MoS_2 with conductive frameworks such as carbon nanotubes or graphene [[28], [29], [30]]. CVD has recently been achieved in large areas on sapphire substrates up to 2-inch diameters, with encouraging thickness control for synthesis [31]. In particular, high-quality films for scale-up can be achieved with metal-organic CVD methods [32]. These approaches are also compatible with both atomic layer deposition and with industrial processes, and are thus highly relevant for practical device fabrication [33].

The emphasis of this work is to optimize CVD conditions for MoS_2 synthesis and then evaluate the effects of such parameters on the film's morphology and structure. The intention is that it will facilitate further developments in MoS_2 electronics, sensing and catalytic applications.

Experimental Methods

Synthesis of MoS_2

In Figure 1, the MoS_2 synthesis process is demonstrated. Molybdenum disulfide has been synthesized by the chemical vapor deposition technique. The sources of molyndenum (MoO_3 99,9%, Sigma Aldrich) and sulfur (S 99,9%, Sigma Aldrich) have been placed onto quartz boats in the reaction zone. In the first zone, the sulfur has been placed, the temperature 250 °C was settled. The MoO_3 has been placed into the second zone, and the maximum synthesis temperature of 780 °C was settled for 15 minutes. Argon (Ar 99,99% Ihsan gas) has been used as the transportation gas. A flow of Ar at 220 sccm transports sulfur and MoO_3 vapors to the silicon substrate (Si). The distance between sulfur and MoO_3 was 25 cm, and between MoO_3 and the silicon substrate was 1.5 cm. This configuration provided optimal conditions for the growth of thin MoS_2 on the substrate under the conditions of the used CVD furnace.

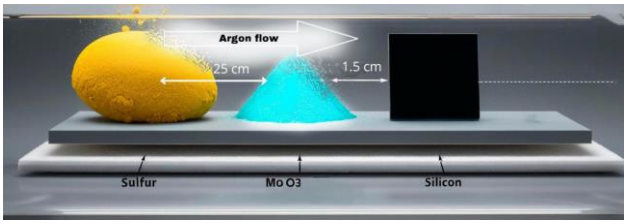

Figure 1 – The process of material synthesis

Investigation of material characteristics

The structural features, such as crystallite shape, size and spatial distribution, were examined for the

samples using scanning electron microscopy (SEM). SEM images were taken using JEOL JSPM-5200 operating at 30 kV accelerating voltage. Energy dispersive X-ray spectroscopy (EDS) measured elemental composition analysis in a JEOL EX-2300 BU detector attached to the SEM system. To keep the spectra consistent with the SEM imaging, EDS spectra were collected under the same conditions.

The layer number and characteristic vibrational mode identification were investigated by Raman spectroscopy. The Raman spectra were obtained using a Jobin-Yvon LabRaman HR800 spectrometer, with monochromatic light of wavelength 632.8 nm.

Results and discussion

The growth conditions are summarized such that the morphological characteristics of the synthesized crystallites are reported in Table 1. Systematic adjustment of the key deposition parameters of CVD synthesis, for example, deposition time and temperature, and the relative positioning of substrate and molybdenum and sulfur sources was done in order to optimize the CVD process. The resulting crystallites were found to have thickness, lateral dimensions and were further confirmed using SEM and Raman spectroscopy.

Figure 2 presents SEM images illustrating the morphology of the synthesized sample. At a magnification of 750× (Figure 2a), the overall surface structure is clearly visible, revealing numerous triangular-shaped crystallites uniformly distributed across the substrate. The lateral dimensions of individual crystallites range from several hundred nanometers to approximately 6 µm, indicating homogeneous growth and a high degree of crystallinity. The observed high nucleation density in certain regions may suggest non-uniform precursor distribution or localized variations in reaction zone parameters such as temperature or reactant concentration [34].

At 9500× magnification (Figure 2b), the fine structure of individual triangular crystallites becomes clearly visible. The well-defined grain boundaries and uniform crystal surfaces observed in the image are indicative of the layered nature of the material and confirm the hexagonal symmetry of the MoS_2 crystal lattice. The formation of triangular and polygonal crystallites can be attributed to anisotropic growth behavior during the CVD process. As Mo and S atoms assemble into hexagonal layers, differences in growth rates along crystallographic directions result in distinct crystal shapes. In particular, when there is an excess of molybdenum, the crystallites tend to adopt a triangular morphology, whereas a more balanced distribution of molybdenum and sulfur leads to more symmetric, nearly hexagonal forms [35].

The results of elemental mapping, which confirm the composition and spatial distribution of elements within the sample structure, are presented in Figure 3. The region selected for analysis is shown in Figure 3a, where triangular and polygonal crystallites are clearly distinguished against the background of the silicon substrate. Figure 3b illustrates the distribution of silicon, which constitutes the underlying substrate. A decrease in silicon signal intensity is observed in the areas covered by MoS_2 crystallites, indicating uniform deposition of the material across the substrate surface.

Figure 3c shows the distribution of molybdenum. The high Mo signal intensity is localized in the regions where MoS_2 crystallites have formed, confirming the presence of molybdenum disulfide. The gradient in signal intensity suggests variations in layer thickness, which may be attributed to growth kinetics under conditions of limited precursor availability. The lower right panel displays the distribution of sulfur, which, in contrast to molybdenum, appears more diffuse. This may indicate compositional variations across the sample or the presence of amorphous sulfur species deposited onto the substrate.

The formation of well-ordered crystallites is governed by a combination of factors, including crystallographic growth anisotropy, thermodynamic constraints, and nucleation mechanisms [34]. The hexagonal structure of MoS_2 promotes preferential growth along low-energy crystal planes, resulting in the formation of triangular and hexagonal platelets. Synthesis temperature plays a particularly critical role; under optimal conditions, a balance between nucleation and crystal growth is achieved, enabling the formation of uniform, highly crystalline structures. The gradient elemental distributions observed in the EDS maps further support the kinetic nature of the deposition process and reflect local compositional fluctuations during film formation.

Table 1 – Morphological characteristics of MoS_2 crystallites under various CVD synthesis conditions

Synthesis Temperature (°C)	Deposition Time (min)	Crystallite Size (μm) and Thickness (nm)	Substrate Position Relative to Mo Source	Comments
620	10	~1–7 μm, ~200–300 nm	Distance between sulfur and MoO_3 - 25 cm between MoO_3 and substrate - 5 cm	Uniform circular structures formed on the substrate surface, with sulfur-rich composition
700	10	~4–7 μm, –	Distance between sulfur and MoO_3 - 30 cm between MoO_3 and substrate - 5 cm	Needle-like structures with molybdenum enrichment
750	10	~2–5 μm, ~0.7 nm	Distance between sulfur and MoO_3 - 30 cm, between MoO_3 and substrate - 1.5 cm	Triangular structures formed with partially developed edges
780	15	~2–6 μm, ~0.7 nm	Distance between sulfur and MoO_3- 25 cm, between MoO_3 and substrate - 1.5 cm	Well-defined triangular crystallites with sharp edges

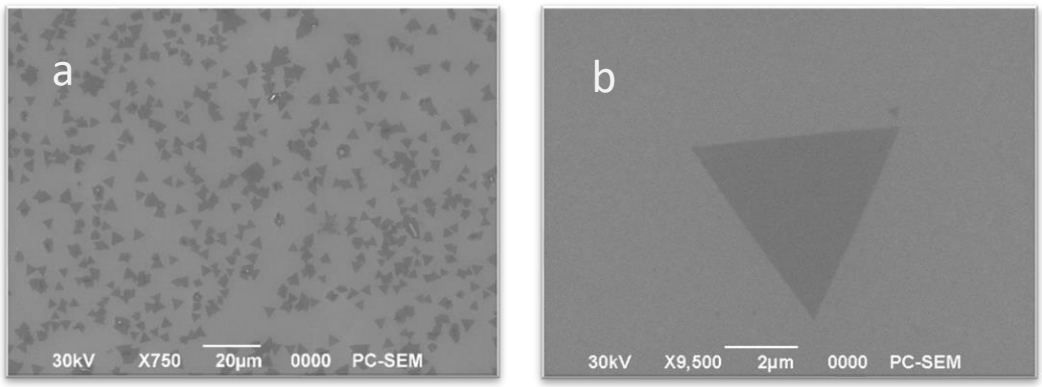

Figure 2 – SEM images of the surface morphology of the MoS_2 sample: (a) 750× magnification; (b) 9500× magnification

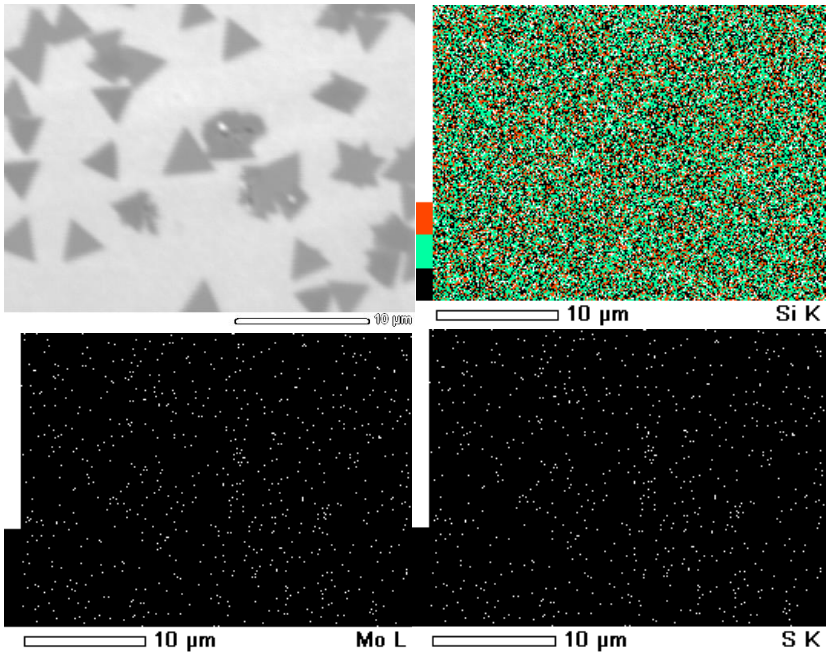

Figure 3 – Elemental mapping of the MoS_2 sample obtained by energy-dispersive X-ray spectroscopy (EDS)

The crystal structure was analyzed using Raman spectroscopy. The spectra were taken at normal temperature with a single-colour light beam at 632.8 nm wavelength. The measurements were done using a 100× objective lens, which focused a laser beam of 1 µm diameter. A single crystallite from the MoS_2 sample provided the spectra presented in Figure 4. The optical image of this sample is shown in the upper-left corner of the spectra. The spectra show two sharp peaks at ~384 cm^{-1} and ~405 $cm^{-1,}$ which are characteristic vibrational modes of MoS_2 known as E_{2g}^1 and A_{1g}. These vibration modes are located at a distance of Δ ≈ 20.9 $cm^{-1,}$ which shows clear signs of a single layer of MoS_2. The Raman spectra exhibit sharp and intense E_{2g}^1 and A_{1g} peaks, indicative of high crystallinity and structural order in the monolayer MoS_2 [36]. A well-defined structure with a high specific surface area facilitates efficient charge carrier separation and offers numerous active sites for hydrogen evolution reactions [37]. The SEM images show clear edge structures and a uniform pattern, which shows that this sample has many surface locations that react efficiently. An effective resistive gas sensor works through specific edge locations that preferentially take gas molecules and alter electrical conductivity [38].

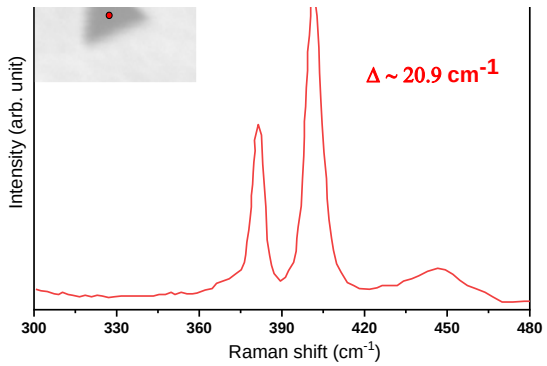

Figure 4 – Raman spectrum of the MoS_2 sample

The two-phonon scattering process at 450 cm^{-1} shows up as a broad peak in the spectrum because this band appears in layered transition metal dichalcogenides [35]. The small peak ratio and narrow lineshapes of E_{2g}^1 and A_{1g} prove the high-quality MoS_2 monolayer formation.

Conclusion

The combined results of SEM imaging and elemental mapping indicate that the synthesized MoS_2 exhibits high crystallinity, well-defined structure, and a characteristic morphology shaped by growth dynamics under CVD conditions. Elemental distribution analysis confirms the uniform incorporation of molybdenum and sulfur within the crystalline domains, along with some compositional variation at grain boundaries. Raman spectroscopy further verifies that the obtained sample corresponds to a monolayer of MoS_2. The interpeak distance of Δ ≈ 20.9 cm^{-1} between the E_{2g}^1 and A_{1g} modes is consistent with high-quality monolayer formation. SEM analysis corroborates the uniform spatial distribution of crystallites and their distinct hexagonal morphology. These findings provide a solid basis for further optimization of MoS_2 synthesis parameters aimed at tailoring morphological characteristics, which is particularly relevant for applications in electronic and optoelectronic devices.

Conflicts of interest. The authors declare no conflict of interest.

CRediT author statement: **Ye.Otunchi**: Methodology; **A. Umirzakov**: Formal analysis; **E. Dmitriyeva** and **A. Shongalova:** Writing-original draft; **A. Kemelbekova**: Writing review. All authors have read and agreed to the published version of the manuscript.

Acknowledgements. This work was financially supported by the Science Committee of the Ministry of Science and Higher Education of the Republic of Kazakhstan under Grant No. BR21881954.

Cite this article as: Otunchi Ye, Umirzakov A, Dmitriyeva E, Shongalova A, Kemelbekova A. Morphological and Crystallographic Investigation of CVD-Grown MoS_2. Kompleksnoe Ispolzovanie Mineralnogo Syra = Complex Use of Mineral Resources. 2026; 339(4):30-37. https://doi.org/10.31643/2026/6445.38

CVD әдісімен алынған MoS_2-нің морфологиясын және кристаллдық тор құрылымын зерттеу

[1] Отунчи Е., [1] Умирзаков А., [1,2]Дмитриева Е., [1] Шонғалова А., [1,2*]Кемелбекова А.

[1] Физико-техникалық институт , Сәтбаев университеті, Алматы, Казахстан
[2] Manul Technologies, Астана, Қазақстан

Мақала келді: *14 ақпан 2025*
Сараптамадан өтті: *8 сәуір 2025*
Қабылданды: *9 маусым 2025*

ТҮЙІНДЕМЕ

Мақалада бу фазасынан химиялық тұндыру (CVD) әдісімен алынған MoS_2 негізіндегі перспективалы материалдың құрылымдық сипаттамалары зерттелген. Қажетті құрылымды алу үшін синтез процесін оңтайландыру нәтижелері де ұсынылған. CVD әдісімен MoS_2 кристалдарын синтездеу үшін оңтайлы параметр күкірттенудің максималды температурасы 780 °C, ұсталу уақыты шамамен 15 минут, күкірт көзі аймағының қыздыру температурасы 250 °C, күкірт пен молибден көздерінің арасындағы қашықтық 25 см, ал молибден көзі мен төсеніш арасындағы қашықтық 1,5 см болды. Алынған үлгілердің морфологиясы мен элементтік құрамы сканерлеуші электронды микроскопия (СЭМ) және энергия-дисперсиялық рентген спектроскопиясы (ЭДС) әдістері арқылы зерттелді. СЭМ нәтижелері бойынша MoS_2 кристалдары үшбұрышты пішінде түзілген және төсеніш бетінде біркелкі таралған. Кристалдардың ең үлкен өлшемі 6 микронға дейін жетеді. ЭДС-картографиялау нәтижесінде молибден мен күкірттің кристал құрылымында біртекті таралуы анықталды, тек түйіршіктер шекараларында аздаған құрам ауытқулары байқалды. Үлгінің сапасы мен қабат саны Раман спектроскопиясы арқылы зерттелді. Спектрде MoS_2 наноқабатының екі сипаттамалық шыңы (E_{2g}^1 және A_{1g} тербеліс режимдерінде) тіркелді, шыңдардың пішіні өткір формада, олар ≈20.9 $см^{-1}$ қашықтықта орналасқан, бұл алынған кристалдардың жоғары құрылымдық сапасын көрсетеді. Алынған нәтижелер таңдалған тәсілдің тиімділігін және жұмыс нәтижелерінің екі өлшемді материалдар технологиясын дамытудағы маңыздылығын дәлелдейді.

Түйін сөздер: молибден дисульфиді, CVD синтезі, 2d материалдар, Раман спектроскопиясы, морфология.

Авторлар туралы ақпарат:

Отунчи Еділ — *Магистрант, Физика-техникалық институты, Сәтбаев университеті, 050032, Алматы, Қазақстан. Email: ye.otunchi@sci.kz; ORCID ID: https://orcid.org/0009-0006-4361-8099*

Умирзаков Арман — *PhD докторант, аға ғылыми қызметкер, Физика-техникалық институты, Сәтбаев университеті, 050032, Алматы, Қазақстан. Email: a.umirzakov@sci.kz; ORCID ID: https://orcid.org/0000-0002-0941-0271*

Дмитриева Елена — *Физика-математика ғылымдарының кандидаты, профессор, Физика-техникалық институты, Сәтбаев университеті, 050032, Алматы, Қазақстан. Email: e.dmitriyeva@sci.kz; ORCID ID: https://orcid.org/0000-0002-1280-2559*

Шонғалова Айгуль — *PhD, Физика-техникалық институты, Сәтбаев университеті, 050032, Алматы, Қазақстан. Email: a.shongalova@sci.kz; ORCID ID: https://orcid.org/0000-0002-7352-9007*

Кемелбекова Айнагуль — *PhD, Физика-техникалық институты, Сәтбаев университеті, 050032, Алматы, Қазақстан; Manul Technologies, Астана, Қазақстан. Email: a.kemelbekova@sci.kz ; ORCID ID: https://orcid.org/0000-0003-4813-8490*

Морфологическое и кристаллографическое исследование MoS_2 выращенных CVD-методом

[1] Отунчи Е., [1] Умирзаков А., [1,2] Дмитриева Е., [1] Шонғалова А. , [1,2*] Кемелбекова А.

[1] Физико- технический институт, Satbayev University, Алматы, Казахстан
[2] Manul technologies, Астана, Казахстан

Поступила: *14 февраля 2025*
Рецензирование: *8 апреля 2025*
Принята в печать: *9 июня 2025*

АННОТАЦИЯ

В данной статье представлено исследование структурных характеристик перспективного материала на основе MoS_2, полученного методом химического осаждения из паровой фазы (CVD). Также представлена оптимизация процесса синтеза для получения желаемой структуры. Оптимальным параметром синтеза методом CVD MoS_2 кристаллов было выявлено максимальная температура сульфуризации 780 °C с выдержкой около 15 минут, температура нагрева зоны источника серы 250 °C, расстояние между источниками серы и молибдена 25 см, а также расстояние между источником молибдена и подложки составляло

	1,5 см. Морфология и элементный состав полученных образцов были изучены с помощью сканирующей электронной микроскопии (СЭМ) с энергодисперсионным рентгеновским спектроскопией (ЭДС). С помощью СЭМ было выявлено, что кристаллы MoS_2 формированы треугольной формы и равномерно распределены по поверхности подложки. Максимальные размеры кристаллитов достигают 6 мкм. ЭДС-картирование кристаллитов подтвердило однородное распределение молибдена и серы в структуре, выявив лишь незначительные вариации состава на границах зерен. Качество, количество слоя образца были изучены с помощью Рамана спектроскопии. Результаты показали два характерных пика (vibrational modes E_{2g}^1 and A_{1g}) наноразмерных MoS_2. Пики имеют острую форму и расположены на расстоянии ≈20,9 $см^{-1}$, что может свидетельствовать о высоком качестве кристаллической структуры полученных кристаллитов. Полученные результаты подчёркивают эффективность выбранного подхода и значимость работы для развития технологий 2D-материалов.
	Ключевые слова: дисульфид молибдена, CVD-синтез, двумерные материалы, Рамановская спектроскопия, морфология.
	Информация об авторах:
Отунчи Еділ	*Магистрант, Физико-технический институт, Satbayev University, 050032, ул. Ибрагимова 11, Алматы, Казахстан. Email: ye.otunchi@sci.kz; ORCID ID: https://orcid.org/0009-0006-4361-8099*
Умирзаков Арман	*PhD докторант, старший научный сотрудник, Физико-технический институт, Satbayev University, 050032, ул. Ибрагимова 11, Алматы, Казахстан. Email: a.umirzakov@sci.kz; ORCID ID: https://orcid.org/0000-0002-0941-0271*
Дмитриева Елена	*Кандидат физико-математических наук, профессор, Физико-технический институт, Satbayev University, 050032, ул. Ибрагимова 11, Алматы, Казахстан. Email: e.dmitriyeva@sci.kz; ORCID ID: https://orcid.org/0000-0002-1280-2559*
Шонғалова Айгуль	*PhD, Физико-технический институт, Satbayev University, 050032, ул. Ибрагимова 11, Алматы, Казахстан. Email: a.shongalova@sci.kz; ORCID ID: https://orcid.org/0000-0002-7352-9007*
Кемелбекова Айнагуль	*PhD, Физико-технический институт, Satbayev University, 050032, ул. Ибрагимова 11, Алматы, Казахстан; Manul technologies, Астана, Казахстан. Email: a.kemelbekova@sci.kz; ORCID ID: https://orcid.org/0000-0003-4813-8490*

References

[1] Ye M, Winslow D, Zhang D, Pandey R, Yap Y. Recent advancement on the optical properties of two-dimensional molybdenum disulfide (MoS_2) thin films. Photonics. 2015; 2(1):288-307. https://doi.org/10.3390/photonics2010288

[2] Tobis M. Controlling structure and morphology of MoS_2 via sulfur precursor for optimized pseudocapacitive lithium intercalation hosts. ChemRxiv. 2024. https://doi.org/10.26434/chemrxiv-2024-7hz4h

[3] Pak S, Lim J, Hong J, Cha S. Enhanced hydrogen evolution reaction in surface functionalized MoS_2 monolayers. Catalysts. 2021; 11(1):70. https://doi.org/10.3390/catal11010070

[4] Zhang G, Liu H, Qu J, & Li J. Two-dimensional layered MoS2: rational design, properties and electrochemical applications. Energy & Environmental Science. 2016; 9(4):1190-1209. https://doi.org/10.1039/c5ee03761a

[5] Khac B, and Chung K. Quantitative assessment of friction characteristics of single-layer MoS_2 and graphene using atomic force microscopy. Journal of Nanoscience and Nanotechnology. 2016; 16(5):4428-4433. https://doi.org/10.1166/jnn.2016.11004

[6] Kong N, Wei B, Li D, Zhuang Y, Sun G, Wang B. A study on the tribological property of MoS_2/Ti– MoS_2/Si multilayer nanocomposite coating deposited by magnetron sputtering. RSC Advances. 2020; 10(16):9633-9642. https://doi.org/10.1039/d0ra01074j

[7] Ermolaev G, Stebunov Y, Vyshnevyy A, Tatarkin D, Yakubovsky D, Novikov S, Volkov V. Broadband optical properties of monolayer and bulk MoS_2. NPJ 2D Materials and Applications. 2020; 4(1). https://doi.org/10.1038/s41699-020-0155-x

[8] Eda G, Yamaguchi H, Voiry D, Fujita T, Chen M, Chhowalla M. Photoluminescence from chemically exfoliated MoS_2. Nano Letters. 2011; 11(12):5111-5116. https://doi.org/10.1021/nl201874w

[9] Lin H, Wang C, Wu J, Xu Z, Huang Y, Zhang C. Colloidal synthesis of MoS_2 quantum dots: size-dependent tunable photoluminescence and bioimaging. New Journal of Chemistry. 2015; 39(11):8492-8497. https://doi.org/10.1039/c5nj01698c

[10] Zhao K. Flexible resistive gas sensor based on molybdenum disulfide-modified polypyrrole for trace NO_2 detection. Polymers. 2024; 16(13):1940. https://doi.org/10.3390/polym16131940

[11] Samy O, Zeng S, Birowosuto M, & Moutaouakil A. A review on MoS_2 properties, synthesis, sensing applications and challenges. Crystals. 2021; 11(4):355. https://doi.org/10.3390/cryst11040355

[12] Zou J, Cai Z, Lai Y, Tan J, Zhang R, Feng S, Cheng HM. Doping concentration modulation in vanadium-doped monolayer molybdenum disulfide for synaptic transistors. ACS Nano. 2021; 15(4):7340-7347. https://doi.org/10.1021/acsnano.0c09349

[13] Pak S. Controlled p-type doping of MoS_2 monolayer by copper chloride. Nanomaterials. 2022; 12(17):2893. https://doi.org/10.3390/nano12172893

[14] Dai X, Du K, Li Z, Liu M, Ma Y, Sun H, Zhang X, Yang Y. Co-doped MoS_2 nanosheets with the dominant CoMoS phase coated on carbon as an excellent electrocatalyst for hydrogen evolution. ACS Applied Materials & Interfaces. 2015; 7(49):27242-27253. https://doi.org/10.1021/acsami.5b08420

[15] Kosnan MA, Azam MA, Munawar RF, Klimkowicz A, Takasaki A. Structural, Morphological, and Electrochemical Properties of MXene/MoS_2-based Supercapacitor. International Journal of Nanoelectronics and Materials (IJNeaM). 2024; 17:263-273. https://doi.org/10.58915/ijneam.v17iJune.867

[16] Morant-Giner M, Brotons-Alcázar I, Shmelev NY, Gushchin AL, Norman LT, Khlobystov AN, & Coronado E. WS_2/MoS_2 heterostructures through thermal treatment of MoS_2 layers electrostatically functionalized with W_3S_4 molecular clusters. Chemistry – A European Journal. 2020; 26(29):6670-6678. https://doi.org/10.1002/chem.202000248

[17] Poudel Y, Sławińska J, Gopal P, Seetharaman S, Hennighausen Z, Kar S, & Neogi A. Absorption and emission modulation in a MoS_2–GaN (0001) heterostructure by interface phonon–exciton coupling. Photonics Research. 2019; 7(12):1511-1520. https://doi.org/10.1364/PRJ.7.001511

[18] Li Z, Bretscher H, Zhang Y, Delport G, Xiao J, Lee A, Rao A. Mechanistic insight into the chemical treatments of monolayer transition metal disulfides for photoluminescence enhancement. Nature Communications. 2021; 12(1):6044. https://doi.org/10.1038/s41467-021-26378-0

[19] Tanoh AOA, Alexander-Webber J, Xiao J, Delport G, Williams CA, Bretscher H, Rao A. Enhancing photoluminescence and mobilities in WS_2 monolayers with oleic acid ligands. Nano Letters. 2019; 19(9):6299-6307 https://doi.org/10.1021/acs.nanolett.9b02431

[20] Wang W, Liu Y, Zeng X. Large size few-layer ambipolar MoS_2 metal-oxide-semiconductor field effect transistors by nitrogen plasma doping. Key Engineering Materials. 2022; 938:89-94. https://doi.org/10.4028/p-h5sa9v

[21] Shaker R, Mohammed S, Abdulsayed Y. Molybdenum disulfide-zirconium dioxide composite with enhance supercapacitance performance. Journal of Metals Materials and Minerals. 2023; 33(4):1791. https://doi.org/10.55713/jmmm.v33i4.1791

[22] Siwińska-Stefańska K, Kurc B, Rymarowicz D, Kubiak A, Piasecki A, Moszyński D, Jesionowski T. Crystallization of TiO_2–MoS_2 hybrid material under hydrothermal treatment and its electrochemical performance. Materials. 2020; 13(12):2706. https://doi.org/10.3390/ma13122706

[23] Ghasemi F, Mohajerzadeh S. Sequential solvent exchange method for controlled exfoliation of MoS_2 suitable for phototransistor fabrication. ACS Applied Materials & Interfaces. 2016; 8(45):31179-31191. https://doi.org/10.1021/acsami.6b07211

[24] Li S, Zhou S, Wang X, Tang P, Pasta M, & Warner J. Increasing the electrochemical activity of basal plane sites in porous 3D edge-rich MoS_2 thin films for the hydrogen evolution reaction. Materials Today Energy. 2019; 13:134-144. https://doi.org/10.1016/j.mtener.2019.05.002

[25] Pudkon W, Bahruji H, Miedziak P, Davies T, Morgan D, Pattisson S, Hutchings G. Enhanced visible-light-driven photocatalytic H_2 production and Cr(VI) reduction of a $ZnIn_2S_4/MoS_2$ heterojunction synthesized by the biomolecule-assisted microwave heating method. Catalysis Science & Technology. 2020; 10(9):2838-2854. https://doi.org/10.1039/d0cy00234h

[26] Zheng W, Wang Q, Li L, Yang R, Zhang G. Monolayer MoS_2 epitaxy. Nano Research. 2020; 14(6):1598-1608. https://doi.org/10.1007/s12274-020-3019-y

[27] Chen S, Gao J, Bharathi M, Zhang Y. A kinetic Monte Carlo study for mono- and bi-layer growth of MoS_2 during chemical vapor deposition. Acta Physico-Chimica Sinica. 2019; 35(10):1119-1127. https://doi.org/10.3866/pku.whxb201812023

[28] Liu L, Liu N, Chen B, Dai C, Wang N. Recent modification strategies of MoS_2 towards electrocatalytic hydrogen evolution. Catalysts. 2024; 14(2):126. https://doi.org/10.3390/catal14020126

[29] Liang J, Wei Z, Wang C, Ma J. Vacancy-induced sodium-ion storage in N-doped carbon nanofiber@MoS_2 nanosheet arrays. Electrochimica Acta. 2018; 285:301-308. https://doi.org/10.1016/j.electacta.2018.07.230

[30] Panjulingam N, Lakshmipathi S. Multiphase MoS_2 monolayer: a promising anode material for Mg-ion batteries. Preprint. 2023. https://doi.org/10.21203/rs.3.rs-3162287/v1

[31] Shinde NB, Francis B, Ramachandra Rao MS, Ryu BD, Chandramohan S, Eswaran SK. Rapid wafer-scale fabrication with layer-by-layer thickness control of atomically thin MoS_2 films using gas-phase chemical vapor deposition. APL Materials. 2019; 7(8):081105. https://doi.org/10.1063/1.5100914

[32] Curtis M, Maryon O, McKibben N, Eixenberger J, Chen C, Chinnathambi K, Estrada D. Assessment of wafer scale MoS_2 atomic layers grown by metal–organic chemical vapor deposition using organo-metal, organo-sulfide, and H_2S precursors. RSC Advances. 2024; 14(31):22618-22626. https://doi.org/10.1039/D4RA04279D

[33] Sun J, Li X, Guo W, Zhao M, Fan X, Dong Y, Fu Y. Synthesis methods of two-dimensional MoS_2: A brief review. Crystals. 2017; 7(7):198. https://doi.org/10.3390/cryst7070198

[34] Suleman M, Lee S, Kim M, Nguyen VH, Riaz M, Nasir N, Seo Y. NaCl-assisted temperature-dependent controllable growth of large-area MoS_2 crystals using confined-space CVD. ACS Omega. 2022; 7(34):30074-30086. https://doi.org/10.1021/acsomega.2c03108

[35] Zhang X, Lee YH, Zhang W, Chang MT, Lin CT, Chang KD, Li LJ. Shape evolution of monolayer MoS_2 crystals grown by chemical vapor deposition. Chemistry of Materials. 2014; 26(22):6371-6379. https://doi.org/10.1021/cm5025662

[36] Chakraborty B, Bera A, Muthu DVS, Bhowmick S, Waghmare UV, Sood AK. Symmetry-dependent phonon renormalization in monolayer MoS_2 transistor. The Journal of Physical Chemistry Letters. 2014; 5(17):2924-2930. https://doi.org/10.1021/jz501230n

[37] Jariwala D, Sangwan VK, Lauhon LJ, Marks TJ, Hersam MC. Emerging device applications for semiconducting two-dimensional transition metal dichalcogenides. Nano Letters. 2014; 14(6):3343-3352. https://doi.org/10.1021/nl501892k

[38] Late DJ, Liu B, Matte HSSR, Dravid VP, Rao CNR. Gas sensing using atomically thin-layered 2D nanomaterials: A review. ACS Applied Materials & Interfaces. 2023; 15(11):13697-13716. https://doi.org/10.1021/acsami.3c04438

Crossref
DOI: 10.31643/2026/6445.39
Engineering and Technology

Use of fly ash and ground tuff as pozzolanic additives in lightweight structural

[1]Zhuginissov M.T., [1]Kuldeyev E.I., [1]Nurlybayev R.E., [1*]Khamza Y.Y., [2]Orynbekov Y.S., [3]Iskakov A.A.

[1] Satbayev University, Almaty, Kazakhstan
[2] LLP International Educational Corporation, Almaty, Kazakhstan
[3] LLP SAVENERGY, Almaty, Kazakhstan

* Corresponding author email: y.khamza@satbayev.university

Received: *April 4, 2025*
Peer-reviewed: *June 4, 2025*
Accepted: *June 11, 2025*

ABSTRACT

This paper investigates the effect of partial replacement of cement with fly ash and ground volcanic tuff on the physical and mechanical properties of concrete. The main focus is on the changes in average density and compressive strength at different contents of replacement materials (from 10% to 35%). The investigated concrete composition (27PPPF) without admixtures has an average density of 1925.5 kg/m³ and compressive strength of 40.1 MPa. The results show that when fly ash is added, the concrete strength first increases, reaching a maximum value of 41.6 MPa at 10% cement replacement and then decreases to 29.1 MPa at 35% replacement. A similar trend is observed when tuff is introduced, but the peak strength (40.7 MPa) is also reached at 10% replacement, after which the strength gradually decreases to 27.9 MPa at 35%. The average density of the specimens changes insignificantly, being in the range of 1910.4-1928.5 kg/m³, which indicates that the dense structure of the concrete is maintained. Thus, the optimum content of fly ash and tuff in the concrete composition is 10-15%, as these values provide the best mechanical characteristics. Higher dosages of substitutes result in lower strength due to thinning of cement stone and lack of binding properties. This study confirms the possibility of using fly ash and volcanic tuff as effective pozzolanic additives to improve the environmental friendliness and sustainability of concrete.

Keywords: fly ash, pozzolanic effect, tuff, binder, lightweight structural concrete.

Information about authors:

Zhuginissov M.T. *Doctor of technical sciences, professor, Satbayev University, Satpayev str., 22, 050013, Almaty, Kazakhstan. Email: m.zhuginissov@satbayev.university; ORCID ID: https://orcid.org/0000-0001-5594-3653*

Kuldeyev E.I. *Professor, Board member - Vice-Rector for Science and Corporate Development, Satbayev University, Satpayev str., 22, 050013, Almaty, Kazakhstan. Email: kuldeyev@satbayev.university; ORCID ID: https://orcid.org/0000-0001-8216-679X*

Nurlybayev R.E. *Doctor of PhD, research professor, Satbayev University, Satpayev str., 22, 050013, Almaty, Kazakhstan. Email: nurlybayev.savenergy@gmail.com; ORCID ID: https://orcid.org/0000-0003-0161-6256*

Khamza Y.Y. *Doctor of PhD, Head of the laboratory of RILA (Research Laboratory of architecture and construction). Satbayev University, Satpayev str., 22, 050013, Almaty, Kazakhstan. Email: y.khamza@satbayev.university; ORCID ID: https://orcid.org/0000-0003-2368-7485*

Orynbekov Y.S. *Candidate of technical sciences, Associate research professor, LLP International Educational Corporation, Ryskulbekov str., 28, 50043, Almaty, Kazakhstan. Email: orynbekov.savenergy@gmail.com; ORCID ID: https://orcid.org/0000-0003-2131-6293*

Iskakov A.A. *Bachelor, Engineer-technologist, LLP SAVENERGY, Akkent Microdistrict, 4, 050038, Almaty, Kazakhstan. Email: isk_888@mail.ru; ORCID ID: https://orcid.org/0000-0002-6403-2066*

Introduction

The use of fly ash from CHP (combined heat and power plant) waste and natural pozzolans in concrete composition as a partial replacement of cement plays an important role in the development of sustainable construction. Cement production is one of the largest sources of CO_2 emissions in the world, and its replacement with secondary and natural materials can significantly reduce the carbon footprint. Fly ash, a by-product of coal combustion, not only reduces the need for clinker cement but also improves the properties of concrete, increasing its strength and durability. Pozzolans such as volcanic tuff and zeolite, reacting with calcium hydroxide formed during cement hydration, promote the formation of additional amounts of strong calcium silicate hydrates, which increases the durability of structures [[1], [2], [3]].

The environmental advantages of such replacement are obvious: utilization of fly ash reduces the volume of waste that would otherwise

accumulate in landfills, polluting soil and water, and the use of pozzolans reduces limestone mining and energy consumption for cement clinker firing. In addition, pozzolanic materials increase concrete's resistance to corrosive environments, reducing the risk of reinforcement corrosion and structural failure. With the global drive to reduce greenhouse gas emissions and rational use of natural resources, the introduction of alternative binders in concrete becomes an important step towards a more environmentally friendly and durable construction industry.

The paper [4] analyzes the use of natural pozzolans such as zeolite and pumcite as a partial replacement of cement in water permeable concrete mixes. The mechanical and hydraulic properties of concrete at different cement replacement percentages (from 0% to 20%) and the effect of plasticizer addition are investigated.

Our study also focused on the development of formulations aimed at reducing cement consumption, a critical step towards more sustainable and cost-effective building materials. Cement production is one of the largest sources of carbon dioxide emissions, making its reduction an important objective in addressing environmental concerns. Reducing cement consumption not only reduces the carbon footprint but also helps to optimize resource utilization without compromising material performance.

To achieve this goal, we investigated the possibility of partially replacing cement with local materials such as ground tuff and fly ash from CHP-2. These materials are by-products or natural resources, which makes them advantageous both economically and environmentally.

This approach is in line with global trends towards sustainable construction and resource management. By using alternative binders, I aim to create lightweight and durable concrete with a lower environmental impact. Such compositions not only advance the science of building materials, but also promote more sustainable construction methods that benefit both industry and the environment.

Several studies have investigated the possibility of using volcanic tuff as a partial replacement for cement in concrete to improve sustainability and reduce environmental impact. For example, studies [5] show the content of natural volcanic tuff in concrete mixtures with replacement levels ranging from 10% to 50%. These studies demonstrate improvements in mechanical properties, such as a 35.6 % increase in flexural strength and a 56.5 % increase in durability by reducing water permeability. The pozzolanic activity of volcanic tuff contributes to the densification of the concrete microstructure (Figure 1), resulting in the following benefits.

Thus, the high pozzolanic activity of natural pozzolanic tuff powder in cement composites is due to the combined action of nucleation, filling and pozzolanic reactions, with the filling and nucleation effects being the dominant factors.

Another study [6] investigated lightweight structural concrete with volcanic tuff and fly ash. This study emphasizes the economic and environmental advantages of using such materials in achieving desired rheological and mechanical properties. In particular, it showed promising applications in self-compacting concrete.

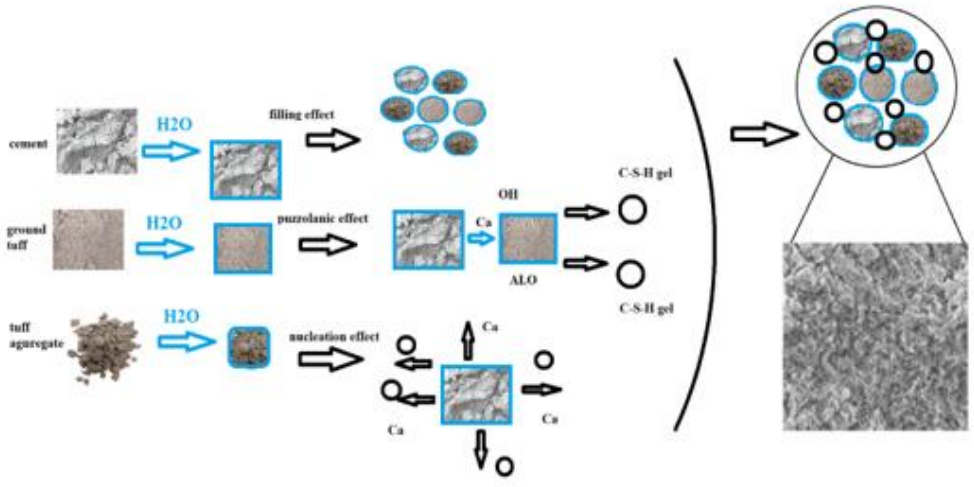

Figure 1 - Improvement of concrete microstructure with volcanic tuff particles and visualization of pozzolanic effect [6]

These findings suggest that volcanic tuff can make a significant contribution to sustainable construction by reducing cement consumption and carbon emissions without compromising concrete performance.

Another study [7] investigated lightweight structural concrete with volcanic tuff and fly ash. This study emphasizes the economic and environmental advantages of using such materials in achieving desired rheological and mechanical properties. In particular, it showed promising applications in self-compacting concrete.

These findings suggest that volcanic tuff can make a significant contribution to sustainable construction by reducing cement consumption and carbon emissions without compromising concrete performance.

Studies show that the use of fly ash in concrete mixtures not only improves strength properties but also significantly reduces cement consumption. Fly ash has pozzolanic activity with respect to cement, which promotes the formation of additional calcium silicate hydrate during concrete curing, improving its durability and strength in the long term.

One of the key benefits is the reduction of environmental impact as fly ash replaces part of the cement, which also contributes to the reduction of CO_2 emissions associated with cement production. Specifically, studies have shown that replacing 15-25% of cement with fly ash can significantly reduce carbon dioxide emissions without significantly compromising the mechanical properties of concrete [8]. In addition, fly ash helps to reduce water consumption and thermal effects during the hydration process, which is particularly important for the development of sustainable and environmentally friendly building materials [9].

Thus, the use of fly ash in concrete mixtures is an effective way to create more sustainable and environmentally friendly building materials while reducing cement costs.

Puzzolan is a material composed of silicates, aluminosilicates or a combination of both. It does not harden on its own when mixed with water. However, when finely ground and in the presence of water at normal temperature, it reacts with calcium hydroxide ($Ca(OH)_2$) to form calcium hydrosilicates and hydroaluminates. These compounds impart strength to the hardened material, similar to the hardening processes of hydraulic binders.

Volcanic tuff is often characterized by a high content of pozzolanic components such as silica and aluminosilicates, making it a valuable raw material for the production of building materials. Due to its high pozzolanic activity, tuff is able to interact effectively with calcium hydroxide in the presence of water to form strong calcium hydrosilicates and hydroaluminates. This property allows it to be used as a natural additive to cements and concretes, improving their strength characteristics, durability and resistance to aggressive media.

Pozzolans are mainly composed of reactive silica (SiO_2) and alumina (Al_2O_3), with smaller amounts of iron oxide (Fe_2O_3) and other oxides. The mass fraction of reactive silica (SiO_2) should be at least 25%.

Fly ash is produced by electrostatic or mechanical precipitation of fine particles from the flue gases from the combustion of pulverized coal or oil shale. The chemical composition of fly ash can be acidic, with high SiO_2 content, or basic, with high CaO content. The acidic ash exhibits pozzolanic properties, while the basic ash can also exhibit hydraulic properties.

The alkali oxide (R_2O) content, converted as Na_2O, should not exceed 2.0% by weight, and the MgO content should not be more than 5%. The loss on ignition of fly ash shall not exceed 5.0%, although fly ash with a loss on ignition of up to 7.0% is acceptable. When fly ash with a loss on ignition above 5.0% but up to 7.0% is used in cement compositions, a maximum loss on ignition of 7% shall be specified on the packaging and in the accompanying documentation. The uniformity of volume change (expansion) of cement with fly ash additives should not exceed 10 mm [10].

The article is devoted to the study of the effect of basaltic pozzolan addition on the strength and durability of concrete. Different levels of cement replacement and their effect on concrete characteristics are considered [11].

Experimental part

Materials. In this paper, cement, ground volcanic tuff, fly ash, tuff sand, tuff crushed stone and polypropylene fiber (PPF) were used as the main components of concrete mixtures. Each of these materials has specific characteristics that affect the properties of the resulting concrete.

Ordinary Portland cement (CEM I 42.5N) was used in the study, produced by HeidelbergCement. Its partial replacement with alternative materials aims to reduce the carbon footprint and improve the durability of the concrete.

Ground volcanic tuff is a natural pozzolan capable of reacting with calcium hydroxide to form

additional calcium silicate hydrates, which helps to increase the density of the cement stone. Volcanic tuff used in this study was obtained from a natural deposit located in the Chundzha region (Almaty oblast, Kazakhstan). The material was preliminarily dried, crushed, and sieved to obtain a powder suitable for use as a mineral additive. Fly ash was sourced from Thermal Power Plant No. 2 (TPP-2) in Almaty.

Fly ash, which is a waste product of coal combustion at thermal power plants, also exhibits pozzolanic properties, improving the structure of concrete and reducing its permeability.

Tuff sand and tuff crushed stone were used as aggregates, which have a porous structure and relatively low density, which can affect the strength properties of concrete. The use of such aggregates makes the concrete lighter and improves its thermal resistance.

In addition, polypropylene fiber (PPF) was introduced into the composition to increase the crack resistance of concrete and prevent shrinkage deformations in the early stages of curing. Polypropylene fibers with a length of 12 mm were used as a reinforcing additive for foam concrete mixtures. The fibers were supplied by LLP "Damu – Khimiya" (Kazakhstan) and were incorporated to enhance the tensile strength, reduce shrinkage cracking, and improve the overall durability of the foam concrete.

The combined use of these materials is aimed at creating a more environmentally friendly and durable concrete by reducing the cement content and improving the performance of the material.

Methods

Elemental analysis of volcanic tuff and fly ash composition. Scanning Electron Microscopy (SEM) and Energy Dispersive X-ray Spectroscopy (EDS) analyses were conducted using a JEOL NeoScope JCM-7000 microscope (JEOL Ltd., Japan) to study the microstructure and elemental composition of the hardened cement matrix. The procedures followed standard protocols for microstructural analysis of cementitious materials, as described in [12]. This state-of-the-art instrument allows for high-resolution imaging and accurate determination of the elemental composition of the materials, making it possible to identify key components in the samples. Using energy dispersive X-ray spectroscopy (EDS), the SEM provided detailed information on the chemical composition of the pellets, including the distribution of silica, alumina and other oxides. The resulting images revealed microstructural features of the granules such as porosity, particle size, and surface morphology. These characteristics are crucial to understanding the pozzolanic activity of the material and its suitability as an additive in cement and concrete. Through this analysis, the reactivity and potential efficacy of volcanic tuff and ash in various applications can be accurately assessed.

The elemental and microstructural analysis performed with the JEOL NeoScope SEM is essential for both scientific research and practical applications. Understanding the composition and structure of volcanic tuffs and ashes helps researchers evaluate their potential as additional cementitious materials. High pozzolanic activity, indicated by the significant presence of reactive silica and alumina, enhances the strength and durability of concrete when these materials are used as additives. SEM images provide insight into how these granules interact in the matrix, affecting factors such as hydration and bonding. These data are not only important for improving material performance, but also contribute to sustainable construction by encouraging the use of natural and industrial by-products. The analysis thus contributes to the development of innovative, environmentally friendly building materials with improved properties.

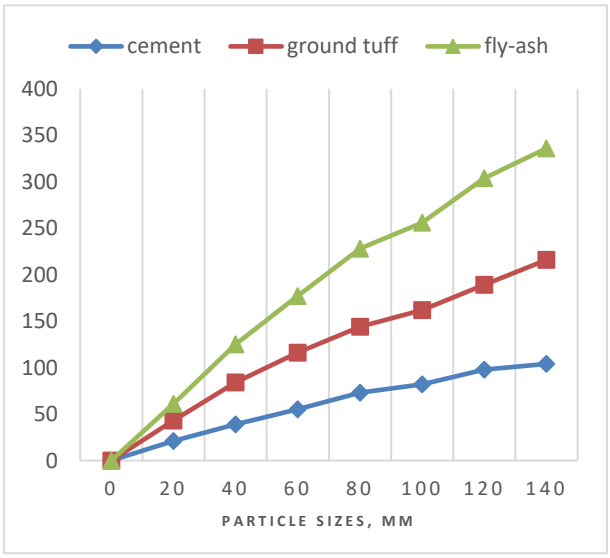

Figure 2 - Granulometric composition of natural volcanic tuff and Portland cement particles

Determination of the fineness of grinding of volcanic tuff and fly ash. The fineness of grinding of volcanic tuff and fly ash of TPP-2 was determined by

the requirements of the standard [13], which sets forth the standard methodology for assessing the fineness of mineral powders. The particle size distribution of natural volcanic tuff and Portland cement, adapted from [14], is shown in Figure 2.

This test is of great importance for assessing the quality of materials used in cement and concrete production, since particle size significantly affects pozzolanic activity, hydration rate and general mechanical properties. The procedure involves determining the residual material on a standard sieve with 45-micron mesh openings. This allows consistent comparison of particle sizes in different samples and ensures that the material meets industry requirements.

The test begins with sample preparation, which is thoroughly dried to remove moisture that could affect the results. A certain mass of material, usually 50 grams, is weighed and placed in a sieve with a mesh size of 45 microns (Figure 3). The sieve is placed on a vibrating bench that is run for 15 minutes to ensure uniform and complete sieving. After sieving, the residue on the sieve is collected and weighed. The percentage of residue is calculated as a fraction of the original mass.

Figure 3 - Determination of grinding fineness of volcanic tuff

The results are then compared with the limit values set by the standard [13]. As a rule, the material is considered fine enough if no more than 10% remains on the sieve. This standard guarantees the high reactivity of the material and its suitability for use in pozzolanic or hydraulic systems. By following this methodology, researchers and manufacturers can guarantee the quality and efficiency of ground volcanic tuff and fly ash in various building materials.

Determination of grinding fineness by specific surface using Le Chatelier's device. The specific surface of ground volcanic tuff and fly ash was determined using the Le Chatelier device (Figure 4) by the standard [13]. This method allows for evaluation of the fineness of grinding by measuring the specific surface of the material (m^2/kg), which is the most important parameter affecting the reactivity, strength set and durability of materials used in cement and concrete. The Le Chatelier method is based on the principle of air permeability, where the time required for air to pass through a compacted specimen serves as an indirect measure of particle size distribution.

To begin the test, the Le Chatelier instrument is calibrated, and the sample is dried to remove moisture. A specified mass of finely ground material, usually 2-5 grams, is weighed and placed in the cell of the instrument. The sample is uniformly compacted using a standard plunger to ensure a consistent packing density. The apparatus is then connected to an air permeation system, and a constant flow of air is passed through the sample.

The time required for a certain volume of air to pass through the sample is recorded. This time is used to calculate the specific surface area of the material using the calibration curve supplied with the instrument. The specific surface area is expressed in square meters per kilogram (m^2/kg).

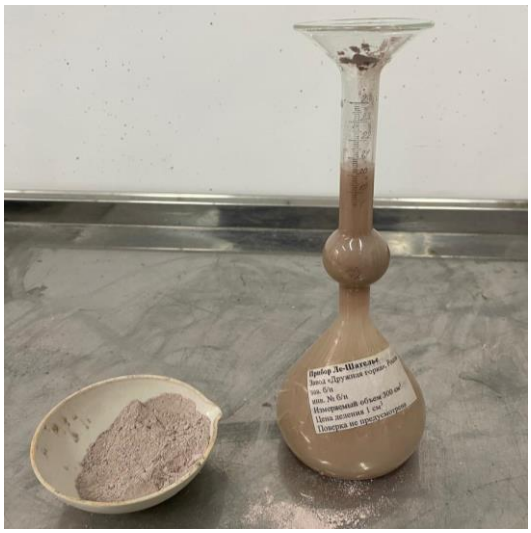

Figure 4 - Determination of specific surface using Le Chatelier's device

The results obtained are compared with the required values for the intended application. For pozzolanic and supplementary cementitious materials, a higher specific surface area usually indicates better reactivity and efficiency in the cement matrix. This method provides a reliable and reproducible way to evaluate the fineness of volcanic tuff and fly ash, ensuring that they meet industry standards for use in building materials.

Selection of lightweight concrete composition using ground tuff and fly ash. To evaluate the potential of volcanic tuff as a partial replacement for cement, a series of concrete mixtures were designed and prepared (Table 1). The mixes included a control mix (27PPF) and variants in which cement was replaced with ground tuff in proportions of 10%, 15%, 20%, 25%, 30% and 35%. In each mix, the ratio of tuff sand, tuff aggregate and polypropylene fibers (PPF) was kept constant at 1.5% by volume to ensure homogeneity of the other components. The water-to-cement (W/C) ratio was adjusted to 0.5 for the control and 10% replacement variants, while for higher percentages of tuff replacement (15% and above), the W/C ratio was increased to 0.6 to account for the altered workability. These adjustments ensured that the mixtures met the practical requirements for casting and testing.

The prepared concrete specimens were subjected to a rigorous testing program to analyze the effect of replacing cement with ground tuff on basic properties such as compressive strength and durability. The objective was to determine the optimum level of replacement that maintains or improves the mechanical performance of the concrete while reducing the cement requirement. This approach not only aims to improve the sustainability of concrete production but also explores the potential of volcanic tuff as a viable supplemental cementitious material to promote resource conservation and environmental improvement.

Table 1 - Selection of formulations with ground tuff as a substitute for binder

No.	Cement, g	Ground tuff, g	Tuff sand, g	Tuff crushed stone, g	Fiber quantity, g	W/C
27PPF	400	-	640	820	6	0.5
27PPF (10%)	360	40	640	820	6	0.5
27PPF (15%)	340	60	640	820	6	0.6
27PPF (20%)	320	80	640	820	6	0.6
27PPF (25%)	300	100	640	820	6	0.6
27PPF (30%)	280	120	640	820	6	0.6
27PPF (35%)	260	140	640	820	6	0.6

Table 2 - Selection of compositions with ash from CHPP 2 as a replacement for the binding agent

No.	Cement, g	Fly-ash, g	Tuff sand, g	Tuff crushed stone, g	Fibres Fibre quantity, g	W/C
27PPF	400	-	640	820	6	0.5
27PPF (10%)	360	40	640	820	6	0.5
27PPF (15%)	340	60	640	820	6	0.6
27PPF (20%)	320	80	640	820	6	0.6
27PPF (25%)	300	100	640	820	6	0.6
27PPF (30%)	280	120	640	820	6	0.6
27PPF (35%)	260	140	640	820	6	0.6

In addition to investigating volcanic tuff as a partial cement replacement, concrete samples were also prepared using CHP-2 fly ash as a binder (Table 2).

For uniformity, the same mix proportions were followed, with cement being partially replaced by fly ash in percentages of 10%, 15%, 20%, 25%, 30% and 35%. In these mixtures, the same aggregate composition, including tuff sand and tuff aggregate, was maintained, and polypropylene fibers (PPF) were added at a dosage of 1.5% by volume. We can observe the manufactured specimens in Figure 5. The water-to-cement ratio (W/C) was also adjusted, kept at 0.5 for the control mix and the mix with 10% ash, and increased to 0.6 for mixes with 15% and above to ensure sufficient workability during casting.

The prepared concrete specimens were subjected to a rigorous testing program to analyze the effect of replacing cement with ground tuff on basic properties such as compressive strength and durability. The objective was to determine the optimum level of replacement that maintains or improves the mechanical performance of the concrete while reducing the cement requirement. This approach not only aims to improve the sustainability of concrete production but also explores the potential of volcanic tuff as a viable supplemental cementitious material to promote resource conservation and environmental improvement.

In addition to investigating volcanic tuff as a partial cement replacement, concrete samples were also prepared using CHP-2 fly ash as a binder (Table 2).

For uniformity, the same mix proportions were followed with cement being partially replaced by fly ash in percentages of 10%, 15%, 20%, 25%, 30% and 35%. In these mixtures, the same aggregate composition, including tuff sand and tuff aggregate, was maintained, and polypropylene fibers (PPF) were added at a dosage of 1.5% by volume. We can observe the manufactured specimens in Figure 5. The water-to-cement ratio (W/C) was also adjusted, kept at 0.5 for the control mix and the mix with 10% ash, and increased to 0.6 for mixes with 15% and above to ensure sufficient workability during casting.

Specimens were prepared to analyze and compare the performance of concrete with volcanic tuff and fly ash as a partial replacement for cement. The testing of properties such as compressive strength and durability is aimed at determining the most effective use of these alternative materials in concrete production.

Figure 5 - Concrete samples with CHPP 2 ash as a partial replacement of binder

The use of fly ash, a by-product of thermal power plants, is in line with the Sustainable Development Goals by utilising industrial waste and potentially improving concrete properties. This parallel study allows a comprehensive evaluation of the environmental and mechanical benefits of these supplementary cementitious materials.

Results and Discussion

1) Chemical composition. Volcanic tuff is characterized by a high SiO content of 69.26 %, determined by X-ray spectral microanalysis (EDS) on an electron probe microanalyzer JCTXA-733. We can observe the percentage of chemical composition in Table 3. This significant proportion of silica indicates a high silicate content, which corresponds to the classification of pozzolans according to standard [10]. According to this standard, the minimum silica content requirement for materials classified as pozzolans is 25%. The exceptionally high silica content in volcanic tuff not only meets but also significantly exceeds this threshold, which allows the finely ground tuff to be classified as pozzolanic materials.

Table 3 - Chemical composition of volcanic tuff

Compound, % by mass								
SiO_2	Al_2O_3	K_2O	Na_2O	CaO	FeO	MgO	TiO_2	MnO
69.26	16.04	6.24	3.44	2.46	1.57	0.57	0.14	0.28

Figure 6 is an energy dispersive X-ray spectrum (EDS) obtained using a JEOL scanning electron microscope. The spectrum shows the presence of the main elements that make up the material, including aluminum (Al), silicon (Si), calcium (Ca), iron (Fe), magnesium (Mg), potassium (K), titanium (Ti), and oxygen (O), confirming its mineral nature. The most intense peaks correspond to AlKα and

SiKα, indicating a high content of aluminosilicate phases characteristic of fly ash. The results confirm the chemical composition of the material and its potential as a pozzolanic admixture in concrete.

These data confirm the possibility of using finely ground volcanic tuff as a partial replacement for traditional binders in cement systems. The pozzolanic properties of the material, due to its high silica content, increase its ability to react with calcium hydroxide during the hydration process, improving the durability and mechanical properties of concrete.

This application is consistent with sustainable construction practices, as it reduces the need for conventional Portland cement, which produces significant CO_2 emissions. The use of volcanic tuff in this context represents an environmentally friendly alternative that allows the use of natural resources while maintaining the quality standards required for modern construction.

In the article [15], chemical parameters of fly ash obtained at Almaty CHPP-2 were determined, including the content of silicon (SiO2), titanium (TiO2), aluminum (Al2O3), iron (Fe2O3), calcium (CaO), magnesium (MgO), sodium (Na2O), potassium (K2O) oxides and other impurities. The results show that the highest content in the ash is silicon oxide (65.0-65.9%), which is typical for materials used in construction, such as cement. Variations in the content of other oxides were also assessed, which allows for a better understanding of the properties and possible applications of this ash in various industries, such as in the production of building materials or in improving soil quality.

Figure 7 shows us fly ash particles captured on an electronic scanning microscope.

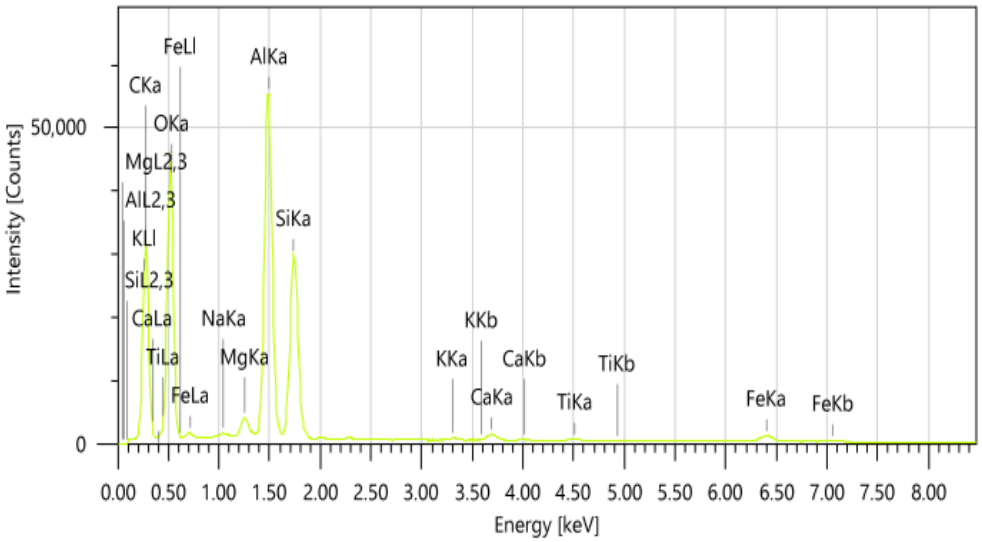

Figure 6 – X-ray energy dispersion analysis (EDS) of fly ash from CHPP 2

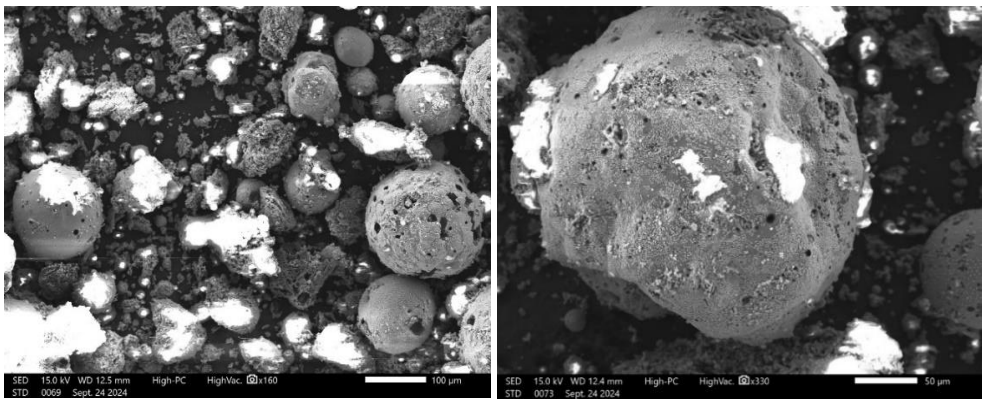

Figure 7 – Scanning electron microscope images of ash from CHPP 2

2) The fineness of grinding of crushed tuff and fly ash was determined in accordance standard [16], which evaluates the material retained on a sieve with a mesh size of 0.08 mm. For both tuff and fly ash, the fineness values were slightly higher than for cement, indicating a somewhat coarser particle distribution. Despite this, the obtained values are in the acceptable range for use as additional cement materials. The grinding process achieved a sufficient reduction in particle size, which ensures good compatibility with cement for partial replacement. The residue on a 0.08 sieve for ground tuff was on average 8.5%, while for ash, this figure was 11.5%. At the same time, the norm for standard cement is no more than 10%.

The slightly higher fineness values for tuff and fly ash reflect their natural characteristics and production processes. However, these results indicate that both materials are reactive enough to contribute to the cement matrix and participate effectively in hydration reactions. These characteristics make them suitable for use in concrete mixtures where partial replacement of cement is required, offering potential environmental benefits and reducing the carbon footprint. In addition, their fineness allows them to mix well with other components of the mixture, while maintaining the required workability and strength development properties of concrete.

The article [17] discusses how the degree of dispersion of components such as lime and slag affects the physical and mechanical properties of autoclaved materials. Reducing the grain size of the binder components helps to improve these properties, but if the grinding is too fine, the particles may stick together, which leads to the opposite effect.

3) The specific surface area of ground tuff and fly ash was determined by GOST 310.2-76. The obtained values were within the standard range for cement. The specific surface area of ground tuff was 241 m²/kg, which is slightly lower than the typical value for ordinary Portland cement. This result indicates good fineness of tuff, which makes it suitable for use as a partial replacement for cement in concrete. A higher specific surface area increases the reactivity of the material, positively affecting the cementitious properties of the mixture.

Several studies have examined the effect of the specific surface area of ash on the properties of building materials. It has been established that an increase in the dispersion of ash, for example, from hydrodecarbonization, increases its pozzolanic activity, which improves the mechanical properties of concrete and the durability of materials. Studies show that optimizing the degree of grinding of ash, with a specific surface area above 250 m²/kg, helps to increase the strength and efficiency of its use in cement and concrete mixtures [[18], [19], [20]].

Similarly, the specific surface area of fly ash was determined to be 229 m²/kg, which is also within the acceptable range. This value confirms the potential of fly ash to be used as a supplementary cementitious material. Sufficient fineness ensures that the material can combine well with cement and contribute to the compaction of the microstructure. Both materials show promise in reducing cement consumption while maintaining or improving the performance of concrete.

4) Strength properties were also determined according to standards, and cube specimens were prepared and tested using a hydraulic press. The specimens included mixtures with ground tuff and fly ash as a partial replacement for cement. The cubes were prepared according to standard procedures to ensure consistency and reliability of the results. The tests were conducted to evaluate the compressive strength of these modified mixtures at different curing times. The inclusion of ground tuff and fly ash was aimed at assessing their effect on the mechanical properties of concrete. The results obtained on the hydraulic press provided valuable information on the feasibility of using these materials as additional cementing components while maintaining or increasing the overall strength of concrete.

The effect of fly ash and pozzolan additives on the strength of concrete has been studied in various studies. In one of them, when replacing up to 40% of cement with ash additives, the strength of concrete after 28 days remained close to the control, and after 60 days it was almost equal to the strength of concrete without the additive. In another study, the use of fly ash and microsilica as mineral additives in concrete showed an increase in compressive strength compared to the control composition. Also, in a study of the effect of pozzolanic additives such as fly ash and metakaolin on the reaction of alkali with silica, a decrease in the expansion of concrete was observed, indicating a positive effect of these additives on strength characteristics. Finally, a study of the effect of ash residues from the processing of municipal solid waste on the properties of concrete showed that concrete with an ash content of 10-20% has the highest compressive strength, reaching about 60 MPa [[21], [22], [23], [24]].

Table 4 – Strength and average density indicators of lightweight concrete using ground tuff and ash as a partial replacement of the binder

No.	Ash or tuff content, %	Average density, kg/m^3	Compressive strength, MPa
27PPF	-	1925.5	40.1
27PPF Tuff	10	1927.0	40.7
27PPF Tuff	15	1928.5	39.6
27PPF Tuff	20	1924.6	37.7
27PPF Tuff	25	1926.8	32.1
27PPF Tuff	30	1920.2	28.3
27PPF Tuff	35	1926.3	27.9
27PPF Fly-ash	10	1924.6	41.6
27PPF Fly-ash	15	1919.5	40.4
27PPF Fly-ash	20	1914.8	38.5
27PPF Fly-ash	25	1913.6	35.8
27PPF Fly-ash	30	1914.5	30.7
27PPF Fly-ash	35	1910.4	29.1

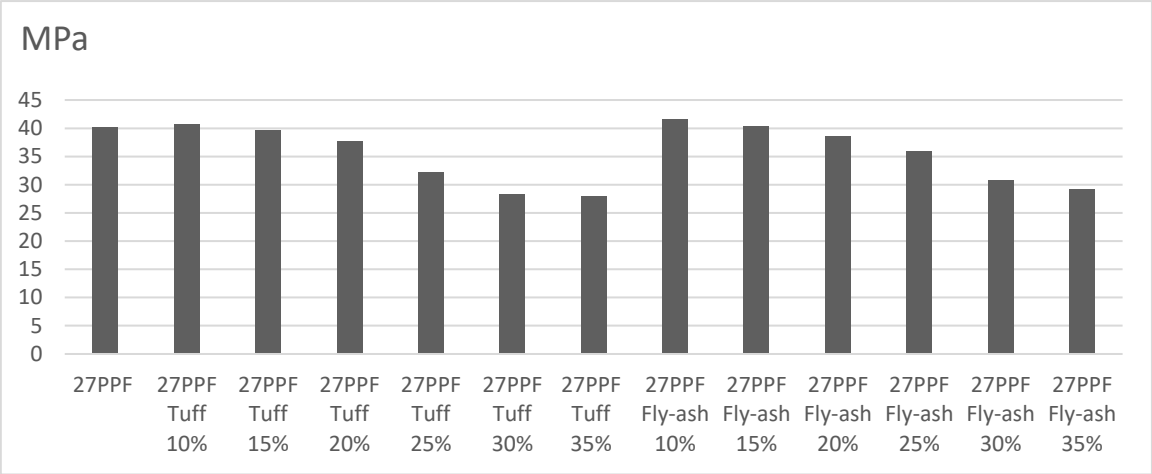

Figure 8 – Graph of the dependence of the strength indicator on the amount of ground tuff and ash as a partial replacement for the binder

The data demonstrate the effect of replacing cement with ground tuff or fly ash on the average density and compressive strength of 27PPF concrete mixtures. For both admixtures, the compressive strength generally decreases with increasing replacement percentage. This trend is more pronounced at higher substitution levels, indicating that excessive cement substitution may weaken the concrete matrix, probably due to a decrease in the binder properties of the mixture, as can be seen in Table 4.

In the case of ground tuff, the compressive strength remains relatively stable up to 15% replacement, after which a slight decrease is observed. After this point, the strength decrease becomes significant, decreasing to 37.7 MPa at 20% and further to 27.9 MPa at 35%. Similarly, the density of the mixtures fluctuates slightly but remains within a narrow range, indicating that the influence of ground tuff on the bulk properties of the material is minimal until higher substitution levels. In Figure 8, we can see the strength as a function of the percentage of ground tuff and ash.

A similar trend is observed for fly ash mixtures, although the compressive strength values are slightly higher compared to tuff at equivalent substitution levels. At 10% ash replacement, the compressive strength increases to 41.6 MPa, indicating the potential of ash to improve early performance. However, when the substitution level reaches 30-35%, the strength drops below 31 MPa, similar to tuff mixtures.

Overall, these results indicate that moderate replacement (10-15%) of ground tuff or fly ash can

maintain acceptable strength and density, while higher replacement levels degrade mechanical performance. Fly ash appears to provide superior performance compared to tuff, especially at lower substitution rates.

Conclusions

1. The results indicate that partial replacement of cement with ground volcanic tuff and fly ash at moderate levels (10–15%) maintains compressive strength and density within acceptable limits, demonstrating the potential of these materials as supplementary cementitious components. Ground tuff shows relatively stable performance with a slight decrease in strength and density, while fly ash exhibits an early strength gain due to its pozzolanic activity, which enhances matrix compaction during the initial hardening phase.

2. At higher substitution rates (20% and above), both materials cause a significant reduction in compressive strength, more pronounced for volcanic tuff, where strength drops below 30 MPa at 35% replacement, limiting its suitability for high-performance concrete applications. Fly ash performs slightly better under similar conditions but still leads to considerable strength loss, emphasizing the need for careful optimization of replacement levels to ensure structural integrity.

3. The chemical composition of volcanic tuff, with a high silica content (69.26% SiO_2), confirms its pozzolanic nature and suitability for partial cement replacement. This contributes to the environmental benefits of reducing cement consumption and associated carbon emissions in concrete production.

4. Although the particle size distribution of volcanic tuff and fly ash is coarser compared to conventional cement, their fineness remains within acceptable ranges that allow effective participation in hydration reactions. This supports their positive effect on the mechanical properties of the resulting concrete mixtures.

5. Strength testing confirms that cement replacement up to 15% with either ground volcanic tuff or fly ash does not compromise concrete performance and may slightly improve early strength in the case of fly ash. These findings highlight the potential of both materials to serve as sustainable alternatives in cementitious systems without significant loss of mechanical properties.

Conflicts of interest. On behalf of all the authors, the corresponding author declares that there is no conflict of interest.

CRediT author statement: **R. Nurlybayev, M. Zhuginissov and E. Kuldeyev:** Conceptualization; **M. Zhuginissov and Y. Khamza:** Methodology; **Y. Khamza, Y. Orynbekov and A. Iskakov:** Software; **R. Nurlybayev, M. Zhuginissov and Y. Orynbekov:** Formal analysis; **M. Zhuginissov and Y. Khamza:** Writing—original draft preparation; **E. Kuldeyev and R. Nurlybayev:** Visualization, Project administration, Funding acquisition. All authors have read and agreed to the published version of the manuscript.

Acknowledgements. This research is funded by the Committee of Science of the Ministry of Science and Higher Education of the Republic of Kazakhstan (Grant No. BR21882292 – “Integrated development of sustainable construction industries: innovative technologies, optimization of production, effective use of resources and creation of technological park”).

Cite this article as: Zhuginissov MT, Kuldeyev EI, Nurlybayev RE, Khamza YY, Orynbekov YS, Iskakov AA. Use of fly ash and ground tuff as pozzolanic additives in lightweight structural concrete composition. Kompleksnoe Ispolzovanie Mineralnogo Syra = Complex Use of Mineral Resources. 2026; 339(4):38-51. https://doi.org/10.31643/2026/6445.39

Жеңіл конструкциялық бетон құрамында пуццоландық қоспалар ретінде күлді және ұнтақталған туфты қолдану

[1]Жугинисов М.Т., [1]Кульдеев Е.И., [1]Нурлыбаев Р.Е., [1*]Хамза Е.Е., [2]Орынбеков Е.С., [3]Искаков А.А.

[1] Сәтбаев Университеті, Алматы, Қазақстан
[2] ЖШС Халықаралық Білім Беру Корпорациясы, Алматы, Қазақстан
[3] ЖШС SAVENERGY, Алматы, Қазақстан

Мақала келді: *4 сәуір 2025*
Сараптамадан өтті: *4 маусым 2025*
Қабылданды: *11 маусым 2025*

ТҮЙІНДЕМЕ

Бұл жұмыста цементті ұшпа күлмен және ұнтақталған жанартаулық туфпен (туф-құрылыс материалы ретінде қолданылатын тау жынысы) ішінара ауыстырудың бетонның физика-механикалық қасиеттеріне әсері зерттеледі. Негізгі назар материалдардың әртүрлі құрамындағы орташа тығыздық пен қысу беріктігінің өзгеруіне (10%-дан 35%-ға дейін) аударылады. Зерттелетін қоспасыз бетон құрамының (27PPPF) орташа тығыздығы 1925,5 кг/м³ және қысымға беріктігі 40,1 МПа. Нәтижелер ұшпа күлді қосқанда алдымен бетонның беріктігі артып, цементті 10% ауыстырғанда максималды мәнге 41,6 МПа жетеді, содан кейін 35% ауыстырғанда 29,1 МПа дейін төмендейтінін көрсетеді. Осыған ұқсас үрдіс туфты енгізген кезде байқалады, бірақ беріктік шыңына (40,7 МПа) 10% ауыстыру кезінде де жетеді, содан кейін беріктік 35% кезінде 27,9 МПа дейін біртіндеп төмендейді. Үлгілердің орташа тығыздығы шамалы өзгереді, 1910,4-1928,5 кг/м³ аралығында болады, бұл бетонның тығыз құрылымының сақталғанын көрсетеді. Осылайша, бетон құрамындағы ұшпа күл мен туфтың оңтайлы мөлшері 10-15% құрайды, өйткені бұл көрсеткіштер ең жақсы механикалық сипаттамалар береді. Ауыстырылатын заттардың жоғары дозалары цемент тасының жұқаруы мен байланыстырушы қасиеттерінің болмауына байланысты беріктіктің төмендеуіне әкеледі. Бұл зерттеу бетонның экологиялық тазалығы мен тұрақтылығын арттыру үшін тиімді пуццоландық қоспалар ретінде ұшпа күлді және жанартау туфын пайдалану мүмкіндігін растайды.

Түйін сөздер: ұшпа күл, пуццоландық әсер, туф, байланыстырғыш, жеңіл конструкциялық бетон.

Авторлар туралы ақпарат:

Жугинисов М.Т. *Техника ғылымдарының докторы, профессор, Сәтбаев Университеті, Сәтбаев к-сі, 22, 050013, Алматы, Қазақстан. Email: m.zhuginissov@satbayev.university; ORCID ID: https://orcid.org/0000-0001-5594-3653*

Кульдеев Е.И. *Профессор, Басқарма мүшесі — Ғылым және корпоративтік даму жөніндегі проректор, Сәтбаев Университеті, Сәтбаев к-сі, 22, 050013, Алматы, Қазақстан. Email: kuldeyev@satbayev.university; ORCID ID: https://orcid.org/0000-0001-8216-679X*

Нурлыбаев Р.Е. *PhD докторы, зерттеуші профессор, Сәтбаев Университеті, Сәтбаев к-сі, 22, 050013, Алматы, Қазақстан. Email: nurlybayev.savenergy@gmail.com; ORCID ID: https://orcid.org/0000-0003-0161-6256*

Хамза Е.Е *PhD докторы, Сәулет және құрылыс ғылыми-зерттеу зертханасының меңгерушісі, Сәтбаев Университеті, Сәтбаев к-сі, 22, 050013, Алматы, Қазақстан. Email: y.khamza@satbayev.university; ORCID ID: https://orcid.org/0000-0003-2368- 7485*

Орынбеков Е.С. *Техника ғылымдарының кандидаты, Қауымдастырылған профессор-зерттеуші, ЖШС Халықаралық білім беру корпорациясы, Рысқұлбеков көшесі, 28, 50043, Алматы, Қазақстан. Email: orynbekov.savenergy@gmail.com; ORCID ID: https://orcid.org/0000-0003-2131-6293*

Искаков А.А *Бакалавр, инженер-технолог, SAVENERGY ЖШС, Ақкент ықшам ауданы, 4, 050038, Алматы, Қазақстан. Email: isk_888@mail.ru; ORCID ID: https://orcid.org/0000-0002-6403-2066*

Использование летучей золы и молотого туфа в качестве пуццолановых добавок в составе легкого конструкционного бетона

[1]Жугинисов М.Т., [1]Кульдеев Е.И., [1]Нурлыбаев Р.Е., [1*]Хамза Е.Е., [2]Орынбеков Е.С., [3]Искаков А.А.

[1] Satbayev University, Алматы, Казахстан
[2] ТОО Международная образовательная корпорация, Алматы, Казахстан
[3] ТОО SAVENERGY, Алматы, Казахстан

Поступила: *4 апреля 2025*
Рецензирование: *4 июня 2025*
Принята в печать: *11 июня 2025*

АННОТАЦИЯ

В данной статье исследуется влияние частичной замены цемента летучей золой и молотым вулканическим туфом на физические и механические свойства бетона. Основное внимание уделяется изменениям средней плотности и прочности на сжатие при различных содержаниях заменяющих материалов (от 10% до 35%). Исследуемый бетонный состав (27PPF) без добавок имеет среднюю плотность 1925,5 кг/м³ и прочность на сжатие 40,1 МПа. Результаты показывают, что при добавлении золы уноса прочность бетона сначала увеличивается, достигая максимального значения 41,6 МПа при 10% замещения цемента, после чего снижается до 29,1 МПа при 35% замены. Аналогичная тенденция наблюдается и при введении туфа, однако пик прочности (40,7 МПа) достигается также при 10% замены, после чего прочность постепенно уменьшается до 27,9 МПа при 35%. Средняя плотность образцов изменяется незначительно, находясь в диапазоне 1910,4–1928,5 кг/м³, что свидетельствует о сохранении плотной структуры бетона. Таким образом, оптимальное

	содержание летучей золы и туфа в составе бетона составляет 10–15%, поскольку при этих значениях обеспечиваются наилучшие механические характеристики. Более высокие дозировки заменителей приводят к снижению прочности, что объясняется разрежением цементного камня и недостатком вяжущих свойств. Данное исследование подтверждает возможность использования летучей золы и вулканического туфа в качестве эффективных пуццолановых добавок, способствующих повышению экологичности и устойчивости бетона.
	Ключевые слова: летучая зола, пуццолановый эффект, туф, вяжущее вещество, легкий конструкционный бетон.
Жугинисов М.Т.	***Информация об авторах:*** *Доктор технических наук, профессор, Satbayev University, ул. Сатпаева, 22, 050013, Алматы, Казахстан. Email: m.zhuginissov@satbayev.university; ORCID ID: https://orcid.org/0000-0001-5594-3653*
Кульдеев Е.И.	*Профессор, член Правления — Проректор по науке и корпоративному развитию, Satbayev University, ул. Сатпаева., 22, 050013, Алматы, Казахстан. Email: kuldeyev@satbayev.university; ORCID ID: https://orcid.org/0000-0001-8216-679X*
Нурлыбаев Р.Е.	*Доктор PhD, профессор-исследователь, Satbayev University, ул. Сатпаева, 22, 050013, Алматы, Казахстан. Email: nurlybayev.savenergy@gmail.com; ORCID ID: https://orcid.org/0000-0003-0161-6256*
Хамза Е.Е	*Доктор PhD, заведующий лабораторией НИЛАС (Научноисследовательская лаборатория архитектуры и строительства), Satbayev University, ул. Сатпаева, 22, 050013, Алматы, Казахстан. Email: y.khamza@satbayev.university; ORCID ID: https://orcid.org/0000-0003-2368-7485*
Орынбеков Е.С.	*Кандидат технических наук, ассоциированный профессор-исследователь, ТОО Международная образовательная корпорация, ул. Рыскулбекова, 28, 50043, Алматы, Казахстан. Email: orynbekov.savenergy@gmail.com; ORCID ID: https://orcid.org/0000-0003-2131-6293*
Искаков А.А	*Бакалавр, инженер-технолог, ТОО SAVENERGY, микрорайон Аккент, 4, 050038, Алматы, Казахстан. Email: isk_888@mail.ru; ORCID ID: https://orcid.org/0000-0002-6403-2066*

References

[1] Khoshroo M, Shirzadi Javid AA, Shalchiyan M, et al. Evaluation of Mechanical and Durability Properties of Concrete Containing Natural Chekneh Pozzolan and Wood Chips. Iran J Sci Technol Trans Civ Eng. 2020; 44:1159-1170. https://doi.org/10.1007/s40996-019-00305-8

[2] Htwe KS, Mon YPP. Effect of Natural Pozzolan on Carbonation and Chloride Penetration in Sustainable Concrete. Int J Adv Sci Eng Inf Technol. 2018; 8(4):1049-1054. https://ijaseit.insightsociety.org/index.php/ijaseit/article/view/4340

[3] Annune JE, Yohanna A, Oguche CA, Wali CB. Experimental Research on Natural Pozzolan as Cement Replacement. ABUAD Int J Nat Appl Sci. 2023; 3(1):28–33. https://journals.abuad.edu.ng/index.php/aijnas/article/view/140

[4] Oviedo I, Pradena M, Link Ó, Balbo JT. Using Natural Pozzolans to Partially Replace Cement in Pervious Concretes: A Sustainable Alternative? Sustainability. 2022; 14(21):14122. https://doi.org/10.3390/su142114122

[5] Abutaqa A, Mohsen MO, Aburumman MO, et al. Eco-Sustainable Cement: Natural Volcanic Tuffs' Impact on Concrete Strength and Durability. Buildings. 2024; 14(9):2902. https://doi.org/10.3390/buildings14092902

[6] Golewski GL. The Role of Pozzolanic Activity of Siliceous Fly Ash in the Formation of the Structure of Sustainable Cementitious Composites. Sustain. Chem. 2022; 3(4):520-534. https://doi.org/10.3390/suschem3040032

[7] Musungu Khaoya L, Abuodha S, Mwero JN. Effects of Volcanic Tuff Use on the Rheological and Mechanical Properties of Self-Compacting Concrete. DJES. 2024; 17(3):78–97.

[8] Hardjito D. The Use of Fly Ash to Reduce the Environmental Impact of Concrete. EnCon2007. Kuching, Malaysia. 2007.

[9] Onyelowe KC, Kontoni D-PN, Ebid AM, et al. Multi-Objective Optimization of Sustainable Concrete Containing Fly Ash Based on Environmental and Mechanical Considerations. Buildings. 2022; 12(7):948. https://doi.org/10.3390/buildings12070948

[10] GOST 31108-2020. Cements. Technical Specifications.

[11] Moawad MS, Younis S, Ragab AER. Assessment of the Optimal Level of Basalt Pozzolana Blended Cement Replacement Against Concrete Performance. J Eng Appl Sci. 2021; 68:42. https://doi.org/10.1186/s44147-021-00046-4

[12] GOST 30744-2001. Cements. Testing Methods Using Polyfractional Sand.

[13] ASTM C1723-10(2015), Standard Guide for Examination of Hardened Concrete Using Scanning Electron Microscopy.

[14] Cobîrzan N, Thalmaier G, Balog A-A, Constantinescu H, Ceclan A, Nasui M. Volcanic Tuff as Secondary Raw Material in the Production of Clay Bricks. Materials 2021; 14(22):6872. https://doi.org/10.3390/ma14226872

[15] Zhuginissov M, Kuldeyev Y, Nurlybayev R, et al. Lightweight Structural Thermal Insulation Concrete Using TPP Ash. Kompleksnoe Ispolzovanie Mineralnogo Syra = Complex Use of Mineral Resources. 2024; 336(1):74–85. https://doi.org/10.31643/2026/6445.07

[16] GOST 310.2-76 Cements. Methods for Determining Fineness of Grinding.

[17] Isaenko AV, Aleksandrova TI. Vliyanie tonkosti pomola negashenoy izvesti na filtratsionnye svoystva shlako-izvestkovykh avtoklavnykh materialov [Influence of the Fineness of Quicklime Grinding on the Filtration Properties of Slag-Lime Autoclaved Materials]. Vestnik Severo-Vostochnogo federalnogo universiteta im. M. K. Ammosova = Bulletin of the North-Eastern Federal University Named After M.K. Ammosov. 2011; 8(2):67–69. (in Russ.). https://cyberleninka.ru/journal/n/vestnik-severo-vostochnogo-federalnogo-universiteta-im-m-k-ammosova?i=1144573

[18] Rashchupkina MA. Vliyanie dispersnosti zoly gidroudaleniya Ekibastuzskikh ugley i dobavki zhidkogo stekla na svoystva melkozernistogo betona [Influence of the Dispersity of Hydraulically Removed Ash from Ekibastuz Coals and the Addition of Liquid Glass on the Properties of Fine-Grained Concrete] (PhD dissertation). Novosibirsk, 2009. VAK RF Specialty 05.23.05. (in Russ.). https://tekhnosfera.com/vliyanie-dispersnosti-zoly-gidroudaleniya-ekibastuzskih-ugley-i-dobavki-zhidkogo-stekla-na-svoystva-melkozernistogo-beton?utm

[19] Kozhikov SN, Dzhusupova MA. Razrabotka sostavov kompozitsionnykh vyazhushchikh veshchestv i izdeliy na ego osnove s ispolzovaniem zoly Ekibastuzskoy TEC [Development of Composite Binders and Products Based on Them Using Ekibastuz TPP Ash.]. Mekhanika i tekhnologii = Mechanics and Technologies. Scientific Journal. 2024; 3(85):240-246. (in Russ.). https://doi.org/10.55956/GJDU7225

[20] Izotov VS, Mukhametrakhimov RH. Vliyanie tonkosti pomola kvartsevogo peska na fiziko-tekhnicheskie svoystva avtoklavirovannykh fibrotsementnykh plit [Influence of Quartz Sand Grinding Fineness on the Physico-Technical Properties of Autoclaved Fiber Cement Boards]. Stroitel'nye materialy, oborudovanie, tekhnologii XXI veka. Krovel'nye i izolyatsionnye materialy = Construction Materials, Equipment, Technologies of the XXI Century. 2013; (10):22–23. (in Russ.). https://rucont.ru/efd/425508?utm

[21] Nath P, Sarker P. Effect of Fly Ash on the Durability Properties of High Strength Concrete. Procedia Engineering. 2011; 14:1149-1156. https://doi.org/10.1016/j.proeng.2011.07.144

[22] Safonov VD, Petrova SP. Analiticheskiy obzor primeneniya zoly TEC v proizvodstve betona [Analytical review of the application of thermal power plant ash in concrete production]. Molodoy uchyonyy = Young scientist. 2020, 13(303):25-28. (in Russ.). https://moluch.ru/archive/303/68468/?utm

[23] Sokolov AA. Vliyanie puccolanovuh dobavok na beton [Influence of Pozzolanic Additives on Concrete]. Jcement.ru. (in Russ.). https://jcement.ru/magazine/vypusk-1-391/vliyanie-puttssolanovykh-dobavok-v-betonakh-na-reaktsiyu-shchelochi-s-kremnezemom-pri-postuplenii-shch/?utm

[24] Ivanov AN, Petrov IM. Issledovanie vliyaniya zolnyh ostatkov pererabotki tverdyh bytovyh othodov na svoistva cementa I betonov na ego osnove [Study of the Influence of Ash Residues from Municipal Waste Processing on the Properties of Concrete]. Cyberleninka.ru. (in Russ.). https://cyberleninka.ru/article/n/issledovanie-vliyaniya-zolnyh-ostatkov-pererabotki-tverdyh-bytovyh-othodov-na-svoystva-tsementa-i-betonov-na-ego-osnove?utm

Crossref
DOI: 10.31643/2026/6445.40
Engineering and Technology

Review of Sustainable Jet Fuel Production through Pyrolysis of Waste Tires: Process, The Physicochemical Properties and Catalyst

[1,2]Fitrianto, [1]Nandy Putra, [1*]Eny Kusrini

[1]Universitas Indonesia, Jl. Lingkar, Pondok Cina, Kecamatan Beji, Kota Depok, Jawa Barat 16424, Indonesia
[2]National Research and Innovation Agency (BRIN), Serpong, 10340 Banten, Indonesia

**Correspondence email: eny.k@ui.ac.id*

Received: *June 2, 2025*
Peer-reviewed: *June 4, 2025*
Accepted: *June 11, 2025*

ABSTRACT
Solid waste, including waste tires, contributes significantly to global environmental pollution, with approximately one billion used tires generated annually. The use of waste tires as a source of sustainable aviation fuel (SAF) has the advantage of not competing with food sources, thus supporting energy needs without sacrificing food security. However, the production of jet fuel from waste tire pyrolysis oil faces major challenges to meet stringent American Society for Testing and Materials (ASTM) quality standards. This article reviews the physicochemical properties of waste tire pyrolysis oil, including viscosity, density, and sulfur content, and compares them with ASTM jet fuel specifications. A bibliometric analysis is carried out on the development of fuel research from waste tires being converted to jet fuel by collecting the number of papers and documents, the number of citations, and the countries that produce the most papers related to waste tires and their research. The development of catalysts for jet fuel production in the cracking process was also discussed in detail. The use of waste tire pyrolysis oil in jet engines was also reviewed as an initial step towards implementing sustainable fuels in the aviation sector.

Keywords: Catalyst, Jet fuel, Physicochemical Properties, Pyrolysis oil, Waste tires.

Information about authors:

Fitrianto
Master Student, Department of Mechanical Engineering, Faculty of Engineering, Universitas Indonesia, 16424 Depok, Jawa Barat, Indonesia. Email: fitrianto21@ui.ac.id; ORCID ID: https://orcid.org/0009-0004-2029-6723

Nandy Setiadi Djaya Putra
Dr.-Ing, Professor, Department of Mechanical Engineering, Faculty of Engineering, Universitas Indonesia, 16424 Depok, Jawa Barat, Indonesia. Email: nandyputra@eng.ui.ac.id; ORCID ID: https://orcid.org/0000-0003-3010-599X

Eny Kusrini
Ph.D., Department of Chemical Engineering, Faculty of Engineering, Universitas Indonesia, Kampus Baru UI, Depok 16424, Indonesia. Email: eny.k@ui.ac.id; ORCID ID: https://orcid.org/0000-0002-7919-0083

Introduction

Recently, global demand for sustainable aviation fuels has been increasing rapidly. Solid waste is an alternative raw material to meet this need [1]. Solid waste significantly contributes to environmental pollution worldwide, including industrial, agricultural, municipal solid waste, waste tires, etc [2]. Waste tires are one type of solid waste generated by various vehicles, including large vehicles, small vehicles, motorcycles, and heavy equipment [[3], [4]]. The problems caused by waste tires are not trivial because they will cause various issues, such as social, economic, and environmental issues [5]. Around one billion waste tires are generated worldwide each year, and the production of this waste will continue to increase over time [[6], [7]]. With such a large amount, it is a real challenge for various stakeholders to manage the waste wisely and in an environmentally friendly manner.

Waste tires have a high potential to be used as fuel [[8, [9], [10], [11]] because they have a high calorific value. Tires have a high calorific value due to their high carbon content, which is a primary fuel component. The calorific value of tires is influenced by their composition, which includes natural rubber, synthetic rubber, carbon black, and fillers [9]. The calorific value of tires can be further enhanced by processing them through pyrolysis, which breaks down the tire components into their basic elements. This process increases the calorific value of the tire. Pyrolysis is a potential method to process waste tires into high-value products such as pyrolysis oil, which has a high calorific value (37-45 MJ/kg) and has the

potential to be used as jet fuel. Waste tire pyrolysis oil has a calorific value of 37-45 MJ/kg [12]. Previous research has shown that around 42 wt% of the waste tire pyrolysis process is pyrolysis oil found in the liquid fraction [13]. The yield of tire pyrolysis oil depends on several factors, including heating rate, temperature, catalyst, and others [[14], [15]].

Global jet fuel consumption is projected to rise from 4 quadrillion Btu in 2010 to 16 quadrillion Btu by 2050 [16]. As demand for fuel increases, the aviation industry faces challenges in reducing carbon emissions caused by the use of fossil fuels [[17], [18]]. Aviation turbine (avtur) or jet fuel is kerosene-based fuel [[19], [20]]. Producing jet fuel from kerosene derived from pyrolysis oil is a significant challenge for researchers. The challenge is that fuels used in the aviation industry must meet certain standards and be certified, according to the American Society for Testing and Materials (ASTM) [21]. These standards ensure the fuel's quality, safety, and performance in jet engines. Pyrolysis oil contains impurities, water, nitrogen, sulfur, oxygen content, high density, and viscosity compared to ideal jet fuel [[20], [22]]. In addition, the kerosene fraction in waste tire pyrolysis oil is relatively small compared to the diesel fraction [23].

Waste tire pyrolysis with a catalyst for aviation fuel production is promising. The main advantage of incorporating catalysts into the pyrolysis is the increase in yield and quality of the resulting pyrolysis oil, and it may be even better for aviation fuels. The works showed that catalytic pyrolysis of waste tires substantially improves the quality of the produced oil. Catalysts can remove sulfur content [1] and oxygen content [24], enhancing the oil's quality and making it more compatible with aviation fuel specifications.

Based on the author's study, there are not many studies that focus on the conversion of waste tires into jet fuel through the pyrolysis process. This study aims to provide information and knowledge about the handling of waste tires and the hopes and challenges of converting waste tires as fuel for aircraft engines in the aviation sector. Catalysts that have the potential to be used in the pyrolysis of waste tires to produce jet fuel are reviewed. The properties of waste tire pyrolysis oil and its impurities, such as nitrogen, sulfur, and oxygen compounds, were also discussed.

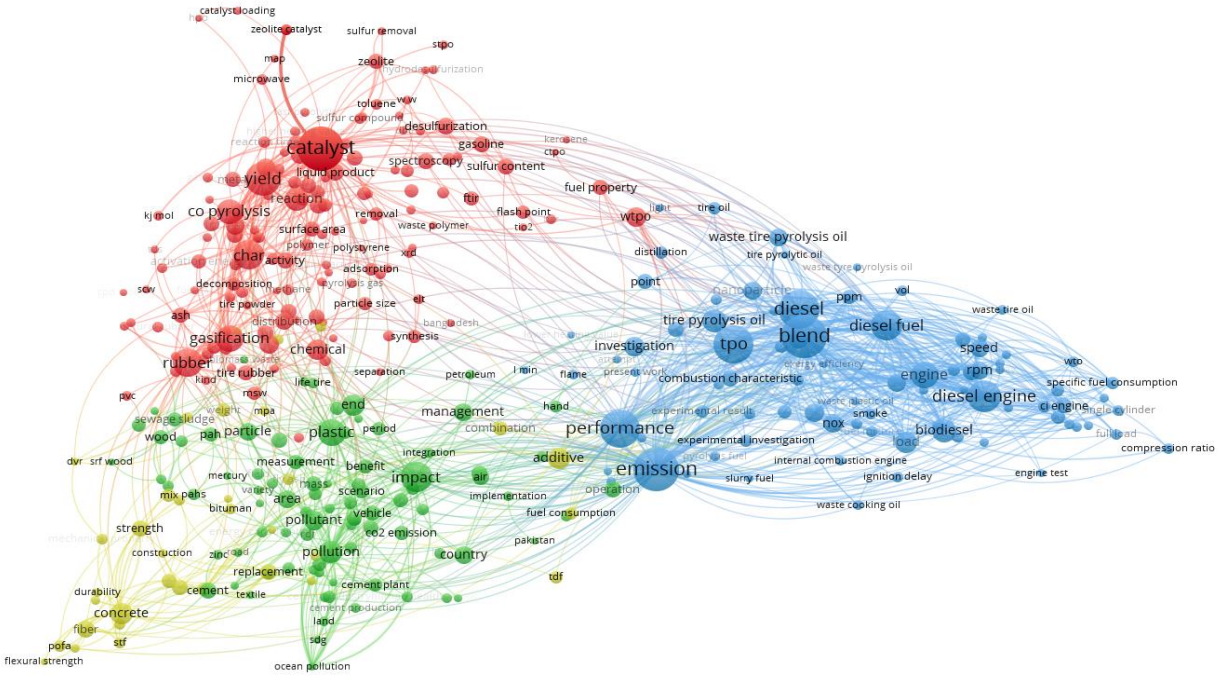

Figure 1 - Map of cluster network visualization showing articles on “waste/scrap tire fuel” published in Scopus. This map is based on 687 documents, with a minimum of ten occurrences

Bibliometric Analysis. Scientific article data was taken based on data from Scopus in February 2025. Scopus was chosen because it is one of the most extensive indexing services and journal database providers today. The keywords used were "(waste OR scrap) AND (tyre* OR tire*) AND fuel" in the Scopus search column. Indexed publications were then filtered in the range of 2015 to 2025, limited to only articles, conference papers, and the final publication stage. The number of publications downloaded was 687 articles. The publication data was then input into VOSviewer (version 1.6.20). VOSviewer was used because it can visualize network maps for bibliometric analysis [25]. A bibliometric analysis is carried out on the development of fuel research from waste tires being converted to jet fuel by collecting the number of paper documents, number of citations, countries that producing the most papers related waste tire and its research.

The bibliometric analysis in

Figure ***1*** shows the relationship between the various clusters in research on waste tire fuel. This mapping shows that related research can be categorized into four main clusters marked with different colors. The red represents research focusing on the catalysis aspect, and the blue describes research on fuel applications in diesel engines. In contrast, green relates to the environmental and sustainability aspects of using fuel from waste tires. The yellow indicates the relationship of research to construction material aspects, such as using pyrolysis residues in concrete or asphalt mixtures.

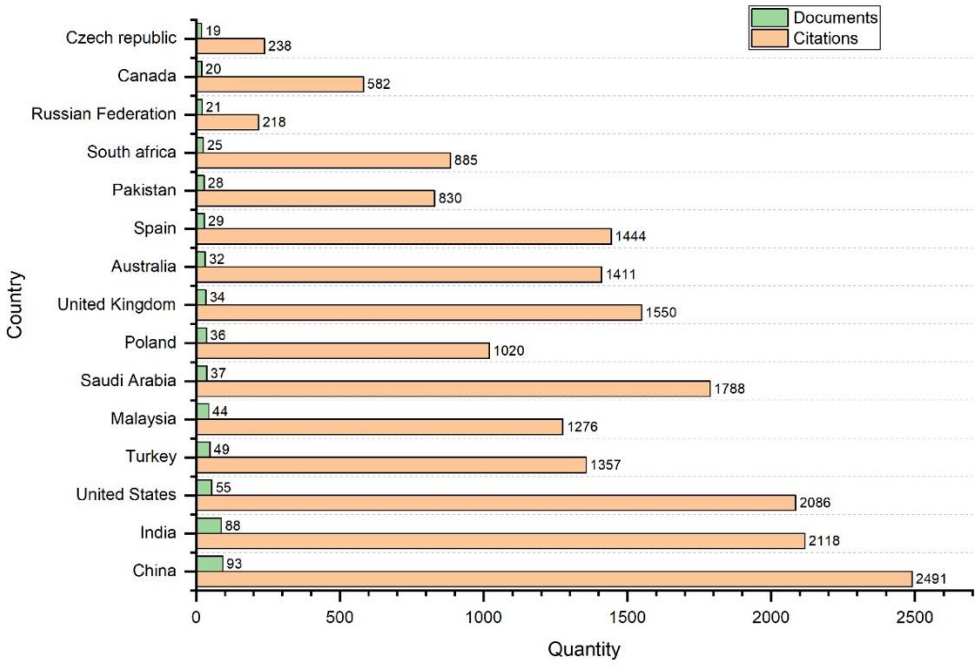

(a)

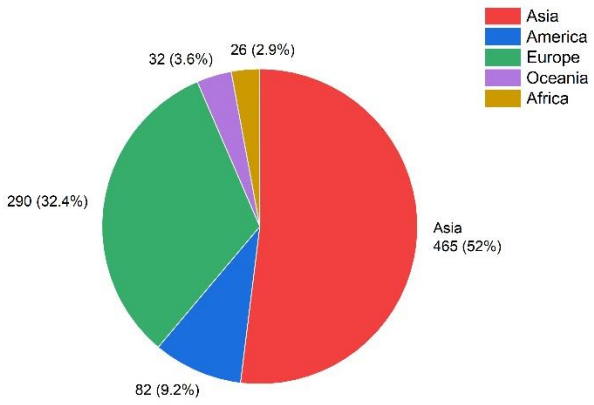

(b)

Figure 2 - (a) Countries of co-authorship involvement in waste tire fuel research, with a minimum of five documents per country, (b) document quantity per continent

From the analysis of the relationship between keywords, it can be seen that terms such as "diesel blend," "engine," and "performance" have a strong connection with "waste tire pyrolysis oil". This shows that many current studies focus on blending waste tire pyrolysis oil with conventional fuels and their effects on engine performance and emission characteristics. However, this map does not find a strong direct relationship with the term "jet fuel" or aviation fuel specifications, although the word kerosene appears in a non-dominant part. This indicates that although many studies are related to the use of WTPO in diesel engines, studies that specifically target its application as jet fuel are still very limited or have not been a primary focus.

China and India are the two countries with the highest number of publications in the provided bibliometric analysis (Figure 2). This dominance can be attributed to several factors, including rapid industrialization, high waste tire generation, strong research funding, and government policies promoting sustainable energy solutions. As the world's largest tire producer and consumer, China has significant research initiatives focused on waste tire management, alternative fuel production, and pyrolysis technology development [5]. China's commitment to reducing carbon emissions and advancing waste-to-energy conversion is evident in its policy support, technological innovation, and financial incentives, integrating waste tire recycling into national carbon reduction frameworks [26]. India faces significant challenges in waste tire management due to increasing motorization and non-biodegradability, prompting the government to introduce the Extended Producer Responsibility (EPR) framework in 2022 to enhance recycling and resource recovery. Upgrading pyrolysis plants, enforcing compliance with regulations, and raising awareness in rural communities are crucial steps to improving waste tire valorization while mitigating environmental and health risks [27].

Waste Tire Handling

Conventional handling of waste tires can be carried out in various ways: recycling, reclamation, landfilling, retreading, reuse, incineration, and combustion [9]. Recycling is the process of creating new products from waste tires. Reclamation involves extracting valuable materials from waste tires, such as steel and fibers, to reuse in other industries. Landfilling is a method of disposal that involves burying waste tires in a specific location. Retreading is the refurbishing of worn-out tires by replacing their treads so they can be used again. Incineration and combustion are waste management methods for waste tires that involve applying heat treatment to reduce the mass massively, but this method results in heavy environmental pollution.

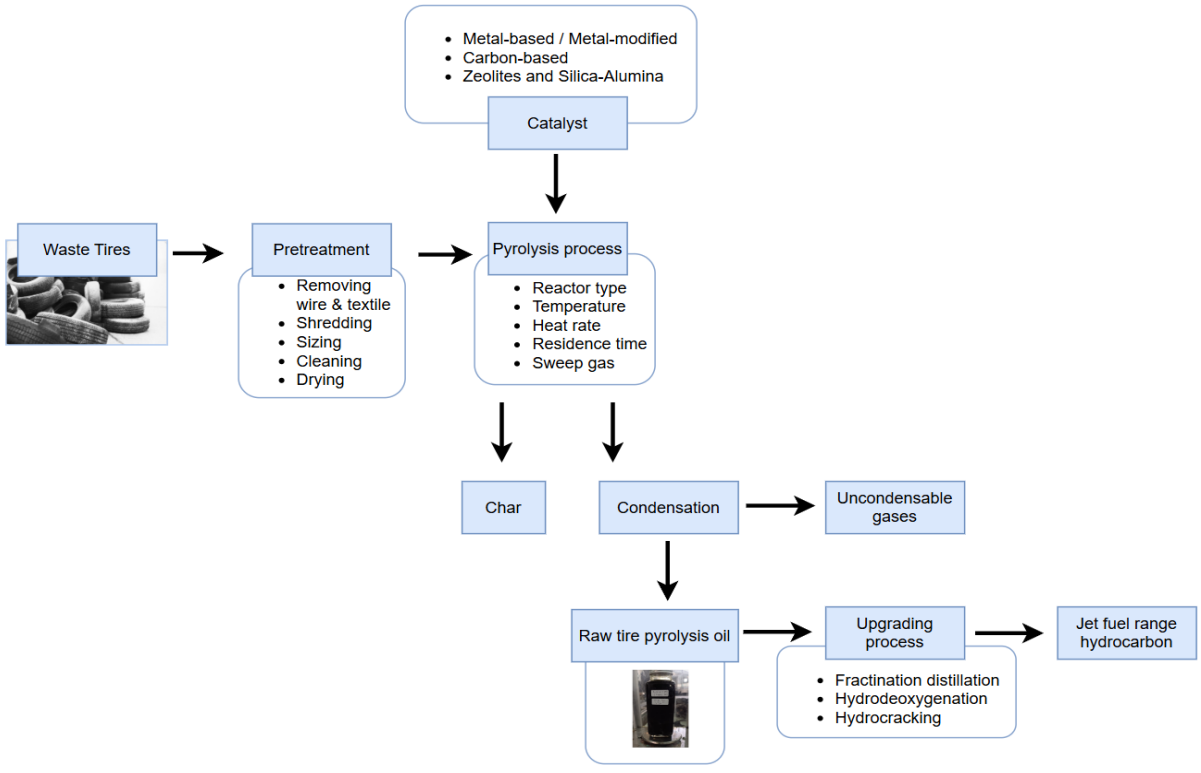

Figure 3 - Waste tire pyrolysis pattern to jet fuel range hydrocarbon.
Adapted from Refs. [[20], [29], [30]]

The chemical composition of waste tires is crucial in understanding their behaviour during pyrolysis. Waste tires typically consist of 60% natural rubber (NR) and synthetic rubber (SR), 30% carbon black, and 10% organic and inorganic fillers [28]. This composition affects elasticity, wear resistance, and shock absorption [28].

Non-conventional waste tire treatment methods such as gasification, liquefaction, hydrothermal liquefaction, and pyrolysis are considered more environmentally friendly [31]. Gasification involves converting tires into syngas, a versatile fuel source. Liquefaction processes break down tires into liquid fuels or chemicals. Hydrothermal liquefaction utilizes high temperatures and pressures to convert tires into bio-oil.

Waste Tire Pyrolysis

Pyrolysis, a thermal decomposition process without oxygen, transforms tires into valuable products like pyrolysis oil, gas, and char. Pyrolysis oil is generally considered the most beneficial among these products [[32], [33], [34], [35]]. Pyrolysis has become one of the most practical chemical recycling and waste utilization techniques [[36], [37], [38]]. When waste tires undergo a pyrolysis process, they will decompose into products with simpler compositions [39]. It breaks down the complex hydrocarbon polymers in waste tires into smaller molecules, producing a mixture of liquid, gas, and solid products [40]. Catalysts added to the pyrolysis process can significantly influence the pyrolysis results. The liquid fraction, often called pyrolysis oil or bio-oil, contains a variety of hydrocarbons that are suitable for further processing into fuels such as gasoline, diesel, and kerosene. In addition, pyrolysis gas, which mainly consists of hydrogen, methane, and other light hydrocarbons, can be used for heat and power generation, while the solid residue, known as char, can be used in a variety of industries, including as a carbon feedstock.

Figure 4 shows the various types of reactors used in tire pyrolysis, such as fixed-bed, fluidized-bed, rotary kiln, and auger or screw reactors. Each type of reactor has a different working method, temperature characteristics, and heating rate. Fluidized-bed provides a higher oil yield due to faster and more even heating, while rotary kiln is used for continuous large-volume pyrolysis [41]. Slow pyrolysis typically uses low heating rates (around 10 °C/min) with long vapor residence times, producing around 30–55% pyrolysis oil yields. Fast pyrolysis with higher heating rates and short residence times can produce pyrolysis oil yields of over 50%. Flash pyrolysis, such as in conical spouted bed reactors, has very high heating rates with vapor residence times of less than 2 seconds, producing pyrolysis oil yields of up to around 58% and limonene yields of up to 14.1% at temperatures around 475 °C[29].

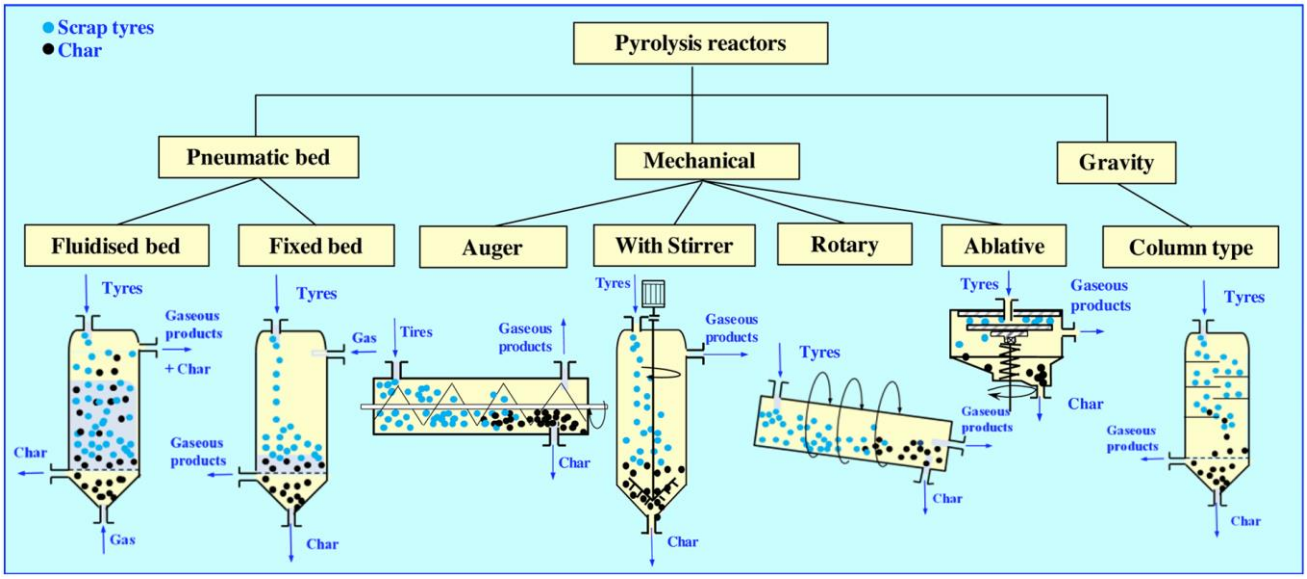

Figure 4 - Reactor types of waste tire pyrolysis [41] with permission No 6033420831611

Properties of Waste Tire Pyrolysis Oil

M.F. Laresgoiti [42] employed gas chromatography (GC) to examine a comprehensive array of over 130 compounds in tire pyrolysis oils with many aromatics. The oil is suitable for automotive and diesel oils based on distillation. It's been reported, too, that oil from waste tires is a blend of aliphatic and aromatic compounds, much like petroleum fuel [12]. Indeed, the properties of the liquid fraction are generally similar to those of the light oil fraction, like gasoline [41].

One of the main problems with jet fuel made from pyrolysis oil is that it contains impurities such as water, nitrogen, sulfur, and oxygen compounds. These impurities can reduce the performance of the jet engine and can even increase the risk of jet engine damage [43]. To comply with established aviation fuel standards, the levels of these impurities must be lowered.

Waste tire pyrolysis oil has been classified based on the property of its density, and interest has been gained in its use as an alternative fuel, more so in comparison with conventional jet fuel. Table 1 shows the properties of waste tire pyrolysis oil. According to Sharma [44], the densities of waste tire pyrolysis oil typically lie around 0.86 g/cm³. This range indicates that waste tire pyrolysis oil is denser than conventional fuels, including jet fuel, generally with a density of about 0.775 kg/m³ [45]. According to Yaqoob et al. [46], the higher density of waste tire pyrolysis oil compared to other kinds of fuel could make a difference in combustion characteristics and suitability for various engines. Thus, while the density of waste tire pyrolysis oil is comparable to jet fuel, its chemical composition and impurities must be further improved to be an ideal drop-in replacement for conventional aviation fuel.

The significant barriers of waste tire pyrolysis oil come from its high viscosity, which often entails complete reconstruction of the engine's construction to be compatible with the specification and not damage the engine [51]. Waste tire pyrolysis oil generally has a higher viscosity than conventional jet fuels. Some reports show the viscosity of waste tire pyrolysis oil at about 3.8 to 15 cSt at ambient temperature, which depends on product composition and operating parameters [52]. It is considerably higher than conventional jet fuels, such as Jet A-1, whose viscosity usually lies much lower at similar temperatures. Indeed, the pyrolysis oil obtained from waste tires is especially identified with dark color and foul smell, with its chemical composition having a high content of BTX (benzene, toluene, and xylene) and polycyclic aromatic hydrocarbons (PAH), which is believed to give rise to its high viscosity [53]. The formation of BTX is strongly influenced by secondary reactions occurring during tire pyrolysis [32].

The calorific value of waste tire pyrolysis oil was about 40.8 MJ/kg, which is competitive with conventional jet fuel, as reported by Islam et al. [48]. However, sulfur compounds in waste tire pyrolysis oil would be a severe problem because of their direct application in aviation use, which may lead to increased emissions and malfunction in operations [54]. The higher polycyclic aromatic hydrocarbons (PAH) concentration in waste tires affects a higher adiabatic flame temperature, leading to a higher heat release rate [[19], [55]].

The flash point is the lowest temperature at which the vapors of pyrolysis oil can ignite.

Table 1 - Comparison of Jet A-1 to waste tire pyrolysis oil.

Properties	Jet A-1	Reference [44]	Reference [47]	Reference [48]	Reference [49]
Density(g/cm3)	0.775 [a]	0.91	0.86	0.97	0.94
Freezing point (°C)	-40 [a]	-	-	-	-
Viscosity (cSt)	8 (at – 20 °C) [a]	3.35 (at 20 °C)	2.47 (at 40 °C)	4.90 (at 30 °C)	4.62 (at 40 °C)
Calorific value (MJ/kg)	42.8 [a]	38.10	41.74	40.80	38.00
Flash point (°C)	38 [a]	49.00	56.54	32.00	41.60
Cetane number	-	-	< 45	-	-
Carbon (%)	86.56[b]	86.92	80.94	84.80	87.57
Hydrogen (%)	13.25[b]	10.46	12.72	9.01	10.35
Nitrogen (%)	-	0.65	-	0.70	< 1.00
Sulfur (%)	0.30[a]	0.95		1.36	1.35

[a] Properties of Jet A-1 are taken from Hemighaus et al. [45], and [b] properties of Jet A-1 are taken from Kumar et al. [50].

Table 2 - Type of sulfur compound in waste tire pyrolysis oil

Sulfur Compound	Removal (% area)	Reducing Method	Ref
Thiophene, Benzothiophene, Dibenzothiophene, and their derivatives	Maximum sulfur removal 87.8% (NiMo/c-Al_2O_3)	Catalytic Hydrodesulfurization (HDS), post-pyrolysis process using NiMo, CoMo, and Mo catalysts	[65]
Benzothiophene, 3-Methylbenzothiophene, Dibenzothiophene derivatives	Sulfur reduction from 1.36% to 0.60% (NiMoS/Al_2O_3)	Pyrolysis followed by simultaneous catalytic desulfurization (cracking + HDS), formation of H_2S	[66]
Benzothiophene, Phenyl thiophene, Dibenzothiophene, Inorganic sulfides, aliphatic sulfur, sulfates	Sulfur removal in gas up to 87.7%; benzothiophene 78.1% (Fe_2O_3)	Catalytic pyrolysis with Fe_2O_3; Fe-S bond formation, C-S bond cleavage, dehydrogenation, oxygen migration	[67]
Thiophene, Benzothiophene, Dibenzothiophene, sulfoxides, sulfones	Sulfur removal 81-84% (solvent fraction and raw oil) via ODS	Oxidative desulfurization (ODS) post-pyrolysis; oxidation of sulfur to sulfoxides/sulfones and adsorption by Al2O3	[68]

The presence of many other compounds formed during pyrolysis can affect the flash point of these oils. For example, López et al. [56] and Martínez et al. [57] studied the continuous pyrolysis of waste tires and then the co-pyrolysis of biomass. In both works, the resultant oils showed different flash point according to feedstock and operating conditions. Co-pyrolysis of biomass with waste tires has been explored to enhance liquid fuel yield [[58], [59]].

During pyrolysis, the tire material degrades with the volatilization of hydrocarbons, nitrogen-containing species, and gases like hydrogen. Waste tires contain a significant amount of nitrogen that may be responsible for generating nitrogenous compounds in pyrolysis products, which may affect the combustion characteristics of the resulting fuels. Nitrogen can form nitrogen oxides when burned, which are harmful gases contributing to air pollution [[60], [61], [62]]. Understanding nitrogen dynamics during pyrolysis is crucial in optimizing fuel quality and reducing emissions.

Its sulfur content must be reduced when it is used as jet fuel. The sulfur content comes from applying additives during the factory tire production process [[63], [64]]. The content of sulfur compounds in waste tire pyrolysis oil consists of thiophenes, benzothiophenes, dibenzothiophenes, and several derivatives [65]. Other researchers who identified sulfur compounds are presented in Table 2.

Several mechanisms carry out the reduction of sulfur compounds in waste tires from pyrolysis. In the post-pyrolysis hydrodesulfurization (HDS) process, sulfur compounds such as thiophene, benzothiophene, and dibenzothiophene are removed by hydrogenation reactions under high hydrogen pressure using catalysts such as NiMo or CoMo on alumina, which convert sulfur to H_2S, thereby significantly reducing sulfur content [65]. In catalytic pyrolysis, catalysts such as Fe_2O_3 help break C-S bonds and form Fe-S bonds and facilitate dehydrogenation and partial oxidation reactions, so that sulfur is trapped in the form of solid or gaseous compounds that are easier to separate [67]. In addition, the oxidative desulfurization (ODS) method, carried out after pyrolysis, oxidizes sulfur compounds into sulfoxides and sulfones, which are then adsorbed by the catalyst surface, such as Al_2O_3. This increases the efficiency of sulfur removal in the final product [68]. The pyrolysis process, followed by simultaneous catalytic desulfurization with NiMoS/Al_2O_3 catalyst, also showed effectiveness in cracking while reducing sulfur in oil products [66].

Waste tire pyrolysis oil has significant amounts of sulfur, leading to pyrolysis equipment corrosion. Therefore, the desulfurization method should be applied to long-lasting [69]. Choi et al. [70] did one- and two-stage pyrolysis of waste tires to study sulfur content in pyrolysis oil, and the result was that temperatures around 500 ◦C had lower sulfur content.

The concentration of sulfur compounds in waste tire pyrolysis oil derived from the pyrolysis process depends on the operating conditions. The mechanism of compound formation depends on the reactor type, reactor temperature, catalyst, heating rate, and time [64]. Catalysts can transfer sulfur elements from the liquid phase product to the solid

Table 3 - Comparison of the operational conditions for the pyrolysis process and sulfur content

Reactor	Catalyst	Temperature (°C)	Sweep gas	Sulfur Content obtained	Ref
Fixed bed	Fe_2O_3	600	Argon	COS, H_2S, and SO_2 were decreased by 77.3 %, 99.7 %, and 85.1 %, respectively.	[67]
Fixed bed	Zeolite	500	Nitrogen	Up to 12.8 % removal	[71]
Rotary Kiln	CaO	400	-	Sulfur content in pyrolysis oil decreased from 0.99 % to 0.91 %	[72]
Solar-powered pyrolysis	CaO	650	Nitrogen	H2S decreased from 1.53 to 0.39 mL/g	[73]

phase in the pyrolysis process. In addition, the type of sweep gas used also has an influence that cannot be ignored.

Table 3 shows the sulfur content produced due to operating conditions in waste tire pyrolysis from several experiments.

Using sweep gas in the pyrolysis process of waste tires increases liquid oil yield while reducing the amounts of solid residue (char) and gas. The sweep gas helps to carry the vaporized products out of the reactor more efficiently. It makes the process more effective and increases the amount of valuable liquid fuel produced. Water vapor as a sweep gas was introduced to minimize sulfur content in the liquid phase and increase the solid phase [74]. That review revealed that the fixed bed produces the highest amount in the oil phase.

Aviation Turbine Fuel Standards and Certification

Aviation turbine fuel (avtur) or jet fuel is used in aircraft. This fuel is a mixture of hundreds of hydrocarbons extracted from crude oil. Crude oil is a black, viscous liquid that cannot be used directly. To be used, crude oil must be processed at oil refineries. The first processing process is carried out by staged distillation, while a more complex process is carried out in the second processing. The fuel produced mostly becomes gasoline and diesel, while a small part becomes avtur. Gasoline has a lighter density and is more volatile than avtur, while diesel is heavier and more prone to clumping into solids.

Avtur must follow strict standards and get certification to ensure quality, safety, and optimal performance in aircraft engines [[20], [75]]. The American Society for Testing and Materials (ASTM) has developed standards for avtur quality and testing procedures. This standard has been widely adopted worldwide. Following ASTM standards is very important for fuel suppliers and aircraft manufacturers because not following these rules can make engines less efficient and unsafe. These standards include fuel composition, purity, volatility, and thermal stability. By following ASTM standards, jet fuel suppliers ensure their products meet the strict requirements for the safe and reliable operation of jet engines.

Table 4 - Specification Properties of Jet Fuels [[76], [77], [78]]

Fuel	Jet A	Jet A-1	TS-1	Jet B	JP-8
Specification	ASTM D 1655	DEF STAN 91-91	GOST 10227	CGSB-3.22	MIL-DTL83133
Sulfur, mass%	0.30	0.30	0.25	0.40	0.3
Flash point, °C, min	38	38	28	—	38
Density, 15°C, kg/m3	775-840	775-840	min 774@20°C	750-801	775-840
Freezing Point, °C, max	–40	–47.0	–50 (Chilling point)	–51	-47
Viscosity, –20°C, mm2/sec, max	8	8.0	8.0 @ –40°C	—	8
Heating value, MJ/kg, min	42.8	42.8	42.9	42.8	42.8

Aviation turbine fuel is commonly divided into two main types: Jet A and Jet A-1, which are widely used in commercial aeroplanes, and JP-8, primarily used by the military [76]. ASTM has issued jet fuel standards for avtur fuels, namely Jet A and Jet A-1 [77]. This standard is usually used in fuel used by commercial airlines. Flights outside the United States and Eastern Europe commonly use the A-1 jet. In the United Kingdom (UK), there is a DEF STAN standard that regulates Jet A-1 fuel. A GOST standard regulates TS-1 jet fuel in Russia and Eastern Europe. The country near the North Pole, Canada, has a standard in the form of the Canadian General Standards Board (CGSB), which accommodates Jet B type fuel regulations. Table 4 specifies the type of jet fuel.

Jet A-1 has a carbon number of 8 to 16, which is highly controlled during fuel refinery processes to meet regulatory standards [79]. It ensures the fuel delivers the required energy density and combustion characteristics for safe and efficient flight operations. The precise formulation of Jet A-1 enhances engine performance and minimises environmental impact by reducing emissions and improving fuel efficiency.

One of the considerations for using fuel is that the plane needs energy to move and resist the force of gravity so that the aircraft can fly. The energy quantity in the fuel is expressed in units of MJ/kg or megajoules per litre (MJ/L) according to the International Metric (SI) units. From Table 4, it can be seen that there is not much of a significant difference between jet fuels above.

Avtur is composed of hundreds of hydrocarbons that have freezing points. The hydrocarbon component that has the highest freezing point will be solid first. The freezing point is the temperature at which the molecules begin to freeze. This parameter is crucial for aviation operating at extreme altitudes where temperatures are very low [75]. A low freezing point will ensure the fuel remains liquid during flight. It will affect the smooth and stable fuel flow to the engine combustion chamber.

Viscosity indicates a viscous fluid level that can be affected by temperature. Too high a viscosity in a fluid, in this case, fuel, can cause significant problems and impair engine performance [80]. Proper viscosity will maintain a smooth supply of fuel to the combustion chamber. The pumping power of jet fuel is affected by viscosity. The greater viscosity will disrupt the smooth supply of fuel and disrupt the stability of fuel flow, especially in icy temperature conditions. An example of standard tests for jet fuel properties is listed in Table 5.

The sulfur content shows the percentage of sulfur in the fuel. Sulfur is an element that causes corrosion and impure gas emissions, such as sulfur dioxide, which is dangerous to health and the environment. 0.30% means the sulfur content of this fuel is relatively low.

The lower the sulfur, the less pollution is generated. It will prevent corrosion in the engine, keeping it in good condition while helping the environment. Usually, fuel with low sulfur content is more expensive as it needs extra refinement.

The flash point refers to the lowest temperature at which a fuel might ignite with the availability of an ignition source. Therefore, a minimum value of 38°C implies that this fuel has reasonable safety and is not easy to burn at low temperatures. The higher the flash point, the safer the fuel against fire hazards in handling and storage applications. This aspect of flash point is quite significant for the transportation and storage of fuel. High flash point acts as a measure to avoid accidental fire outbreaks.

Table 5 - ASTM Standard for fuel jet quality testing (adapted from [77] and [81])

Property	Standard test method	Description
Viscosity	ASTM D 445 /IP 71	Test method for measuring the kinematic viscosity of petroleum products and liquid fuels at various temperatures
Sulfur	ASTM D 1266 /IP 107	The test method used to determine sulfur content in petroleum products and other materials through the Lamp Combustion method.
Flash Point	ASTM D 56	The test method used to determine the flash point of liquids using a Tag Closed Cup apparatus, commonly applied to assess the flammability of petroleum products.
Density	ASTM D 1298 / IP 160	The test method used to determine the density or relative density (specific gravity) of petroleum products and liquid hydrocarbons is a hydrometer.
Heating Value	ASTM D4809	Test method for determining the heat of combustion of liquid hydrocarbon fuels using a bomb calorimeter, providing critical data for fuel performance evaluation and quality control

Density is the measure of how compact the fuel is. It would mean that a range of 775-840 kg/m³ indicates a density of this fuel at 15°C. Density impacts the volume and weight that can fit in any given tank. Since this fuel is denser, it possibly contains more energy per volume. Consistent density ensures that for an engine to perform optimally, the appropriate amount of fuel reaches the engine for efficient combustion.

ASTM D7566-18 has set five synthetic paraffinic kerosene (SPK) types as blending components with conventional jet fuel [79]. SPK is made from renewable sources like vegetable oil and waste. The goal is greenhouse gas emissions reduction. It will make flights more environmentally friendly. The types of SPK are Fischer-Tropsch SPK (FT-SPK), Hydroprocessed Esters and Fatty Acids SPK (HEFA-SPK), Synthesized Iso-Paraffinic SPK (SIP-SPK), Alcohol to Jet SPK (ATJ-SPK), and Alcohol to Jet SPK (HC-HEFA-SPK). FT-SPK is processed from biomass or natural gas. HEFA-SPK is made from vegetable oil or animal fats. SIP-SPK is made from fermented sugar, and ATJ-SPK is made from alcohol turned into jet fuel. HC-HEFA-SPK is made from sugar through chemical and biotechnology processes. Each SPK type can be mixed up to a certain percentage with conventional jet fuel. Benefits include lower emissions, the use of renewable resources, and less reliance on petroleum. However, ASTM has not recognized the pyrolysis process as a pathway in production or blending with jet fuel.

Catalytic Cracking as an Approach to Producing Jet Fuel

The role of catalysts in the pyrolysis process for producing avtur is to optimize yields and quality. Without a catalyst, pyrolysis can depend only on high temperatures to degrade long hydrocarbon chains into smaller compounds, often forming products of uncontrolled composition and quality [82]. Catalysts drive the pyrolysis reaction along more selective pathways and produce a hydrocarbon fraction [83] that can be driven more closely to match the jet fuel specification. Catalysts improve product selectivity, whereby the pyrolysis process affords more light hydrocarbons and preferred fuel components like aromatic and aliphatic C8-C16 in agreement with jet fuel characteristics [84]. Catalysts can also improve energy efficiency in the pyrolysis process [85]. Catalysts allow lower reaction temperatures and cut reaction times compared to pyrolysis without catalysts, reducing energy consumption [86]. Catalyst for jet fuel production in the cracking process is listed in Table 6. Table 6 provides information on using various catalysts in the high-temperature cracking process for jet fuel production from various feedstocks. Catalysts have been widely used by researchers in pyrolysis. Not a few have also researched the use of catalysts to produce avtur, which can potentially be used in waste tire pyrolysis. Prasad et al. [87] studied an experiment on producing bio-jet fuels through catalytic pyrolysis of sawdust using MgO-modified activated biochar. These studies have evidenced that the optimum composition of catalysts improves yields of jet fuels, with a maximum yield of 29% at 600°C with 10 wt% MgO. Poor performance was noticed for AC alone due to strong surface -OH and -COOH groups; hence, adding MgO neutralises them and gives higher yields of bio-jet fuel. The results explained that the acid and base sites of the catalyst played a vital role in the conversion process; hence, this method is one of the green ways of producing bio-jet fuel. It can be concluded that MgOAC has been considered one of the promising, efficient, and economical catalysts in biomass pyrolysis.

Fu et al. [88] studied catalytic co-pyrolysis of lignin and polypropylene (PP) using Fe/AC as a catalyst. The research included evaluating the effect of reactants, such as iron loading, reaction temperature, catalyst/feedstock, and ligament/PP ratio, on the yield and distribution of the jet fuel range hydrocarbons. Adding PP increased the H/C ratio in the pyrolysis system and improved the quality of pyrolytic oil. PP was manifested as a hydrogen donor, which supplied hydrogen radicals that suppressed the polycondensation and cross-linking of the lignin pyrolysis intermediate. It led to increased pyrolysis oil from using both FP and lignin instead of using only FP, proving that PP and lignin had a synergistic relationship with each other.

Increased Fe loading on the catalyst led to improved jet fuel range hydrocarbon production and encouraged the development of cycloalkanes and aromatics. Deoxygenation and alkylation reactions were mediated by the Fe^{3+} sites, converting phenols into high-carbon aromatics, improving the distribution of hydrocarbons in the jet fuel range. The study established the optimal conditions of 550 °C, 1:1 lignin/Polypropylene ratio, and 1:2 catalyst/feedstock ratio for maximizing the production of jet fuel range hydrocarbons. However, excessive amounts of catalysts negatively affected high carbon hydrocarbon and cycloalkane yields.

Table 6 - Catalyst for jet fuel production in the cracking process

Catalyst	Catalyst Category	Feedstock	Reactor Type	Temperature (°C)	Avtur Fraction (%)	Ref
MgO modified	Metal oxide	Sawdust	Batch	600	29	[87]
Fe/AC	Activated carbon	Lignin/polypropylene	Fixed bed	550	35.39	[88]
Activated carbon	Activated carbon	Soapstock	Fixed bed	500	98	[89]
Zeolite Y	Zeolite	Municipal plastic	Fixed bed	500	30	[90]
Metal-loaded activated carbon	Activated carbon	LDPE	Fixed bed	600	96.17*	[91]
Activated carbon	Activated carbon	LDPE/wheat straw	Fixed bed	550	95.4*	[92]
Activated carbon	Activated carbon	Waste plastics	Fixed bed	500	100*	[93]
CaO and Zn-modified HBeta	Metal oxide/Zeolite	Camphorwood/LDPE	Fixed bed	550	18.45	[94]
Sulfonated activated carbon	Activated carbon	Sawdust/LDPE	Fixed bed	500	97.51*	[95]
Metal/HZSM-5(38)	Metal/Zeolite	Sawdust	Fixed bed	550	~55*	[96]
Fe/biochar	Metal/Biochar	Syringe	Fixed bed	500	78	[97]
SBA-15	Mesoporous silica	Coconut oil	Fixed bed	500	NA	[98]
Ni-Mo/silica-alumina	Metal/Aluminosilicate	Waste cooking oil	Fixed bed	420	55.6	[99]
Bentonite	Mineral	Jatropha oil	Batch	350	40	[100]
Carbon-loaded platinum	Metal/Carbon	Polyisoprene rubbers	Fixed bed	460	83.6	[101]
NiAg/SAPO-11	Metal/Silica alumina	Pure alkanes	Fixed bed	380	67	[43]

Duan [89] reported in the paper focused on the catalytic pyrolysis of soapstock using an H_3PO_4-activated corn cob-derived activated carbon catalyst to produce jet fuel, gasoline-range hydrocarbons, and H_2-enriched biogas. The loading concentration of H_3PO_4 was essential for developing acid groups and porous properties of the ACC, which significantly impacted the yield and chemical profile of the produced bio-oil and biogas. The maximum selectivities of jet fuel (98.78%) and gasoline (91.03%) were achieved under the optimal conditions with a pyrolysis temperature of 500°C and a soapstock-to-ACC ratio of 1:1.5. This study had novelty and an efficient route for waste soapstock transformation into valuable energy products. At the same time, further investigations should be conducted to improve catalysts and detailed reaction mechanisms at the molecular level.

The type of catalyst used significantly impacts the production of jet fuel fractions. Activated carbon can significantly break down feedstock into jet fuel, especially for waste plastic feedstock. Jet fuel produced using this catalyst can reach 100% area. Meanwhile, metal-loaded activated carbon used in LDPE produces 96.17%. In addition, operating temperature also plays an important role in conversion efficiency. Most of the process occurs in the range of 500–600°C, which is the optimal temperature for thermal decomposition and catalytic reactions that produce medium-chain hydrocarbons (C8-C16), following jet fuel specifications. For example, Ni-Mo/silica-alumina used in a fixed bed reactor at 420°C produces 55.6% of the avtur fraction, indicating that this catalyst has high activity in the cracking reaction despite the lower temperature. Considering this, these catalysts also have the potential to be used on waste tires to be converted into jet fuel.

Experiments Attempting to Produce Jet Fuel Base from Waste Tires

Producing high-quality oil from pyrolysis due to impurities and contaminants is tough. Various methods have been proposed to improve the quality of oil derived from pyrolysis to produce jet fuel. One method involves strict testing methodologies necessary for jet fuel to be accepted for aviation use. Most of these test methods typically involve the analysis of key parameters such as sulfur content, density, viscosity, and composition to meet aviation fuel requirements. Using modern testing equipment and methodology, one would be able to obtain an appropriate estimation of the quality of jet fuel derived from pyrolysis oil. Table 7 lists researchers attempting to obtain jet fuel range from waste tire pyrolysis.

Table 7 - Experiments attempting to produce jet fuel base from waste tires

Reactor type	Feed Stock	Catalyst	Working Temperature (◦C)	Sweep Gas	Upgrading Process	Ref.
Semi-batch	Tire	-	550, 650, 700	-	Distillation 149–232 ◦C	[102]
Fixed	Tire	Pt/Zeolite	500, 600, 700	Nitrogen	Polar-aromatic fractionation	[103]
Fixed	Tire	Zeolite	600	Nitrogen	-	[104]
Fixed	Tire	-	500	-	Distillation 131–225 ◦C	[19]

Lopez et al. [102] experimented with the GRAUTHERMIC-Tires process. GRAUTHERMIC-Tires was a novel process developed to efficiently valorize granulated scrap tires through thermolysis at moderate temperatures at atmospheric pressure. In the GRAUTHERMIC-Tires process, vertical, parallel, tubular reactors without internal moving parts restrict the entrance of oxygen into the thermolysis environment to prevent combustion. In this work, the effect of thermolysis temperature in the range of 500 to 700 °C was investigated for the yields of solid-char, liquid tire-derived oil, waste tire pyrolysis oil, and gaseous products from granulated scrap tires (GST) in a semi-batch pilot plant. Results showed that high gas yields, waste tire pyrolysis oil, and char fractions could be achieved. Gas yields varied in the range of 15-22 wt.%, and the waste tire pyrolysis oil yields varied in the range of 34-46 wt.%, and char yields in the range of 39-44 wt.%, attesting to the goodness of the process for the valorization of valuable materials from GST. Waste tire pyrolysis oil was distilled into the following categories: gasoline (<149 ◦C), jet fuel (149–232 ◦C), diesel (232–343 ◦C), fuel oil (343–371 ◦C), and heavy vacuum gas oil (>371 ◦C). Jet fuel fraction was obtained in a significant amount. The waste tire pyrolysis oil recovered had a GCV of 41-44 MJ/kg and could be qualified as heating oils and, therefore, usable as a fuel. The fraction of incondensable gas can also be used for electricity production with a gas turbine and can yield 4.1-6.5 kWh of electricity per gram of treated GST. The value of the resulting char was much higher for other industries, with a GCV of 27-28 MJ/kg and high ash and zinc contents. Although the results from this study were positive, it was realised that market demand for the obtained products was an important factor affecting the economic viability of pyrolytic treatment of waste tires.

Dung et al. [103] focused on the influence of pyrolysis temperature and the use of Pt-loaded catalysts on polar-aromatic content in waste tire pyrolysis oils. An increase in pyrolysis temperature increased the production of polar-aromatic compounds, often unwanted, given their complex structure and environmental implications. This work noted that bifunctional catalysts, such as Pt/HBETA, significantly improved polar-aromatic reduction in comparison with Pt/HMOR since HBETA enjoys a better surface area and Pt dispersion, and these improvements in hydrogenation activity were, in turn, responsible for the improvement in reduction. This work also noted that the preparation of catalysts via calcination and impregnation was one of the key steps in optimizing catalytic performance. The results also indicated that the hydrogenation rate catalysed by Pt was higher compared to the conversion into heavier polar-aromatic compounds, thus minimising their concentration in pyrolytic oils. The work, in general, highlighted useful insights toward pyrolysis conditions and catalyst design, which could potentially reduce the yield of undesirable polar-aromatic compounds and improve the quality of tire oils.

Osayi et al. [104] aimed to investigate the properties of the pyrolytic oil obtained from waste tires through pyrolysis using synthesized zeolite NaY as the catalyst. Pyrolysis was conducted at 600 °C with different catalyst concentrations in the range of 1 to 10 wt%. The maximum yield of CPO was 21.3 wt.% at the catalyst-to-tire ratio of 7.5 wt.%, though lower than the yield of noncatalyzed pyrolytic oil that reached 34.40 wt.%. The chemical composition of the pyrolytic oil was tremendously enhanced with a significantly increased yield of valuable compounds like benzene, ethylbenzene, toluene, and xylenes in order of CPO (5 wt.%) > CPO (1 wt.%) > CPO (10 wt.%) > CPO (7.5 wt.%) > noncatalyzed pyrolytic oil in terms of the yield of benzene. GC-MS, FT-IR, and NMR techniques were separately applied to the present study to evaluate the chemical composition and present functional groups within the pyrolytic oil. The CPO consisted of a complex mixture of aromatics, olefins, and paraffins that represented a wide hydrocarbon profile. Besides,

the zeolite NaY catalyst also showed the possibility of increasing hydrocarbon yield in the carbon range of C6-C15, which corresponds to the available gasoline and jet fuel yields with lower yields of diesel and fuel oils. In general, synthesised NaY zeolite was a highly active catalyst that improved both the quality and yield of the pyrolysis oil from waste tires; hence, it demonstrated its potential for industrial applications in the production of valuable chemical compounds.

Suchocki et al. [19] experimented on the performance-emission characteristics of a miniature GTM-140 gas turbine engine fired with blends of jet fuel with waste tire pyrolysis oil, which is presented in this paper. Before blending, waste tire pyrolysis oil was distilled at 131–225 ◦C to meet the kerosene base property and to reduce impurities. The research work met the demand for alternative fuels depleted by fossil fuels and the environmental concern for waste tires that are difficult to recycle. The pyrolysis process transformed the tires into pyrolysis in a liquid fuel form, which is usable instead of conventional fuels in gas turbines. The work reported an experimental study that aims to find out the potential impacts of using various concentrations of waste tire pyrolysis oil blended with kerosene on turbine performance, given static thrust, thrust-specific fuel consumption (TSFC), and emission of harmful gases such as NO_x, CO, and SO_2. The experimental results revealed that waste tire pyrolysis oil blends give good enough thrust, while to maintain the same rotational speed, the fuel flow rate needs to be higher than that of pure kerosene. This increased the TSFC, which points to efficiency issues when waste tire pyrolysis oil is used. It was further found in the study that NO_x emissions tend to increase with a higher waste tire pyrolysis oil concentration, indicating a potential linkage between fuel composition and nitrogen oxide formation. On the other hand, the SO_2 emission results were below for all the blends, which may be considered an environmental merit for the application of waste tire pyrolysis oil. The testing methodology ranged from turbine inlet and outlet temperatures to fuel flow and emissions measured at different load conditions to comprehensively present the operational characteristics of the gas turbine running on waste tire pyrolysis oil blend. Test results also proved that waste tire pyrolysis oil can be considered as an alternative fuel. However, further optimisation of its viscosity and combustion characteristics was necessary for better performance and reduction of the emission level. In general, this paper provided useful insight into the feasibility study of applying waste-derived fuels to gas turbines, opening up a path toward more sustainable energy solutions for power generation.

Sajdak et al. [30] explored the conversion of pyrolysis oil from car tires into jet fuel, focusing on optimizing hydrodeoxygenation (HDO) and hydrocracking (HC) processes to maximize the kerosene fraction yield. The study used NiMo/γ−Al_2O_3 catalysts under varying temperature, pressure, and time conditions to refine tire pyrolysis oil (TPO) and then analyzed the impact of these conditions on the oil's composition and properties. The research indicates that hydrodeoxygenation (HDO) and hydrocracking (HC) processes can effectively upgrade tire pyrolysis oil (TPO) into a substance with properties similar to aviation fuel fractions. During the HDO process, the sulfur and nitrogen contents were significantly reduced. HDO generally increasing the content of paraffins, iso-paraffins, and naphthenes, while aromatics can be reduced.

Discussion

Jet fuel is a complex fuel made up of hundreds of different types of hydrocarbons derived from crude oil. Aircraft use aviation turbine fuel, which is a complex fuel manufactured from hundreds of different hydrocarbons obtained from crude oil processing. Jet fuel has to meet strict standards for safety and efficiency in aircraft engines, as set out by organisations such as the ASTM. These internationally accepted standards relate to fuel characteristics such as composition, purity, volatility, and thermal stability. For example, ASTM specifies Jet A and Jet A-1 for commercial aircraft, while other states have their specifications, such as the UK with DEF STAN, Russia and Eastern Europe with GOST, and CGSB in Canada for Jet B. The existence of such regulations ensures that jet fuel will be able to meet even the most stringent requirements to safely and reliably power jet engines anywhere in the world.

Jet fuel comes with essential requirements in aircraft, which include the energy content, freezing point, viscosity, sulfur content, flash point, and density, which are all great concerns in ensuring safety in their operations. Several standards in jet fuel, like ASTM, have been set for all these parameters to ensure dependability for high-altitude and low-temperature conditions that require low freezing points and proper viscosity for a continued smooth flow of fuel toward the engine. More

recently, ASTM introduced SPK types derived from renewable sources, such as FT-SPK, HEFA-SPK, SIP-SPK, and ATJ-SPK, which can be blended into conventional jet fuel to reduce greenhouse gas emissions. Although the previous pathways have been approved by ASTM for blending, all pyrolysis-derived fuels remain unapproved as a jet fuel production or blending pathway [20]. The difference indicates that sources of renewable jet fuel are still being explored, and more tests should be done to ensure they meet the strict standards set for aviation fuels.

Waste tire pyrolysis with distillation purification, as mentioned in the previous literature, was used to start mini turbine engines, although there are differences in terms of properties. The results of the study showed that there were no significant problems in the combustion chamber operating the mini-turbine engine [20]. On the side of combustion results, there are still gases that are harmful and pollute the environment produced from the combustion process. However, the study requires a larger test scale to determine the effect of waste tire pyrolysis on aviation turbine fuel over a longer and comprehensive period.

Such catalysts play an important role in optimising pyrolysis processes toward the production of jet fuel by improving product yield and selectivity, and adding energy efficiency. This means that catalytic pyrolysis of biomass, lignin, polypropylene, waste tires, and other materials on MgO-modified activated biochar, Fe/AC, and zeolites will break them down into desirable jet-fuel-range hydrocarbons. On the other hand, catalyst selectivity prefers to move toward producing specific hydrocarbon fractions, such as C8-C16 aliphatic and aromatic compounds, within the jet fuel specifications. MgO-modified-activated biochar increases the yield of sawdust toward jet fuel. Fe/AC acts as a catalyst for co-pyrolysis between lignin and polypropylene, producing hydrocarbons of jet-fuel quality. Moreover, catalysts like H_3PO_4-activated carbon and zeolites offer some promise for improving the selectivity and lowering the impurities in pyrolysis oils of soapstock and waste tires. Waste tire pyrolysis oil, for instance, may be refined and can be mixed with kerosene for consumption in turbines, though further improvement in the viscosity and management of emissions is required. Although promising, pyrolysis has not yet been approved as a certified pathway to jet fuel by ASTM because additional research and validation will be needed to meet the strict aviation standards.

The next step that can be taken after getting tire pyrolysis oil is to do hydrodeoxygenation (HDO) and hydrocracking (HC). Some literature states that this process can bring tire pyrolysis oil (TPO) properties closer to the jet fuel fraction by reducing contaminants and sulfur content. The distillation process is necessary to obtain the right boiling point and meet the volatility requirements of jet fuel. Even so, processes that need to be carried out, such as isomerization and additives, still need to be carried out. Isomerization improves the branching of hydrocarbon molecules, leading to better cold flow properties. Additives will improve its stability, prevent corrosion, and enhance other properties. Adding appropriate additives is necessary before the fuel can be certified for use.

Conclusion

Waste tire pyrolysis is a promising pathway for sustainable aviation fuel production. Pyrolysis offers dual benefits in waste tire handling and alternative energy production. The bibliometric analysis shows the development of research on waste tire fuels. The study of keyword relationships shows that current research is highly focused on mixing waste tire pyrolysis oil with conventional fuels, and application as jet fuel is still a relatively unexplored area. From several previous studies, tire pyrolysis oil has been tried to be used in micro turbine engines on a laboratory scale. These results need to be validated on a larger scale and for a longer time to find a more significant impact. Although jet fuel derived from waste tires shows promise, there are still challenges to overcome, especially in meeting stringent aviation standards such as ASTM. These challenges include optimizing properties such as viscosity, density, freezing point, and sulfur content, as well as addressing emissions of harmful compounds such as nitrogen oxides. Catalyst development has shown potential for improving the yield and quality of pyrolysis oil to meet aviation fuel specifications. MgO, Fe/AC, and zeolite are some of the catalysts used on biomass to produce jet fuel and have potential applications in waste tire pyrolysis. However, further refining processes such as hydrodeoxygenation, hydrocracking, distillation, and isomerization are necessary to bring waste tire pyrolysis oil closer to jet fuel specifications. Future work should focus on refining pyrolysis processes, developing advanced catalysts, and conducting large-scale testing to validate the long-term viability of this pathway for sustainable jet fuel production.

Conflict of Interest. The authors declare that there is no conflict of interest regarding the publication of this article.

CRediT author statement. **Fitrianto**: Conceptualization, Methodology, Investigation, Manuscript drafting; **Nandy Putra**: Conceptualization, review, Supervision; **Eny Kusrini**: Conceptualization, Manuscript revision, Supervision.

Acknowledgments. The first author wishes to express gratitude to the Lembaga Pengelola Dana Pendidikan (LPDP) of the Republic of Indonesia for funding the author's master's studies and supporting this research project through the LPDP Master Scholarship.

Cite this article as: Fitrianto, Nandy Putra, Eny Kusrini. Review of Sustainable Jet Fuel Production through Pyrolysis of Waste Tires: Process, The Physicochemical Properties and Catalyst. Kompleksnoe Ispolzovanie Mineralnogo Syra = Complex Use of Mineral Resources. 2026; 339(4):52-70. https://doi.org/10.31643/2026/6445.40

Қалдық шиналардың пиролизі арқылы тұрақты реактивті отын өндірісіне шолу: процесс, физика-химиялық қасиеттері және катализаторы

[1,2]Fitrianto, [1]Nandy Putra, [1*]Eny Kusrini

[1] Индонезия университеті, Jl. Lingkar, Pondok Cina, Бежи ауданы, Депок қаласы, Батыс Ява 16424, Индонезия
[2]Ұлттық зерттеулер және инновациялар агенттігі (BRIN), Serpong, 10340 Бантен, Индонезия

Мақала келді: *2 маусым 2025*
Сараптамадан өтті: *4 маусым 2025*
Қабылданды: *11 маусым 2025*

ТҮЙІНДЕМЕ

Қатты қалдықтар, соның ішінде шиналар қалдығы жаһандық қоршаған ортаның ластануына айтарлықтай үлес қосады, жыл сайын шамамен бір миллиард пайдаланылған шиналар пайда болады. Қалдық шиналарды тұрақты авиациялық отынның (SAF) көзі ретінде пайдалану азық-түлік көздерімен бәсекелеспейді, осылайша азық-түлік қауіпсіздігіне нұқсан келтірместен энергия қажеттіліктерін қамтамасыз етеді. Дегенмен, шиналардың пиролиз майынан авиакеросин өндіру Американдық сынақтар мен материалдар қоғамының (ASTM) қатаң сапа стандарттарына байланысты айтарлықтай қиындықтарға тап болады. Бұл мақалада тұтқырлықты, тығыздықты және күкіртті қоса алғанда, шиналардың пиролиз майының физика-химиялық қасиеттері қарастырылады және оларды ASTM реактивті отынның техникалық сипаттамаларымен салыстырады. Мақалалар мен құжаттардың санын, дәйексөздер санын, шина қалдықтарына қатысты ең көп мақаларды жариялайтын елдер мен олардың зерттеулерін жинау арқылы авиакеросинге айналдырылатын шина қалдықтарынан жанармай зерттеулерін дамытуға библиометриялық талдау жүргізіледі. Сондай-ақ крекинг процесінде авиакеросин өндіруге арналған катализаторларды әзірлеу жайы да жан-жақты талқыланды. Реактивті қозғалтқыштарда шиналардың пиролиз майының қалдықтарын пайдалану авиация секторында тұрақты отынды енгізудің бастапқы қадамы ретінде қарастырылады.

Түйін сөздер: катализатор, реактивті отын, физико-химиялық қасиеттері, пиролиз майы, қалдық шиналар.

Авторлар туралы ақпарат:

Fitrianto
Магистр, машина жасау бөлімі, инженерлік факультеті, Индонезия университеті, 16424 Депок, Джава Барат, Индонезия. Email: fitrianto21@ui.ac.id; ORCID ID: https://orcid.org/0009-0004-2029-6723

Nandy Setiadi Djaya Putra
Доктор, машина жасау кафедрасының профессоры, Инженерлік факультеті, Индонезия университеті, 16424 Депок, Джава Барат, Индонезия. Email: nandyputra@eng.ui.ac.id; ORCID ID: https://orcid.org/0000-0003-3010-599X

Eny Kusrini
PhD, Химиялық инженерия бөлімі, Инженерлік факультеті, Индонезия университеті, Кампус Бару UI, Депок 16424, Индонезия. Email: eny.k@ui.ac.id; ORCID ID: https://orcid.org/0000-0002-7919-0083

Обзор устойчивого производства реактивного топлива путем пиролиза изношенных шин: процесс, физико-химические свойства и катализатор

[1,2]Fitrianto, [1]Nandy Putra, [1*]Eny Kusrini

[1]Университет Индонезии, Jl. Лингкар, Пондок Чина, Кекаматан Беджи, Кота Депок, Джава Барат 16424, Индонезия
[2]Национальное агентство исследований и инноваций (BRIN), Серпонг, 10340 Бантен, Индонезия

Поступила: *2 июня 2025*
Рецензирование: *4 июня 2025*
Принята в печать: *11 июня 2025*

АННОТАЦИЯ

Твердые отходы, включая отработанные шины, вносят значительный вклад в глобальное загрязнение окружающей среды, ежегодно образуется около одного миллиарда отработанных шин. Использование отработанных шин в качестве источника устойчивого авиационного топлива (SAF) имеет то преимущество, что они не конкурируют с источниками продовольствия, тем самым поддерживая потребности в энергии без ущерба для продовольственной безопасности. Однако производство реактивного топлива из пиролизного масла отработанных шин сталкивается с серьезными проблемами, связанными со строгими стандартами качества Американского общества по испытаниям и материалам (ASTM). В этой статье рассматриваются физико-химические свойства пиролизного масла отработанных шин, включая вязкость, плотность и содержание серы, и сравниваются со спецификациями реактивного топлива ASTM. Проводится библиометрический анализ развития топливных исследований из отработанных шин, перерабатываемых в реактивное топливо, путем сбора количества статей и документов, количества цитирований и стран, которые выпускают больше всего статей, связанных с отработанными шинами и их исследованиями. Также подробно обсуждалась разработка катализаторов для производства реактивного топлива в процессе крекинга. Использование пиролизного масла из отработанных шин в реактивных двигателях также рассматривалось как первый шаг на пути к внедрению экологически чистых видов топлива в авиационном секторе.

Ключевые слова: катализатор, реактивное топливо, физико-химические свойства, пиролизное масло, отработанные шины.

Информация об авторах:

Fitrianto *Магистр кафедры машиностроения инженерного факультета Университета Индонезии, 16424 Депок, Джава Барат, Индонезия. Email: fitrianto21@ui.ac.id; ORCID ID: https://orcid.org/0009-0004-2029-6723*

Nandy Setiadi Djaya Putra *Доктор технических наук, профессор кафедры машиностроения инженерного факультета Университета Индонезии, 16424 Депок, Джава Барат, Индонезия. Email: nandyputra@eng.ui.ac.id; ORCID ID: https://orcid.org/0000-0003-3010-599X*

Eny Kusrini *Доктор философии, кафедра химической инженерии, инженерный факультет, Университет Индонезии, Кампус Бару UI, Депок 16424, Индонезия. Email: eny.k@ui.ac.id; ORCID ID: https://orcid.org/0000-0002-7919-0083*

References

[1] Emmanouilidou E, et al. Solid waste biomass as a potential feedstock for producing sustainable aviation fuel: A systematic review. Renewable Energy. 2023; 206:897-907. https://doi.org/10.1016/j.renene.2023.02.113

[2] Jadav K, et al. Investigation of nano catalyst to enhance fuel quality in waste tyre pyrolysis. Energy Sources, Part A: Recovery, Utilization and Environmental Effects. 2022; 44(1):1468-1477. https://doi.org/10.1080/15567036.2019.1645245

[3] Valentini F, and Pegoretti A. End-of-life options of tyres. A review. Advanced Industrial and Engineering Polymer Research. 2022; 5(4):203-213. https://doi.org/10.1016/j.aiepr.2022.08.006

[4] Hoang AT, NguyenTH, and Nguyen HP. Scrap tire pyrolysis as a potential strategy for waste management pathway: a review. Energy Sources, Part A: Recovery, Utilization, and Environmental Effects. 2020; 46(1):6305-6322. DOI: https://doi.org/10.1080/15567036.2020.1745336

[5] Xu J, et al. High-value utilization of waste tires: A review with focus on modified carbon black from pyrolysis. Sci Total Environ. 2020; 742:140235. https://doi.org/10.1016/j.scitotenv.2020.140235

[6] Dabic-Miletic S, Simic V, and Karagoz S. End-of-life tire management: a critical review. Environ Sci Pollut Res Int. 2021; 28(48):68053-68070. https://doi.org/10.1007/s11356-021-16263-6

[7] Tushar Q, et al. Recycling waste vehicle tyres into crumb rubber and the transition to renewable energy sources: A comprehensive life cycle assessment. J Environ Manage. 2022; 323:116289. https://doi.org/10.1016/j.jenvman.2022.116289

[8] Karagöz M, Ağbulut Ü, and Sarıdemir S. Waste to energy: Production of waste tire pyrolysis oil and comprehensive analysis of its usability in diesel engines. Fuel. 2020, 275. https://doi.org/10.1016/j.fuel.2020.117844

[9] Rogachuk BE, and Okolie JA. Waste tires based biorefinery for biofuels and value-added materials production. Chemical Engineering Journal Advances. 2023, 14. https://doi.org/10.1016/j.ceja.2023.100476

[10] Carmo-Calado L, et al. Co-Combustion of Waste Tires and Plastic-Rubber Wastes with Biomass Technical and Environmental Analysis. Sustainability. 2020; 12(3). https://doi.org/10.3390/su12031036

[11] Zerin NH, et al. End-of-life tyre conversion to energy: A review on pyrolysis and activated carbon production processes and their challenges. Sci Total Environ. 2023; 905:166981. https://doi.org/10.1016/j.scitotenv.2023.166981

[12] Zhang G, et al. Properties and utilization of waste tire pyrolysis oil: A mini review. Fuel Processing Technology. 2021; 211. https://doi.org/10.1016/j.fuproc.2020.106582

[13] Muelas Á, et al. Production and droplet combustion characteristics of waste tire pyrolysis oil. Fuel Processing Technology. 2019; 196. https://doi.org/10.1016/j.fuproc.2019.106149

[14] Abedeen A, et al. Catalytic cracking of scrap tire-generated fuel oil from pyrolysis of waste tires with zeolite ZSM-5. International Journal of Sustainable Engineering. 2021; 14(6):2025-2040. https://doi.org/10.1080/19397038.2021.1951883

[15] Mello M, Rutto H, and Seodigeng T. Waste tire pyrolysis and desulfurization of tire pyrolytic oil (TPO) - A review. J Air Waste Manag Assoc. 2023; 73(3):159-177. https://doi.org/10.1080/10962247.2022.2136781

[16] Fitriasari EI, Won W, and Jay Liu J. Sustainability assessment of biojet fuel produced from pyrolysis oil of woody biomass. Sustainable Energy and Fuels. 2023; 7(15):3625-3636. https://doi.org/10.1039/d3se00468f

[17] Jing L, et al. Understanding variability in petroleum jet fuel life cycle greenhouse gas emissions to inform aviation decarbonization. Nat Commun. 2022; 13(1):7853. https://doi.org/10.1038/s41467-022-35392-1

[18] Why ESK, et al. Single-step catalytic deoxygenation of palm feedstocks for the production of sustainable bio-jet fuel. Energy. 2022; 239:122017. https://doi.org/10.1016/j.energy.2021.122017

[19] Suchocki T, et al. Experimental investigation of performance and emission characteristics of a miniature gas turbine supplied by blends of kerosene and waste tyre pyrolysis oil. Energy. 2021; 215:119125.

[20] Gunerhan A, Altuntas O, and Caliskan H. Utilization of renewable and sustainable aviation biofuels from waste tyres for sustainable aviation transport sector. Energy. 2023; 276:127566. https://doi.org/10.1016/j.energy.2023.127566

[21] Gunerhan A, Altuntas O, and Caliskan H. Utilization of renewable and sustainable aviation biofuels from waste tyres for sustainable aviation transport sector. Energy. 2023; 276. https://doi.org/10.1016/j.energy.2023.127566

[22] Aramkitphotha S, et al. Low sulfur fuel oil from blends of microalgae pyrolysis oil and used lubricating oil: Properties and economic evaluation. Sustainable Energy Technologies and Assessments. 2019; 31:339-346. https://doi.org/10.1016/j.seta.2018.12.019

[23] Straka P, et al. Production of transportation fuels via hydrotreating of scrap tires pyrolysis oil. Chemical Engineering Journal. 2023; 460. https://doi.org/10.1016/j.cej.2023.141764

[24] Sanahuja-Parejo O, et al. Ca-based catalysts for the production of high-quality bio-oils from the catalytic co-pyrolysis of grape seeds and waste tyres. Catalysts. 2019; 9(12). https://doi.org/10.3390/catal9120992

[25] Qi J, et al. Machine learning-driven prediction and optimization of pyrolysis oil and limonene production from waste tires. Journal of Analytical and Applied Pyrolysis. 2024; 177. https://doi.org/10.1016/j.jaap.2023.106296

[26] Zhao Q, et al. Pathways to Carbon Neutrality: A Review of Life Cycle Assessment-Based Waste Tire Recycling Technologies and Future Trends. Processes. 2025; 13(3). https://doi.org/10.3390/pr13030741

[27] Khan W, Shyamal DS, and Kazmi AA. Management of end-of-life tyres in India: current practices, regulatory framework, challenges, and opportunities. Journal of Material Cycles and Waste Management. 2024; 26(3):1310-1325. https://doi.org/10.1007/s10163-024-01937-3

[28] Han W, Han D, and Chen H. Pyrolysis of Waste Tires: A Review. Polymers (Basel). 2023; 15(7). https://doi.org/10.3390/polym15071604

[29] Lopez G, et al. Waste truck-tyre processing by flash pyrolysis in a conical spouted bed reactor. Energy Conversion and Management. 2017; 142:523-532. https://doi.org/10.1016/j.enconman.2017.03.051

[30] Sajdak M, et al. Design of experiments method into upgrading pyrolytic oil for sustainable aviation fuel additives by hydrotreating and hydrocracking. Waste Manag. 2025; 194:258-269. https://doi.org/10.1016/j.wasman.2025.01.012

[31] Durak H. Comprehensive Assessment of Thermochemical Processes for Sustainable Waste Management and Resource Recovery. Processes. 2023; 11(7). https://doi.org/10.3390/pr11072092

[32] Zheng D, et al. Influences and mechanisms of pyrolytic conditions on recycling BTX products from passenger car waste tires. Waste Management. 2023; 169:196-207. https://doi.org/10.1016/j.wasman.2023.07.001

[33] Abnisa F, and Alaba PA. Recovery of liquid fuel from fossil-based solid wastes via pyrolysis technique: A review. Journal of Environmental Chemical Engineering. 2021; 9(6):106593. https://doi.org/10.1016/j.jece.2021.106593

[34] Wu Q, et al. Resource and environmental assessment of pyrolysis-based high-value utilization of waste passenger tires. Waste Management. 2021; 126:201-208. https://doi.org/10.1016/j.wasman.2021.03.008

[35] Wang K, et al. Thermo-chemical conversion of scrap tire waste to produce gasoline fuel. Waste Management. 2019; 86:1-12. https://doi.org/10.1016/j.wasman.2019.01.024

[36] Shehata M, Okeily MA, and Hammad AS. Valorisation of shredded waste tyres through sequential thermal and catalytic pyrolysis for the production of diesel-like fuel. Results in Engineering. 2024; 21. https://doi.org/10.1016/j.rineng.2023.101718

[37] Igliński B, Kujawski W, and Kiełkowska U. Pyrolysis of Waste Biomass: Technical and Process Achievements, and Future Development—A Review. Energies. 2023; 16(4). https://doi.org/10.3390/en16041829

[38] Haryanto A, et al. Valorization of Indonesian Wood Wastes through Pyrolysis: A Review. Energies. 2021; 14(5). https://doi.org/10.3390/en14051407

[39] Ruwona W, Danha G, and Muzenda E. A Review on Material and Energy Recovery from Waste Tyres. Procedia Engineering. 2019; 35:216-222. https://doi.org/10.1016/j.promfg.2019.05.029

[40] Alsaleh A, and Sattler ML. Waste Tire Pyrolysis: Influential Parameters and Product Properties. Current Sustainable/Renewable Energy Reports. 2014; 1(4):129-135. https://doi.org/10.1007/s40518-014-0019-0

[41] Lewandowski WM, Januszewicz K, and Kosakowski W. Efficiency and proportions of waste tyre pyrolysis products depending on the reactor type—A review. Journal of Analytical and Applied Pyrolysis. 2019; 140:25-53. https://doi.org/10.1016/j.jaap.2019.03.018

[42] Laresgoiti MF, et al. Characterization of the liquid products obtained in tyre pyrolysis. Journal of Analytical and Applied Pyrolysis. 2004; 71(2):917-934. https://doi.org/10.1016/j.jaap.2003.12.003

[43] Chen YK, Hsieh CH, and Wang WC. The production of renewable aviation fuel from waste cooking oil. Part II: Catalytic hydro-cracking/isomerization of hydro-processed alkanes into jet fuel range products. Renewable Energy. 2020; 157:731-740. https://doi.org/10.1016/j.renene.2020.04.154

[44] Sharma A, and Murugan S. Potential for using a tyre pyrolysis oil-biodiesel blend in a diesel engine at different compression ratios. Energy Conversion and Management. 2015; 93:289-297. https://doi.org/10.1016/j.enconman.2015.01.023

[45] Hemighaus G, et al. Aviation fuels technical review. Chevron Corporation. 2006.

[46] Yaqoob H, et al. Current status and potential of tire pyrolysis oil production as an alternative fuel in developing countries. Sustainability (Switzerland). 2021; 13(6):3214. https://doi.org/10.3390/su13063214

[47] Karagöz M. Investigation of performance and emission characteristics of an CI engine fuelled with diesel – waste tire oil – butanol blends. Fuel. 2020; 282. https://doi.org/10.1016/j.fuel.2020.118872

[48] Islam MR, Tushar MSHK, and Haniu H. Production of liquid fuels and chemicals from pyrolysis of Bangladeshi bicycle/rickshaw tire wastes. Journal of Analytical and Applied Pyrolysis. 2008; 82(1):96-109. https://doi.org/10.1016/j.jaap.2008.02.005

[49] Ucar S, et al. Evaluation of two different scrap tires as hydrocarbon source by pyrolysis. Fuel. 2005; 84(14):1884-1892. https://doi.org/10.1016/j.fuel.2005.04.002

[50] Kumar M, and Karmakar S. Combustion characteristics of butanol, butyl butyrate, and Jet A-1 in a swirl-stabilized combustor. Fuel. 2020; 281. https://doi.org/10.1016/j.fuel.2020.118743

[51] Suchocki T, et al. Experimental investigation of performance and emission characteristics of a miniature gas turbine supplied by blends of kerosene and waste tyre pyrolysis oil. Energy. 2021; 215. https://doi.org/10.1016/j.energy.2020.119125

[52] İlkılıç C, and Aydın H. Fuel Production From Waste Vehicle Tires by Catalytic Pyrolysis and Its Application in a Diesel Engine. Fuel Processing Technology. 2011; 92(5):1129-1135. https://doi.org/10.1016/j.fuproc.2011.01.009

[53] Pšeničkа M, et al. Pyrolysis Oils from Used Tires and Plastic Waste: A Comparison of a Co-Processing with Atmospheric Gas Oil. Energies. 2022; 15(20):7745. **https://doi.org/10.3390/en15207745**

[54] Trongkaew P, et al. Photocatalytic Desulfurization of Waste Tire Pyrolysis Oil. Energies. 2011; 4(11):1880-1896. https://doi.org/10.3390/en4111880

[55] Kalargaris I, Tian G, and Gu S. Combustion, performance and emission analysis of a DI diesel engine using plastic pyrolysis oil. Fuel Processing Technology. 2017; 157:108-115. https://doi.org/10.1016/j.fuproc.2016.11.016

[56] López G, et al. Continuous Pyrolysis of Waste Tyres in a Conical Spouted Bed Reactor. Fuel. 2010; 89(8):1946-1952. https://doi.org/10.1016/j.fuel.2010.03.029

[57] Martínez JD, et al. Co-Pyrolysis of Biomass With Waste Tyres: Upgrading of Liquid Bio-Fuel. Fuel Processing Technology. 2014; 119:263-271. https://doi.org/10.1016/j.fuproc.2013.11.015

[58] Babajo SA. Production of liquid fuel from co-pyrolysis of jatropha cake with tyre waste. Environmental Research and Technology. 2022; 5(2):111-118. https://doi.org/10.35208/ert.1024788

[59] Ahmed A, Khan SR, and Zeeshan. Application of low-cost natural zeolite catalyst to enhance monoaromatics yield in co-pyrolysis of wheat straw and waste tire. Journal of the Energy Institute. 2022; 105:367-375. https://doi.org/10.1016/j.joei.2022.10.014

[60] Seljak T, Rodman Oprešnik S, and Katrašnik T. Microturbine combustion and emission characterisation of waste polymer-derived fuels. Energy. 2014; 77:226-234. https://doi.org/10.1016/j.energy.2014.07.020

[61] Rizzo AM. Biomass pyrolysis for liquid biofuels: production and use. 2015.

[62] Seljak T, and Katrašnik T. Designing the microturbine engine for waste-derived fuels. Waste Management. 2016; 47:299-310. https://doi.org/10.1016/j.wasman.2015.06.004

[63] Kan T, Strezov V, and Evans T. Fuel production from pyrolysis of natural and synthetic rubbers. Fuel. 2017; 191:403-410. https://doi.org/10.1016/j.fuel.2016.11.100

[64] Toteva V, and Stanulov K. Waste tires pyrolysis oil as a source of energy: Methods for refining. Progress in Rubber, Plastics and Recycling Technology. 2019; 36(2):143-158. https://doi.org/10.1177/1477760619895026

[65] Jantaraksa N, et al. Cleaner alternative liquid fuels derived from the hydrodesulfurization of waste tire pyrolysis oil. Energy Conversion and Management. 2015; 95:424-434. https://doi.org/10.1016/j.enconman.2015.02.003

[66] Saeng-Arayakul P, and Jitkarnka S. An Attempt on Using a Regenerated Commercial NiMoS/Al2O3 as a Catalyst for Waste Tyre Pyrolysis. 2013; 35:1339-1344.

[67] Jiang H, et al. Desulfurization and upgrade of pyrolytic oil and gas during waste tires pyrolysis: The role of metal oxides. Waste Manag. 2024; 182:44-54. https://doi.org/10.1016/j.wasman.2024.04.020

[68] Zhang Q, et al. Desulfurization of Spent Tire Pyrolysis Oil and Its Distillate via Combined Catalytic Oxidation using H2O2 with Formic Acid and Selective Adsorption over Al2O3. Energy & Fuels. 2020; 34(5):6209-6219. https://doi.org/10.1021/acs.energyfuels.9b03968

[69] Papuga S, et al. Pyrolysis of Tyre Waste in a Fixed-Bed Reactor. Symmetry. 2023; 15(12). https://doi.org/10.3390/sym15122146

[70] Choi G-G, Oh S-J, and Kim J-S. Non-catalytic pyrolysis of scrap tires using a newly developed two-stage pyrolyzer for the production of a pyrolysis oil with a low sulfur content. Applied Energy. 2016; 170:140-147. https://doi.org/10.1016/j.apenergy.2016.02.119

[71] Muenpol S, Yuwapornpanit R, and Jitkarnka S. Valuable petrochemicals, petroleum fractions, and sulfur compounds in oils derived from waste tyre pyrolysis using five commercial zeolites as catalysts: Impact of zeolite properties. Clean Technologies and Environmental Policy. 2015; 17(5):1149-1159. https://doi.org/10.1007/s10098-015-0935-8

[72] Tian X, et al. Waste resource utilization: Spent FCC catalyst-based composite catalyst for waste tire pyrolysis. Fuel. 2022; 328. https://doi.org/10.1016/j.fuel.2022.125236

[73] Cao C, et al. Insights into the role of CaO addition on the products distribution and sulfur transformation during simulated solar-powered pyrolysis of waste tires. Fuel. 2022; 314. https://doi.org/10.1016/j.fuel.2021.122795

[74] Yongrong Y, Jizhong C, and Guibin Z. Technical advance on the pyrolysis of used tires in China. in China–Japan International Academic Symposium Enviromental Problem in Chinese Iron Steelmaking Industries and Effective Technology Transfer, Japan. 2000.

[75] Fabiana P de Sousa, Gustavo P dos Reis, Vânya MD Pasa. Catalytic pyrolysis of vegetable oils over NbOPO4 for SAF and green diesel production. Journal of Analytical and Applied Pyrolysis. 2024; 177:106314. https://doi.org/10.1016/j.jaap.2023.106314

[76] Shahriar MF, and Khanal A. The current techno-economic, environmental, policy status and perspectives of sustainable aviation fuel (SAF). Fuel. 2022; 325. https://doi.org/10.1016/j.fuel.2022.124905

[77] Hemighaus G, et al. Aviation fuels: Techincal review. Chevron Products Company. 2007.

[78] Yontar AA. Injection parameters and lambda effects on diesel jet engine characteristics for JP-8, FAME and naphtha fuels. Fuel. 2020; 271:117647. https://doi.org/10.1016/j.fuel.2020.117647

[79] Yang J, et al. An overview on performance characteristics of bio-jet fuels. Fuel. 2019; 237:916-936. https://doi.org/10.1016/j.fuel.2018.10.079

[80] Yaşar F. Mixing of Biodiesels Produced From Different Sources to Jet Fuels and Comparison of Specifications of Fuel Blends. European Journal of Technic. 2020; 10(1):86-96. https://doi.org/10.36222/ejt.710457

[81] Tsanaktsidis CG, Christidis SG, and Favvas EP. A novel method for improving the physicochemical properties of diesel and jet fuel using polyaspartate polymer additives. Fuel. 2013; 104:155-162. https://doi.org/10.1016/j.fuel.2012.09.076

[82] Giudici C, et al. Chapter One - Catalytic and non-catalytic chemical kinetics of hydrocarbons cracking for hydrogen and carbon materials production, in Advances in Chemical Engineering, M. Pelucchi and M. Maestri, Editors. Academic Press. 2023, 1-62.

[83] Moorthy Rajendran K, et al. Review of catalyst materials in achieving the liquid hydrocarbon fuels from municipal mixed plastic waste (MMPW). Materials Today Communications. 2020; 24:100982. https://doi.org/10.1016/j.mtcomm.2020.100982

[84] Duan D, et al. A novel production of phase-divided jet-fuel-range hydrocarbons and phenol-enriched chemicals from catalytic co-pyrolysis of lignocellulosic biomass with low-density polyethylene over carbon catalysts. Sustainable Energy & Fuels. 2020; 4:3687-3700. https://doi.org/10.1039/D0SE00419G

[85] Reza MS, et al. Influence of Catalyst on the Yield and Quality of Bio-Oil for the Catalytic Pyrolysis of Biomass: A Comprehensive Review. Energies. 2023; 16(14):5547. https://doi.org/10.3390/en16145547

[86] Wang K, et al. Study on pyrolysis characteristics, kinetics and thermodynamics of waste tires catalytic pyrolysis with low-cost catalysts. Fuel. 2024; 356. https://doi.org/10.1016/j.fuel.2023.129644

[87] Reddy Kannapu H, et al. MgO-modified activated biochar for biojet fuels from pyrolysis of sawdust on a simple tandem micro-pyrolyzer. Bioresource Technology. 2022; 359. https://doi.org/10.1016/j.biortech.2022.127500

[88] Fu H, et al. Jet fuel range hydrocarbon generation from catalytic pyrolysis of lignin and polypropylene with iron-modified activated carbon. Journal of Analytical and Applied Pyrolysis. 2024; 177:106360. https://doi.org/10.1016/j.jaap.2024.106360

[89] Duan D, et al. Production of renewable jet fuel and gasoline range hydrocarbons from catalytic pyrolysis of soapstock over corn cob-derived activated carbons. Energy. 2020. 209 https://doi.org/10.1016/j.energy.2020.118454

[90] Seyed Mousavi SAH, Sadrameli SM, and Saeedi Dehaghani AH. Catalytic pyrolysis of municipal plastic waste over nano MIL-53 (Cu) derived @ zeolite Y for gasoline, jet fuel, and diesel range fuel production. Process Safety and Environmental Protection. 2022; 164:449-467. https://doi.org/10.1016/j.psep.2022.06.018

[91] Li P, et al. Jet fuel-range hydrocarbon production from catalytic pyrolysis of low-density polyethylene by metal-loaded activated carbon. Sustainable Energy & Fuels. 2022; 6:2289-2305. https://doi.org/10.1039/D2SE00129B

[92] Huo E, et al. Jet fuel range hydrocarbons production by co-pyrolysis of low density polyethylene and wheat straw over activated carbon catalyst. Sustainable Energy & Fuels. 2021; 5:6145-6156. https://doi.org/10.1039/D1SE01108A

[93] Zhang Y, et al. Jet fuel production from waste plastics via catalytic pyrolysis with activated carbons. Appl. Energy. 2019; 251: 113337.

[94] Tang H, et al. Aviation fuel hydrocarbons from camphorwood and low-density polyethylene: Cascade catalytic approach with CaO and Zn/HBeta. Fuel. 2024; 369. https://doi.org/10.1016/j.fuel.2024.131770

[95] Mateo W, et al. Synthesis and characterization of sulfonated activated carbon as a catalyst for bio-jet fuel production from biomass and waste plastics. Bioresource Technology. 2020; 297. https://doi.org/10.1016/j.biortech.2019.122411

[96] Farooq A, et al. Jet fuel-range hydrocarbons generation from the pyrolysis of saw dust over Fe and Mo-loaded HZSM-5(38) catalysts. Fuel. 2023; 333(1). https://doi.org/10.1016/j.fuel.2022.126313

[97] Zhou L, et al. Pyrolysis-catalysis of medical waste over metal-doping porous biochar to co-harvest jet fuel range hydrocarbons and H2-rich fuel gas. Journal of Analytical and Applied Pyrolysis. 2023; 175. https://doi.org/10.1016/j.jaap.2023.106157

[98] Miro de Medeiros A, et al. Catalytic pyrolysis of coconut oil with Ni/SBA-15 for the production of bio jet fuel. RSC Advances, 2022; 12(16):10163-10176. https://doi.org/10.1039/d2ra00866a

[99] Verma V, et al. Catalytic hydroprocessing of waste cooking oil for the production of drop-in aviation fuel and optimization for improving jet biofuel quality in a fixed bed reactor. Fuel. 2023; 333(1). https://doi.org/10.1016/j.fuel.2022.126348

[100] Hassan SH, et al. Catalytic hydrocracking of jatropha oil over natural clay for bio-jet fuel production. Scientific Reports. 2023; 13(1). https://doi.org/10.1038/s41598-023-40500-2

[101] Wang J, et al. Converting polyisoprene rubbers into bio-jet fuels via a cascade hydropyrolysis and vapor-phase hydrogenation process. Energy Conversion and Management. 2022; 270. https://doi.org/10.1016/j.enconman.2022.116250

[102] López FA, et al. The GRAUTHERMIC-Tyres process for the recycling of granulated scrap tyres. Journal of Analytical and Applied Pyrolysis. 2013; 103:207-215. https://doi.org/10.1016/j.jaap.2012.12.007

[103] Dũng NA, Wongkasemjit S, and Jitkarnka S. Effects of pyrolysis temperature and Pt-loaded catalysts on polar-aromatic content in tire-derived oil. Applied Catalysis B: Environmental. 2009; 91(1-2):300-307. https://doi.org/10.1016/j.apcatb.2009.05.038

[104] Osayi J, and Osifo P. Utilization of Synthesized Zeolite for Improved Properties of Pyrolytic Oil Derived from Used Tire. International Journal of Chemical Engineering. 2019; 2019:1-12. https://doi.org/10.1155/2019/6149189

Crossref
DOI: 10.31643/2026/6445.41
Engineering and Technology

Decomposition of Magnesite-Sparing Waste in Sulfuric Acid with a High Concentration: Empirical Modeling and Determination of Optimal Conditions

Atashev E.A.

Urgench State University named after Abu Rayhon Beruni, Uzbekistan

Corresponding author email: elyor.a@urdu.uz

Received: *June 3, 2025*
Peer-reviewed: *June 10, 2025*
Accepted: *June 17, 2025*

ABSTRACT

This article describes the processes of decomposition of magnesite waste in sulfuric acid, which is formed during flotation enrichment of the Zinelbulak talc-magnesite deposit. As a result of the research, the influence of concentration and temperature of the reaction medium on the dissolution of magnesite in H_2SO_4 solution was investigated and melting degrees were determined. Based on the data obtained, a mathematical model of the process was formed: the melting kinetics were described by equations, and the parameters were calculated using regression analysis. The modelling results were based on the rate at which magnesite melts, with a focus on acid concentration and temperature factors. The value of the coefficient of determination of the constructed mathematical model justified the fact that this model was 97.2% accurate. Based on the reliability of the mathematical model, optimal conditions are determined through experimental and model analysis. The optimum conditions are a temperature of T = 81.45 °C and an acid concentration of C = 74.05%, resulting in a decomposition rate of Y_{max} = 93.57%. The results of this work establish a scientific foundation for treating waste products containing magnesium and producing products such as magnesium sulfate from them. Initially, the article describes the composition of raw materials and experimental methods, then the mathematical model and the results obtained are analysed, and conclusions and proposals are presented.

Keywords: Zinelbulak mine, talc-magnesite waste, magnesite, dissolution in sulfuric acid, mathematical model, kinetic analysis, regression analysis.

Atashev Elyor Atashevich

Doctor of Philosophy in Technical Sciences, Associate Professor at the Faculty of Chemical Technology, Urgench State University named after Abu Rayhon Beruni, Urgench, H. Olimjon Street 14, 220100, Uzbekistan. Email: elyor.a@urdu.uz; ORCID ID: https://orcid.org/0000-0003-4070-5665

Introduction

The Zinelbulak talc-magnesite deposit reserve is the only major talc rock deposit in Central Asia with an output of 200 million tonnes. Mining ore has a complex composition containing 52% talc, 43% carbonate minerals (mainly magnesite) and 5% iron oxides [[1], [2], [3]]. Qualitative and quantitative analyses showed that the main mineralogical composition of ore consists of talc and magnesium components, and the magnesium content is 31.7 wt%. It has also been found that such impurities as serpentine, quartz, hematite, and magnetite are found in this raw material [[1], [2]].

When talc concentrate is isolated from the talc-magnesite raw material by gravitational or flotation methods, a magnesite waste consisting mainly of magnesite is formed. This magnifying waste can be chemically processed into a valuable product. In particular, when the magnesium is decomposed in sulfuric acid, magnesium sulfate ($MgSO_4$) is formed, a compound that is widely used in industry and agriculture. Therefore, obtaining a variety of products through the recycling of magnetic waste can provide additional economic benefits as well as reduce environmental problems.

Globally, it has been reported that by dissolving magnesite waste in hydrochloric acid, the process kinetics obeys the "pseudo-secondary" model and the activation energy is 62.4 kJ/mol [4]. However, there are also several general studies on the melting kinetics of magnesite feedstock in acids and the optimization of process parameters. Specifically, [5] in their study, they set the reaction duration to 60 min with a solid-liquid part ratio of 1:20 at an acid concentration of 2 M at a temperature of 65°C, as optimal conditions for dissolving magnesite in H_2SO_4

solution. The melting kinetics of magnesite in sulfuric acid were studied by the process of magnesium extraction in sulfuric acid on the example of the mineral serpentinite. As a result of the process, a magnesium release of 98.35% was achieved. As a result, the authors found that high-purity $Mg(OH)_2$ and $4MgCO_3$· Synthesis of $Mg(OH)_2 \cdot 4H_2O$ obtained [6]. The influence of indicators such as acid concentration, temperature, mixing rate, and particle size as factors influencing the efficiency of the magnetite acid refining process was investigated, and conclusions about optimal conditions were drawn [[7], [8], [9]].

According to the above-mentioned sources of literature analysis, the process of decomposition of magnesite waste formed by flotation enrichment of talc-magnesite from the Zinelbulak mine using sulfate, nitrate or hydrochloric acids and its mathematical model have not been studied. In this regard, this study investigated experimentally and theoretically the process of disintegration of magnite-sparing wastes by processing in H_2SO_4, the main component of which is magnesite.

The purpose of the research is to define its parameters and equations by mathematical modeling of a process and determine the optimal technological conditions for the complete process.

Experimental part

The object of the study was the magnesite-containing waste generated during the flotation beneficiation process of the Zinelbulak talc-magnesite rock. The material composition of the Zinelbulak talc-magnesite rock has been studied in our previous research [2] using modern physico-chemical methods. The magnesite-containing waste sample formed during the flotation beneficiation of this raw material was comprehensively analyzed using an X-ray fluorescence spectrometer (Figure 1).

Based on the analyses, the chemical composition of the raw material is presented in Table 1.

The phase composition of this raw material was analyzed using X-ray diffraction, and the results were processed using the BGMN/Profex Rietveld software package to determine the qualitative and quantitative mineralogical composition of the samples (Figure 2 and Table 2) [[10], [11], [12]].

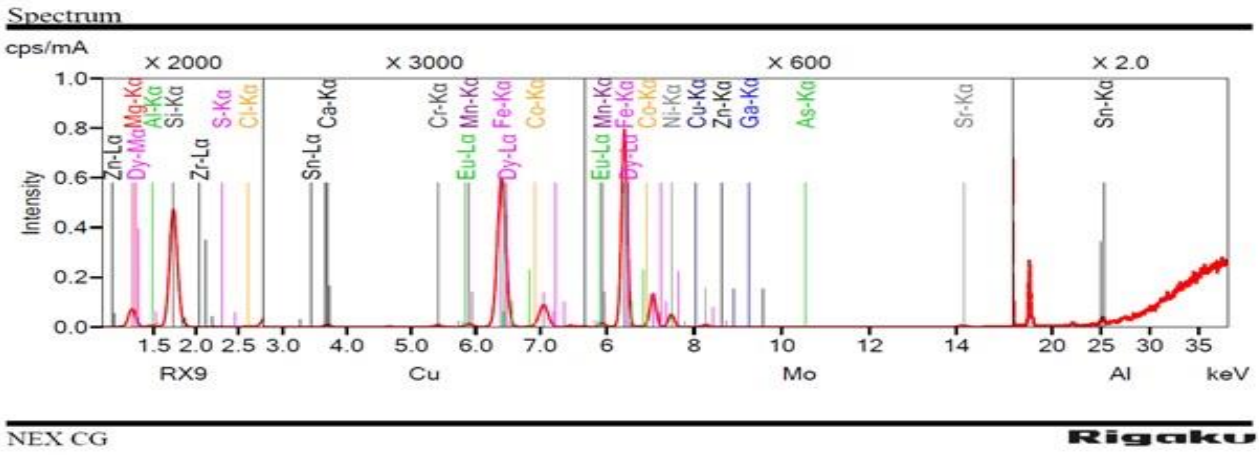

Figure 1 - Extended analysis of the magnesite-containing waste using an X-ray fluorescence spectrometer

Table 1 - Chemical composition of the magnesite precipitate obtained from the flotation process as determined by X-ray fluorescence spectrometry

Tarkibdagi oksidlarning ulushi, %										
SiO_2	MgO	Fe_2O_3	$A1_2O_3$	CaO	Cr_2O_3	MnO	SO_3	NiO	ZrO_2	N_2O
39.15	39.46	5.93	2.42	2.78	0.14	1.62	1.34	1.56	1.78	3.82

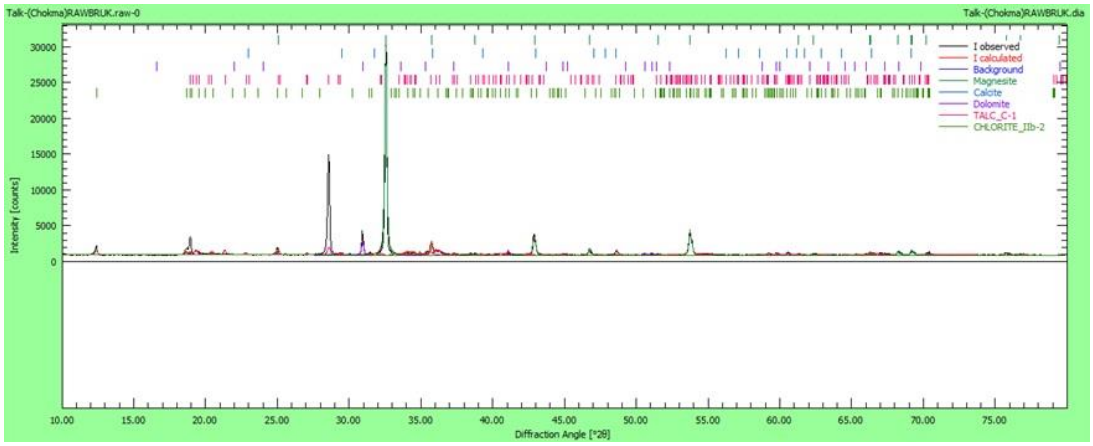

Figure 2 - X-ray diffraction pattern of the magnesite-containing waste

Table 2 - Mineralogical composition of the magnesite-containing waste sample

Mineral name	Chemical formula	Content in the waste, %
Magnesite	$MgCO_3$	53.70
Talc	$3MgO{\cdot}4SiO_2{\cdot}H_2O$	27.20
Kemmererite	$5MgO{\cdot}5FeO{\cdot}Al_2(SiO_3)_3{\cdot}H_2O$	10.01
Dolomite	$MgCO_3{\cdot}CaCO_3$	7.75
Calcite	$CaCO_3$	1.34
Total		**100**

For conducting the research, a static chemical solvent (liquid–solid leaching) method was used in the laboratory. Dried to a constant mass were weighed at an extraction of 5g from a sample with a moderate particle size to −100µm. Disintegration processes were carried out with a solid-to-liquid ratio of 5:100 (g/ml) with the sample measured in a glass tube with a volume of 100 or 250 ml of sulfuric acid solution. For preparation of the acid solution, chemically clean high concentration H_2SO_4 was used, and concentrations of 20–96% were prepared by dilution.

Theoretically, in the process of the decomposition of magnitous boar with sulfuric acid, the following reactions have been observed:

$MgCO_3 + H2SO4 = MgSO_4 + H_2O + CO_2$
$CaMg(CO_3)_2 + 2H_2SO_4 + (n-2)H_2O = CaSO_4{\cdot}nH_2O + MgSO_4 + 2CO_2$
$CaCO_3 + H_2SO_4 = CaSO_4 + H_20 + CO_2$
$2Mg(OH)_2{\cdot}MgSiO_3{\cdot}3SiO_2 + 2H_2SO_4 = 2MgSO_4 + 4H_2O + MgSiO_3 + 3SiO_2$
$Mg(OH)_2{\cdot}4MgFeO_2{\cdot}FeO{\cdot}Al_2(SiO_3)_3 + 10H_2SO_4 = 5MgSO_4 + 5FeSO_4 + Al_2(SiO_3)_3 + 11H_2O$

The amount of magnesium contained in talc-magnesite raw materials and separated magnesite porridges was determined according to the requirements of State standart 19728.8-2001, and the amount of calcium oxide was determined according to the requirements of State standart 19728.7-2001 using volumetric complexometric methods of titration with 0.05. normal Trilon-B solution, chromium black-blue and fluorescein indicators were used. The results were calculated using the following calculation formulas (1 and 2) [[13], [14]].

$$X_{CaO} = \frac{VCV_1 100}{V_2 m} \quad (1)$$

Here: V- Volume flow rate of trilon-B, см^3; *C*- concentration of trilon-B, g/см^3; V_1- total volume of solution, см^3; V_2- volume of solution taken for titration, см^3; *m*- amount of sample, g.

$$X_{MgO} = \frac{VCV_1}{V_2 m} \times 100 - 0{,}719X_1 \quad (2)$$

Here: *V*- volumetric flow rate of Trilon-B used for titration of calcium and magnesium content in the control solution, см^3; *C*- concentration of Trilon-B, g/см^3; V_1- total volume of solution, см^3; V_2- volume

of solution taken for titration, см^3; *m*- amount of sample, g; X_1- mass fraction of calcium oxide, %.

During the analytical processes, a solution is prepared according to the method specified in the literature [15] for determining the general form of P_2O_5 in phosphate raw materials and magnesium phosphate fertilizers. The filtered sample was measured in a photo colourimeter at a wavelength of λ=440 and the results were calculated using the following formula 3:

$$C_{P_2O_5} = \frac{a \times 250 \times 100}{g \times V \times 1000} \quad (3)$$

Here: *a*-the amount of P_2O_5 found from the calibration graph, mg; g - the amount of the analyzed sample, g; V-solution volume, см^3

Calcium and magnesium oxides contained in phosphate raw materials and magnesium phosphate fertilizers were determined by titration with a Trilon-B solution using the complexometric method presented in the literature [[16], [17]]. To determine the general form of P_2O_5 for analysis, a fixed amount of 250 cm^3 of a 0.05 N solution of trilon-B was taken from the prepared solution and analyzed in the presence of chromium black-blue. The results were calculated using the following formulas (4 and 5).

$$C_{CaO} = \frac{a \times 0.0014 \times 50 \times 100}{g \times V \times 50}; \quad (4)$$

$$C_{MgO} = \frac{(b-a) \times 0.001 \times 250 \times 250 \times 100}{g \times V \times 50}; \quad (5)$$

Here: α-volume of Trilon-B used to determine the amount of calcium, ml; β-the volume of Trilon-B used to determine the amount of magnesium, ml; g - amount of analyzed sample, g; V-Volume of solution, cm^3.

In order to determine the optimal conditions for the sulfuric acid decomposition process of this magnifying waste with a complex composition, a quadratic regression model with dependence on the kkita independent variable C-acid concentration (%) and T - process temperature (°C) was used to predict.

In the creation of a mathematical model, the mathematical model equation is expressed only from a mathematical point of view, depending on their quadratic, i.e. curved effect on the degree of decay when the basic initial values, i.e. temperature and concentration are 0, when the acid concentration and process temperatures increase by one unit value, depending on their quadratic, i.e. curved effect:

$$Y = a + bC + cT + dC^2 + eCT + fT^2$$

Where *a, b, c, d, e, f are the coefficients determined on the basis of experimental data.*

To predict the maximum extent of the disintegration process, the two main independent variables are the concentration of acidity (%) and T (°C) by solving all the maximum values and conditions of the process temperature.

$$\frac{\partial Y}{\partial C} = 0; \ \frac{\partial Y}{\partial T} = 0$$

The model determines the coefficient of determination depending on the total –T_{dis} and residual –R_{des} dispersions, i.e

$$R^2 = 1 - \frac{T_{dis}}{R_{des}}$$

The total and residual dispersions in the formula are determined depending on the actual observed value as well as the values predicted by the model. In this case, the general dispersion $T_{dis} = \sum_{i=1}^{n}(y_i - \bar{y})^2$ and residual dispersion $R_{dis} = \sum_{i=1}^{n}(y_i - \hat{y})^2$are determined from the dispersion formulas [[18], [19]].

Results and Discussion

The prepared reaction mixture was carried out in a digital tube heater with magnetic stirring brand MS7-H550-Pro for 180 min at a temperature interval of 10°C, temperature range 30-100°C (with thermostat control ±1 °C accuracy) and constant stirring at 300 rpm. The resulting solid residue was filtered, separated, washed and dried. The amount of magnesium in the samples was determined by the complexometric method (using EDTA).

The results obtained during the studies are shown in Table 3 below, which shows that the degree of decomposition of the magnetite ash relative to MgO is due to a variation of 20–96% concentration of kp acid (C%) and temperature of 30–100°C (T).

Table 3 - Degrees of decomposition of magnesite precipitate at different concentrations, absolute values, and temperatures of H_2SO_4

Acid concentration, %	Degree of brocade of magnesite chips, %, $k_P = \frac{MgO_{сув.}}{MgO_{ум.}}$;							
	30°C	40°C	50°C	60°C	70°C	80°C	90°C	100°C
20	39.33	50.32	51.02	51.03	53.12	54.48	55.12	55.32
30	48.21	74.64	71.24	71.65	72.15	73.52	74.15	74.32
40	49.48	76.64	74.14	74.03	77.97	78.01	78.07	83.89
50	50.38	79.04	79.21	79.46	80.06	80.26	83.94	84.56
60	54.78	79.86	79.64	82.04	82.76	82.02	85.36	85.65
70	57.56	82.01	82.95	83.02	84.56	85.01	87.46	87.92
80	53.35	83.02	83.76	84.16	85.02	85.21	88.56	88.72
90	58.82	83.89	84.50	85.02	86.01	87.01	88.69	89.08
96	59.01	84.40	85.12	85.56	87.08	87.92	89.02	90.14

When the acid concentration was 20% in the process, the rate of decomposition increased by 1.40 times compared to MgO water (k_P), reaching from 39.33% to 55.32%. When the concentration was 30%, the decomposition rate was observed to increase from 48.21% to 65.66% to 1.54 times, and these dependencies increased to 1.69 and 1.68 times, respectively, at concentrations of 40% and 50% of sulfuric acid. It was found that in processes where the acid concentration was increased from 60% to 96%, these values increased by 1.56 and 1.53 times, respectively. At all concentrations of acid, an increase in decomposition at the temperature range of 30-40°C was observed by 1.23 and 1.43 times, and at the temperature range of 50-100°C, up to 1.08 times. Based on the research carried out, it was found that the process is desirable to conduct the process at high concentrations of acid, 80-96%, at a temperature of 40°C.

In the studies, the maximum value was determined at the boundary points, having the concentration of acid (C) in the range of 20% ≤ C ≤ 96% and the process temperature ranges (T) between 30°C ≤ T ≤ 100°C.

$$Y = a + bC + cT + dC^2 + eCT + fT^2$$

The coefficients *a, b, c, d, e, and f in the mathematical model* were calculated using the method of least squares and were determined to be equal to *a = -27.21; b = 0.6257; c = 2.4094; d = -0.0023; e = -0.0035* and *f = -0.0132*. Based on these coefficients, the following equation was formed.

$$Y = -27.721 + 0.6257C + 2.4094T - 0.0023C^2 - 0.0035CT - 0.0132T^2$$

The number of *values of the kP* – experimental decomposition levels in Table 1 above is 9 on the acid, concentration – *9* on C and temperature – 8 on T. So, in the calculations, it will be equal. On the basis of this value, the levels of decay calculated according to the model were determined by the formula $\hat{Y}n = CT = 9 \times 8 = 72$

$$\hat{Y} = \frac{1}{n}\sum_{i=1}^{n}(Y_i) = \frac{1}{72} \times (5780.88) = 80.29\%$$

The determination coefficient of this structure. model – R^2 total –T_{dis} and residual – R_{des} was determined depending on the dispersions.

$$R^2 = 1 - \frac{T_{dis}}{R_{des}} = 1 - \frac{\sum_{i=1}^{n}(y_i - \bar{y})^2}{\sum_{i=1}^{n}(y_i - \hat{y})^2} = \frac{365.12}{13067.93} = 0.972$$

The value of the coefficient of determination indicated that this model was suitable for experimental data with 97.2% accuracy. In the graph shown in Figure 3 below, the experimental values of the degree of decomposition were compared with the values of the degree of decomposition calculated according to the model. The fact that all the points in the graph are located close to it along the regression line once again justified the accuracy of this model. $R^2 = 0.972$

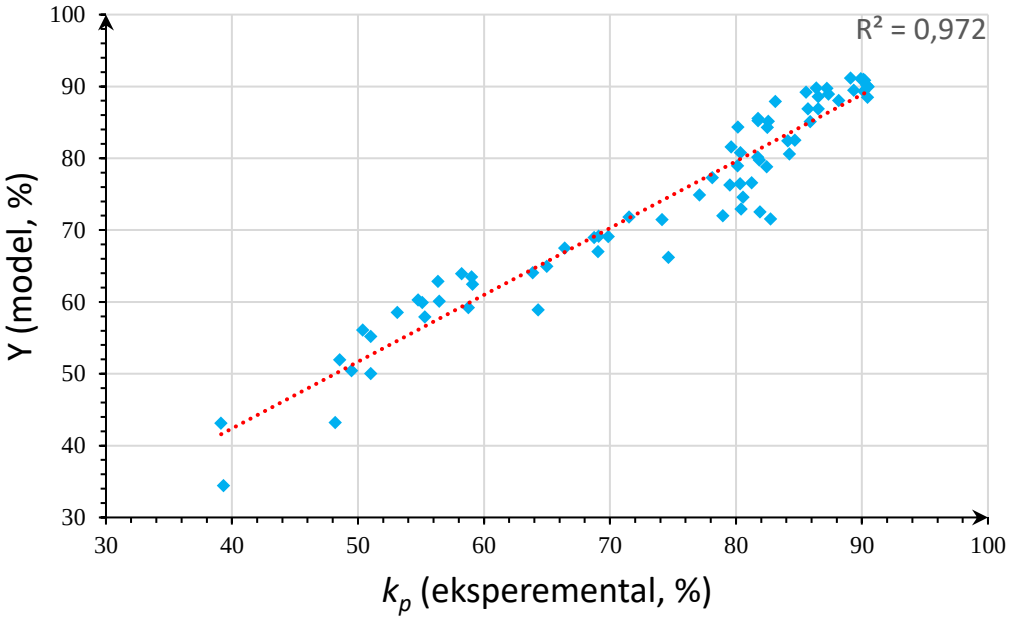

Figure 3 - Comparative comparison of model and experimental values

It has been proven that the model is suitable for research to predict optimal conditions in terms of acid concentration and process temperature parameters.

Conclusion

Based on the above model equation, the optimal conditions and conditions of acid concentration and temperature were deduced. $\frac{\Delta Y}{\Delta C} = 0$; $\frac{\Delta Y}{\Delta T} = 0$

$$\frac{\Delta Y}{\Delta C} = 0.6257 - 2 \times 0.0023C - 0.0035T$$

$$\frac{\Delta Y}{\Delta T} = 2.4094 - 2 \times 0.0132T - 0.0035C$$

Calculations were performed by zeroing the first-order derivatives. As a result of the calculations, the decomposition rate is Y_{max} = 93.57% when the temperature is T = 81.45°C and the concentration of acidity required for the process is C=74.05%.

On the basis of the studies conducted, the model created to determine the possibility of processing magnesitic waste in sulfuric acid under optimal conditions was found and proved to be theoretically useful. This model has made it possible to use the acid decomposition process efficiently and efficiently in the studies because it operates at high precision.

Conflicts of interest. The author declares that there is no conflict of interest regarding the conduct and publication of this study.

Acknowledgements. We would like to express our deep gratitude to Sherzod Raimberganovich Kurambayev, Dean of the Faculty of Chemical Technologies at Urgench State University named after Abu Rayhon Beruni, for his practical assistance in conducting the experiments for this research. We also extend our sincere appreciation to Arslon G‘anibek o‘g‘li Jumaniyazov for his support in translation and language-related matters, and to my colleague Azamat Shomuratovich Khadjiev for his valuable contributions to the writing and editing of this article.

Formatting of funding sources. This research did not receive any specific grant from funding agencies in the public, commercial, or not-for-profit sectors.

Cite this article as: Atashev EA. Decomposition of Magnesite-Sparing Waste In Sulfuric Acid With a High Concentration: Empirical Modeling and Determination of Optimal Conditions. Kompleksnoe Ispolzovanie Mineralnogo Syra = Complex Use of Mineral Resources. 2026; 339(4):71-78. https://doi.org/10.31643/2026/6445.41

Құрамында магнезит қоспасы бар қалдықтардың жоғары концентрациялы күкірт қышқылында ыдырауы: эмпирикалық модельдеу және оңтайлы шарттарды анықтау

Аташев Э.А.

Әбу Райхан Бируни атындағы Үргеніш мемлекеттік университеті, Өзбекстан

Мақала келді: *3 маусым 2025*
Сараптамадан өтті: *10 маусым 2025*
Қабылданды: *17 маусым 2025*

ТҮЙІНДЕМЕ

Бұл мақалада Зинелбулак тальк-магнезит кен орны шикізатын флотациялық байыту кезінде алынатын магнезит қалдығының күкірт қышқылында ыдырау процестері қарастырылған. Зерттеу нәтижесінде магнезиттің H_2SO_4 ерітіндісінде еруіне реакциялық орта концентрациясы мен температурасының әсері зерттеліп, еру дәрежелері анықталды. Алынған мәліметтер негізінде процестің математикалық моделі жасалды: еру кинетикасы теңдеулер арқылы сипатталып, параметрлері регрессиялық талдау көмегімен есептелді. Модельдеу нәтижелері магнезиттің еру жылдамдығы негізінен қышқыл концентрациясы мен температура факторларына тәуелді екенін көрсетті. Құрылған математикалық модельдің детерминация коэффициентінің R^2=0,972 мәні бұл модельдің 97,2% дәлдікпен жұмыс істейтінін дәлелдеді. Математикалық модельдің дәлдігінің негізінде оңтайлы шарттар температура T=81,45°C және қажетті қышқыл концентрациясы C=74,05% кезінде ыдырау деңгейі Y_{max}=93,57% тең болатыны тәжірибелік және модельдік талдаулар арқылы анықталды. Бұл зерттеу нәтижелері магнезит құрамындағы қалдықтарды қайта өңдеу және олардан магний сульфаты сияқты өнімдерді алу үшін ғылыми негіздерді құруға мүмкіндік береді. Мақалада алдымен шикізат құрамы мен эксперименттік әдістер баяндалып, кейін математикалық модель мен алынған нәтижелер талданып, қорытындылар мен ұсыныстар берілді.

Түйін сөздер: Зинелбулак кені; тальк-магнезит қалдығы; магнезит; күкірт қышқылында еріту; математикалық модель; кинетикалық талдау; регрессиялық талдау.

Авторлар туралы ақпарат:

Atashev Elyor Atashevich

Техника ғылымдары бойынша философия докторы, Әбу Райхон Беруни атындағы Үргеніш мемлекеттік университетінің химия-технология факультетінің доценті, Үргеніш қ. Х.Олимжон, 14, 220100, Өзбекстан. Email: elyor.a@urdu.uz; ORCID ID: https://orcid.org/0000-0003-4070-5665

Разложение магнезитсодержащих отходов в высококонцентрированной серной кислоте: эмпирическое моделирование и определение оптимальных условий

Аташев Э.А.

Ургенчский государственный университет имени Абу Райхона Беруни, Узбекистан

Поступила: *3 июня 2025*
Рецензирование: *10 июня 2025*
Принята в печать: *17 июня 2025*

АННОТАЦИЯ

В данной статье рассматриваются процессы разложения магнезитсодержащих отходов, образующихся при флотационном обогащении тальк-магнезитовой руды Зинелбулакского месторождения, в серной кислоте. В результате проведённых исследований изучено влияние концентрации реакционной среды и температуры на растворение магнезита в растворе H_2SO_4, а также определены степени растворения. На основе полученных данных была разработана математическая модель процесса: кинетика растворения описана уравнениями, а параметры рассчитаны с использованием регрессионного анализа. Результаты моделирования показали, что скорость растворения магнезита в основном зависит от факторов концентрации кислоты и температуры. Коэффициент детерминации построенной математической модели R^2=0,972 подтвердил, что точность модели составляет 97,2%. На основе достоверности математической модели определены оптимальные условия: при температуре T=81,45°C и концентрации кислоты C=74,05% степень разложения составляет Y_{max}=93,57%, что установлено на основе экспериментальных и модельных анализов. Результаты данной работы закладывают научные основы для переработки отходов, содержащих магнезит, и получения из них таких продуктов, как сульфат магния. В статье сначала изложены состав сырья и экспериментальные методы, затем приведён анализ математической модели и полученных результатов, а также даны выводы и предложения.

Ключевые слова: Зинелбулакское месторождение, тальк-магнезитовый отход, магнезит, растворение в серной кислоте, математическая модель, кинетический анализ, регрессионный анализ.

Аташев Элёр Аташевич

Информация об авторах:
Доктор философии в области технических наук, доцент факультета химической технологии Ургенчского государственного университета имени Абу Райхона Беруни, Ургенч, улица Х. Олимжона, 14, 220100, Узбекистан. Email: elyor.a@urdu.uz; ORCID ID: https://orcid.org/0000-0003-4070-5665

References

[1] Umirov FE, Shodikulov JM, Aslonov AB, Sharipov SSh. Material composition of talc-magnesite rocks of the Zinelbulak deposit in Uzbekistan. Obogashchenie Rud. 2023; 4. https://doi.org/10.17580/or.2023.04.05

[2] Jumaniyazov M, Kurambayev Sh, Atashev E, Jumaniyozov A, Buranova M. Determination of the composition of the Zinelbulak talc-magnesite deposit rock using modern physicochemical methods. E3S Web of Conferences. 2025; 633:06002. https://doi.org/10.1051/e3sconf/202563306002

[3] Hojamberdiev M, Arifov P, Tadjiev K, Yunhua XU. Characterization and processing of talc-magnesite from the Zinelbulak deposit. Mining Science and Technology (China). 2010; 20(3): 411–415. https://doi.org/10.1016/S1674-5264(09)60218-0

[4] Özdemir M, Çakır D, Kıpçak İ. Magnesium recovery from magnesite tailings by acid leaching and production of magnesium chloride hexahydrate. International Journal of Mineral Processing. 2009; 93(2):209-212.

[5] Abalı Y, Çopur M, Yavuz M. Determination of the optimum conditions for dissolution of magnesite with H_2SO_4 solutions. Indian Journal of Chemical Technology. 2006; 13(4):391-397.

[6] Chen M, Fang Y, Wang X, & Wu Y**.** Selective recovery of magnesium from serpentine using two-stage counter-current leaching with sulfuric acid and synthesis of $4MgCO_3 \cdot Mg(OH)_2 \cdot 4H_2O$. Minerals. 2023; 3(3):318. https://doi.org/10.3390/min13030318

[7] Li W, Bai G, & Huang S. Effect of acid concentration and temperature on leaching kinetics of magnesium carbonate. *Hydrometallurgy*. 2022; 209:105790. https://doi.org/10.1016/j.hydromet.2021.105790

[8] Wang L, Zhang L, & Yu J. Optimization and kinetics of sulfuric acid leaching of magnesite for magnesium sulfate production. Journal of Cleaner Production. 2020; 276:124201. https://doi.org/10.1016/j.jclepro.2020.124201

[9] Zhou T, Yang J, & Li W. Leaching behavior and kinetics of MgO from calcined magnesite in hydrochloric acid solution. Minerals Engineering. 2021; 173:107201. https://doi.org/10.1016/j.mineng.2021.107201

[10] Agarwal BK. X-ray spectroscopy. Berlin, Heidelberg, New York: Springer. 1991, 419.

[11] Zschornack G. Spravochnik po rentgenovskim dannim. Berlin, Geydelberg: Springer-Verlag. 2007, 969.

[12] Monina LM. X-ray Diffraction. Qualitative X-ray Phase Analysis. Publisher: Prospekt. 2017, 120.

[13] State standart 19728.8-2001. Talc and talcomagnesite. Methods for determination of magnesium oxide. M.: IPK Publishing House of Standards. 2001, 7.

[14] State standart 19728.7-2001. Talc and talc-magnesite. Methods for determination of calcium oxide. I.: IPC Publishing House of Standards. 2001, 7.

[15] State standart EN 16198-2016. Determination of magnesium by the complexometric method. Date of introduction. 2017-07-01

[16] Jin Yao (2024) Research advancement of efficient flotation separation technologies for magnesium-containing minerals, Green and Smart Mining Engineering, 1 (2) : 140. https://doi.org/10.1016/j.gsme.2024.05.003

[17] Vinnik MM, Erbanova LN, Zaitsev PM. Methods for the analysis of phosphate raw materials, phosphate and complex fertilizers, feed phosphates, Chemistry, Moscow. 1975.

[18] Fatih Demir, Bünyamin Dönmez, Sabri Çolak. Leaching Kinetics of Magnesite in Citric Acid Solutions. Journal of chemical engineering of Japan. 2003; 36(6):683-688. https://doi.org.10.1252/jcej.36.683

[19] A Compilation of Rate Parameters of Water-Mineral Systems, USGS. U.S. GEOLOGICAL SURVEY. 2004.

[20] Yessengaziyev AM, Ultarakova AA, Burns PC. Fluoroammonium method for processing of cake from leaching of titanium-magnesium production sludge. Kompleksnoe Ispol'zovanie Mineral'nogo Syr'a = Complex Use of Mineral Resources. 2022;320(1):67-74. https://doi.org/10.31643/2022/6445.08

Crossref
DOI: 10.31643/2026/6445.42
Engineering and Technology

Mathematical Analysis of CaO Content Variation in Acidic Wastewater and Mineralized Mass Mixture from Central Kyzylkum Phosphorite Based on Exponential Decay Model

Yuldasheva A.P., *Shamuratov S.Kh., Kurambayev Sh.R., Radjabov M.F.

Urgench State University named after Abu Rayhon Beruni, Urgench, Uzbekistan

**Corresponding author email: sanjar.sh@urdu.uz*

Received: *July 1, 2025*
Peer-reviewed: *July 10, 2025*
Accepted: *July 15, 2025*

ABSTRACT

This article investigates the reduction behavior of calcium oxide (CaO) content in mixtures of mineralized mass (MM) from Central Kyzylkum phosphorite and acidic wastewater (AWW) from the oil and fat industry, using experimental data and a mathematical approach. The study was conducted at 60°C, with the AWW: MM ratio varying from 100:10 to 100:40. The CaO content in each mixture was determined and analysed in terms of its mass ratio. Results demonstrated a systematic decrease in CaO content with an increasing proportion of MM. The initial rate of decline was rapid and then gradually slowed. An exponential decay model was employed and characterized by parameters. A first-order differential equation was applied and refined using experimental data. The initial value and decay constant were found to be C_0 = 67.39 and k = 0.0401, respectively. The resulting exponential equation showed a high degree of correlation with experimental points ($R^2 \approx 0.98$). This study offers a structured evaluation of CaO behavior in complex systems through mathematical modeling, which can be used to control processes in real technological conditions. The modeling outcomes may serve as a methodological basis for developing kinetic models involving other ions and components in future research.

Keywords: CaO, exponential decay, mineralized mass, wastewater, mathematical modeling, predictive model.

Information about authors:

Yuldasheva Asal Pulat kizi — *Student, faculty of Chemical Technology, Urgench State University named after Abu Rayhon Beruni, Urgench, H. Olimjon Street 14, 220100, Uzbekistan. Email: shamuratovsx@gmail.com*

Shamuratov Sanjarbek Khusinbay ugli — *Doctor of Philosophy in Technical Sciences, Associate Professor at the Faculty of Chemical Technology, Urgench State University named after Abu Rayhon Beruni, Urgench, H. Olimjon Street 14, 220100, Uzbekistan. Email: sanjar.sh@urdu.uz; ORCID ID: https://orcid.org/0000-0002-1040-1807*

Kurambayev Sherzod Raimbergenovich — *Doctor of Technical Sciences, Dean of the Faculty of Chemical Technology, Urgench State University named after Abu Rayhon Beruni, Urgench, H. Olimjon Street 14, 220100, Uzbekistan. Email: sherzod.sh@urdu.uz; ORCID ID: https://orcid.org/0009-0003-3986-5079*

Radjabov Mansur Farkhadovich — *Candidate of Technical Sciences, Head of the Department of Food Technology, Urgench State University named after Abu Rayhon Beruni, Urgench, H. Olimjon Street 14, 220100, Uzbekistan. Email: mansur.ra@urdu.uz; ORCID ID: https://orcid.org/0000-0003-2068-0595*

Introduction

Acidic wastewater generated during processing operations in the oil and fat industry represents one of the most pressing environmental issues today. In particular, wastewater produced during the separation and refining of soapstock contains high concentrations of ions such as H^+, SO_4^{2-}, Cl^-, Na^+, and Mg^{2+}. These chemically aggressive components significantly disrupt the pH balance in aquatic environments [[1], [2], [3], [4], [5]].

This leads to severe damage to natural ecological systems. It negatively impacts the quality of groundwater. It disrupts the microbiology of soils. It reduces biodiversity [[6], [7]]. It also destabilizes the food chain and natural biocycles. Such wastewaters degrade very slowly in nature. In most cases, they are discharged directly into surface water bodies. This dramatically increases environmental risk. Industrial facilities often release these wastes without treatment [[8], [9], [10], [11]].

Such practices contradict global environmental protection standards. Especially when the wastewater has a pH below 4, the high acid load makes neutralization absolutely essential. Neutralization is the chemical conversion of harmful acidic components into stable, environmentally safe forms. It is a crucial step in ensuring ecological safety in industrial processes. When selecting neutralizing agents, several criteria must be considered. Economic viability, environmental safety, technological compatibility,

and local availability are key among them [[12], [13], [14], [15], [16]].

Considering these factors, this study selected the mineralized mass derived from the Central Kyzylkum Phosphorite Complex as the neutralizing material. This material is an industrial byproduct from phosphorite processing. It contains chemically active oxides such as CaO, MgO, Al_2O_3, and SiO_2. These oxides can react with acidic ions. The material is natural, locally sourced, cost-effective, and environmentally safe. It exists in large quantities as a byproduct and is typically unused [[13], [14], [15], [16], [17]].

Utilizing it for neutralization offers dual benefits. First, it helps detoxify acidic industrial wastewater. Second, it enables the reuse of industrial mineral waste. This approach aligns with the concept of waste-from-waste technology. Additionally, the Central Kyzylkum mineralized mass demonstrates stable neutralizing behavior against a variety of ionic contaminants [18]. It performs consistently under mechanical mixing and elevated temperature conditions. It does not generate toxic byproducts, forming inert residues instead. Previous studies have not sufficiently evaluated this material's potential. Its kinetic behavior and consumption rate in neutralization processes have not been thoroughly analyzed [[19], [20], [21]].

Most earlier studies rely on laboratory observations without theoretical modeling. This limits their applicability in real industrial scenarios. Therefore, the present research focuses on assessing this material's efficiency in neutralizing real acidic wastewater. Samples of acidic wastewater were treated with varying doses of mineralized mass [[13], [14]]. The decrease in CaO concentration during treatment was analyzed. Neutralization efficiency and reagent consumption were evaluated [[22], [23]]. From a practical perspective, this approach aids in optimizing reagent dosage. It also allows for analysis of how waste composition affects neutralization. The results guide industrial applications. The findings help establish a technological basis for achieving regulatory compliance in wastewater treatment. In essence, this study offers an effective, sustainable, and economically feasible solution for neutralizing acidic industrial effluents. It contributes directly to environmental protection, resource conservation, and waste valorization [13].

Experimental part

The AWW sample was collected from an oil and fat processing plant in Uzbekistan. Preliminary chemical analysis revealed a pH ≈ 2.8 and high concentrations of SO_4^{2-} (1190 mg/L), Cl^- (2120 mg/L), Na^+, Mg^{2+}, and H^+ ions [[13], [14], [15], [16]]. The chemical composition of acidic wastewater produced during the process of extracting fatty acids from soapstock is presented in Table 1.

MM was obtained from Central Kyzylkum's limestone-rich deposits and contained CaO (43,17%), CO_2 (14,01%), P_2O_5 (15,09%), and SO_3 (2,17%). Samples were mixed at 60 ± 1°C in the following mass ratios: 100:10, 100:15, 100:20, 100:25, 100:30, 100:35, and 100:40.

Each sample consisted of 100 g AWW and the corresponding MM amount. They were stirred for 30 minutes at 400 rpm. CaO content was determined from the dry residue using gravimetric methods. Each experiment was repeated three times, and average values were recorded. Based on the data, a mathematical model was constructed to describe CaO decrease with increasing MM.

Modeling was conducted in Origin 2021 Pro using scatter plots and exponential regression:

$$C_{(x)} = C_0 \cdot e^{-kx}$$

Table 1 - Chemical composition of acidic wastewater (AWW) produced during the process of extracting fatty acids from soapstock

Cations	mg/l	meq / l	% -eq / l	Anions	mg/l	meq / l	% -eq / l
H^+	100	100	81	Cl^-	38114	1073	50
Na^+	431560	1876.41	11	SO_4^{2-}	48165	1003.13	46
K^+	-	-	-	NO_2^-	20.11	-	-
NH_4^+	99	5.44	-	NO_3^-	842	13.65	-
Ca^{2+}	299	11	1	CO_3^-	-	-	-
Mg^{2+}	1831	151	7	HCO_3^-	3447	55.18	4
Fe^{3+}	0.4	0.03	-	**Total**		**2148.08**	**100**
Fe^{2+}	32	1.08	-				
Total		**2144.96**	**100**				

Modeling was performed using the "Nonlinear Curve Fit" function based on the sample function “ExpDec1”.

The initial values of the parameters C_o and k were automatically determined, and their optimal values, along with confidence intervals, were provided.

Based on the modeling results, the coefficient of determination (R^2) was found to be higher than 0.98, indicating a strong fit of the exponential model.

All graphs were plotted using the Origin 2021 Pro software environment.

Model-predicted CaO (%) values were calculated using the exponential equation above.

Absolute deviation (Δ) was calculated as the difference between modeled and experimental CaO values [[24], [25]]:

$$\Delta = C_{model} - C_{experimental}$$

Relative error (%) was determined using the formula:

$$\text{Relative error} = \left|\frac{\Delta}{C_{experimental}}\right|$$

Results and Discussion

The CaO content in the resulting products was determined experimentally by preparing mixtures of acidic wastewater and mineralized mass in different mass ratios.

The experiments were conducted at a temperature of 60 °C, with each trial repeated three times, and average values were calculated. The mass ratios of AWW: MM (Acidic Wastewater: Mineralized Mass) were gradually increased from 100:10 to 100:40.

The results indicate that as the proportion of MM increases, the percentage of CaO in the mixture decreases sharply.

This can be explained by the reaction of CaO present in the MM with H^+ ions and other acidic ions found in the AWW, leading to its gradual reduction.

Table 2 and Figure 1 below show the AWW: MM ratio and the corresponding observed CaO content (%).

Table 2 - CaO content in mixtures at increasing AWW:MM ratios

№	AWW:MM Ratio	CaO (%)
1	100:10	46.52
2	100:15	36.49
3	100:20	28.98
4	100:25	23.39
5	100:30	18.94
6	100:35	17.65
7	100:40	16.17

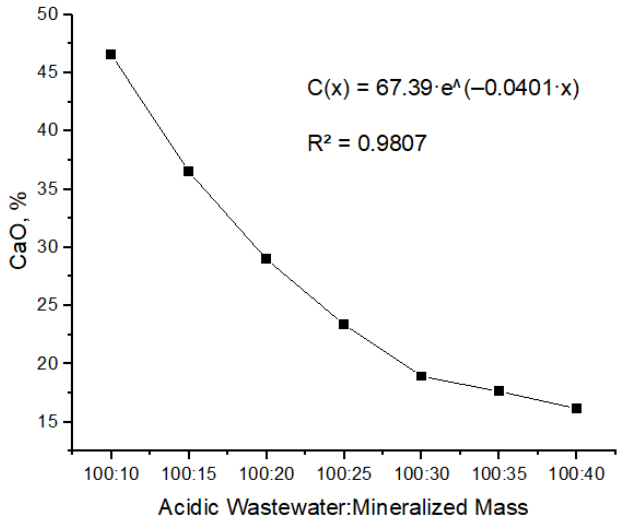

Figure 1 - Exponential decrease in CaO content in the mixture depending on the increase in the AWW:MM ratio

In the sample with a mass ratio of 100:10, the CaO content was 46,52%, whereas at the 100:40 ratio, it dropped to 16,17%. A sharp decline in CaO content was observed during the initial three stages -from 100:10 to 100:25-indicating that reactive CaO actively participated in neutralization reactions with the acidic components of the AWW. This range represents the zone of highest neutralization efficiency for CaO, where the most significant changes occurred. From 100:25 to 100:40, the decrease became more gradual, suggesting that the remaining CaO content declined slowly due to residual reactions.

The exponential decay behavior observed in the graph was confirmed by the model, and the high R^2 value (0,9807) indicates excellent agreement between the model and the experimental data.

The trajectory of CaO reduction was accurately described by the following model:

$$C_{(x)} = 67{,}39 \cdot e^{-0.0401\mathrm{x}}$$

In this case, $C_{(x)}$ -represents the percentage of CaO depending on the amount xxx of mineralized mass (MM); 67,39 is the initial maximum reactive capacity (i.e., the CaO value when the MM amount is close to zero); 0,0401 is the decay coefficient.

According to the graph analysis, the functional decrease of CaO corresponds to the characteristics of a classical kinetic model. This behavior reflects similar reactivity trends observed during the neutralization of real industrial wastewater. The values given in the table are very close to the results of the mathematical model, with an average relative error of approximately 3–4%. Such closeness demonstrates the reliability of the model and enables the identification of optimal technological regimes for various AWW: MM (Acidic Wastewater : Mineralized Mass) mass ratios.

Based on these observations, it was determined that applying CaO in a calculated dose allows effective adjustment of the mixture to meet regulatory pH levels. The decreasing trend of CaO percentage in AWW: MM mixtures was described using an exponential regression model based on experimental data. In this model, the independent variable is the amount of MM (g), while the dependent variable is the CaO percentage (%). As a result of exponential regression performed in Origin 2021 Pro, the following mathematical model equation was obtained.

The model's goodness-of-fit is represented by the value:

$$R^2 = 0{,}9807$$

which indicates a strong correlation between the experimental results and the model.

The linearized graph generated from the model nearly fully encompasses the experimental data points, visually confirming the high degree of conformity.

The high rate of decrease in the initial stages suggests that CaO acts more actively as a neutralizing agent during the early increases in MM quantity.

Using the model equation, one can calculate in advance either the required amount of MM for neutralizing AWW or the residual CaO percentage. This enables the optimization of reagent consumption, technological process control, and effective adjustment of waste to meet pH standards in practical applications. The exponential nature of the model reflects the progressively slowing behavior of the process, which may be attributed to the gradual depletion of reactive components.

The mathematical analysis also provides theoretical justification for the dynamic decrease of CaO content depending on the AWW:MM ratio. This mathematical approach enables digital control, optimization, and forecasting of reagent requirements in the neutralization process.

Table 3 presents the experimentally determined CaO percentages for various AWW:MM mass ratios, as well as the values calculated based on the exponential model.

As shown in Table 3, the relative error in most cases does not exceed 5–7%, indicating high model accuracy. In particular, for MM amounts between 10-30 g, the model closely matches the experimental data. Although deviations slightly increase at 35–40 g, the overall trend remains consistent. These results confirm the reliability of the model and its practical predictive value.

Table 3 - Experimental vs. modeled CaO content and relative errors

AWW:MM	Exp. CaO (%)	Model CaO (%)	Δ (%)	Rel. Error (%)
100:10	46.52	45.13	+1.39	2.99
100:15	36.49	36.93	–0.44	1.20
100:20	28.98	30.22	–1.24	4.28
100:25	23.39	24.73	–1.34	5.73
100:30	18.94	20.24	–1.30	6.85
100:35	17.65	16.56	+1.09	6.17
100:40	16.17	13.56	+2.61	16.14

As observed from the table, the CaO percentages calculated using the model closely match the experimental values. For each data point, both the absolute difference in CaO content and the relative error are indicated separately. In most cases, the relative error remains below 5%, demonstrating the high accuracy of the model. Only at the MM ratio of 40 g does the relative error reach approximately 16%, which may be attributed to possible experimental uncertainties or secondary influencing factors in the reaction process. Overall, the modeled CaO reduction closely follows the trajectory of the experimental values, indicating high reliability of the developed exponential model. This table was provided to verify the agreement between the results of mathematical modeling and empirical data, assess the level of accuracy, and justify the applicability of the model in industrial practice. Furthermore, the table facilitates forecasting of CaO consumption and supports technological planning through analytical interpretation of experimental results.

The column labeled "Difference (Δ)" in the table represents the direction of deviation between the model and actual measurements (+/–), helping identify whether the model underestimates or overestimates the values. Such a table enhances the scientific credibility of the analysis results and plays an important role in documenting the modeling process.

Conclusion

The research findings confirmed that the decrease in CaO content within AWW and MM mixtures exhibits an exponential trend. As the AWW:MM mass ratio increased, a consistent reduction in CaO percentage was observed, which is explained by the complete reaction of the reagent with the acidic environment. The coefficient of determination (R^2) of the model was found to be 0,9807, indicating a high degree of agreement between experimental results and theoretical predictions. The difference between modeled and experimental values ranged between 3–6 %, with the relative error remaining minimal. The analytical table visually and quantitatively confirms the discrepancy between the model and actual measurements. Based on this model, it is possible to pre-calculate the required amount of MM or CaO for neutralizing industrial wastewater, optimize reagent consumption, and bring the pH of the effluent to regulatory levels. The high initial reactivity of CaO and the subsequent slowdown observed in the later stages of the neutralization process are well reflected in the model, further demonstrating that exponential regression accurately represents real chemical-technological behavior. The model's simple structure allows for its practical application in rapid calculations in industrial settings. This scientific approach helps fill the existing gap in mathematical modeling for acidic wastewater neutralization. The study enables a deeper understanding of the interaction mechanism between industrial effluents and neutralizing reagents, with validation and prediction supported by empirical data. Moreover, the findings lay a scientific foundation for the development of cost-effective and efficient neutralization methods utilizing MM-containing technogenic waste materials.

Conflicts of interest. On behalf of all authors, the corresponding author states that there is no conflict of interest.

CRediT author statement: **S. Shamuratov**: Conceptualization, Methodology, Software, Data curation, Writing draft preparation, Reviewing and Editing; **Sh. Kurambayev**: Visualization, Investigation, Supervision; **M. Radjabov and A. Yuldasheva**: Software, Validation.

Formatting of funding sources. This research did not receive any specific grant from funding agencies in the public, commercial, or not-for-profit sectors.

Cite this article as: Yuldasheva AP, Shamuratov SKh, Kurambayev ShR, Radjabov MF. Mathematical Analysis of CaO Content Variation in Acidic Wastewater and Mineralized Mass Mixture from Central Kyzylkum Phosphorite Based on Exponential Decay Model. Kompleksnoe Ispolzovanie Mineralnogo Syra = Complex Use of Mineral Resources. 2026; 339(4):79-86. https://doi.org/10.31643/2026/6445.42

Орталық Қызылқұм фосфоритінен алынған қышқыл ағынды сулар мен минералданған масса қоспасындағы CaO құрамының өзгерісін экспоненциалды ыдырау моделінің негізінде математикалық талдау

Юлдашева А.П., *Шамуратов С.Х., Курамбаев Ш.Р., Раджабов М.Ф.

Әбу Райхан Бируни атындағы Үргеніш мемлекеттік университеті, Үргеніш, Өзбекстан

Мақала келді: *1 шілде 2025*
Сараптамадан өтті: *10 шілде 2025*
Қабылданды: *15 шілде 2025*

АННОТАЦИЯ

Бұл мақалада Орталық Қызылқұм фосфоритінің минералданған массасы (ММ) мен май өнеркәсібінің қышқыл ағынды суларының (ҚАС) қоспаларындағы кальций оксиді (CaO) мөлшерінің төмендеу үрдісі эксперименттік деректер мен математикалық әдісті қолдана отырып зерттеледі. Зерттеу 60°C температурада жүргізілді, ҚАС:ММ ара қатынасы 100:10-нан 100:40-қа дейін өзгертілді. Әр қоспадағы CaO мөлшері оның массалық қатынасына байланысты анықталып, талданды. Нәтижелер ММ үлесі артқан сайын CaO мөлшерінің жүйелі түрде азаятынын көрсетті. Бастапқыда төмендеу жылдамдығы жоғары болып, кейіннен біртіндеп баяулады. Экспоненциалды ыдырау моделі қолданылып, тиісті параметрлермен сипатталды. Бірінші ретті дифференциалдық теңдеу эксперименттік деректер негізінде қолданылып, жетілдірілді. Анықталған бастапқы мән мен ыдырау тұрақтысы сәйкесінше C_0 = 67,39 және k = 0,0401 болды. Алынған экспоненциалды теңдеу эксперименттік нүктелермен жоғары дәрежелі корреляцияны көрсетті (R^2 ≈ 0,98). Бұл зерттеу математикалық модельдеу арқылы күрделі жүйелердегі CaO әрекетін құрылымдық тұрғыдан бағалауды ұсынады, оны нақты технологиялық жағдайларда процестерді басқару үшін қолдануға болады. Модельдеу нәтижелері болашақ зерттеулерде басқа иондар мен компоненттерді қамтитын кинетикалық модельдерді әзірлеуге методологиялық негіз бола алады.

Түйін сөздер: CaO, экспоненциалды ыдырау, минералданған масса, ағынды су, математикалық модельдеу, болжамдық үлгі.

Авторлар туралы ақпарат:

Юлдашева Асал Пулат қызы — *Студент, Әбу Райхан Беруни атындағы Үргеніш мемлекеттік университетінің химиялық технология факультеті, Үргеніш қаласы, Х. Олимжан көшесі, 14, 220100, Өзбекстан. Email: shamuratovsx@gmail.com*

Шамұратов Санжарбек Хұсынбайұлы — *Техника ғылымдары бойынша философия докторы, Әбу Райхан Беруни атындағы Үргеніш мемлекеттік университетінің химиялық технология факультетінің қауымдастырылған профессоры, Үргеніш қаласы, Х. Олимжан көшесі, 14, 220100, Өзбекстан. Email: sanjar.sh@urdu.uz; ORCID ID: https://orcid.org/0000-0002-1040-1807*

Құрамбаев Шерзод Райымбергенович — *Техника ғылымдарының докторы, Әбу Райхан Беруни атындағы Үргеніш мемлекеттік университетінің химия-технология факультетінің деканы, Үргеніш қаласы, Х.Олимжон көшесі 14, 220100, Өзбекстан. Email: sherzod.sh@urdu.uz; ORCID ID: https://orcid.org/0009-0003-3986-5079*

Раджабов Мансур Фархадович — *Техника ғылымдарының кандидаты, Әбу Райхан Беруни атындағы Үргеніш мемлекеттік университетінің Тағам технологиясы кафедрасының меңгерушісі, Үргеніш қаласы, Х. Олимжан көшесі, 14, 220100, Өзбекстан. Email: 6ansur.ra@urdu.uz; ORCID ID: https://orcid.org/0000-0003-2068-0595*

Математический анализ изменения содержания CaO в кислых сточных водах и смеси минерализованной массы из фосфоритов Центральных Кызылкумов на основе модели экспоненциального распада

Юлдашева А.П., *Шамуратов С.Х., Курамбаев Ш.Р., Раджабов М.Ф.

Ургенчский государственный университет имени Абу Райхона Беруни, Ургенч, Узбекистан

Поступила: *1 июля 2025*
Рецензирование: *10 июля 2025*
Принята в печать: *15 июля 2025*

АННОТАЦИЯ

В данной статье исследуется поведение снижения содержания оксида кальция (CaO) в смесях минерализованной массы (ММ) из фосфоритов Центральных Кызылкумов и кислых сточных вод (КСВ) масложировой промышленности, используя экспериментальные данные и математический подход. Исследование проводилось при температуре 60°C, при этом соотношение КСВ:ММ варьировалось от 100:10 до 100:40. Содержание CaO в каждой смеси определялось и анализировалось в зависимости от ее массового соотношения. Результаты показали систематическое снижение содержания CaO при увеличении доли ММ. Первоначальная скорость снижения была высокой, а затем постепенно замедлялась. Для характеристики процесса использовалась модель экспоненциального распада с соответствующими параметрами. Дифференциальное уравнение первого порядка было применено и уточнено с использованием экспериментальных данных. Начальное значение и константа распада были определены как C_0 = 67,39 и k = 0,0401 соответственно. Полученное экспоненциальное уравнение продемонстрировало высокую степень корреляции с экспериментальными точками ($R^2 \approx 0,98$). Данное исследование предлагает структурированную оценку поведения CaO в сложных системах посредством математического моделирования, которое может быть использовано для управления процессами в реальных технологических условиях. Результаты моделирования могут служить методологической основой для разработки кинетических моделей с участием других ионов и компонентов в будущих исследованиях.

Ключевые слова: CaO, экспоненциальный распад, минерализованная масса, сточные воды, математическое моделирование, прогнозная модель.

Информация об авторах:

Юлдашева Асал Пулат кизи
Студент, факультет химической технологии Ургенчского государственного университета имени Абу Райхона Беруни, Ургенч, улица Х. Олимжона, 14, 220100, Узбекистан. Email: shamuratovsx@gmail.com

Шамуратов Санжарбек Хусинбай угли
Доктор философии в области технических наук, доцент факультета химической технологии Ургенчского государственного университета имени Абу Райхона Беруни, Ургенч, улица Х. Олимжона, 14, 220100, Узбекистан. Email: sanjar.sh@urdu.uz; ORCID ID: https://orcid.org/0000-0002-1040-1807

Курамбаев Шерзод Раимбергенович
Доктор технических наук, декан химико-технологического факультета Ургенчского государственного университета имени Абу Райхана Беруни, Ургенч, улица Х. Олимжона, 14, 220100, Узбекистан. Email: sherzod.sh@urdu.uz; ORCID ID: https://orcid.org/0009-0003-3986-5079

Раджабов Мансур Фархадович
Кандидат технических наук, заведующий кафедрой технологии пищевых продуктов Ургенчского государственного университета имени Абу Райхана Беруни, Ургенч, улица Х. Олимжона, 14, 220100, Узбекистан. Email: mansur.ra@urdu.uz; ORCID ID: https://orcid.org/0000-0003-2068-0595

References

[1] Dumont M-J, & Narine SS. Soapstock and deodorizer distillates from North American vegetable oils: Review on their characterization, extraction and utilization. Food Research International. Elsevier BV. 2007; 40(8):957-974. https://doi.org/10.1016/j.foodres.2007.06.006

[2] Haas Michael J. Improving the Economics of Biodiesel Production through the Use of Low Value Lipids as Feedstocks: Vegetable Oil Soapstock. Fuel Processing Technology. Elsevier BV. 2005; 86(10):1087-1096. https://doi.org/10.1016/j.fuproc.2004.11.004

[3] Dowd Michael K. Compositional Characterization of Cottonseed Soapstocks. Journal of the American Oil Chemists' Society. Wiley. 1996. https://doi.org/10.1007/bf02525458

[4] Barbusiński, Krzysztof, Sławomir Fajkis, and Bartosz Szeląg. Optimization of Soapstock Splitting Process to Reduce the Concentration of Impurities in Wastewater. Journal of Cleaner Production. Elsevier BV. January 2021; 280(2):124459. https://doi.org/10.1016/j.jclepro.2020.124459

[5] Ahmad, Talha, Tarun Belwal, Li Li, Sudipta Ramola, Rana Muhammad Aadil, Abdullah, Yanxun Xu, and Luo Zisheng. Utilization of Wastewater from Edible Oil Industry, Turning Waste into Valuable Products: A Review. Trends in Food Science & Technology. Elsevier BV. 2020; 99:21-33. https://doi.org/10.1016/j.tifs.2020.02.017

[6] Qasim, Wael, and Mane AV. Characterization and Treatment of Selected Food Industrial Effluents by Coagulation and Adsorption Techniques. Water Resources and Industry. Elsevier BV. 2013; 4:1-12. https://doi.org/10.1016/j.wri.2013.09.005

[7] Geetha Devi M, Shinoon Al-Hashmi ZS, and Chandra Sekhar G. Treatment of Vegetable Oil Mill Effluent Using Crab Shell Chitosan as Adsorbent. International Journal of Environmental Science and Technology. Springer Science and Business Media LLC. 2012; 9:713-718. https://doi.org/10.1007/s13762-012-0100-4

[8] Pintor Ariana MA, Andreia G Martins, Renata S Souza, Vítor JP Vilar, Cidália MS Botelho, and Rui AR Boaventura. Treatment of Vegetable Oil Refinery Wastewater by Sorption of Oil and Grease onto Regranulated Cork – A Study in Batch and Continuous Mode. Chemical Engineering Journal. Elsevier BV. 2015; 268:92-101. https://doi.org/10.1016/j.cej.2015.01.025

[9] Ahmad Ashfaq, Azizul Buang, and Bhat AH. Renewable and Sustainable Bioenergy Production from Microalgal Co-Cultivation with Palm Oil Mill Effluent (POME): A Review. Renewable and Sustainable Energy Reviews. Elsevier BV. 2016; 65:214-234. https://doi.org/10.1016/j.rser.2016.06.084

[10] Hmidi K, Ksentini I, and Mansour LB. Treatment of Olive-Pomace Oil Refinery Wastewater Using Combined Coagulation-Electroflotation Process. Journal of Water Chemistry and Technology. Allerton Press. 2017; 39:275-280. https://doi.org/10.3103/s1063455x17050046

[11] Mirshafiee Amir, Abbas Rezaee, and Rasol Sarraf Mamoory. A Clean Production Process for Edible Oil Removal from Wastewater Using an Electroflotation with Horizontal Arrangement of Mesh Electrodes. Journal of Cleaner Production. Elsevier BV. 2018; 198:71-79. https://doi.org/10.1016/j.jclepro.2018.06.201

[12] Ahmad Talha, Rana Muhammad Aadil, Haassan Ahmed, Ubaid ur Rahman, Bruna CV Soares, Simone LQ Souza, Tatiana C Pimentel, et al. Treatment and Utilization of Dairy Industrial Waste: A Review. Trends in Food Science & Technology. Elsevier BV. 2019; 88:361-372. https://doi.org/10.1016/j.tifs.2019.04.003

[13] Shamuratov Sanzharbek, Umid Baltaev, Umarbek Alimov, Namazov Shafoat, Sherzod Kurambaev, and Bazar Ibadullaev. Utilization Process Research of the Soap Industry Acid Waste Water with High Carbonate Phosphorite of Central Kyzylkum. E3S Web of Conferences. EDP Sciences. 2021. https://doi.org/10.1051/e3sconf/202126404079

[14] Shamuratov Sanjarbek, Umid Baltaev, Sanobar Achilova, Umarbek Alimov, Shafoat Namazov, and Najimuddin Usanbaev. Enhancement of Availability of High Calcareous Phosphorite by Neutralization of Acid Effluent and Composting of Cattle Manure. E3S Web of Conferences. EDP Sciences. 2023. https://doi.org/10.1051/e3sconf/202337703004

[15] Shamuratov Sanjarbek, Umid Baltaev, Olga Myachina, Umarbek Alimov, Elyor Atashev, and Tokhir Kuramboev. Agrochemical Efficiency of Slow Release Phosphate Fertilizers Derived on the Base of Phosphorite Activation. E3S Web of Conferences. EDP Sciences. 2023. https://doi.org/10.1051/e3sconf/202343403014

[16] Sotimboev Ilgizarbek, Umidbek Baltaev, Sanjarbek Shamuratov, Ruzimov Shamsiddin, Umarbek Alimov, and Mirzabek Saporboyev. Technical and Economic Efficiency of Processing Acidic Wastewater from the Oil and Fat Industry into Necessary Agricultural Products. E3S Web of Conferences. EDP Sciences. 2024. https://doi.org/10.1051/e3sconf/202456303072

[17] Turatbekova Aidai, Malokhat Abdukadirova, Sanjarbek Shamuratov, Bakhodir Latipov, Mirzabek Saporboyev, Jafar Shamshiyev, and Yusuf Makhmudov. Investigation of the Effect of Fertilizers on the Biochemical and Physical Characteristics of Carrots (Daucus Carota L.). E3S Web of Conferences. EDP Sciences. 2024. https://doi.org/10.1051/e3sconf/202456303074

[18] Sultonov BE, Kholmatov DS, Rasulov AA, and Temirov USh. Treatment of Phosphate Waste Generated during Thermal Processing of Phosphorites of the Central Kyzylkum. Obogashchenie Rud. Ore and Metals Publishing House. 2024. https://doi.org/10.17580/or.2024.04.06

[19] Shaymardanova Mokhichekhra, Kholtura Mirzakulov, Gavkhar Melikulova, Sakhomiddin Khodjamkulov, Abror Nomozov, and Oybek Toshmamatov. Studying of The Process of Obtaining Monocalcium Phosphate Based on Extraction Phosphoric Acid from Phosphorites of Central Kyzylkum. Baghdad Science Journal. College of Science for Women, University of Baghdad. 2024. https://doi.org/10.21123/bsj.2024.9836

[20] Sultonov BE, Nozimov ES, and Kholmatov DS. Recycling of Local Phosphate Waste - Mineralized Mass into Activated Phosphorus Fertilizers. Chemical Science International Journal. Sciencedomain International. 2023; 32(6). https://doi.org/10.9734/csji/2023/v32i6875

[21] Temirov Uktam, Nodir Doniyarov, Bakhrom Jurakulov, Najimuddin Usanbaev, Ilkhom Tagayev, and Abdurasul Mamataliyev. Obtaining Complex Fertilizers Based on Low-Grade Phosphorites. E3S Web of Conferences. EDP Sciences. 2021. https://doi.org/10.1051/e3sconf/202126404009

[22] Sedghkerdar Mohammad Hashem, Ehsan Mostafavi, and Nader Mahinpey. Investigation of the Kinetics of Carbonation Reaction with Cao-Based Sorbents Using Experiments and Aspen Plus Simulation. Chemical Engineering Communications. Informa UK Limited. 2015. https://doi.org/10.1080/00986445.2013.871709

[23] Sun Ping, John R Grace, Jim Lim C, and Edward J Anthony. Determination of Intrinsic Rate Constants of the CaO–CO2 Reaction. Chemical Engineering Science. Elsevier BV. 2008; 63(1):47-56. https://doi.org/10.1016/j.ces.2007.08.055

[24] Fritz Matthew S. An Exponential Decay Model for Mediation. Prevention Science. Springer Science and Business Media LLC. 2013; 15:611-622. https://doi.org/10.1007/s11121-013-0390-x

[25] Atashev E. Decomposition of Magnesite-Sparing Waste in Sulfuric Acid with a High Concentration: Empirical Modeling and Determination of Optimal Conditions. Kompleksnoe Ispolzovanie Mineralnogo Syra = Complex Use of Mineral Resources. 2025; 339(4):71-78. https://doi.org/10.31643/2026/6445.41

Crossref
DOI: 10.31643/2026/6445.43
Earth sciences

Methods for Analysis and Improvement of Dynamic Loads on the Steel Wire Rope Holding the Boom of Steel Wire Rope Excavators

[1] Toshov J.B., [2*] Rabatuly M., [3] Khaydarov Sh.,[3] Kenetayeva A.A., [3] Khamzayev A., [3] Usmonov M., [2]Zheldikbayeva A.T.

[1] Tashkent state technical university, Tashkent, Uzbekistan
[2] Abylkas Saginov Karaganda Technical University, Karaganda, Kazakhstan
[3] Navoi state university of mining and technologies, Navoi, Uzbekistan

** Corresponding author email: mukhammedrakhym@mail.ru*

Received: *May 16, 2025*
Peer-reviewed: *June 9, 2025*
Accepted: *July 21, 2025*

ABSTRACT

The article analyzes the dynamic loads on the booms of single-bucket quarry excavators and steel cables between two supports and develops design solutions to reduce them. The boom of quarry excavators and steel cables between two supports are located separately on both sides, and as a result of stretching the steel cables, the tension force on the steel cable on one side of the boom increases, which not only has a dynamic effect on the steel cable of this side, but also leads to curvature of the boom. The methods used in the article are analyzed based on the equilibrium equations of the distribution of static and dynamic loads and the finite element method. Based on the programs, a new model of the structural arrangement of the boom and two supports is created and an analysis of the results obtained from the calculations is obtained. As a result of creating a new design model by installing steel cables supporting the excavator boom on two supports as a half-block, uniform distribution of steel cable tension and maintaining automatic tension balance are achieved, which reduces dynamic loads and extends the service life of working mechanisms, and also reduces the risk of accidents by monitoring the dynamic loads of steel cables in real time, which leads to a significant contribution to ensuring the safety of workers. The practical significance of the article is that installing half-blocks on two supports serves to increase the operational reliability of excavators and prevents operating costs and the appearance of cracks in the boom by increasing the efficiency of maintenance, preventing ruptures and defects resulting from improper tension of steel cables, due to ensuring the balance of loads on steel cables, excessive loads on the working mechanisms are eliminated, which leads to an increase in the service life of the steel cable by 15-20%.

Keywords: excavator, steel wire ropes, loading, dynamic balance, static balance, design solution, operation, maintenance, section.

Information about authors:

Toshov Javokhir Buriewicz — *Doctor of Technical Sciences, Professor, Islam Karim Tashkent State Technical University, 100095 Republic of Uzbekistan, Tashkent, Almazar district, Universitetskaya street 2. E-mail: j.toshov@tdtu.uz; ORCID ID: https://orcid.org/0000-0003-4278-1557*

Rabatuly Mukhammedrakhym — *Ph.D., Associate Professor, Department of Development of Mineral Deposits of Abylkas Saginov Karaganda Technical University, 100027, The Republic of Kazakhstan, Karaganda, Ave. Nursultan Nazarbayev, 56. E-mail: mukhammedrakhym@mail.ru; ORCID ID: https://orcid.org/0000-0002-7558-128X*

Khaydarov Shokhidjon — *PhD, Associate Professor, Department of Mining Electromechanics, Navoi State Mining and Technological University, Navoi, Uzbekistan. E-mail: shohidh@mail.ru; ORCID ID: https://orcid.org/0009-0005-5661-3919*

Kenetaeva Aigul Akanovna — *lecturer of Abylkas Saginov Karaganda Technical University, Master of Engineering and Technology specialty Mining, Karaganda, Kazakhstan. E-mail: aigul_tate@bk.ru; ORCID ID: https://orcid.org/0000-0001-7943-3279*

Khamzaev Akbar — *PhD, Associate Professor, Department of Mining Electromechanics, Navoi State Mining and Technological University, Navoi, Uzbekistan. E-mail: akbar-86-86@mail.ru; ORCID ID: https://orcid.org/0009-0005-4362-2488*

Usmonov Maftunjon — *Assistant in Mining Electrical Mechanics, Navoi State Mining and Technological University, Navoi, Uzbekistan. E-mail: usmonovmaftunjon@gmail.com; ORCID ID: https://orcid.org/0000-0002-0716-4775*

Zheldikbayeva Aisaule Takenovna — *PhD student, Department of Automation of manufacturing processes of Abylkas Saginov Karaganda Technical University, 100027, The Republic of Kazakhstan, Karaganda, Ave. Nursultan Nazarbayev, 56. E-mail: aisaule89@mail.ru; ORCID ID: https://orcid.org/0009-0005-1325-5576*

Introduction

Steel wire ropes of excavators that are used in mining environment play an important role in the working process of the excavator. These steel wire ropes enter the suspension system of the excavator and participate in controlling its arm and bucket movements [1].

Research is being conducted around the world to improve the reliability of excavator working members. Steel wire ropes have been analyzed from a mechanical point of view to improve the load-bearing efficiency and reliability of excavators [2]. Also, methods of dynamic analysis of excavator mechanisms with steel wire ropes based on a virtual prototype were proposed [3], which allows optimizing the loads on steel wire ropes. A dynamic analysis of the excavator boom section of steel wire ropes was carried out using the FEA (finite element analysis) method [4]. These studies are aimed at theoretically and experimentally studying the loading process of excavator steel wire ropes, which provides a basis for studying advanced approaches in this area. In Western Europe and the USA, mainly intelligent monitoring systems are being introduced to solve problems related to excavator steel wire ropes. Steel wire ropes recommended the use of new composite materials to increase the load-bearing capacity of the excavator boom and its main parts. This approach allowed increasing the durability of the cables by 10-15% [5].

In Russia and China, the main focus is on automating the load distribution of steel wire rope excavators, where algorithms have been developed to optimize the loading of the trusses and reduce moment imbalance. According to the results of this study, it was found that the load difference can be reduced by 5-10% [[6], [7]].

Steel wire ropes and their main function - Steel wire ropes are one of the main elements of the lifting and balancing system that moves the working members of the excavator. Their main functions are to ensure the lifting and lowering of the bucket, ensure the stability of the excavator boom, and ensure the forward and backward movement of the bucket.

The scientific novelty of the research presented in this article and the difference from the results of previous works is that a new design solution and an automatic balancing model have been created to reduce the dynamic loads of steel cables of the excavator rack, the effectiveness of which has been proven by modeling and precise calculations.

The essence of scientific novelty is as follows:

By proposing an automatic dynamic force equalization mechanism, the problem of uneven distribution of forces between several parallel steel cables in the boom section of the excavator was analyzed for the first time in the scientific work, and an automatic equalization mechanism was created. This mechanism allows for the synchronization and balancing of the dynamic loads applied to the steel cables during movement.

Analysis of the dynamics of forces in real time was carried out by means of mechanical modeling, i.e., the change in dynamic forces acting on steel cables as a function of time. This provides accuracy not only in calculating static, but also dynamic loads (Table 1).

Table 1 - The difference from previous scientific research

Direction	Previous research	In this article
Dynamic load analysis	Static or general theoretical analyses	Complete dynamic analysis (graphs, time functions)
Constructive solutions	Mainly material substitution or algorithms	New structural system - automatic power balance
Modeling method	Classical methods or general FEA	Complete mechanical modeling based on COMPAS-3D
Scientific results	Partial effect, load reduction up to 5-10%	Efficiency at load balance 20-50%, service life increase 30-40%

This research is distinguished as a scientific and practical innovation in the modernization of steel cable boom systems, which are of great importance for quarry excavators. It covers the stages of not only identifying the existing problem, but also proposing, calculating, and proving a specific technical solution for its solution. This work demonstrates a new level of analytical, technical, and engineering approach to previous research.

Types of steel wire ropes Steel wire ropes used in excavators of the EKG-8I, EKG-10 and EKG-15 types are divided into:

- bucket lifting steel wire ropes - used to raise and lower the bucket;
- boom holding steel wire ropes - hold the boom in the desired position;
- traction steel wire ropes - participate in moving the bucket forward;
- balancing steel wire ropes - help to keep the excavator in a stable position.

The material and properties of steel wire ropes of the 52.0 G-V-O-N-160 brand are as follows [[8], [9]]:

- bucket lifting steel wire ropes - made of special alloys that can withstand high tension;
- tensile strength - since the excavator is subjected to repeated bending and stretching during operation, the cables must be resistant to bending;
- corrosion-resistant coating - special coatings are used to resist moisture and dust in quarry conditions.

Steel wire ropes are mainly used in excavators, with φ 39 mm diameter steel wire ropes in EKG-5A excavators, φ45.5 mm diameter steel wire ropes in EKG-8I excavators, φ52 mm diameter steel wire ropes in EKG-10 excavators, and φ57 mm diameter steel wire ropes in EKG-15 excavators. These steel wire ropes are manufactured in accordance with GOST 2688-80 standards, depending on the manufacturer [[10], [11]].

The experimental part

Currently, the steel wire ropes of excavators of the EKG-8I, EKG-10 and EKG-15 types are constructed based on the design shown in Figure 1 below, in which case the excavator boom is subjected to a large load due to the imbalance of the tension forces in the steel wire ropes holding it[[12], [13]]. When installing steel wire ropes on the boom, the incorrect distribution of the load on the rope leads to a decrease in the service life of the excavator boom, defects and breakage of the steel wire ropes. The boom of excavators of the EKG-8I, EKG-10 and EKG-15 types consists of a head block 1, 2- steel wire ropes 2, a saddle bearing 4 is located between the upper 3 and lower 6 sections of the boom for installing a single-beam lever, and the boom is held by a two-legged column 7 and a holder 5 [[14], [15]].

Figure 1 - View of the excavator boom and steel wire rope

1- head block; 2- cable; 3- boom upper section; 4- saddle bearing; 5- retainer; 6- boom lower section; 7- two-legged column [14].

If the steel wire ropes of an excavator are not of the same length or tension, the boom will be unevenly positioned under dynamic and static loads. This will result in the following forces [21]:

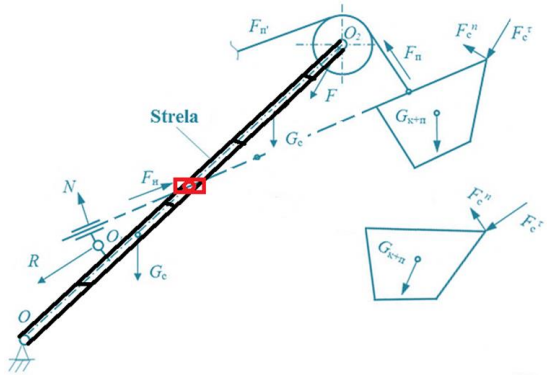

Figure 2 - Scheme for determining lifting and compressive forces

The main forces acting on the boom Fig. 2 shows the movement of the excavator boom under static and dynamic loads. Based on this diagram, the following forces act:

- G_c - arrow weight, directed downwards, *t*.
- G_{k+m} - weight of the load-bearing block and steel cable, *t*.
- F - tensile force applied by the steel cable, N.
- F_H - horizontal reaction force (support reaction), *N*.
- N - normal reaction force, *N*.
- R - total reaction force). ($R = \sqrt{N^2 + F_H^2}$)

- $F_n, F_{n'}$ - projections in the direction of the forces, *N*.

- $F_c, F_{c'}$ - centripetal forces, *N*.

Equilibrium equations of the resulting forces Equilibrium equations are formulated based on Newton's second law for the equilibrium of an arrow in a stationary state:

Equilibrium equations for the projections of load forces:

Horizontal (OX) direction:

$$\sum F_x = 0 \rightarrow F_H + F_{n'} - F_c \cdot cos\,\theta = 0 \quad (1)$$

Vertical (OY) direction:

$$\sum F_y = 0 \rightarrow N + F_{c'} - G_c - G_{k+m} = 0 \quad (2)$$

Equilibrium of rotational moments:

$$\sum M_0 = 0 \rightarrow M_{Gc} + M_{Gk+m} - M_F = 0 \quad (3)$$

Here, the moments are expressed as follows:

$$M = F \cdot d$$

here; d - shoulder distance relative to the center of rotation of the force *m*, θ - angle of rotation, F - effective value of the force *N*.

Dynamic loads act on the excavator boom during the process of lifting and lowering the load. [[16], [17]]. Dynamic loads are mainly caused by the following reasons:

- Inertial forces - steel wire change depending on the speed and acceleration of the rope:

$$F_{iner} = m \cdot a$$

-Oscillations and compression (tension) deformations - caused by the elasticity of the steel cable :

$$F_{pruj} = k \cdot \Delta l$$

Static load distribution on the boom in position 1

$$\sum F_k = 0, T_A + T_B - P = 0 \quad (4)$$

$$T_A + T_B = P, T_A = P - T_B \quad (5)$$

Taking into account elastic tension

$$\frac{T_A}{k_A} = \frac{T_B}{k_B} \qquad T_A = T_B \cdot \frac{k_A}{k_B} \qquad T_B = \frac{P}{1+\frac{k_A}{k_B}} \quad (6)$$

We add the inertial forces for the dynamic state.

$$F_1 = m \cdot a \quad (7)$$

$$T_A(t) + T_B(t) = P(t) + m \cdot a(t) \quad (8)$$

here; T_A-strength of the right rope *N*, T_B-strength of the left rope *N*, k_A-rigidity of the right rope, k_B-rigidity of the left rope, P-all forces of gravity arising *N*, F_{iner} -inertial force *N*, F_{pruj} -elastic force arising in the rope *N*, Δl -relative elongation of the rope *m*.

In this case, it is modeled by differential equations of oscillation. However, this can lead to two reasons:

1- dynamic resonance occurs when steel cables differ in stiffness and length;

2- If one of the steel cables stretches longer than the other, this causes the boom to deflect.

As a result of the load on one rope for such reasons, we obtain the following expression.

$$\Delta L = \frac{T}{k_A}, \; k_A = \frac{E_A}{L_A} \quad (9)$$

If steel cable A stretches by 5 cm, then steel cable B needs 5 cm to stretch. In this case, according to expression (4)

$$ma(t) = T_A(t) + T_B(t) - P(t) \quad (10)$$

The force of inertia arises.

$$ma(t) = k \cdot \Delta x, \quad ma(t) = k \cdot d\vartheta \cdot dt \quad (11)$$

$$k \cdot \vartheta(t) = T_A(t) + T_B(t) \quad (12)$$

In such cases:

1 - steel cable can quickly wear out and break;

2-a one-sided deflection of the arrow;

3- malfunctions occur based on static (1) and dynamic (4) expressions.

where; v-relative velocity arising on the rope, m-rope mass, a-rope acceleration, t-time.

The equations of static equilibrium and moment equilibrium are used to check the state of the boom [18].

Discussion of the results

Figure 3 shows the change in the tension forces generated in the left and right steel wire ropes over the operating time, which shows the imbalance of the tension forces in the two steel wire ropes. This, in turn, causes the rapid failure of the excavator working members. In addition, due to exploitation and improper installation, it can also affect the efficiency of the excavator working members and the safety of the service personnel.

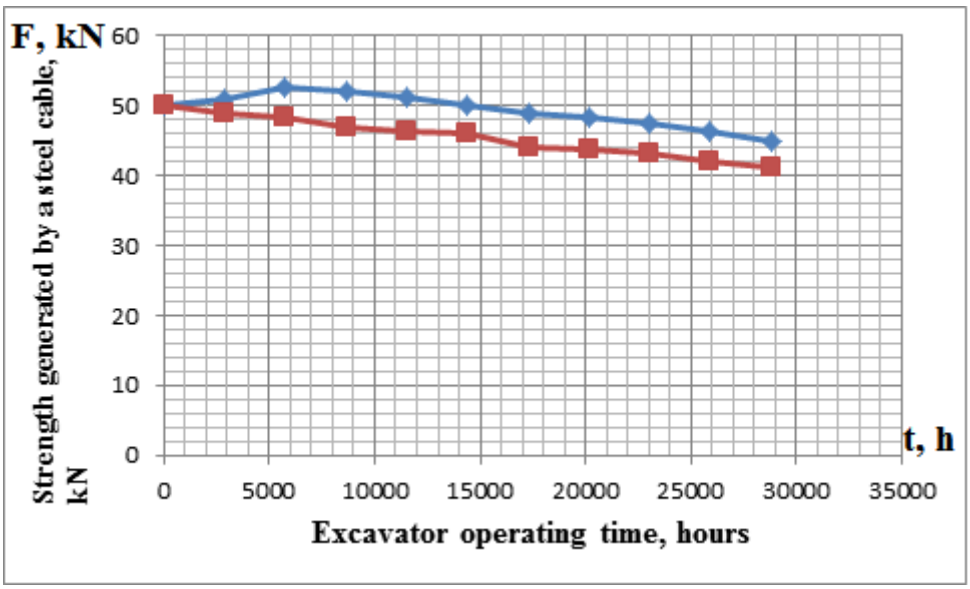

Figure 3 - Variation of tensile forces over time in the left and right steel wire ropes of the excavator boom.
Simulation results obtained using COMPAS-3D software. Horizontal axis – Time (t), s; Vertical axis – Tensile force (F), N.

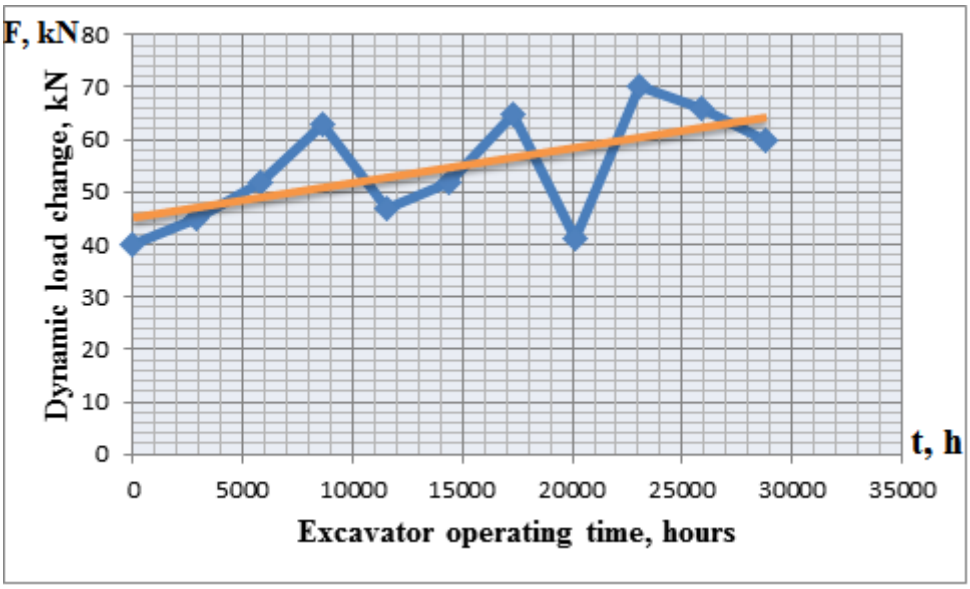

Figure 4 - Dynamic load variation on the excavator boom caused by imbalance in tensile forces of steel ropes.
Results obtained via finite element method (FEM) analysis. Horizontal axis – Time (t), s;
Vertical axis – Dynamic load (F_{dyn}), N.

During the operation of excavators, a dynamic load is created on the working parts. The formation of such a dynamic load changes over time. Figure 4 shows the change in the dynamic load on the excavator boom due to the difference in the tensile forces of the steel cables on the left and right sides of the excavator boom, where the main straight line is in normal operating conditions, and the dynamic load on the excavator boom changes due to the difference in the tensile forces of the steel cables on the left and right sides. In this case, the excavator's operation leads to the rapid failure of the boom.

As a new constructive solution, methods for reducing disproportions and dynamic loads arising in steel cables are presented. Figure 5 shows the view of the structure with a half-block installed on both supports of the excavator. Then 1-main block; 2-polar cable between the boom and two supports; 3 - upper section of the boom; 4 - lever; 5-two supports; 6 - half-block; 7 - lower sections of the boom. As a result of theoretical calculations, as a result of automatic correction and adjustment of the imbalance in steel cables, the tension forces and dynamic loads on the excavator boom are brought

to a normal level. As a result, high efficiency is achieved due to the efficiency of the excavator boom and steel cables, as well as savings in operating time and repair time [[18], [19]].

Cable material: 52.0 G-V-O-N-160 (σ_i = 1400 MPa, E = $2.1 \cdot 10^5$ MPa)

Cable diameter: ϕ = 52 mm

Boom length: L = 6.8 m

Boundary conditions: fixed support at base, pinned connection at top.

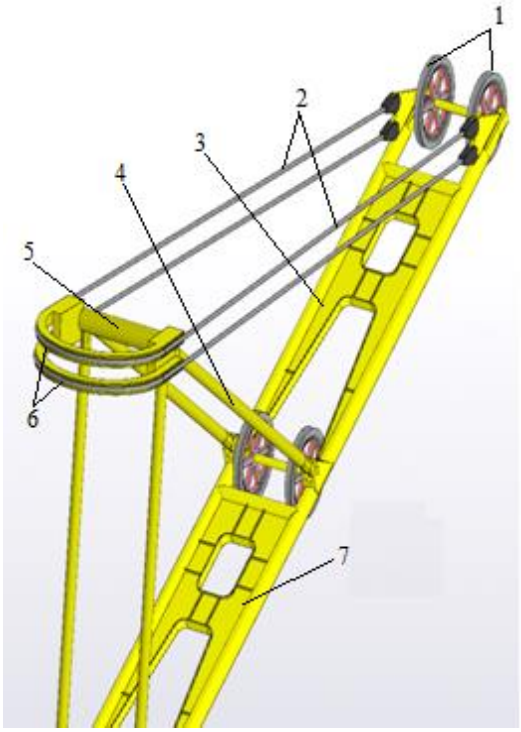

Figure 5 - View of the structure with a half-block installed on the two supports of the excavator

1 - main block; 2-polar cable between the boom and two supports; 3 - upper section of the boom; 4 - lever; 5-two supports; 6 - half-block; 7 - lower section of the boom;

In case 2, to resolve the issue:

$$\sum F_k = 0 \quad ma(t) = 0 \tag{13}$$

We accept the terms.

$\sum F_k \neq 0$ case, $F_q \neq 0$ condition is generated.

$F_q \neq 0$ this occurs when additional external forces arise (in vibrations, resonance, and mechanical oscillations).

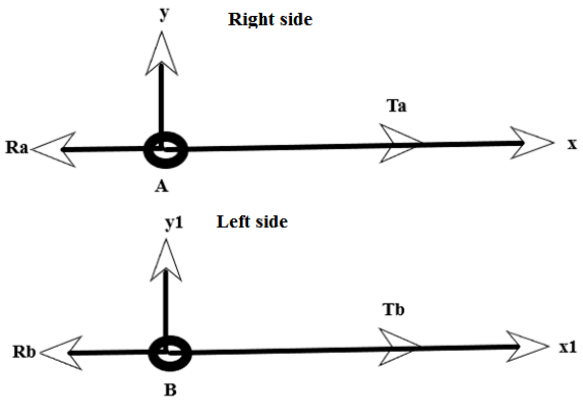

Figure 6 - Tension forces arising on the steel wire rope of the excavator boom: a) tension in right cable; b) tension in left cable

Through the semi-block system, the forces acting on the left and right wire ropes are automatically equalized. This balances the disproportionate loads that arise from any differences in length or stiffness of the ropes during movement [[20], [21], [22]].

The tensile forces arising in the steel cables of the excavator boom shown in fig. 6 are obtained using the following expressions (14), (15) and (16).

$$\sum F_x = 0, -R_A + T_A = 0 \tag{14}$$

$$\sum F_{x1} = 0, -R_B + T_B = 0 \tag{15}$$

$$R_A = T_A \quad R_B = T_B \quad T_A \neq T_B \tag{16}$$

here; R_A-reaction force of the right rope,
R_B-left rope reaction force.

According to the structural rules about static bonding and their reactions, the bonding reaction consisting of a taut thread is directed along the tension of this thread. Based on this, we have the following constructive solution to maintain the same tension of the steel cable and equalize the reaction force counteraction.

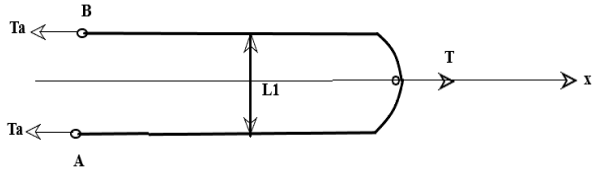

Figure 7 - Excavator boom tension forces

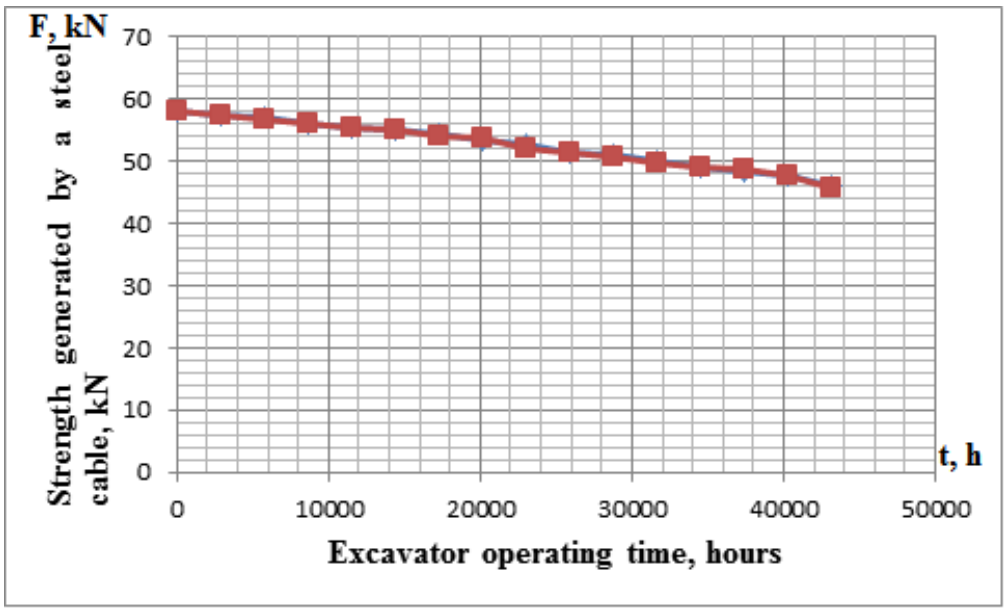

Figure 8 - Graph of the dependence of tensile forces on time on the left and right steel cables of the new design

The tension forces generated by the excavator boom shown in fig. 7 are determined by the following expressions (21), (22), (23) and (24) and we accept the conditions.

$$\sum F_x = 0, T_A + T_B - T = 0 \quad (17)$$

$$\sum M_A(F_k) \neq 0, -T \cdot \frac{l_1}{2} + T_A \cdot l_1 = M_A \quad (18)$$

$$\sum M_B(F_k) \neq 0, -T \cdot \frac{l_1}{2} + T_B \cdot l_1 = M_B \quad (19)$$

$$\sum M(F_k) = 0, M_A - M_B = 0, M_A = M_B \quad (20)$$

$M_A = T_A \cdot l_1, M_B = T_B \cdot l_1, T_A \cdot l_1 = T_B \cdot l_1 T_A = T_B$ condition is accepted.

In this case, an external inertial force arises, according to expression (4).

$$T_A(t) + T_B(t) = P(t) + ma(t) \quad (21)$$

$$F_x \neq k \cdot \Delta x = k \cdot d\vartheta \cdot dt \quad (22)$$

$$\Delta x = 0, d\vartheta = 0, \quad (23)$$

$$2T_A(t) = P(t) + ma(t) \quad (24)$$

$$2T_A(t) - P(t) = ma(t) \quad (25)$$

$$a = \frac{d\vartheta}{dt}, d\vartheta = 0, \quad (26)$$

$2T_A(t) = P(t)$ causes uniform load distribution.

here; *dv*-rope speed change,
Δx-change in rope length,
M_A - right rope torque,
M_B-left rope torque.

The beneficial outcomes achieved based on the proposed model are presented in Table 2 below.

Table 2 - The difference from previous scientific research

Parameters	Before	Suggested system	Change (%)
Rope tension (max)	18.4 kN	12.9 kN	29.8 %
Dynamic load peak	16.2 kN	8.1 kN	50 %
Service life	14 month	19 month	35.7 %

In Figure 8, shows the dependence of the tension forces arising from the use of the new design solution on the left and right sides of the boom steel cables on the operating time of the excavator.

Conclusion

If the steel wire ropes of excavators of the EKG-8I, EKG-10 and EKG-15 types do not have the same tension, an imbalance of moments will occur, which will lead to uneven positioning of the boom. It is necessary to identify and eliminate this problem in advance by calculating the balance of moments and forces based on the equations. During maintenance, the efficiency of operation will increase by regularly checking the cables, pulleys and reaction forces. In addition, by using the new design considered above, the efficiency of the excavator's working members will increase by 20-25% due to the efficiency of their work and the time spent on work and repairs. As a result of preventing unbalanced loads, the probability of failure of steel wire ropes will be reduced by 40-50%. Real-time monitoring of

dynamic loads will reduce the risk of accidents by 30-40% and reduce maintenance costs by 20-25%. Overall, these solutions lead to a 25-35% increase in excavator efficiency and significant improvements in service life and safety. The results of the study show that the boom of single-bucket mining excavators used in the mining industry and steel cables between the two supports improve reliability and reduce maintenance costs.

Conflict of interest. On behalf of all the authors, the correspondent author declares that there is no conflict of interest.

***CRediT author statement*: J. Toshov, M. Rabatuly:** Conceptualization, Methodology, Software; **Sh. Khaydarov, A. Zheldikbayeva**: Data curation, Writing- Original draft preparation; **A. Khamzayev, A. Kenetayeva:** Visualization, Investigation, M. Usmonov: Software, Validation.

Cite this article as: Toshov JB, Rabatuly M, Khaydarov Sh, Kenetayeva AA, Khamzayev A, Usmonov M, Zheldikbayeva AT. Methods for Analysis and Improvement of Dynamic Loads on the Steel Wire Rope Holding the Boom of Steel Wire Rope Excavators. Kompleksnoe Ispolzovanie Mineralnogo Syra = Complex Use of Mineral Resources. 2026; 339(4):87-96. https://doi.org/10.31643/2026/6445.43

Болат арқанды экскаватор жебесін (стреласын) ұстайтын болат арқандағы динамикалық жүктемелерді талдау және оларды азайту әдістері

[1] Тошов Ж.Б., [2] Рабатұлы М., [3] Хайдаров Ш., [2] Кенетаева А. А., [3] Хамзаев А., [3] Усмонов М., [2] Желдикбаева А. Т.

[1] Ислам Кәрім атындағы ташкент Мемлекеттік Техникалық Университеті, Ташкент, Өзбекстан
[2]Ә. Сағынов атындағы Қарағанды Техникалық Университеті, Қарағанды, Қазақстан
[3] Навои Мемлекеттік Тау-Кен Технологиялық Университеті, Навои, Өзбекстан

Мақала келді: *16 мамыр 2025*
Сараптамадан өтті: *9 маусым 2025*
Қабылданды: *21 шілде 2025*

ТҮЙІНДЕМЕ

Мақалада бір шөмішті карьер экскаваторларының жебе элементіне және екі тірек арасындағы болат арқандарға әсер ететін динамикалық жүктемелер талданып, оларды азайтуға арналған конструкциялық шешімдер ұсынылған. Жебе мен болат арқандар әр жақта жеке орналасқан жағдайда, бір жақтағы арқанның тартылу күші артады, бұл тек сол жақтағы арқанға динамикалық әсер етіп қана қоймай, сонымен қатар жебенің майысуына әкеледі. Зерттеу әдістері ретінде статикалық және динамикалық жүктемелердің таралуына арналған тепе-теңдік теңдеулері мен соңғы элементтер әдісі қолданылды. Бағдарламалық модельдер негізінде жебе мен екі тіректің жаңа конструкциялық сызбасы жасалып, есептеу нәтижелері талданды. Екі тірекке жартылай блок түрінде орнатылған болат арқандар арқылы экскаватор жебесінің жаңа конструкциялық моделі жасалып, тартылу күшінің біркелкі таралуы мен автоматты тепе-теңдігі қамтамасыз етіледі. Бұл динамикалық жүктемелерді төмендетіп, жұмыс механизмдерінің қызмет ету мерзімін арттырады, сондай-ақ нақты уақыт режимінде арқандардағы жүктемелерді бақылау арқылы жұмысшылардың қауіпсіздігін қамтамасыз етеді. Мақаланың практикалық маңыздылығы – екі тірекке жартылай блок орнату арқылы экскаваторлардың сенімділігін арттыру, техникалық қызмет көрсету шығындарын азайту, жебедегі сызаттардың пайда болуына жол бермеу болып табылады. Арқандардағы жүктеме балансын қамтамасыз ету жұмыс механизмдерінің шамадан тыс жүктелуін болдырмайды, болат арқандардың қызмет ету мерзімін 15–20%-ға арттырады.

Түйін сөздер: экскаватор, болат арқан, жүктеме, динамикалық теңгерім, статикалық теңгерім, құрылымдық шешім, пайдалану, техникалық қызмет көрсету, секция.

Авторлар туралы ақпарат:

Тошов Жавохир Буриевич — *Техника ғылымдарының докторы, Ислам Карим атындағы Ташкент Мемлекеттік Техникалық Университетінің профессоры, 100095, Алмазар ауданы Университетская көшесі 2, Ташкент, Өзбекстан. E-mail: j.toshov@tdtu.uz; ORCID ID: https://orcid.org/0000-0003-4278-1557*

Рабатұлы Мұхаммедрахым — *PhD докторы, Әбілқас Сағынов атындағы Қарағанды Техникалық Университетінің Пайдалы қазбалар кенорындарын өндіру кафедрасының доценті, 100027, Нұрсұлтан Назарбаев даңғ. 56, Қарағанды, Қазақстан. E-mail: mukhammedrakhym@mail.ru; ORCID ID: https://orcid.org/0000-0002-7558-128X*

Хайдаров Шохидижон — *PhD, Тау-кен электр механика кафедрасының ассистенті, Навои Мемлекеттік Тау-Кен Технологиялық Университеті, Навои, Өзбекстан. E-mail: shohidh@mail.ru; ORCID ID: https://orcid.org/0009-0005-5661-3919*

Кенетаева Айгуль Акановна	*Техника ғылымдарының магистрі, Әбілқас Сағынов атындағы Қарағанды Техникалық Университетінің Геология және пайдалы қазбалар кен орындарын барлау кафедрасының оқытушысы, 100027, Нұрсұлтан Назарбаев 56, Қарағанды, Қазақстан. E-mail: aigul_tate@bk.ru ; ORCID: https://orcid.org/0000-0001-7943-3279*
Хамзаев Акбар	*PhD докторы, Тау-кен электромеханика кафедрасының қауымдастырылған профессоры, Навои Мемлекеттік Тау-Кен Технологиялық Университеті, Навои, Өзбекстан. E-mail: akbar-86-86@mail.ru; ORCID ID: https://orcid.org/0009-0005-4362-2488*
Усмонов Мафтунжон	*Тау-кен электр механика кафедрасының ассистенті, Навои Мемлекеттік Тау-кен технологиялық Университеті, Навои, Өзбекстан. E-mail: usmonovmaftunjon@gmail.com; ORCID ID: https://orcid.org/0000-0002-0716-4775*
Желдикбаева Айсауле Такеновна	*Әбілқас Сағынов атындағы Қарағанды Техникалық Университетінің Өндірістік процестерді автоматтандыру кафедрасының PhD докторанты, 100027, Нұрсұлтан Назарбаев даңғ. 56, Қарағанды, Қазақстан. E-mail: aisaule89@mail.ru; ORCID ID: https://orcid.org/0009-0005-1325-5576*

Методы анализа и снижения динамических нагрузок на стальной канат, удерживающий стрелу экскаваторов с канатным приводом

[1] Тошов Ж.Б., [2] Рабатұлы М., [3] Хайдаров Ш., [2] Кенетаева А. А., [3] Хамзаев А., [3] Усмонов М., [2] Желдикбаева А. Т.

[1] Ташкентский Государственный Технический Университет имени Ислама Карима, Ташкент, Узбекистан
[2]Карагандинский Технический Университет имени А. Сагинова, Караганда, Казахстан
[3] Навойский Государственный Горно-Технологический Университет, Навои, Узбекистан

Поступила: *16 мая 2025*
Рецензирование: *9 июня 2025*
Принята в печать: *21 июля 2025*

АННОТАЦИЯ

В статье проведён анализ динамических нагрузок, действующих на стрелу одноковшовых карьерных экскаваторов и на стальные тросы, расположенные между двумя опорами. Предложены конструктивные решения, направленные на снижение указанных нагрузок. Показано, что при отдельном размещении стрелы и стальных тросов по обе стороны, натяжение троса с одной стороны приводит к его усиленной нагрузке, что оказывает не только динамическое воздействие на трос, но и вызывает изгиб стрелы. В качестве методов исследования использованы уравнения равновесия для распределения статических и динамических нагрузок, а также метод конечных элементов. На основе расчетов разработана новая модель конструктивного расположения стрелы и двух опор, проведен анализ полученных результатов. Предложенная модель, в которой стальные тросы устанавливаются на двух опорах в виде полублока, обеспечивает равномерное распределение усилий натяжения и автоматическое балансирование, что снижает динамические нагрузки, увеличивает срок службы рабочих механизмов и способствует повышению безопасности труда за счёт мониторинга тросов в реальном времени. Практическая значимость работы заключается в том, что установка полублоков на двух опорах повышает эксплуатационную надежность экскаваторов, снижает затраты на обслуживание и предупреждает возникновение трещин на стреле. Обеспечение баланса нагрузок предотвращает перегрузку рабочих механизмов и способствует увеличению срока службы тросов на 15–20%.

Ключевые слова: экскаватор, стальные канаты, нагрузка, динамический баланс, статический баланс, конструктивное решение, эксплуатация, обслуживание, секция.

Информация об авторах:

Тошов Жавохир Буриевич	*Доктор технических наук, профессор Ташкентского Государственного Технического Университета имени Ислама Карима, 100095, Алмазарский район, ул. Университетская 2, Ташкент, Узбекистан. E-mail: j.toshov@tdtu.uz; ORCID ID: https://orcid.org/0000-0003-4278-1557*
Рабатулы Мухаммедрахым	*Доктор PhD, доцента кафедры Разработки месторождений полезных ископаемых Карагандинского Технического Университета имени Абылкаса Сагинова, 100027, пр. Нурсултана Назарбаева, 56, Караганда, Казахстан. E-mail: mukhammedrakhym@mail.ru; ORCID ID: https://orcid.org/0000-0002-7558-128X*
Хайдаров Шохидижон	*PhD, ассистент кафедры Горной электромеханики, Государственный Горно-Технологический Университет Навои, Навои, Узбекистан. E-mail: shohidh@mail.ru; ORCID ID: https://orcid.org/0009-0005-5661-3919*
Кенетаева Айгуль Акановна	*Магистр технических наук кафедры Геология и разведка месторождений полезных ископаемых Карагандинского Технического Университета имени Абылкаса Сагинова, 100027, пр. Нурсултана Назарбаева, 56, Караганда, Казахстан. E-mail: aigul_tate@bk.ru; ORCID: https://orcid.org/0000-0001-7943-3279*

Хамзаев Акбар	*PhD, ассоциированный профессор кафедры горной электромеханики, Государственный Горно-Технологический Университет Навои, Узбекистан. E-mail: akbar-86-86@mail.ru; ORCID ID: https://orcid.org/0009-0005-4362-2488*
Усмонов Мафтунжон	*Ассистент кафедры Горной электромеханики, Государственный Горно-Технологический Университет Навои, Узбекистан. E-mail: usmonovmaftunjon@gmail.com ; ORCID ID: https://orcid.org/0000-0002-0716-4775*
Желдикбаева Айсауле Такеновна	*PhD докторант кафедры Автоматизации производственных процессов Карагандинского Технического Университета имени Абылкаса Сагинова, 100027, пр. Нурсултана Назарбаева, 56, Караганда, Казахстан. E-mail: aisaule89@mail.ru; ORCID ID: https://orcid.org/0009-0005-1325-5576*

References

[1] Haydarov SB, & Usmonov MZ. Analysis of factors influencing the efficiency of excavator workers. Digital technologies in industry. 2023; 1 (2):70-78.

[2] Raza MA, Frimpong S. Mechanics of electric rope shovel performance and reliability in formation excavation. Lagrangian mechanics. 2017, 107-133

[3] Yuan Y, et al. Dynamic analysis of the rigid-flexible excavator mechanism based on virtual prototype. Facta Universitatis, Series: Mechanical Engineering. 2022; 20(2):341-361.

[4] Juhasz A, Virag Z. Dynamic Analysis of a Bucket Wheel Excavator Boom Using FEA. Mining Revue.Revista Minelor. 2024; 30.

[5] Solazzi L, Assi A, Ceresoli F. Excavator arms: Numerical, experimental and new concept design. Composite Structures. 2019; 217:60-74.

[6] Dolganov A, Letnev K. Developing expert control systems for automated complexes of technical operation of vehicles. AIP Conference Proceedings. AIP Publishing. 2022; 2456(1).

[7] Lukashuk O, Letnev K, Komissarov A. Efficiency increase in excavation control as primary reserve of performance increase for open-pit excavators. International Conference on Modern Trends in Manufacturing Technologies and Equipment, ICMTMTE 2018. EDP Sciences, 2018; 224.

[8] Alshanskaya AA. Improving the Reliability of Excavators Based on Failure Forecasting and Digital Models of Structural Load Conditions: Dissertation. Siberian Federal University. 2024.

[9] Tkachev RE. Modernization of the EKG-10 Single-Bucket Excavator to Increase Its Productivity: Dissertation. Siberian Federal University. 2021.

[10] Toshov JB, Fozilov DM, Yelemessov KK, Ruziev UN, Abdullayev DN, Baskanbayeva DD, Bekirova LR. Povysheniye stoykosti zub'yev burovykh dolot putem izmeneniya tekhnologii ikh izgotovleniya [Increasing the durability of drill bit teeth by changing its manufacturing technology]. Obrabotka metallov-tekhnologiya, oborudovanie, instrumenty = Metal Working and Material Science. 2024; 26(4):112-124. http://dx.doi.org/10.17212/1994-6309-2024-26.4-112-124

[11] Toshov ZhB, Rahutin MG, Toshov BR, Baratov BN. The method of constructing the scans of the toroidal belts of the faces during drilling wells. Eurasian Mining. 2024; 1:62-66.

[12] Andryushenkov DN. Justification and Selection of Basic Parameters of Quarry Loading and Transport Machines: PhD Thesis in Technical Sciences, Specialty 05.05.06. Yekaterinburg. 2015, 127.

[13] Komissarov AP, Lagunova YA, Shestakov VS. Comparative Evaluation of Energy Characteristics of Quarry Excavators. Mining Equipment and Electromechanics. 2014; 2:14-16.

[14] Komissarov AP, Pobegailo PA, Shestakov VS. Methodology for Rapid Analysis of Energy Consumption During Rock Excavation. Mining Information and Analytical Bulletin. Scientific and Technical Journal. 2014; 12:138-141.

[15] Dragoljub V, Olgica L, Vojislav B. Development of dynamic-mathematical model of hydraulic excavator [J]. Journal of Central South University. 2017; 24(9):2010-2018.

[16] Mylnikov VV, Kondrashkin OB. Mechanization Tools in Construction: Lifting and Earthmoving Machines. 2021.

[17] Chukin MV, Pesin AM, Rydz D, Torbus N, Polyakova MA, Gulin AE. The use of intentionally created high-speed asymmetry in bimetal Ti-Ni rolling. Vestnik of Nosov Magnitogorsk state technical university. 2013; 4(45):49-50.

[18] Patent No. 2163. Shamsutdinov MM, Tashtanbaeva VO. Rope tension control device for mine hoisting installations. July 31, 2019.

[19] Lukashuk OA, Letnev KYu. Determination of Operating Parameters of the Lever Mechanism of a Quarry Excavator. Proceedings of Higher Educational Institutions. Mining Journal. 2021; 2:94-102.

[20] Lukashuk OA. Patterns in the Formation of Operating Parameters of the Main Mechanisms of Quarry Excavators During the Excavation of Rock. Mining Equipment and Electromechanics. 2019; 3(143):14-17.

[21] Rabatuly M, Demin VF, Kenetaeva AA, Steflyuk YuYu, Toshov JB. Evaluation of modern methods and techniques for calculating parameters during coal bed degassing. Kompleksnoe Ispolzovanie Mineralnogo Syra = Complex Use of Mineral Resources. 2025; 334(3):110-120. https://doi.org/10.31643/2025/6445.33

[22] Komissarov AP, et al. Justification of the Operating Characteristics of a Quarry Excavato. Mining Equipment and Electromechanics. 2017; 2:7-10.

Crossref

DOI: 10.31643/2026/6445.44
Earth Sciences

Block modeling reserves estimation

[1]Mussin R.A., [1*] Yachsishin M.G., [2]Golik A.V., [1]Akhmatnurov D.R.

[1]A. Saginov Karaganda Technical University, Karaganda, Kazakhstan
[2] I-Geo Kazakhstan LLP, Karaganda, Kazakhstan

** Corresponding author email: maxim.yachshishin@gmail.com*

Received: *June 9, 2025* Peer-reviewed: *July 14, 2025*
Accepted: *August 18, 2025*

ABSTRACT

The article presents a methodology for resource estimation of a phosphate deposit based on block modeling. The advantages of applying regularization and geometric optimization algorithms for mineable units are demonstrated, ensuring more accurate differentiation of ore grades and a reduction in ore losses and dilution. A comparative analysis is conducted on the excavation of pit benches with varying slope angles and equipment configurations. It is established that a block size of 5m ×5m provides an optimal balance between model accuracy and equipment productivity. The most effective slope angle of the benches is determined based on equipment performance and cost-efficiency. The results contribute to improving the accuracy of resource forecasting and the overall economic viability of deposit development by significantly reducing operating costs and enhancing the quality of extracted material. The study outlines practical approaches to selecting appropriate equipment configurations for different mining scenarios. Special attention is paid to the influence of excavation geometry on the performance of hydraulic excavators. The methodology proposed can be applied to similar deposits with complex morphology. The research findings may serve as a basis for developing more adaptive and data-driven mine planning strategies.

Keywords: block modeling, reserves model, regularization, mineable shapes optimization, losses and dilution, economic efficiency, selective mining.

Information about authors:

Mussin Ravil Altavovich — *PhD, Acting Associate Professor at the Department of Development of Mineral Deposits of the Abylkas Saginov Karaganda Technical University, Nursultan Nazarbayev Ave., 56, 100027, Republic of Kazakhstan, Karaganda. E-mail: r.a.mussin@mail.ru; ORCID ID: https://orcid.org/0000-0002-1206-6889*

Yachsishin Maxim Grigorievich — *Master student at the Department of Development of Mineral Deposits of the Abylkas Saginov Karaganda Technical University, Nursultan Nazarbayev Ave., 56, 100027, Republic of Kazakhstan, Karaganda. E-mail: maxim.yachshishin@gmail.com; ORCID ID: https://orcid.org/0009-0006-2326-8335*

Golik Andrey Vasilyevich — *Director of LLP I-Geo Kazakhstan (Karaganda, Kazakhstan), Novoselov st., 190/1, 100017, Republic of Kazakhstan, Karaganda. E-mail: andrey.golik@i-geo.kz; ORCID ID: https://orcid.org/0009-0008-5179-0002*

Akhmatnurov Denis Ramilievich — *PhD, Head of Laboratory of the Abylkas Saginov Karaganda Technical University, Nursultan Nazarbayev Ave., 56, 100027, Republic of Kazakhstan, Karaganda. E-mail: d.akhmatnurov@gmail.com; ORCID ID: https://orcid.org/0000-0001-9485-3669*

Introduction

At the current stage of mining industry development, block models have become the primary tool for the geological and economic evaluation of mineral deposits. Building a block model allows for a more accurate representation of the spatial distribution of ore bodies and their quality characteristics, as well as a sound basis for resource estimation and economic assessment of the deposit.

A block model is a digital representation of the subsurface in the form of a set of blocks of defined size, each assigned specific attributes [[1], [2], [3], [4]]. The primary purpose of a block model is to provide a comprehensive assessment of the mineral resource and to design the most rational mining options, taking into account geological, geotechnical, and economic factors [[5], [6]].

In many cases, the estimation of mineable reserves is based on the "Methodological Recommendations for Technological Design of Open-Pit Mining Enterprises" dated September 19, 2013 [7]. At the same time, average benchmark indicators for the entire deposit are typically used for calculating operational losses and dilution [[8],

[9], [10]]. This approach assumes bulk extraction of the deposit without differentiating between high-grade and low-grade ore types, leading to the loss of benefit in the final product and potential enterprise profit.

Rational subsoil use and achieving high economic efficiency in the development of solid mineral deposits are key priorities in today's mining industry. Accurate estimation of recoverable reserves, based on geological modeling and analysis of discrepancies between actual and projected parameters, has become especially important [[11], [12], [13]].

Resource block models reflect the total amount of mineral material in situ, without accounting for mining and technical constraints. Consequently, a resource model does not provide a full picture of the reserves that can feasibly be extracted during deposit exploitation.

Experimental part

To improve the accuracy of recoverable resource forecasting, a reserve model is developed. This model represents an operational geological block model that incorporates cut-off grade, the geometry of mining units, ore losses, and dilution. The reserve model is essential for pit optimization, pit contour design, and mine scheduling with a higher degree of reliability.

In global practice, the Lerchs-Grossmann algorithm is widely recognized and commonly applied for pit limit optimization [14]. This method is actively used by leading mining companies due to its ability to identify the most economically feasible pit outline based on the balance between the value of recoverable minerals and stripping costs.

A critical preliminary stage in reserve model construction for subsequent optimization is regularization—the process of converting block model cells to a uniform size that corresponds to the concept of a minimum mining unit [15]. Regularization enhances the realism of recoverable resource estimation [16].

Regularization of the reserve model was carried out using three different mining unit sizes:

3 m × 3 m – the minimum size based on bucket width;

5 m × 5 m – aligned with the blast hole pattern (Figure 1);

7 m × 7 m – used to evaluate the effect of increasing the mining unit size on ore loss and dilution indicators.

In all variants, the height of the mining unit was 7.5 meters, which corresponds to the adopted bench height parameters. To differentiate ore grades, the cut-off grade (COG) [17] for P_2O_5 was applied: 28% for high-grade ore and 15% for low-grade ore.

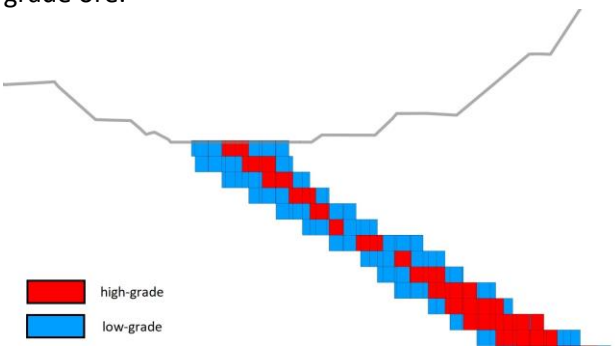

Figure 1 - Reserves model section with 5m x 5m excavation unit size

Table 1 presents the variation in average P_2O_5 content, ore losses, and dilution levels depending on the size of the mining block. As block size increases from 3×3 m to 7×7 m, a consistent decline in ore grade is observed, accompanied by higher dilution and losses. These changes are particularly important for thin-layered phosphate deposits, where selective mining and ore quality preservation are critical.

Table 1 - P_2O_5 content, ore losses and dilution depending on the size of the mining block

Indicator	Resource Model	3m × 3m	5m × 5m	7m × 7m
P_2O_5	27.0%	24.7%	24.6%	24.4%
Losses	0.0%	15.7%	16.3%	17.3%
Dilution	0.0%	9.1%	9.5%	10.3%

Consequently, a block size of 5×5 m was selected as optimal for further analysis, as it provides a balance between modeling accuracy and the technical feasibility of extraction. It corresponds to the typical blast-hole drilling grid used on site and maintains acceptable levels of dilution (9.5%) and losses (16.3%), while still preserving the geometry of the orebody more effectively than larger blocks. This makes the 5×5 m configuration optimal for balancing modeling accuracy and production feasibility in subsequent mine planning stages.

A more advanced and accurate tool for creating block models of mineral reserves is the Mineable Stope Optimiser (MSO). This stope optimization method features extensive configuration options that define the areas within the resource model that

can be economically extracted, taking into account the specified geometry [[18], [19]].

MSO employs optimization algorithms to generate mineable shapes based on financial, geotechnical data, and operational constraints. It is used to determine the ideal extraction geometry of an orebody based on a block model. The primary objective of MSO is to maximize financial returns by generating mining units that align with geometric and geotechnical parameters. The shape, geometry, and geotechnical constraints are defined independently for different zones of the same orebody. Examples of geometric constraints include the height, as well as the maximum and minimum width of the mining units. These geometrical constraints were applied to reflect realistic mining conditions and evaluate the impact of varying slope geometries on the shape and continuity of the generated mineable units.

For inclined phosphorite ore bodies with a dip angle ranging from 25° to 35°, MSO optimization was carried out using two slope angle scenarios: 30°, which approximates the average natural dip of the deposit, and 40°, which simulates a steeper extraction geometry aimed at increasing ore recovery in areas with favorable geotechnical conditions (Figure 2).

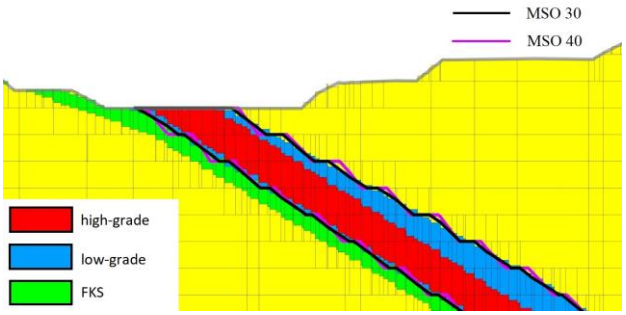

Figure 2 - Section of resource block model with MSO frames with slope angles of 30° and 40°

The purpose of applying different slope angles in the optimization process was to assess the sensitivity of mineable shapes to variations in dip-related constraints, as well as to compare the trade-offs between ore recovery, operational selectivity, and stability. By applying these angular parameters during MSO geometrization, it was possible to generate mineable units that better conform to the geometry of the orebody, reduce over-excavation of barren host rock, and improve the accuracy of production planning.

The results of geometrization facilitate the identification of grade distribution patterns within the deposit, which are used in mine planning processes and in the development of more efficient ore preparation technologies at the mining operation [20].

Table 2 - Comparison of Regularized and MSO Block Model

Indicator	5m×5 m	MSO 40	MSO 30
P2O5	24.6%	25.1%	25.6%
Losses	16.3%	9.4%	7.4%
Dilution	9.5%	4.1%	3.1%

The comparison between the regularized block model (5×5 m) and the MSO-generated geometries at slope angles of 30° and 40° demonstrates a clear improvement in orebody selectivity and overall resource utilization when using MSO-based optimization in Table 2.

The regularized 5×5 m block model yielded an average P_2O_5 grade of 24.6%, with ore losses amounting to 16.3% and dilution reaching 9.5%. In contrast, the MSO-based geometry with a 40° slope produced a higher P_2O_5 content of 25.1%, while significantly reducing ore losses to 9.4% and dilution to 4.1%. The most favorable results were obtained with the 30° MSO scenario, where the P_2O_5 grade increased to 25.6%, ore losses were minimized to 7.4%, and dilution dropped to just 3.1%.

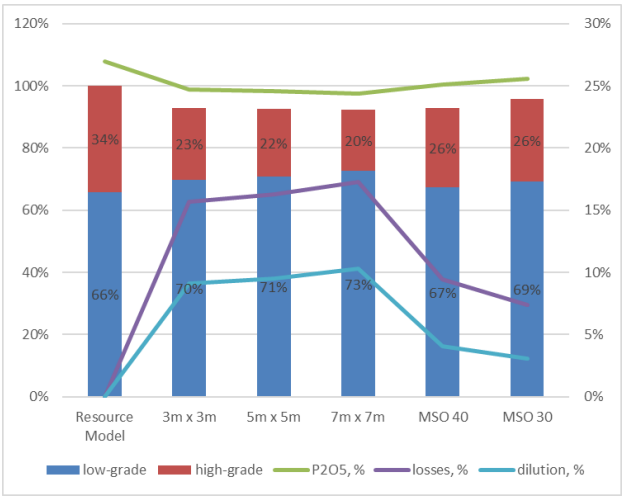

Figure 3 - Relative analysis of block reserves models

As a result of the comparative analysis (Figure 3), it was established that the regularization of the block model is associated with a number of shortcomings. Among the main identified issues is the insufficiently accurate separation of ore grades, which leads to a significant reduction in the volume of high-quality (rich) ore. Furthermore, the

application of this approach results in elevated levels of ore losses and dilution, which adversely affect the economic performance of the project.

These findings indicate that the application of MSO optimization, especially with a slope angle of 30°, allows for more accurate alignment of the mineable shapes with the dip and geometry of the orebody. This results in better preservation of high-grade zones and minimizes the incorporation of barren material. The significant reduction in both losses and dilution contributes directly to higher operational efficiency and improved product quality during downstream processing.

In contrast, the use of the MSO algorithm allows for a more precise and accurate delineation of boundaries between ore, waste rock, and different ore grades. The implementation of MSO contributes to more effective reserve management and improves the economic indicators of deposit development.

Results and Discussions

In the course of analyzing the extraction parameters for ore blocks, a technical and economic feasibility assessment was carried out for the application of different bench slope angles—30° and 40°—taking into account geometric constraints and the operational capabilities of the selected mining equipment. As a representative example, a Komatsu PC1250 hydraulic backhoe excavator was chosen, equipped with arms of varying lengths: 5.7 m, 4.5 m, and 3.4 m [21]. The diagram (Figure 4) visually presents three operational configurations of this excavator. For comparative analysis, the contours of the designed benches—generated using MSO software frameworks—were superimposed: the red line indicates the 30° slope bench, the blue line represents the 40° slope bench, both designed for bottom-digging operations. The purple line illustrates the minimum feasible angle for top digging, with a corresponding bench height of 7.5 meters.

The results of the conducted analysis indicate that when the bench slope angle is 30°, excavation is feasible only by performing two separate passes. This significantly reduces excavator productivity, extends operational cycle time, and leads to additional costs associated with preparing working platforms. In contrast, with a bench slope angle of 40°, efficient single-pass excavation becomes possible, especially when using an excavator equipped with a short boom (3.4 m). This configuration allows for a considerable increase in operational productivity, minimizes cycle time, and optimizes costs related to the excavation process.

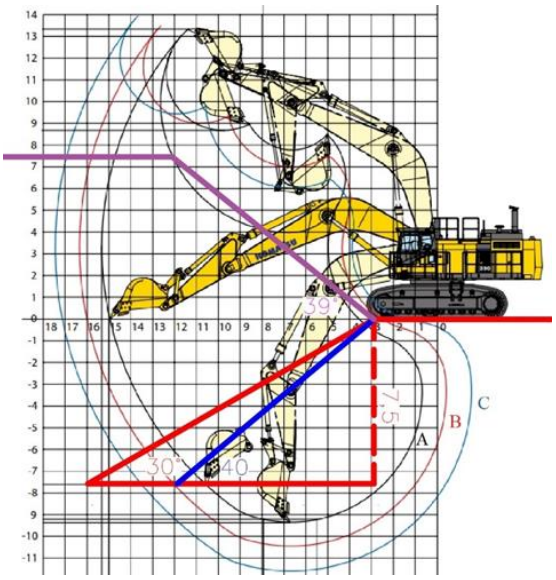

A - arm length 3.4m; B - arm length 4.5m;
C - arm length 5.7m.

Figure 4 - Scheme of ore blocks mining options at angles of 30° and 40°

A comparative analysis of extractable ore volumes based on models generated using the MSO algorithm revealed no significant differences between the 30° and 40° slope angle configurations. Taking into account equipment performance and the technological advantages of the steeper 40° slope, the optimal mining solution involves the use of a Komatsu PC1250 backhoe excavator with a 3.4-meter arm lengh and a bucket capacity of 5.2 m³, or equivalent equipment. In other cases, it becomes necessary to use a smaller 3.4 m³ bucket, resulting in a noticeable decrease in productivity.

Thus, considering the identified technological and economic advantages, the reserve model constructed using the MSO algorithm with a 40° bench slope angle was selected for the further optimization of pit boundaries. This approach ensures an optimal balance between equipment productivity, operational safety, and overall economic efficiency of the project.

Conclusion

Resource estimation using block modeling significantly enhances the accuracy and reliability of forecasts related to recoverable reserves. This approach provides not only a detailed geometric

representation of the ore body but also integrates data on qualitative and economic parameters, making the model more adaptable to actual mining conditions.

One of the key advantages is the ability to implement selective mining, achieved through the precise delineation of zones with varying concentrations of the valuable component. This enables minimization of losses and dilution, increases the degree of reserve utilization, and ensures consistent raw material quality.

Based on the block model, it becomes possible to make a justified selection of mining equipment. Block dimensions, dip angles, and geotechnical parameters form the technical requirements for the type and specifications of equipment used, including excavators, drilling rigs, and haulage systems.

Block modeling contributes to transparent decision-making and control at all stages of mine development — from design and planning to operational production management. It creates a unified digital environment in which deviations can be easily tracked and adjustments to mine plans promptly made. As a result, the enterprise gains additional profit and increased project profitability through the maximization of recoverable reserves, while minimizing losses and reducing operational costs.

Conflicts of interest. On behalf of all authors, the corresponding author states that there is no conflict of interest.

CRediT author statement: **R. Mussin:** Supervision, Validation; **M. Yachsishin:** Writing draft preparation, Software, Visualization; **A. Golik:** Support for the project, Revision; **D. Akhmatnurov:** Reviewing, Editing.

Acknowledgements. This research wasfunded by the Science Committee of the Ministry of Science and Higher Education of the Republic of Kazakhstan (Grant No.BR24993009).

Cite this article as: Mussin RA, Yachsishin MG, Golik AV, Akhmatnurov DR. Block modeling reserves estimation. Kompleksnoe Ispolzovanie Mineralnogo Syra = Complex Use of Mineral Resources. 2026; 339(4):97-103. https://doi.org/10.31643/2026/6445.44

Блоктық модельдеуді қолдана отырып кен орындарының қорларын бағалау

[1]Мусин Р.А., [1*]Ящишин М.Г., [2]Голик А.В., [1]Ахматнуров Д.Р.

[1]А. Сағынов атындағы Қарағанды техникалық университеті, Қарағанды, Қазақстан
[2] I-Geo Kazakhstan ЖШС, Қарағанды, Қазақстан

Мақала келді: *9 маусым 2025*
Сараптамадан өтті: *14 шілде 2025*
Қабылданды: *18 тамыз 2025*

ТҮЙІНДЕМЕ

Мақалада фосфор кен орнының қорларын бағалау үшін блоктық модельдеуге негізделген әдістеме ұсынылған. Қазып алынатын блоктар геометриясын реттеу мен оңтайландыру алгоритмдерін қолданудың артықшылықтары көрсетілген. Бұл тәсіл кеннің түрлі сорттарын дәлірек ажыратуға, кен жоғалуларын және құнарсыздандыруды азайтуға мүмкіндік береді. Әртүрлі еңіс бұрыштары мен жабдық конфигурацияларымен жұмыс істейтін карьерлік сатыларды қазу бойынша салыстырмалы талдау жүргізілді. 5 м × 5 м болатын блок өлшемінде модельдің дәлдігі мен тау-кен техникасының өнімділігі арасында оңтайлы тепе-теңдік болатыны анықталды. Техника өнімділігі мен шығын тиімділігіне негізделе отырып, сатылардың ең тиімді еңіс бұрышы анықталды. Бұл нәтижелер ресурстарды болжаудың дәлдігін және кен орнын игерудің экономикалық тиімділігін арттыруға ықпал етеді, сонымен қатар операциялық шығындарды едәуір азайтып, алынатын материал сапасын жақсартады. Зерттеу әртүрлі тау-кен жағдайларына сәйкес келетін жабдық конфигурациясын таңдаудың практикалық тәсілдерін ұсынады. Қазу геометриясының гидравликалық экскаваторлардың жұмыс тиімділігіне әсеріне ерекше назар аударылған. Ұсынылған әдістеме морфологиясы күрделі кен орындары үшін де қолданылуы мүмкін. Бұл зерттеу нәтижелері тау-кен жұмыстарын жоспарлау стратегияларын бейімдеуге және деректерге негізделген шешім қабылдауға негіз бола алады.

Түйін сөздер: блоктық модельдеу, қорлар моделі, тұрақтандыру, алынатын бірліктерді оңтайландыру, шығындар және құнарсыздану, экономикалық тиімділік, селективті өндіру.

Мусин Равиль Альтавович

Авторлар туралы ақпарат:
PhD, Әбілқас Сағынов атындағы Қарағанды техникалық университетінің пайдалы қазбалар кенорындарын игеру кафедрасының доцентінің м.а., 100027, Нұрсұлтан Назарбаев 56, Қарағанды, Қазақстан. E-mail: r.a.mussin@mail.ru; ORCID ID: https://orcid.org/0000-0002-1206-6889

Ящишин Максим Григорьевич	*Магистрант, Әбілқас Сағынов атындағы Қарағанды техникалық университетінің пайдалы қазбалар кенорындарын игеру кафедрасы, 100027, Нұрсұлтан Назарбаев 56, Қарағанды, Қазақстан. E-mail: maxim.yachshishin@gmail.com; ORCID ID: https://orcid.org/0009-0006-2326-8335*
Голик Андрей Васильевич	*I-Geo Kazakhstan ЖШС директоры, 100027, Новоселов 190/1, Қарағанды, Қазақстан. E-mail: andrey.golik@i-geo.kz; ORCID ID: https://orcid.org/0009-0008-5179-0002*
Ахматнуров Денис Рамильевич	*PhD, Әбілқас Сағынов атындағы Қарағанды техникалық университетінің зертхана меңгерушісі, 100027, Нұрсұлтан Назарбаев 56, Қарағанды, Қазақстан. E-mail: d.akhmatnurov@gmail.com; ORCID ID: https://orcid.org/0000-0001-9485-3669*

Оценка запасов с применением блочного моделирования

[1]Мусин Р.А., [1*]Ящишин М.Г., [2]Голик А.В., [1]Ахматнуров Д.Р.

[1]Карагандинский технический университет имени А. Сагинова, Караганда, Казахстан
[2]ТОО I-Geo Kazakhstan, Караганда, Казахстан

Поступила: *9 июня 2025*
Рецензирование: *14 июля 2025*
Принята в печать: *18.08.2025*

АННОТАЦИЯ

В статье представлена методика оценки запасов фосфоритового месторождения с использованием блочного моделирования. Продемонстрированы преимущества применения регуляризации и алгоритмов геометрической настройки выемочных единиц, обеспечивающих более точное разделение сортов руды и снижение потерь и разубоживания. Проведён сравнительный анализ отработки уступов с различными углами откоса и конфигурациями оборудования. Установлено, что размер блока 5 м × 5 м обеспечивает оптимальный баланс между точностью модели и производительностью оборудования. Определён наиболее эффективный угол откоса уступов с точки зрения производительности техники и экономической целесообразности. Полученные результаты способствуют повышению точности прогнозирования запасов и общей экономической эффективности освоения месторождений за счёт существенного сокращения эксплуатационных затрат и повышения качества добываемого сырья. В исследовании изложены практические подходы к выбору подходящих конфигураций оборудования для различных горных условий. Особое внимание уделено влиянию геометрии выемки на эффективность работы гидравлических экскаваторов. Предлагаемая методика может быть применена к аналогичным месторождениям со сложной морфологией. Полученные результаты могут служить основой для разработки более адаптивных и обоснованных стратегий планирования горных работ.

Ключевые слова: блочное моделирование, модель запасов, регуляризация, оптимизация выемочных единиц, потери и разубоживание, экономическая эффективность, селективная отработка.

Мусин Равиль Альтавович	***Информация об авторах:*** *PhD, и.о. доцента кафедры разработки месторождений полезных ископаемых Карагандинского технического университета имени Абылкаса Сагинова, 100027, пр. Нурсултана Назарбаева, 56, Караганда, Казахстан. E-mail: r.a.mussin@mail.ru; ORCID ID: https://orcid.org/0000-0002-1206-6889*
Ящишин Максим Григорьевич	*Магистрант кафедры разработки месторождений полезных ископаемых Карагандинского технического университета имени Абылкаса Сагинова, 100027, пр. Нурсултана Назарбаева, 56, Караганда, Казахстан. E-mail: maxim.yachshishin@gmail.com; ORCID ID: https://orcid.org/0009-0006-2326-8335*
Голик Андрей Васильевич	*Директор ТОО I-Geo Kazakhstan, 100017, ул. Новоселов, 190/1, Караганда, Казахстан. E-mail: andrey.golik@i-geo.kz; ORCID ID: https://orcid.org/0009-0008-5179-0002*
Ахматнуров Денис Рамильевич	*PhD, руководитель лаборатории Карагандинского технического университета имени Абылкаса Сагинова, 100027, пр. Нурсултана Назарбаева, 56, Караганда, Казахстан. E-mail: d.akhmatnurov@gmail.com; ORCID ID: https://orcid.org/0000-0001-9485-3669*

References

[1] McManus S, Rahman A, Coombes J, Horta A. Uncertainty assessment of spatial domain models in early stage mining projects – A review. Ore Geology Reviews. 2021; 131:104098. https://doi.org/10.1016/j.oregeorev.2021.104098

[2] Stadnik DA, Stadnik NM, Zhilin AG, Lopushnyak EV. Methodological framework for implicit modeling of solid mineral deposits in automated design. Gornyi Zhurnal. 2023; 51:185–194. https://doi.org/10.25018/0236_1493_2023_51_0_185

[3] Rossi ME, Deutsch CV. Mineral resource estimation. Dordrecht: Springer. 2014. https://doi.org/10.1007/978-1-4020-5717-5

[4] Emery X, Matheron G. Uncertainty quantification in mineral resource estimation. Natural Resources Research. 2024; 33: 1101–1125. https://doi.org/10.1007/s11053-024-10394-6

[5] Kantemirov VD, Yakovlev AM, Titov RS. Primenenie geoinformatsionnykh tekhnologiy blochnogo modelirovaniya dlya sovershenstvovaniya metodov otsenki kachestvennykh pokazateley poleznykh iskopaemykh [Application of GIS-based block modeling technologies to improve methods of assessing quality indicators of mineral resources]. Izvestiya vysshikh uchebnykh zavedeniy. Gornyy zhurnal = Journal of Mining Science. 2021;(1):63–73. (in Russ.). https://doi.org/10.21440/0536-1028-2021-1-63-73

[6] Vostrikov AV, Prokofeva EN, Gribanov IV, Goncharenko SN. Analytical modeling for the modern mining industry. Eurasian Mining. 2019; (2):30–35. https://doi.org/10.17580/em.2019.02.07

[7] Plan gornykh rabot dobychi fosforitov otkrytym sposobom na mestorozhdenii Kokzhon uchastka Kistas na 2024–2040 gg. Poyasnitelnaya zapiska. Kniga 1 [Mining plan for open-pit phosphate mining at the Kokzhon deposit, Kistas mine, for 2024–2040. Explanatory note. Book 1]. Ust-Kamenogorsk. 2023, 142. (in Russ.).

[8] Marinin M, Marinina O, Wolniak R. Assessing of losses and dilution impact on the cost chain: case study of gold ore deposits. Sustainability. 2021; 13(7):3830. https://doi.org/10.3390/su13073830

[9] Kantemirov VD, Titov RS, Yakovlev AM, Timokhin AV. Metodika otsenki sverkhnormativnykh poter poleznogo iskopaemogo pri razrabotke slozhnostrukturnykh mestorozhdeniy [Methodology for evaluating excess mineral losses in the development of structurally complex deposits]. Problemy nedropol'zovaniya = Subsoil Use Issues. 2024, 47–56. (in Russ.). https://doi.org/10.25635/2313-1586.2024.01.047

[10] Kantemirov VD, Titov RS, Timochin AV, Yakovlev AM. Sovershenstvovanie metodov ucheta povyshennykh poter' i razubozhivaniya poleznogo iskopaemogo pri dobyche [Improvement of methods for accounting increased losses and dilution of mineral resources during mining]. Gornyi informatsionno-analiticheskii byulleten' = Mining Informational-Analytical Bulletin. 2020; 3-1:453–464. (in Russ.). https://doi.org/10.25018/0236-1493-2020-31-0-453-464

[11] Alikulov Sh, Toshov J, Mussin R, Rabatuly M, Tolovkhan B, Bogzhanova Zh, Gabitova A. Study of rational solution parameters during in-situ uranium leaching. Mining of Mineral Deposits. 2025; 19(1):37–46. https://doi.org/10.33271/mining19.01.037

[12] Zamaliyev NM, Zhalbypov ZhD, Valiev NG, Akhmatnurov DR, Zhansejtov AT. Development of proposals to improve the inpit crushing and conveying system (IPCC) for the Bozshakol deposit. Ugol. 2024; 2:58–64. https://doi.org/10.18796/0041-5790-2024-2-58-64

[13] Zhong D-Y, Wang L-G, Jia M-T, Bi L, Zhang J. Orebody modeling from non-parallel cross sections with geometry constraints. Minerals. 2019; 9(4):229. https://doi.org/10.3390/min9040229

[14] Dimitrakopoulos R. Conditional simulation algorithms for modelling orebody uncertainty in open pit optimisation. Geostatistics for Natural Resources Characterization. 2007; 2:173–179. https://doi.org/10.1080/09208118908944041

[15] Serdyukov AL, Zaporozhets VYu, Kudryashov VS, Levin EL. Komp'yuternoe proektirovanie i planirovanie gornykh rabot v kar'ere s dinamicheskoy otsenkoy poter' i zasoreniya poleznogo iskopaemogo pri dobyche [Computer-aided design and mine planning with dynamic assessment of mineral losses and contamination during extraction]. Trudy Instituta Gornogo Dela im. D.A. Kunayeva (Proceedings of the D.A. Kunayev Mining Institute). 2015; 87:180–185. (in Russ.). http://www.igd.com.kz/pdf/87.pdf

[16] Bertinshaw R, Lipton I. Estimation of mining factors (ore dilution and loss) in open pits. Australasian Institute of Mining and Metallurgy (AusIMM). 2007, 13–18. https://www.ausimm.com/publications/conference-proceedings/sixth-large-open-pit-mining-conference-2007/estimating-mining-factors-dilution-and-ore-loss-in-open-pit-mines/

[17] Muttaqin BIA, Ciptomulyono U, Siswanto N. Optimizing cut-off grades under stochastic price: A model for open-pit lateritic nickel mining with multiple products. Resources Policy. 2025; 87:105630. https://doi.org/10.1016/j.resourpol.2025.105630

[18] Kaputin YuE. Modelirovanie mestorozhdeniy i otsenka mineral'nykh resursov s ispol'zovaniem STUDII 3: uchebnyi kurs [Modeling of deposits and mineral resource estimation using Studio 3: training course]. Saint Petersburg. 2007, 188. (in Russ.). https://www.geokniga.org/bookfiles/geokniga-modelirovanie-mestorozhdeniy-i-ocenka-resursov.pdf

[19] Mokos P, Glover I. Mineable Shape Optimizer. Version 5.0.2. Alford Mining Systems. 2022, 217.

[20] Kantemirov VD, Yakovlev AM, Titov RS. Primenenie geoinformatsionnykh tekhnologiy blochnogo modelirovaniya dlya sovershenstvovaniya metodov otsenki kachestvennykh pokazateley poleznykh iskopaemykh [Application of GIS block modeling technologies for improving methods of assessing quality indicators of mineral resources]. Izvestiya vysshikh uchebnykh zavedeniy. Gornyi zhurnal = News of Higher Educational Institutions. Mining Journal. 2021; 1:63–73. (in Russ.). https://doi.org/10.21440/0536-1028-2021-1-63-73

[21] Komatsu Ltd. Hydraulic Excavator PC1250-11: Product Brochure. Tokyo: Komatsu Ltd. 2022. https://www.komatsu.co.za/sites/default/files/2022-02/PC1250-11R_CEN00903-00_0.pdf

МАЗМҰНЫ
СОДЕРЖАНИЕ
CONTENTS

METALLURGY

Berkinbaeva A.N., Surkova T.Yu., Dosymbayeva Z.D., Umirbekova N.S., Kebekbaeva A.A., Kyussubayeva N.A. INVESTIGATION OF ZINC LEACHING FROM CLINKER WITH PRETREATMENT OF RAW MATERIALS BY ULTRAHIGH FREQUENCY RADIATION (MICROWAVE)……. 5

Kenzhaliyev B.K., Karshyga Z.B., Yersaiynova A.A., Muhammad N.A.A., Yessengaziyev A.M. PHYSICOCHEMICAL PARAMETERS OF LITHIUM SORPTION FROM HYDROMINERAL RAW MATERIALS USING SYNTHESIZED INORGANIC SORBENTS ……... 14

Jumadilov T.K., Kabzhalelov K.R., Khimersen Kh., Totkhuskyzy B., Mukatayeva Zh.S. STUDY OF THE KINETICS OF SORPTION OF PRASEODYMIUM AND NEODYMIUM IONS USING INTERPOLYMER SYSTEMS BASED ON KU-2-8 and AB-17-8 IN SALT FORMS ……... 21

ENGINEERING AND TECHNOLOGY

Otunchi Ye., Umirzakov A., Dmitriyeva E., Shongalova A., Kemelbekova A. MORPHOLOGICAL AND CRYSTALLOGRAPHIC INVESTIGATION OF CVD-Grown MoS_2 …….. 30

Zhuginissov M.T., Kuldeyev E.I., Nurlybayev R.E., Khamza Y.Y., Orynbekov Y.S., Iskakov A.A. USE OF FLY ASH AND GROUND TUFF AS POZZOLANIC ADDITIVES IN LIGHTWEIGHT STRUCTURAL ……. 38

Fitrianto, Nandy Putra, Eny Kusrini REVIEW OF SUSTAINABLE JET FUEL PRODUCTION THROUGH PYROLYSIS OF WASTE TIRES: PROCESS, THE PHYSICOCHEMICAL PROPERTIES AND CATALYST ……. 52

Atashev E.A. DECOMPOSITION OF MAGNESITE-SPARING WASTE IN SULFURIC ACID WITH A HIGH CONCENTRATION: EMPIRICAL MODELING AND DETERMINATION OF OPTIMAL CONDITIONS…… 71

Yuldasheva A.P., Shamuratov S.Kh., Kurambayev Sh.R., Radjabov M.F. MATHEMATICAL ANALYSIS OF CAO CONTENT VARIATION IN ACIDIC WASTEWATER AND MINERALIZED MASS MIXTURE FROM CENTRAL KYZYLKUM PHOSPHORITE BASED ON EXPONENTIAL DECAY MODEL …….. 79

EARTH SCIENCES

Toshov J.B., Rabatuly M., Khaydarov Sh., Kenetayeva A.A., Khamzayev A., Usmonov M., Zheldikbayeva A.T. METHODS FOR ANALYSIS AND IMPROVEMENT OF DYNAMIC LOADS ON THE STEEL WIRE ROPE HOLDING THE BOOM OF STEEL WIRE ROPE EXCAVATORS …….. 87

Mussin R.A., Yachsishin M.G., Golik A.V., Akhmatnurov D.R. BLOCK MODELING RESERVES ESTIMATION …….. 97

Техникалық редакторлар:
Г.К. Қасымова, Н.М.Айтжанова, Т.И. Қожахметов

Компьютердегі макет:
Г.К. Қасымова

Дизайнер:
Г.К. Қасымова, Н.М.Айтжанова

“Металлургия және кен байыту институты” АҚ
050010, Қазақстан Республикасы, Алматы қаласы, Шевченко к-сі, 29/133

Жариялауға 20.08.2025 жылы қол қойылды

Технические редакторы:
Г.К. Касымова, Н.М. Айтжанова, Т.И. Кожахметов

Верстка на компьютере:
Г.К. Касымова

Дизайнер:
Г.К. Касымова, Н.М.Айтжанова

АО “Институт металлургии и обогащения”
050010, г. Алматы, Республика Казахстан. ул. Шевченко, 29/133

Подписано в печать 20.08.2025г.

Technical editors:
G.K. Kassymova, N.M. Aitzhanova, T.I. Kozhakhmetov

The layout on a computer:
G.K. Kassymova

Designer:
G.K. Kassymova, N.M. Aitzhanova

“Institute of Metallurgy and Ore Beneficiation” JSC
050010, Almaty city, the Republic of Kazakhstan. Shevchenko str., 29/133

Signed for publication on 20.08.2025